2013

Novel N-heterocyclic dicarbene ligands and molybdenum and dimolybdenum N-heterocyclic carbene complexes

Ross David Bemowski
University of Iowa

NOVEL N-HETEROCYCLIC DICARBENE LIGANDS AND MOLYBDENUM AND DIMOLYBDENUM N-HETEROCYCLIC CARBENE COMPLEXES

by

Ross David Bemowski

A thesis submitted in partial fulfillment of
the requirements for the Doctor of
Philosophy degree in Chemistry in the
Graduate College of The University of Iowa

August 2013

Thesis Supervisor: Associate Professor Louis Messerle

Graduate College
The University of Iowa
Iowa City, Iowa

CERTIFICATE OF APPROVAL

_____

PH.D THESIS

_____

This is to certify that the Ph. D. thesis of

Ross David Bemowski

has been approved by the Examining Committee for the thesis requirement for the Doctor of Philosophy degree in Chemistry at the August 2013 graduation.

Thesis Committee: _____
Louis Messerle, Thesis Supervisor

_____
Edward G. Gillan

_____
Daniel M. Quinn

_____
James B. Gloer

_____
Lynn M. Teesch

ACKNOWLEDGMENTS

During my tenure at the University of Iowa I have been very lucky to be surrounded by exceptional people, always willing to lend a helping hand. To these friends, colleagues, faculty, and staff, I extend my sincerest gratitude.

First and foremost, I thank my advisor, Prof. Lou Messerle. He has been a patient and encouraging advisor, allowing me to take my own path and providing me with moral support when it seemed that my chemistry would never work. But what I am most thankful for is his helpful criticism, always questioning my work in a way that challenged me to become a better scientist. It is his voice I hear in my head constantly saying "Don't tell me what you think, tell me what you know."

There are also a number of staff members that deserve my thanks. I thank Dr. Santhana Velupillai for all the help with NMR over the years. I also thank Dr. Lynn Teesch and Vic Parcell for their help with mass spectrometry and hiring me to work on their crappy project (pun intended). Sharon Robertson also deserves thanks for guiding me through the university bureaucracy and always knowing who to call to fix a problem. Dr. Dale Swenson deserves my thanks for all his help solving my crystal structures.

I must also thank my group members, both past and present, for making my stay in Iowa much more enjoyable. I thank Adil Mohammad and Dave Rotsch for their nearly constant harassment, making sure my work was held to the highest standard. Justine Olson deserves my thanks for all of her help editing this thesis and helping to keep me sane in general. Kallyn Buschkamp is thanked for his help solving the structure of the dicarbene dimer by 2D NMR methods.

I thank Prof. Dan Quinn for many helpful discussions about organic chemistry mechanisms during the course of my research. I also thank Prof. Jim Gloer for all of his considerable help in solving the structure of the dicarbene dimer, as I really could not have done it without him.

I am deeply grateful to my family, whose confidence in my abilities was unwavering. Without their support, I could have never made it this far.

And lastly, I thank my wife, Kirsten. Her love and support kept me motivated even when my chemistry seemed hopeless. I also can't thank her enough for her help in editing this thesis.

ABSTRACT

The syntheses of a new class of polycyclic TriAmino DiCarbenes (TADCs), based on 3,9-diazajulolidine, and their precursors and adducts are described.

Starting with 2,6-dimethyl-nitrobenzene, 2,6-bis ((alkylamino)methyl)anilines (alkyl = isopropyl, mesityl, and tert-butyl) were synthesized in 40% yield over five steps. These triamines were then di-cyclized stepwise to diformamidinium dications or formamidinium/2-methoxyformaminals using oxonium salts and trialkyl orthoformates. A diformamidinium dication was characterized by single-crystal X-ray diffractometry. Treatment with various bases, particularly lithium hexamethyldisilylazide, led to the novel TADCs and monocarbenes, two of which were isolated and characterized by ^{1}H and ^{13}C NMR spectroscopies. In both cases, treatment with elemental sulfur trapped the TADCs as dithiobiurets. No TADC-transition metal complexes were successfully isolated from reactions of the diformamidinium dications or LiHMDS TADC complex with a number of transition metal complexes.

With the exception of these two cases, all other TADCs were not isolated because they rapidly reacted to form dimers, trimers, and tetramers. One of these dimers was isolated and its structure determined using 1D and 2D NMR spectroscopies, along with high-resolution electrospray ionization mass spectrometry. This revealed that the TADC had dimerized to form an ene-triamine, likely via 1,3-shift of a benzylic proton.

Novel N-heterocyclic Carbene (NHC) complexes of molybdenum were also synthesized and characterized. Reaction of $Cp_2Mo_2(CO)_4$ ($Cp = C_5H_5$) with dimesityl-imidazol-2-ylidenes (IMes) or dimesityl-imidazolidin-2-ylidenes (SIMes) yielded the

molybdoradicals $CpMo(CO)_2(NHC)$ (NHC = IMes or SIMes). The carbonyl infrared stretching frequencies and the relative metal-to-NHC π-backbonding for IMes and SIMes complexes are compared. Reaction of the less bulky dimethylimidazol-2-ylidene (IMe) with $Cp_2Mo_2(CO)_4$ yielded the Mo-Mo triple bond complex $Cp_2Mo_2(CO)_3(IMe)$ by CO substitution. This is the first example of an NHC-ligated metal-metal multiply bonded complex. Single crystal X-ray diffractometry of these new organomolybdenum and organodimolybdenum complexes is discussed.

TABLE OF CONTENTS

LIST OF TABLES

LIST OF FIGURES

LIST OF REACTION SCHEMES

CHAPTER I: INTRODUCTION

A carbene is a neutral carbon with two substituents and six valence electrons. For most of their history, carbenes have been laboratory curiosities as only transiently-stable reaction intermediates. That changed in 1991, when Arduengo crystallized the first free N-Heterocyclic Carbene (NHC) (Scheme 1.1).[1] Since that time, NHCs have become ubiquitous as ligands in transition metal catalysis,[2] valued for their excellent electron-donating properties and steric tunability. The introduction of new structural variations continues to expand catalytic uses for NHCs.

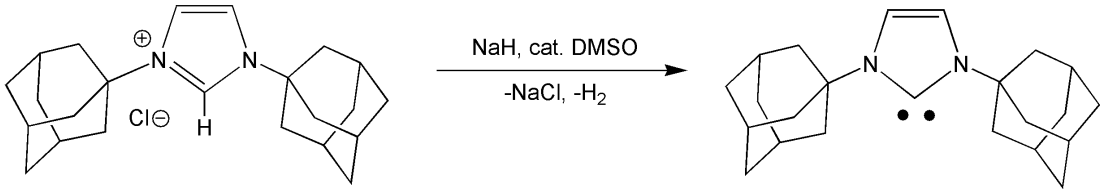

Scheme 1.1. Arduengo's carbene[1]

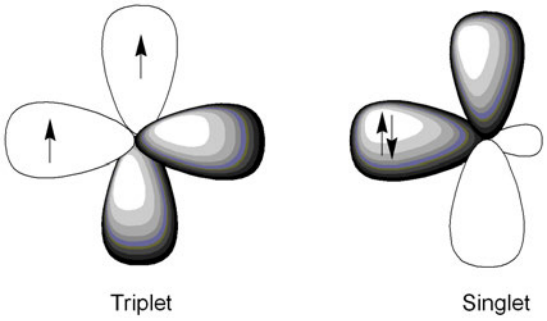

Figure 1.1. Triplet vs. singlet carbenes

Carbenes exist in either the triplet or singlet state (Figure 1.1). Triplet carbenes have alkyl or aryl substituents on the carbene carbon that are unable to donate significant electron density. This relative lack of electron donation results in a ground state with the

two unpaired electrons in separate p orbitals, while the carbon is *sp* hybridized. This carbene is considered a diradical and is only stable for short periods of time when free, though there are examples of isolable triplet carbenes.[3] When bound to a metal they form Schrock alkylidene complexes. The metal-alkylidene bond is covalent in nature, seen as the coupling of two triplet fragments[4] resulting in a double bond (Figure 1.2). In these types of complexes, the alkylidene carbon is nucleophilic and reacts with electrophiles.[5]

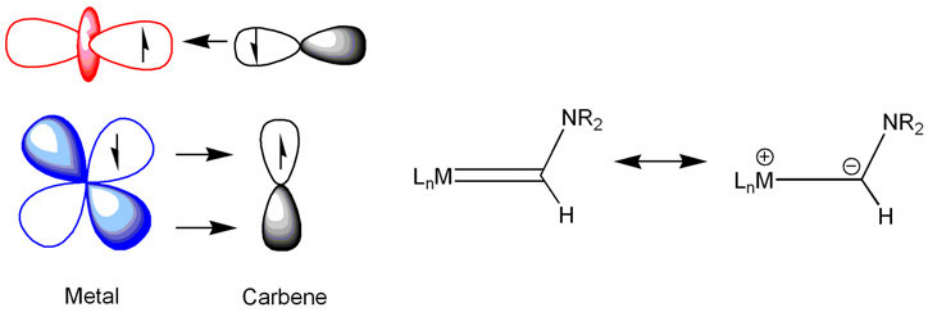

Figure 1.2. Bonding in Schrock alkylidene complexes

While triplet carbenes usually have alkyl or aryl substituents, singlet carbenes have one or two heteroatom α-substituents (N, O, S, or P) that are good electron donors. This electron donation results in a singlet ground state with a lone pair of electrons in an sp^2 type orbital and an empty p orbital that can be filled by the lone pairs from the adjacent heteroatom(s) (Figure 1.3). When bound to a metal, singlet carbenes form Fisher carbene complexes. Bonding in these complexes is seen as a strong carbene-to-metal σ-donation and weaker metal-to-carbene π-backbonding (Figure 1.4). The extent to which the metal backbonds is inversely related to how well the α-substituents stabilize the p-orbital of the carbene. Diaminocarbenes, which include NHCs, have a nominally empty p-orbital completely filled by the adjacent amino groups, resulting in negligible

metal-to-carbene π-backbonding (see Chapter IV for a more in-depth discussion of π-backbonding to NHCs). Additionally, Fischer carbenes are electrophilic, being susceptible to nucleophilic attack.[6]

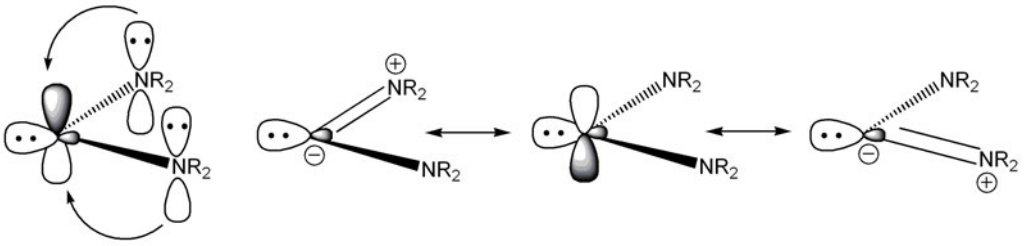

Figure 1.3. Mesomeric structures of diaminocarbenes

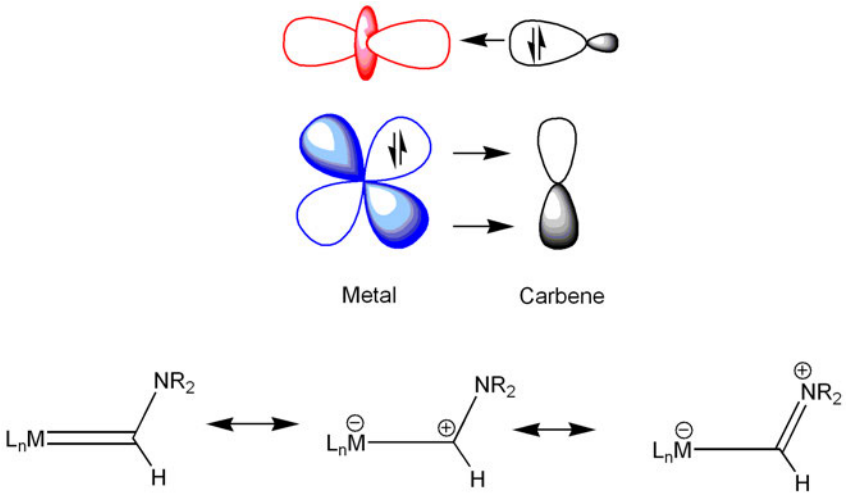

Figure 1.4. Bonding in Fischer carbene complexes

General Reactivity of NHCs

NHCs can dimerize to form enetetramines (Scheme 1.2). The tendency of NHCs to dimerize is based on two factors: the steric bulk of the R-groups on the α-nitrogens and whether or not the heterocycle is aromatic[7] (see Figure 1.5 for nomenclature of

common NHCs and R-groups). When the heterocycle is non-aromatic, dimerization occurs unless

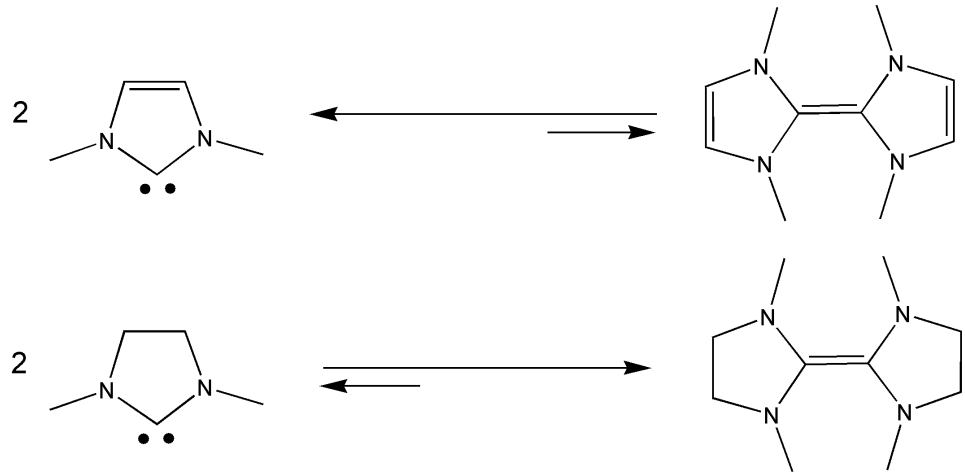

Scheme 1.2. Dimerization of N,N'-dimethyl NHCs

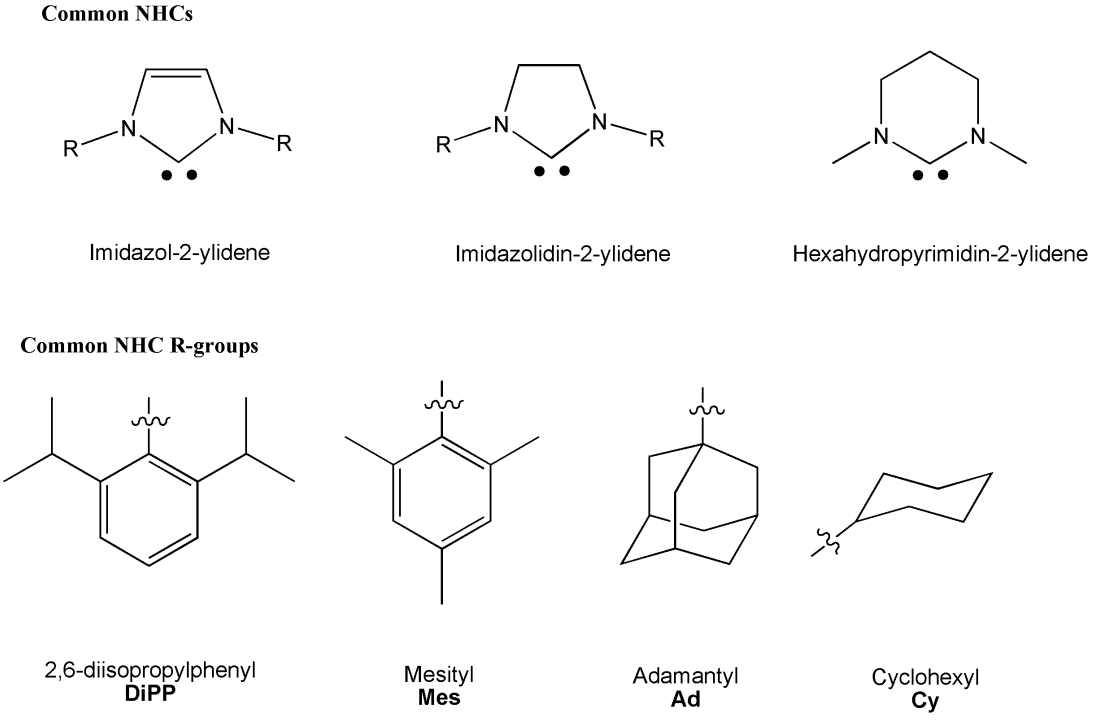

Figure 1.5. Nomenclature of common NHCs and NHC R-groups

the R groups are sufficiently bulky. For imidazolidin-2-ylidenes, the point at which dimerization occurs is ^{t}Bu vs. ^{i}Pr for alkyl and mesityl vs. phenyl for aryl.[8] For the six-membered hexahydropyrimidinylidene, ^{i}Pr groups are sufficient to prevent dimerization because the R groups are angled more toward the carbene in comparison to five-membered rings.[9] If the heterocycle is aromatic, however, as is the case of imidazole-2-ylidenes, the carbene is stable to dimerization even if the R groups are very small (i.e., methyl). In this case, dimerization disrupts the aromaticity of the imidazole ring, which is thermodynamically disfavored.

With calculated conjugate acid pKa's ranging from ≈ 20-30 (in DMSO),[10] NHCs are some of the strongest neutral organic bases available, allowing them to be used as organo-catalysts in a number of reactions.[11] NHCs are extremely moisture-sensitive, reacting with water to form the acyclic amino-formamide; however, NHCs are stable to triplet dioxygen.[12]

Carbenes as Ligands

As ligands, NHCs are often compared to trialkylphosphines. Nolan published an excellent study comparing the steric and electronic properties of NHC and phosphine complexes of nickel.[13] In the study, $Ni(CO)_4$ was reacted with one equivalent of NHC (imidazol-2-ylidenes and imidazolidin-2-ylidenes with various R-groups) or trialkyl phosphine to form $Ni(L)(CO)_x$ (L = NHC or phosphine and x = 2 or 3) (Scheme 1.3). By comparing the carbonyl IR stretching frequencies, it was possible to compare the electron density on the metal center, and thus the electron donating ability of the ligand. The nickel π-backbonds into the C-O π* orbital, weakening the C-O bond and lowering the

energy of the IR stretching frequency. Using these data, it was shown that NHCs are better electron donors than even the most basic trialkylphosphines. Additionally, it was shown that when trialkyl phosphines or less strictly hindered NHCs (where the R-group is Mes, DiPP, or Cy) were used, $Ni(L)(CO)_3$ (L = NHC or phosphine) was formed; however, if an NHC with very bulky R-groups (*tert*-butyl or adamantyl) was used, $Ni(NHC)(CO)_2$ was formed (Scheme 1.3). This demonstrated that NHCs can be more sterically demanding than even the bulkiest trialkylphosphines. This combination of excellent electron donating ability and steric tunability has allowed NHCs to replace trialkyl and triaryl phosphines in many catalytic systems.[2a]

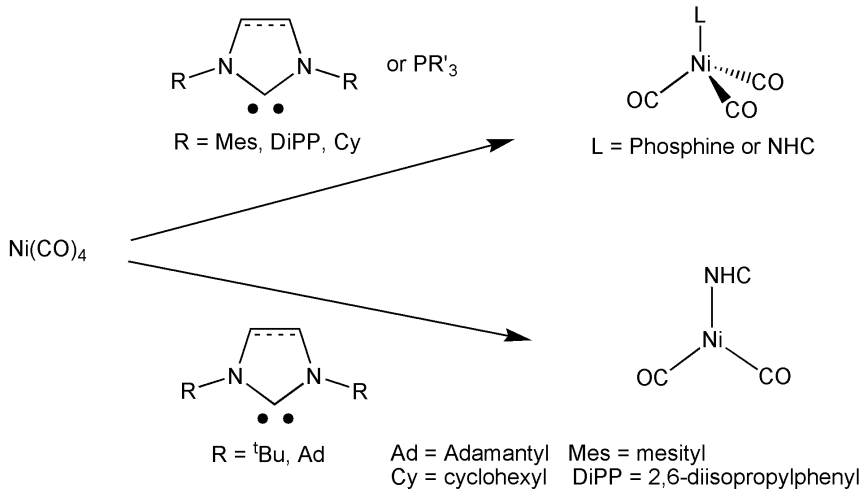

Scheme 1.3. Nolan's syntheses of NHC and phosphine complexes of nickel[13]

Methods to Prepare Free NHCs

Of the various methods for synthesizing free NHCs, the most common is deprotonation of a formamidinium or imidazolium salt. The choice of base can be very important and is largely dependent on the target NHC. For the synthesis of imidazol-2-ylidenes, a wide variety of strong bases are effective, though sodium hydride with a

catalytic amount of potassium *tert*-butoxide has been the most widely used.[14] Other types of NHCs are much more sensitive to the base because they lack aromatic stabilization, making them more electrophilic. In order to avoid the formation of nucleophilic addition products, very non-nucleophilic bases are required. Where treatment of an imidazolium salt with potassium *tert*-butoxide leads to the NHC, the same conditions lead to nucleophilic addition in the case of its saturated congener[15] (Scheme 1.4). In these cases, sterically-hindered amide bases, such as lithium diisopropylamide (LDA) or potassium hexamethyldisilazide (KHMDS), form the free NHC.

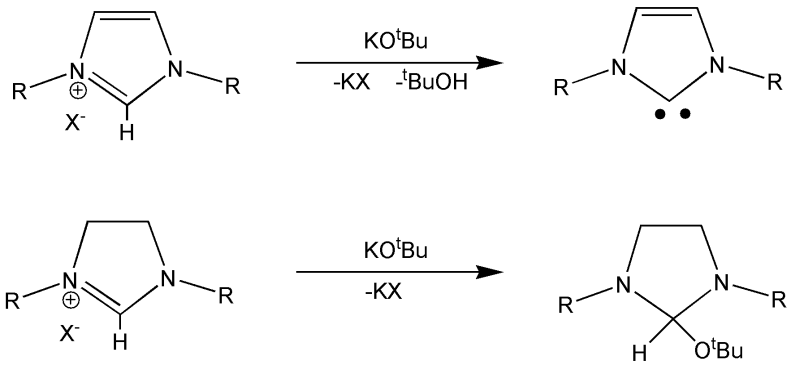

Scheme 1.4. Reaction of KO^{t}Bu with imidazolium and formamidinium salts

When very strong bases are used (e.g., LDA), deprotonation can occur at positions other than the carbenic center.[16] Weaker bases, such as KHMDS, selectively deprotonate the carbenic carbon, forming the NHC.

The choice of the base's counter-cation can also be important for successful NHC synthesis. NHCs have been known to coordinate to alkali metal cations, which can complicate their isolation and purification.[9] This is especially true of lithium, and less so for sodium and potassium, cations.

NHCs can also be obtained by thermolysis of N-heterocyclic rings that contain an alkoxy- or trichloromethyl- group[17] on the carbon being converted to a carbene (Scheme 1.5). Upon heating, either an alcohol or chloroform is eliminated, leading to the NHC. This can be performed under vacuum in order to obtain the free carbene; however, it is more common to form the NHC directly by refluxing the precursor in a high-boiling-point solvent with the metal complexing species.

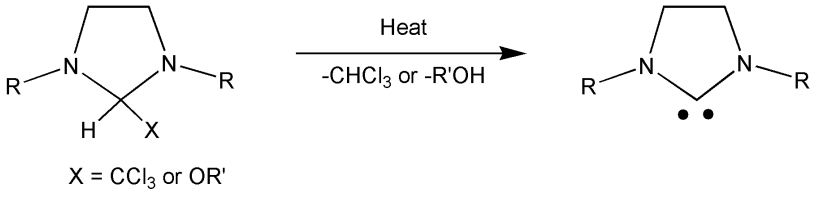

Scheme 1.5. Example of thermolysis to form NHCs

Desulfurization of thioureas with K or Na/K in refluxing tetrahydrofuran (THF) or toluene also produces NHCs (Scheme 1.6).[18] The reaction can be performed at room temperature, though it can require up to 20 days. Despite these conditions, this method provides NHCs in high yields.

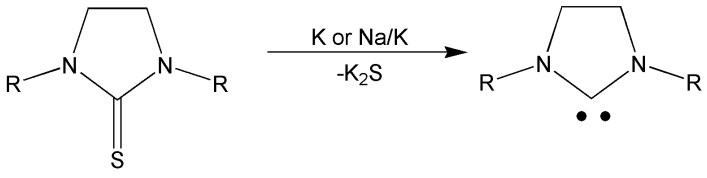

Scheme 1.6. Example of desulfurization of thioureas to form NHCs

Routes to NHC Metal Complexes

The most direct route to NHC metal complexes is addition of the isolated free NHC to a metal complex precursor. Complexation usually proceeds by displacement of another neutral two-electron donor ligand, such as THF, CO, phosphine, or pyridine (Scheme 1.7). This method has the advantage of being straightforward and clean; however, it requires previously isolating the free NHC.

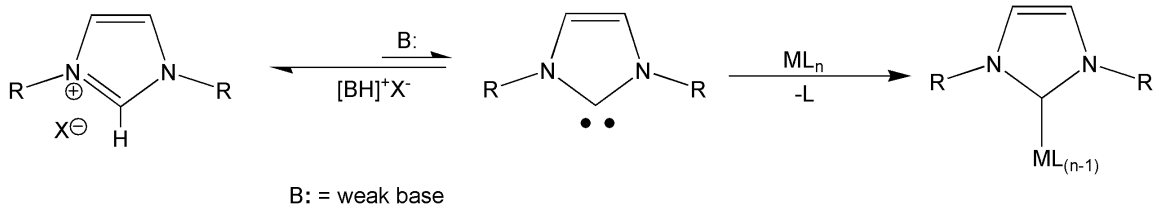

Scheme 1.7. Proposed mechanism for NHC metal complex formation using a weak base

Alternatively, the imidazolium or formamidinium salts can be deprotonated *in situ*. One route to accomplish this is a step-wise deprotonation: addition of a strong base to the imidazolium or formamidinium salt to form the NHC followed by addition of the metal complex reactant. This is convenient because it does not require isolation of the NHC. However, it still requires dry conditions and often low temperature for the deprotonation step. Deprotonation is also possible through use of a weak base, such as triethylamine (TEA),[19] sodium acetate,[20] or cesium carbonate[21] in the presence of the metal complex reactant. This approach is surprising given the disparity between the pKa's of the carbene precursors (pKa = 20-30) and the weak bases (pKa = 4-10). The accepted

explanation is that there is a very low concentration of the NHC at equilibrium that can coordinate to the metal, stabilizing the carbene and making the reaction irreversible.[15]

The third methodology for *in situ* deprotonation uses a ligand on the metal complex reactant to act as a base. Suitable basic ligands include hydrides,[22] acetates,[23] alkyls,[24] or amides.[25] A complicating factor for this reaction is that it formally replaces an anionic ligand with a neutral one, resulting in the counter anion of the imidazolium/formamidinium salt being incorporated into the resulting metal complex. This route is particularly useful for carbenes that have sensitive moieties, such as methylene-bridged imidazolium salts (Scheme 1.8).[23]

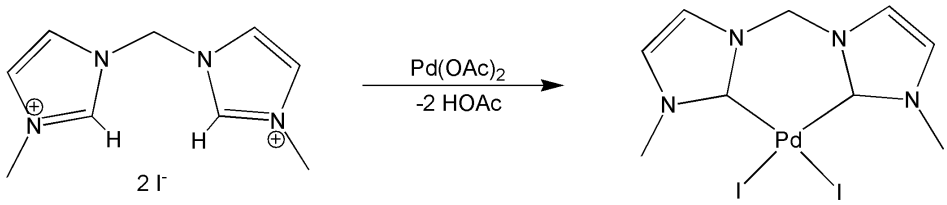

Scheme 1.8. Deprotonation with a basic ligand

Silver oxide reacts with imidazolium and formamidinium salts to form mono or bis(NHC) adducts.[26] Because of the labile Ag^{+}-NHC bond, transmetallation can occur and is driven by the precipitation of the insoluble silver halide (Scheme 1.9). Transmetallation has only been demonstrated with late transition metals. This reaction has seen more success with imidazole-2-ylidenes than with other types of NHCs. One major benefit of this route to NHC complexes is that it is not necessary to maintain anhydrous reaction conditions.

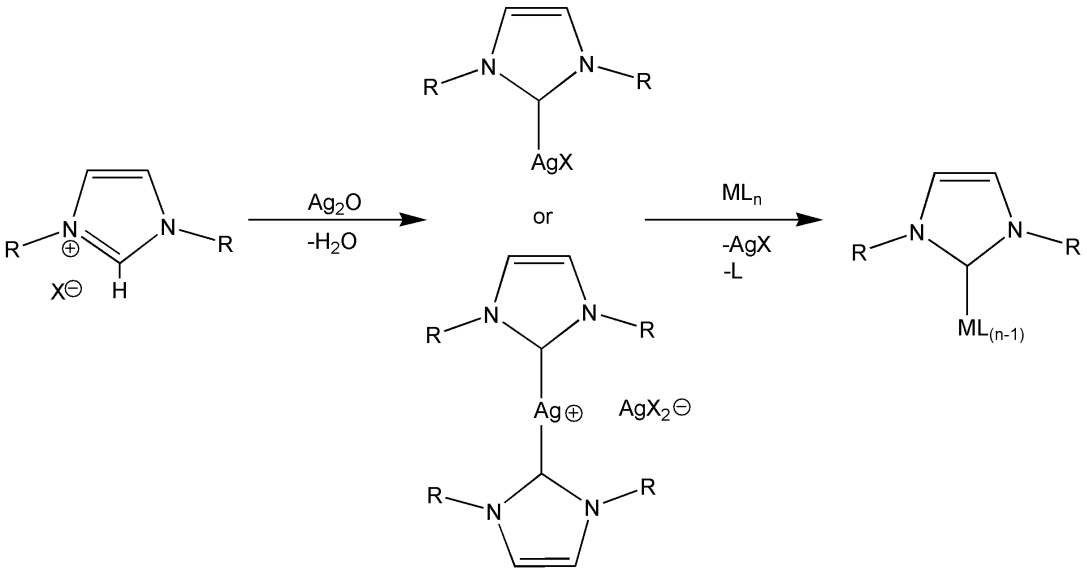

Scheme 1.9. Deprotonation and transmetallation with silver(I) oxide

Synthesis of NHC Precursors

The most commonly used precursors to NHCs, by far, are imidazolium salts. There are a number of synthetic routes to both symmetric (both R groups being the same) and asymmetric (R groups differ) imidazolium salts. Treating glyoxal with two equivalents of a primary amine bearing the desired R-group leads to the diimine, which can then be treated with formaldehyde and an acid to form the symmetric imidazolium salt in good yields (Scheme 1.10).[27] For asymmetric imidazolium salts, glyoxal is treated with one equivalent each of a primary amine, formaldehyde, and ammonium chloride in one flask to form the mono-substituted imidazole. This can then be alkylated to form the asymmetrically-substituted imidazolium salt (Scheme 1.11).[28]

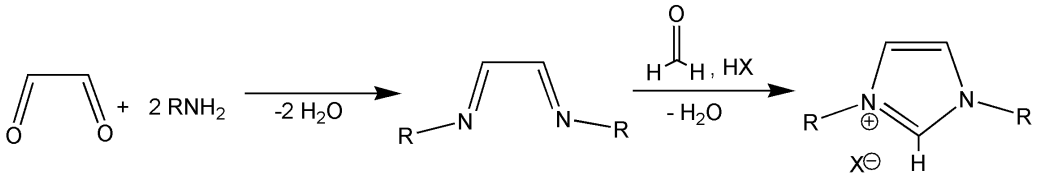

Scheme 1.10. Synthesis of symmetrically-substituted imidazolium salts

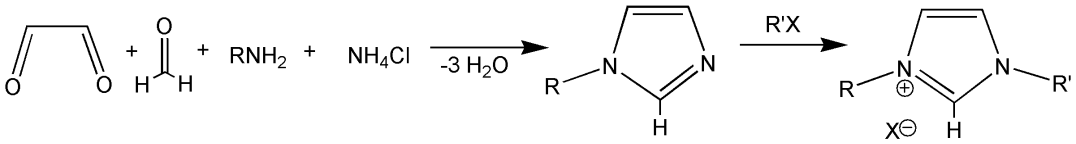

Scheme 1.11. Synthesis of asymmetrically-substituted imidazolium salts

Alternatively, it is possible to start with imidazole, which leads to the anion by treatment with potassium (Scheme 1.12).[28] This anion is then alkylated to form the monosubstituted imidazole. A second alkylation forms the imidazolium salt.

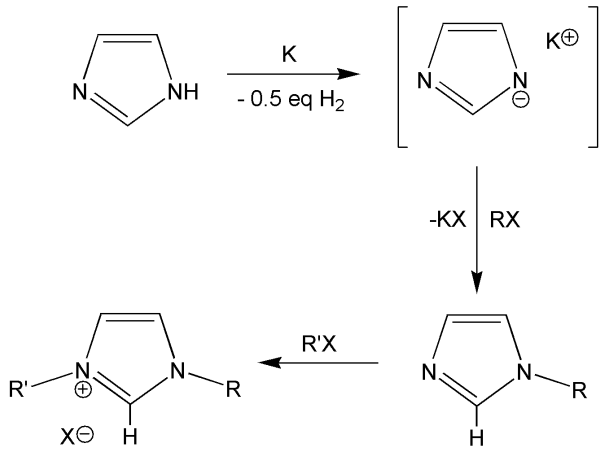

Scheme 1.12. Synthesis of imidazolium salts from imidazole

Cyclic formamidinium salts are produced via a number of methods, almost always starting with a diamine. Diamines can be synthesized via reductive amination of aldehydes or ketones or by nucleophilic substitution of alkyl halides (Scheme 1.13).[29] The most common reagents for converting diamines to formamidinium salts are trialkylorthoformates [$CH(OR)_3$]. Heating the diamine with a trialkylorthoformate and a proton source (usually an ammonium salt) leads to the cyclic formamidinium with the loss of three equivalents of alcohol (Scheme 1.14).[30]

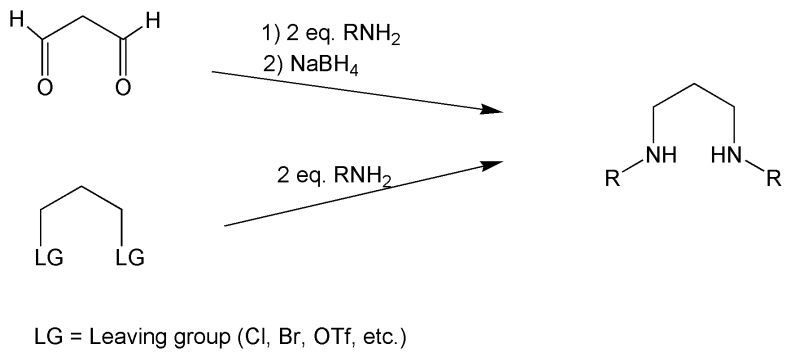

Scheme 1.13. Methods for synthesis of N,N'-disubstituted diamines

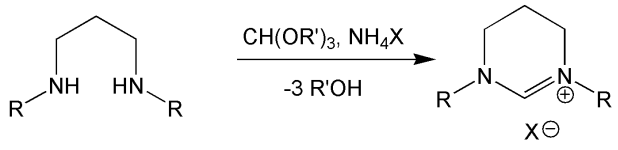

Scheme 1.14. Synthesis of cyclic formamidinium salts from N,N'-disubstituted diamines with trialkylorthoformate

Cyclic formamidinium salts can also be formed by formamidinium exchange. This proceeds by heating the diamine with an acyclic formamidinium salt (typically

N,*N*,*N*',*N*'-tetramethylformamidinium chloride) (Scheme 1.15).[31] The equilibrium is shifted to the desired product by driving off the volatile by-product, dimethylamine.

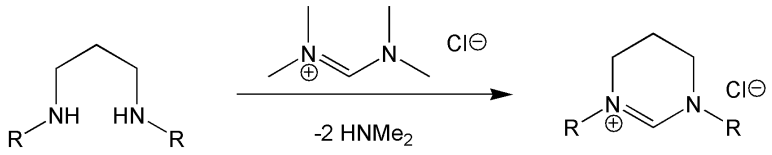

Scheme 1.15. Synthesis of formamidinium salts by formamidinium exchange

Oxonium salts can also be used to form formamidinium salts. Because acyclic oxonium salts can also lead to N-alkylation, sterically-hindered, cyclic oxonium salts are more often used. Oxonium salts are synthesized by treating an orthoformate with tetrafluoroboric acid or boron trifluoride (Scheme 1.16).[31] The reaction of the diamine with the oxonium salt at low temperatures yields the formamidinium salt.

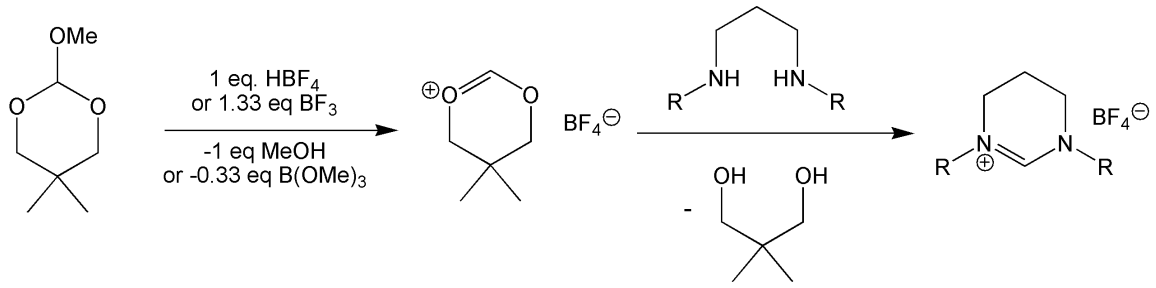

Scheme 1.16. Synthesis of formamidinium salts with oxonium salts

Diamine cyclization to the formaminal with formaldehyde, then oxidation with N-bromosuccinimide (NBS), leads to formamidinium salts (Scheme 1.17).[32]

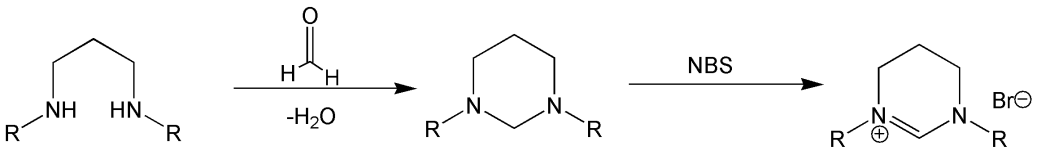

Scheme 1.17. Cyclization of diamine to formamidine with formaldehyde, then oxidation to formamidinium salt with NBS

Thioureas, as precursors to NHCs, can also be produced via cyclization of diamines. A number of reagents are available for this transformation, with carbon disulfide being the most common (Scheme 1.18).[33]

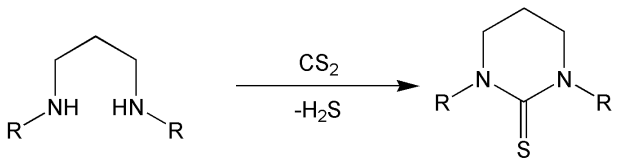

Scheme 1.18. Synthesis of thiourea with carbon disulfide

Appropriate precursors for thermolysis, 2-alkoxy- or 2-trichloromethyl-formaminal, are formed, respectively, by treatment of a formamidinium salt with an alkoxide or chloroform and sodium hydroxide.[34] The same method does not apply to imidazolium salts.

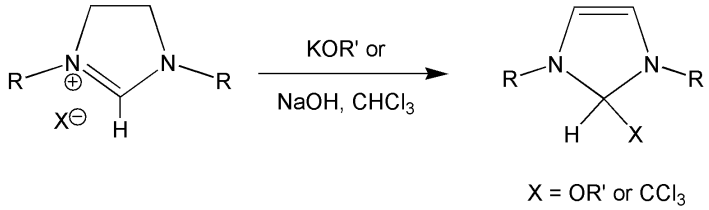

Scheme 1.19. Synthesis of 2-alkoxy- or 2-trichloromethyl-formaminal from formamidinium salt

Uses of NHCs in Catalysis

NHCs are excellent ligands for catalysts, as demonstrated by numerous examples of NHCs improving catalytic properties of catalysts with other ligands.[2a] The exceptional ability of NHCs to donate electron density allows them to stabilize electron-deficient intermediates. NHCs are also very sterically tunable, allowing further modification of the catalyst's reactivity. Furthermore, the strong bonding between NHCs and metals prevents dissociation, which is one of the main mechanisms of catalyst decomposition.

An excellent example of the use of an NHC in catalysis is Grubb's second-generation olefin metathesis catalyst (Scheme 1.20).[35] Replacing one of the phosphine ligands of the first-generation catalyst with an NHC increased the activity. This second-generation catalyst reacted with substrates that were previously inert to metathesis, such as sterically-hindered dienes and tetrasubstituted cycloalkenes. The second-generation catalyst also initiates much faster, producing low polydispersity polymers during ring-opening metathesis polymerization (ROMP). The initiation step involves the dissociation of the phosphine, which is more favorable in the second-generation catalyst because of the strong *trans*-effect of the NHC.

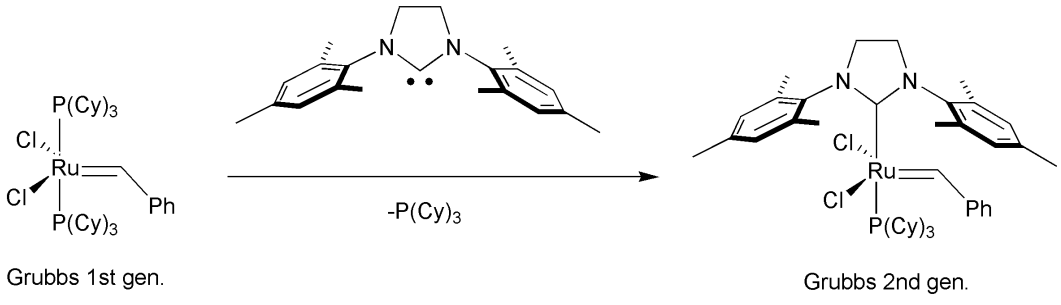

Scheme 1.20. Synthesis of Grubbs 2nd generation catalyst[35]

NHCs have also been used in Pd-catalyzed Suzuki coupling in aqueous media (Scheme 1.21).[36] In this application, the R-groups on the NHC are sulfonated in order to make the NHC-Pd complex water-soluble. This catalytic system has excellent activity, with complete conversion at catalyst loadings as low as 0.1 mol%. This catalyst also demonstrates how robust the NHC-metal bond is, with the catalyst being stable in refluxing water for extended periods.

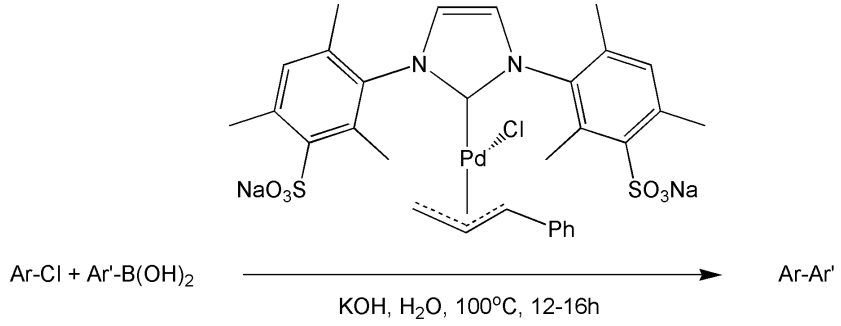

Scheme 1.21. Palladium-catalyzed Suzuki Coupling in aqueous media

NHCs have also proven useful in the realm of organocatalysts. They show excellent activity for catalysis of the benzoin condensation (Scheme 1.22).[37] Modifying the R groups of the NHC may impart useful properties to an organocatalyst. For instance, if the R groups are very long alkyl groups, the NHC will form micelles in water, allowing

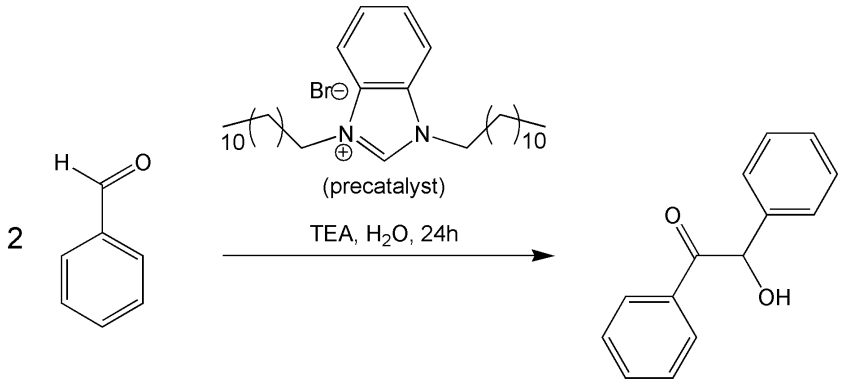

Scheme 1.22. Benzoin condensation using NHC organocatalyst

the catalysis to be performed in aqueous media. If the R groups are asymmetric, high enantioselectivities can be achieved (>90% ee).[38]

Bis(carbenes)

Many bis(carbenes) are known, with the vast majority being two imidazol-2-ylidenes or imidazolin-2-ylidenes connected by an alkyl or aryl group.[39] These types of bis(NHC)s usually chelate and have higher reactivity and stability than mono(NHC)s when used in catalysis.[40]

There are also examples of bis(NHC)s where both of the carbenes are part of a fused ring system, with the NHCs linearly apposed (Janus-type ligand). The Bielawski group prepared a number of organometallic complexes that contain two metal centers bridged by this type of bis(NHC) (Scheme 1.23).[41] Because the bis(NHC)s were

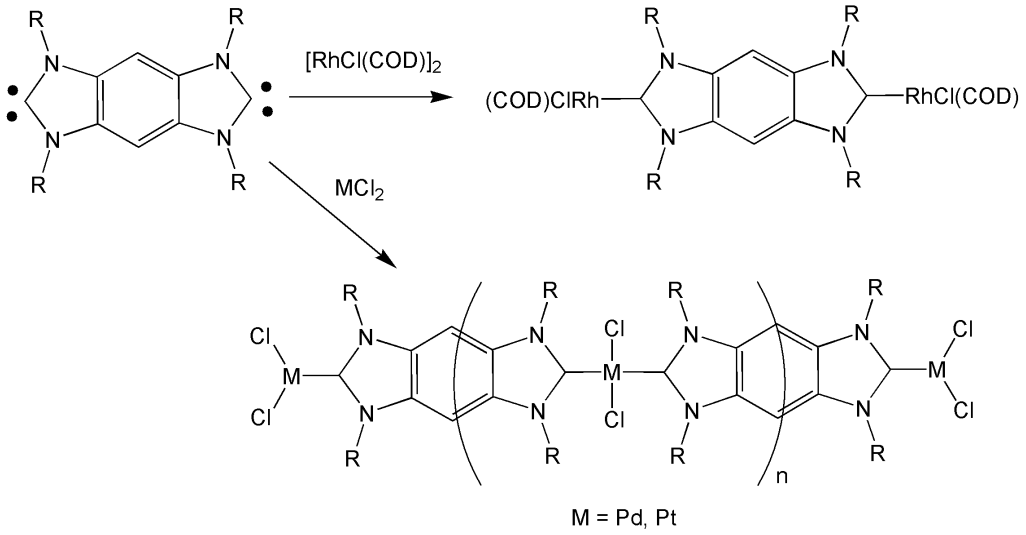

Scheme 1.23. Janus-type NHC can form discrete molecules or polymers

connected with an aromatic linker, the two metal centers could communicate electronically.[42] In addition to discrete organometallic compounds, the Bielawski group

synthesized organometallic polymers with useful properties, such as electrical conductivity and the ability to self-heal.[43]

Another Janus-type bis(NHC), triazole-di-ylidene (ditz) was first synthesized by Bertrand as a polymeric silver complex (Scheme 1.24).[44] It has since been used to prepare homo- and heterobimetallic complexes of rhodium and iridium.[45] This bis(NHC) donates less electron density than other NHCs, and is most electronically similar to phosphines. In spite of their inferior electron donation ability, the iridium and rhodium ditz complexes are very active catalysts for transfer hydrogenation and intramolecular cyclization of alkynoic acids.

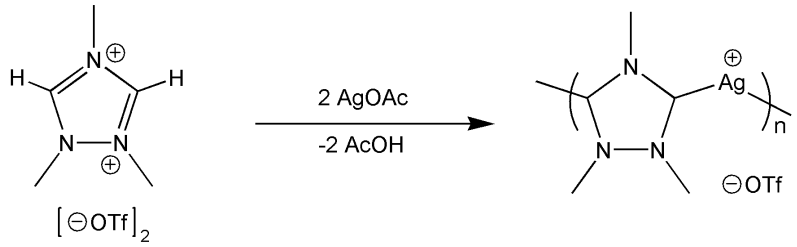

Scheme 1.24. Synthesis of silver ditz complex from the dication

Thesis Overview

NHCs are excellent donors of electron density that have been used to make many mononuclear organometallic complexes, mostly of late transition metals. This thesis will be focused on the synthesis and characterization of dinuclear and early transition NHC metal complexes. Chapters II and III will detail our attempts to synthesize a new type of N-heterocyclic dicarbene capable of dinucleating two metal centers. Chapter IV will discuss the synthesis and characterization of molybdenum mono- and dinuclear NHC complexes.

CHAPTER II: SYNTHESIS AND CHARACTERIZATION OF N-HETEROCYCLIC TRAMINO DICARBNES

A core principle in chemistry is the *functional group*, a linked multiple–atom subset that is the basis for reactivity. Molecules with a *multiple bond* functional group are more reactive than those with single bonds; thus, C-C double and triple bonds are more reactive than C–C single bonds. While the reactivity of carbon multiple bonds is well understood, a comparative understanding of reactivity of non-carbon multiple bonds is far less developed.

Dinuclear complexes with M–M multiple bonds are often supported by dinucleating ligands that bridge two metals. Among these, methylene bis(phosphines) (i.e. $Ph_2PCH_2PPh_2$) have led to considerable amount of dinuclear late transition metal chemistry. Acetates are common anionic dinucleating ligands that yield complexes such as $Mo_2(O_2CCH_3)_4$ and $Re_2(O_2CR)_4Cl_2$. Dinucleating amidinates, which have proven more metallation resistant, have yielded a greater variety of such complexes, particularly of the earlier transition metals.[46]

F. A. Cotton and coworkers studied hexahydropyrimidopyrimidinate (hpp^-), the anion derived from deprotonation of the bicyclic guanidine hppH, as a metallation-resistant ligand. Their efforts[47] and those[48] of the Chisholm group led to the remarkable W-W quadruply-bonded tetragonal lantern-type complex $W_2(hpp)_4$, so highly reducing that it is more easily oxidized in the gas phase than Cesium metal (Figure 2.1). Chemistry has few soluble molecular reductants of high reduction potential, so this discovery attracted considerable attention.[49] Connelly and Geiger noted in their review[50]

of organometallic oxidants and reductants that "Far fewer reagents have been reported for the reduction of organometallic complexes, when compared to the large number of oxidants… There is ample need to develop new reducing agents."

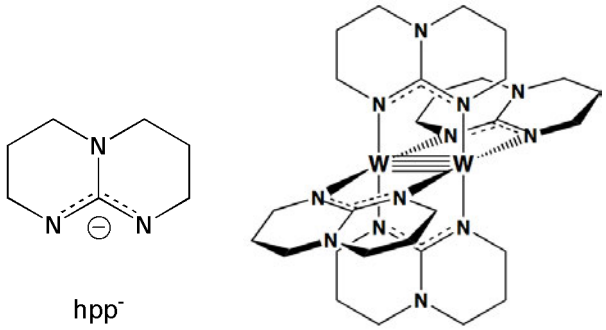

Figure 2.1. hpp- and Cotton's $W_2(hpp)_4$

While hpp- has proven very useful for dinucleation, it is an anionic ligand, requiring the metal center to be in a higher oxidation state. If a neutral analog of hpp- could be synthesized, new, lower oxidation state M-M multiply bonded systems could be created. In theory, these metal complexes should be even more reducing than $W_2(hpp)_4$.

Bis(NHC)s would be an excellent ligand for this application as they would be neutral ligands but still form very strong bonds to metal centers. They would be excellent σ-donors, putting even more electron density on the metal center, which should make the M-M multiple bond even more reducing. However, to date, there have been no bis(NHC)s specifically designed to bridge two metal centers. Thus, we proposed the synthesis of the N-heterocyclic triamino dicarbene (TADC), **A** (Scheme 2.1).

This TADC has the two carbenes as part of a fused six-membered bicyclic ring system. Cotton and Chisholm's work has shown that this type of ring system is optimal

for dinucleation.[51] One of the challenges to designing this ligand was that the bridgehead carbon would be sp^3 hybridized in the simplest fused six-membered bicyclic ring system and the structure would adopt a puckered conformation. Consequently, if two or more TADCs are bridging a dinuclear structure, various geometric isomers are possible, complicating the characterization of these complexes. One approach to circumvent this problem is to make the bridgehead carbon sp^2 hybridized and therefore planar. For our synthesis, this is most easily accomplished by incorporating the bridgehead position into an aromatic ring.

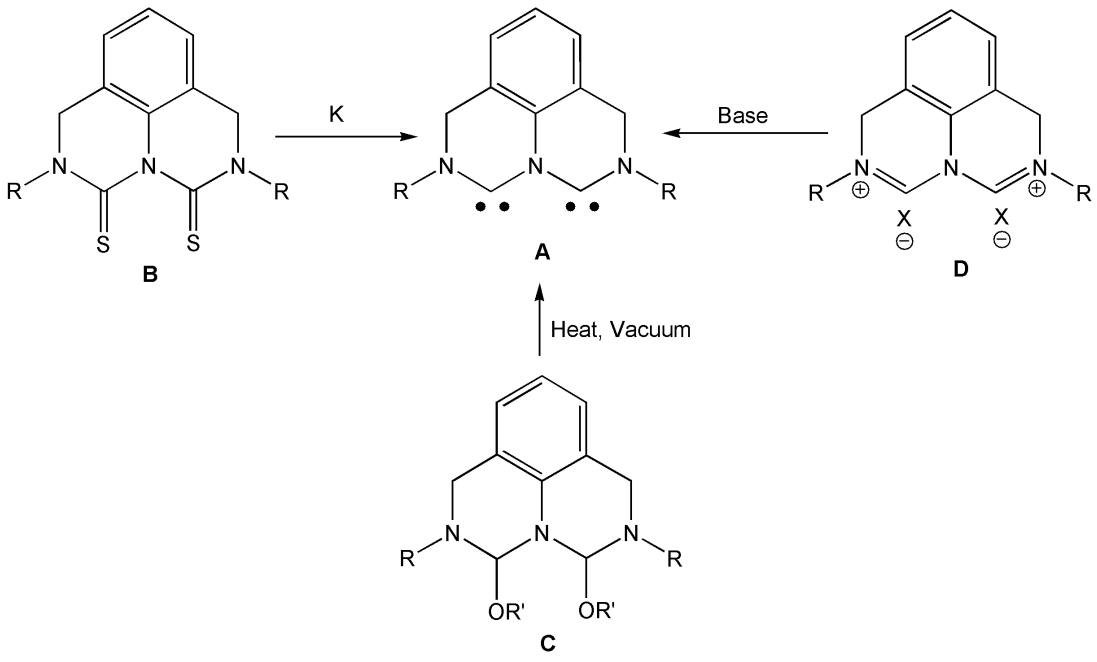

*Scheme 2.1. Plausible synthetic routes to form proposed TADC, **A***

Given the methods previously discussed to form NHCs, the targeted dicarbene **A** could be synthesized from dithiobiuret **B**, 2,4-dialkoxy-N-aminomethylformaminal **C**, or diformamidinium dication **D** (Scheme 2.1). Dithiobiuret is a known functionality with

the most straightforward synthesis; however, the conditions for desulfurization are quite harsh, requiring high temperatures or lengthy reaction times (up to 20 days).[18] If the dicarbene was stable for only a short period of time or at low temperatures, then this methodology would be ineffective. The 2,4-dialkoxy-N-aminomethylformaminal group is an unknown functionality, and its synthesis could prove problematic. Additionally, heat is necessary to induce the loss of alcohol, which increases the likelihood of dicarbene decomposition. The diformamidinium dication is also an unknown functionality, and its synthesis could be challenging. However, unlike the previous two options for preparing TADC **A**, there are a number of methodologies to convert a formamidinium cation to a carbene, such as deprotonation with a strong base or basic ligand on a transition metal complex. Because of the numerous pathways available for transformation of a formamidinium cation into a carbene, a molecule containing a diformamidinium dication moiety was chosen for the first attempted synthesis.

No matter which method is used to prepare the proposed dicarbene (deprotonation, thermolysis, or desulfurization), it is necessary to synthesize a triamine precursor where the 'outer' amines are secondary and the center amine is primary (**E**, Scheme 2.2).

This can be accomplished via reduction of the nitro-diamide, **F**. The nitro-diamide can be synthesized by condensation of the corresponding nitro-diacid chloride with a primary amine. Oxidation of 2,6-dimethyl-nitrobenzene, **G**, to 2-nitro-isophthalic acid, followed by chlorination, would provide the nitro-diacid chloride. This synthetic method has the advantage of using simple, well-known organic transformations, while still allowing the R groups on the 'outer' amines to be easily changed as needed.

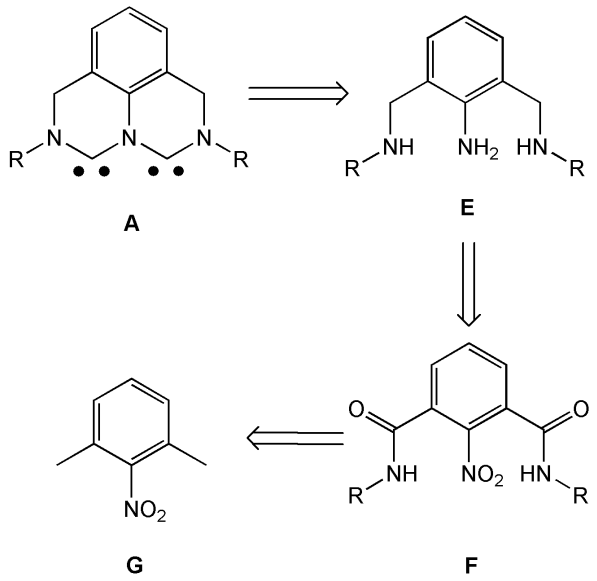

*Scheme 2.2. Retrosynthetic analysis of TADC, **A***

Synthesis of 1,3,5-Triamines

The synthesis started with oxidation of 2,6-dimethylnitrobenzene with $KMnO_4$ in water to afford 2-nitroisophthalic acid, **1** (Scheme 2.3). This was then suspended in 1,1,2,2-tetrachloroethane and combined with excess thionyl chloride.[52] This mixture was heated to reflux for 5 hours, resulting in a clear solution that provided the diacid chloride (**2**) as colorless crystals upon cooling to -40°C. Via solid addition funnel, **2** was then added to an ice-cooled solution of primary amine (isopropyl amine for **3a**, mesityl amine for **3b**, and *tert*-butyl amine for **3c**) in CH_2Cl_2, forming the diamides, **3a-c**, as precipitates in quantitative yield. These were then reduced to the corresponding anilines, **4a-c**, via hydrogenation with 10% palladium on carbon. The reduction of **4b** to the triamine, **5b,** was accomplished via reduction with $LiAlH_4$ in refluxing 1,4-dioxane. When the same conditions were applied to **4a** or **4c**, only starting material was recovered. Additionally, treatment of **4a** or **4c** with BH_3•THF, $Zr(BH_4)_4$[53] or catalytic reduction using ruthenium

carbonyl and silanes[54], did not result in the formation of the triamine. However, when **4a** or **4c** were treated with $NaAlH_2(OC_2H_4OCH_3)_2$ (Red-Al®) in refluxing diglyme, the triamines **5a** or **5c** were afforded in good yield (75% and 89%, respectively).

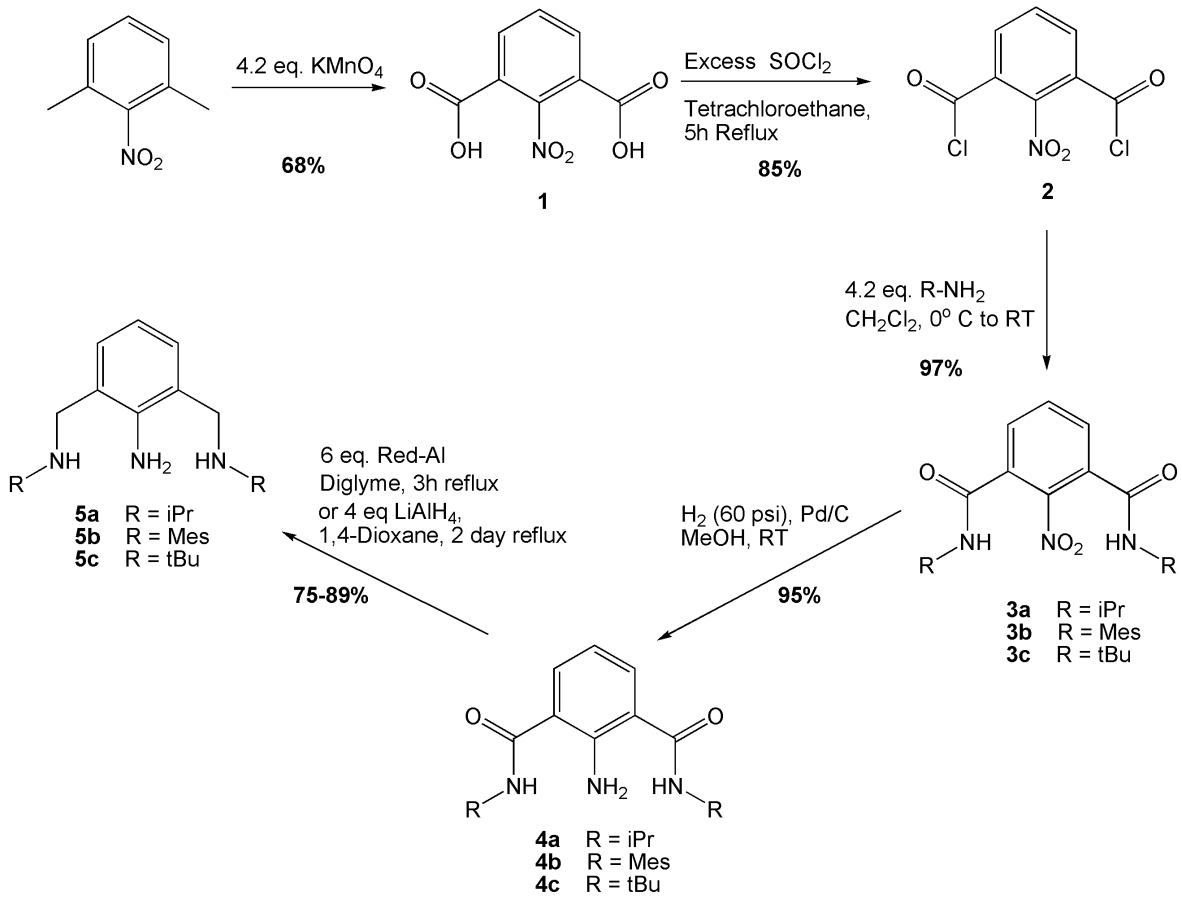

*Scheme 2.3. Synthesis of triamines **5a-c** from 2,6-dimethylnitrobenzene*

Cyclization of 1,3,5-Triamines

Formamidinium salts are usually formed by heating a diamine with a trialkylorthoformate ($CH(OR)_3$) and a proton source, often an ammonium salt. When this methodology was applied to **5a**, only oligomers were formed, as shown by electrospray ionization mass spectrometry (ESI-MS) (Scheme 2.4). However, if [**5a**][HBF_4]$_2$ was

used, the tricyclic diformamidinium salt, **7a**, was formed, albeit in low yield (22%). The same methodology using [**5a**][HCl]$_2$ or [**5a**][TsOH]$_2$ resulted in the formation of a complex mixture or the dicyclic dication [**6a**][HOTs]$_2$, respectively.

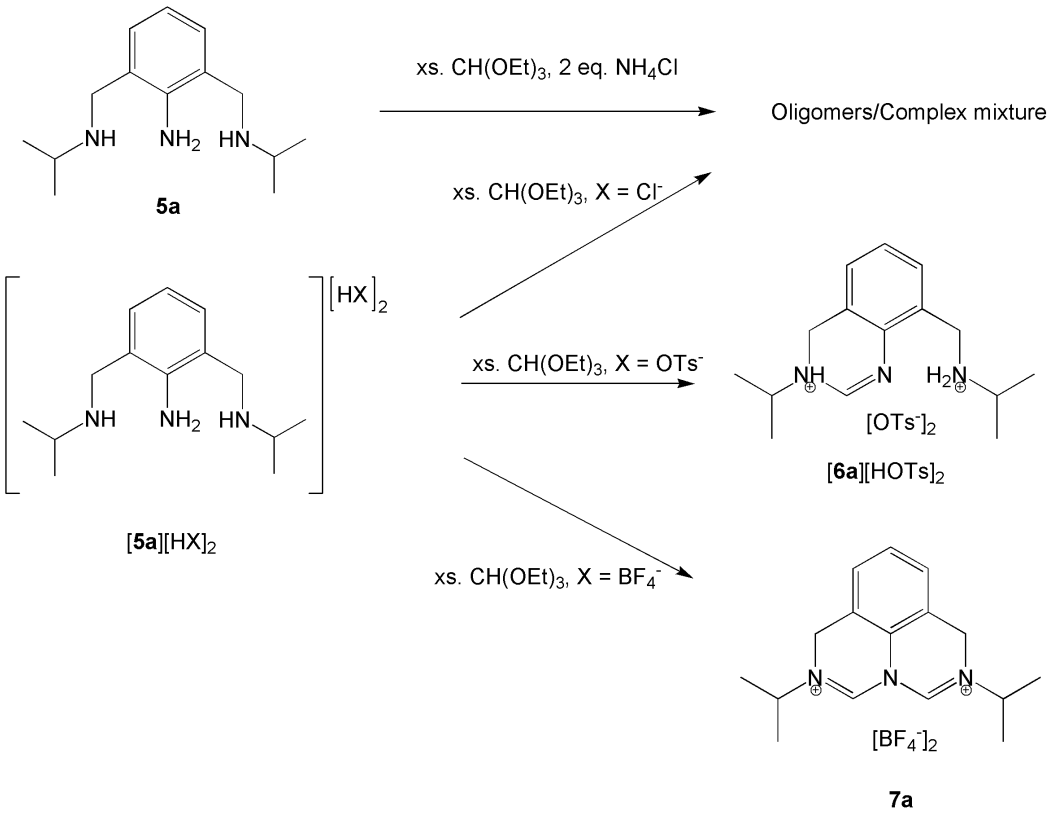

*Scheme 2.4. Attempted cyclizations of triamine **5a***

A different route to formamidinium salts uses formamidinium exchange to create the desired product. The reagent most commonly used is *N,N,N',N'*-tetramethylformamidinium chloride. When **5a** and two equivalents of this reagent were refluxed overnight in acetonitrile (Scheme 2.5), a yellow oil was formed. ^{1}H NMR spectroscopy showed a non-C_2 symmetric molecule, consistent with a monocyclized product, [**6a**][HCl].

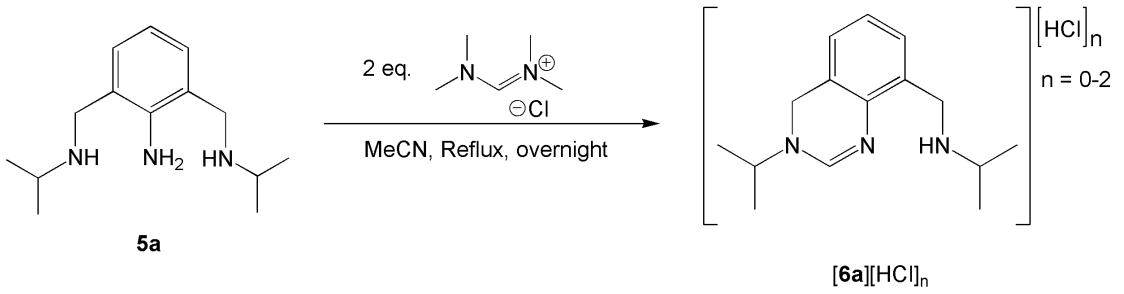

*Scheme 2.5. Reaction of triamine **5a** with N,N,N',N'-tetramethylformamidinium chloride*

Less commonly used cyclization reagents are the cyclic oxonium tetrafluoroborate salts that can generate formamidinium salts. The oxonium reagents were synthesized by the reaction of a diol with trimethylorthoformate ($CH(OMe)_3$) to form the cyclic orthoester (Scheme 2.6).[31] Treatment with tetrafluoroboric acid etherate or boron trifluoride etherate eliminated methanol or trimethylborate, respectively, forming the oxonium salts $\mathbf{Ox_a}$ and $\mathbf{Ox_b}$.

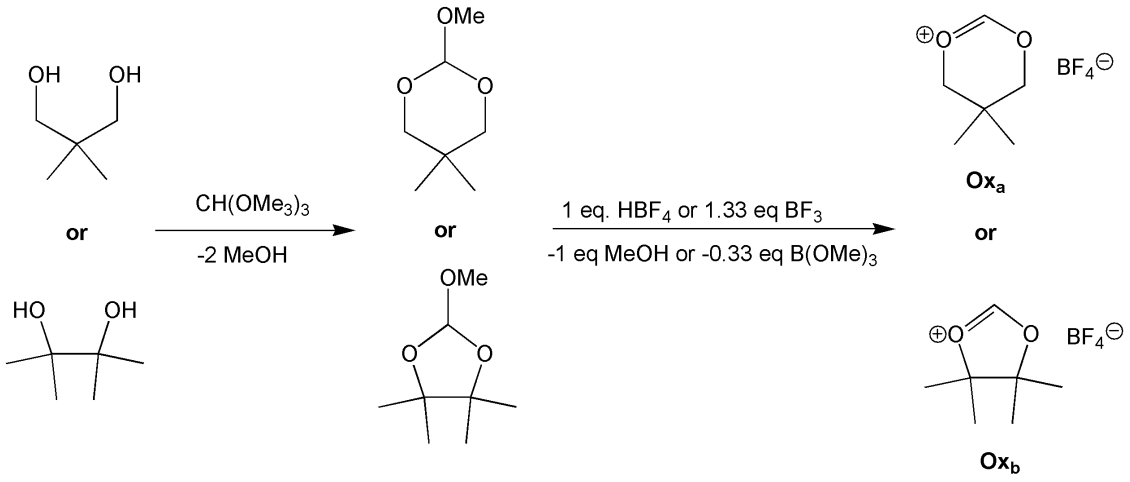

Scheme 2.6. Synthesis of oxonium salts from diols

Addition of two equivalents of $\mathbf{Ox_a}$ to **5b** at room temperature in methylene chloride precipitated a 9:1 mixture of [**6a**][HBF_4]$_2$ and **7a** (Scheme 2.7). At low

temperature (-78ºC), the product ratio was unaltered, while at elevated temperature (40ºC), almost no **7a** was produced. Stepwise cyclization was also studied; addition of one equivalent of $\mathbf{Ox_a}$ to **5a** led to [**6a**][HBF_4] in excellent yields (92%). The reaction of [**6a**][HBF_4] with an additional equivalent of $\mathbf{Ox_a}$ gave the same 9:1 mixture of [**6a**][HBF_4]$_2$ and **7a**. If an excess of $\mathbf{Ox_a}$ (five equivalents) was used, an intractable mixture of $\mathbf{Ox_a}$, [**6a**][HBF_4]$_2$, and **7a** was formed. Changing the solvent from methylene chloride to acetonitrile resulted in the production of only trace quantities of **7a**. Treatment of **5a** with two equivalents of $\mathbf{Ox_b}$ produced [**6a**][HBF_4]$_2$ exclusively.

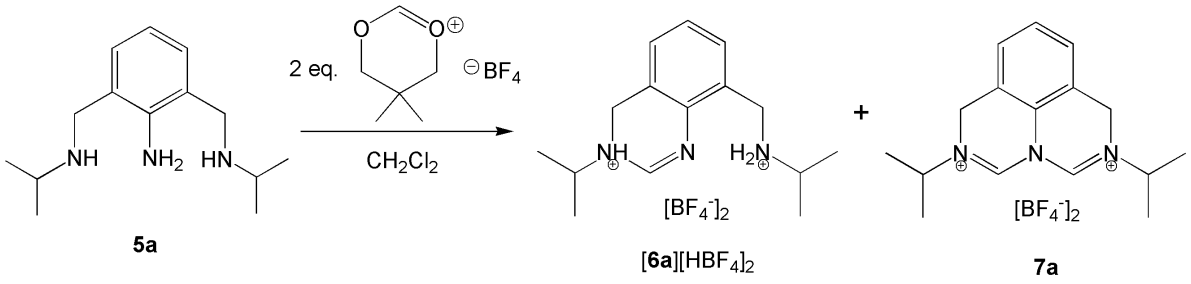

*Scheme 2.7. Reaction of triamine **5a** with oxonium salt $\mathbf{Ox_a}$*

Next, acyclic oxonium salts were employed, with mixed results (Scheme 2.8). Addition of two equivalents of dimethyl oxonium ($\mathbf{Ox_c}$) to **5a** formed less of the desired tricyclic product, **7a,** compared to that formed with reaction with $\mathbf{Ox_a}$ **(**a 12:1 mixture of [**6a**][HBF_4]$_2$ to **7a**). However, diethyl oxonium ($\mathbf{Ox_d}$) and diisopropyl oxonium ($\mathbf{Ox_e}$) gave mixtures enriched in **7a** ([**6a**][HBF_4]$_2$:**7a** = 4:1). When an excess of $\mathbf{Ox_d}$ was used, **7a** was formed in minor amounts, along with [**6a**][HBF_4]$_2$, and, based on ^{1}H NMR spectroscopy, an N-ethylated **6a**. Most researchers avoid acyclic oxonium salts for the production of formamidinium moieties, as they are also very potent alkylating reagents.

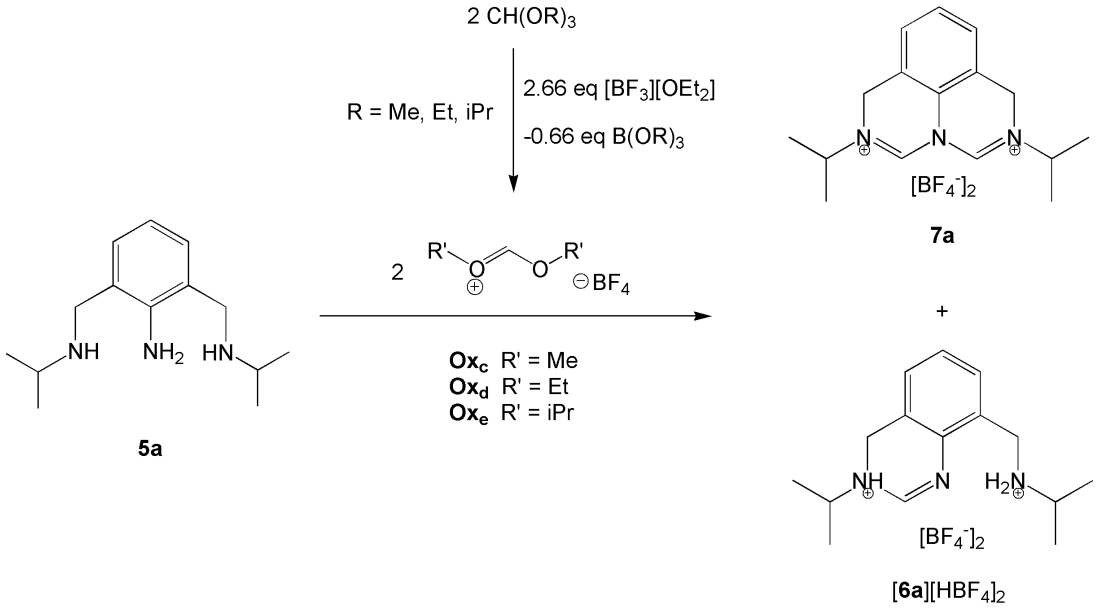

*Scheme 2.8. Reaction of triamine **5a** with acyclic oxonium salts*

Separation of [**6a**][HBF_4]$_2$ and **7a** was difficult because they have very similar solubilities. However, when triethylamine (TEA) was added to a suspension of [**6a**][HBF_4]$_2$ and **7a** in methylene chloride, [**6a**][HBF_4] was formed and dissolved, leaving **7a** as the only precipitate. While this allowed for the isolation of pure **7a**, the yields were very poor because the mixtures from the reaction of **5a** and oxonium salts contained only small quantities of **7a**.

Fortunately, it was found that sequential cyclization of **5a** using $\mathbf{Ox_a}$ and then trimethyl orthoformate led to **7a** in good yield. First, **5a** was treated with one equivalent of the cyclic oxonium salt $\mathbf{Ox_a}$, followed by one equivalent of tetrafluoroboric acid etherate, resulting in [**6a**][HBF_4]$_2$. This was then refluxed in acetonitrile with excess trimethylorthoformate, forming **7a** in 72% yield. This methodology was also used to synthesize **7b-c.**

A single crystal of **7a** was grown by diffusion of toluene into a concentrated solution in acetonitrile at room temperature and studied by X-ray diffractometry. The molecule is planar, with all carbon and nitrogen atoms co-planar except for the methyls on the isopropyl R groups. Unlike other formamidinium salts, the carbenic carbon-nitrogen bond distances are not equal. For example, Alder, *et al.*, published a structure of a six-membered-mono-formamidinium salt that had N(1)-C(1) and N(2)-C(1) bond distances both equal to 1.311(3) Å (Figure 2.2).[9] In the structure of **7a,** the bond lengths alternate, with N(1)-C(1) equal to 1.285(3) Å, while N(2)-C(1) is equal to 1.355(3) Å (the same is true for N(2)-C(2) and N(3)-C(2)) (Figure 2.3). This is presumably because of the electrostatic repulsion of the two cations, forcing more of the cationic character to be on the outer nitrogens. Concordantly, there is more double bond character in the

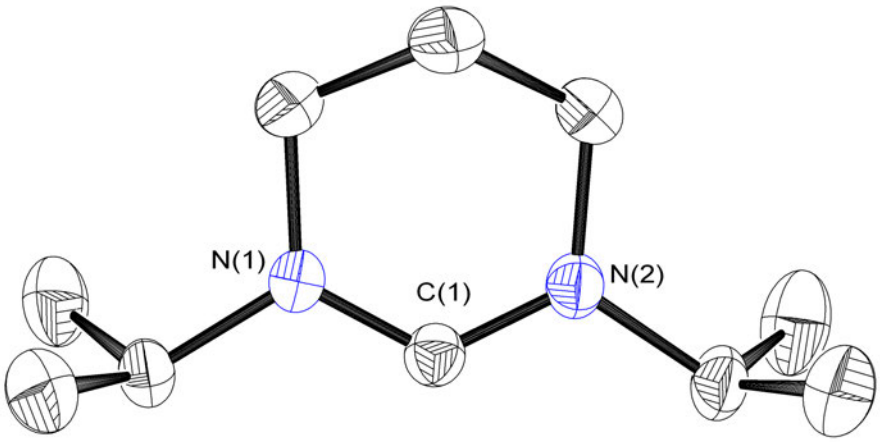

Figure 2.2. Solid-state structure of a six-membered mono-formamidinium salt by Alder, et al.[9] *(hydrogens and BF_4^- omitted for clarity)*

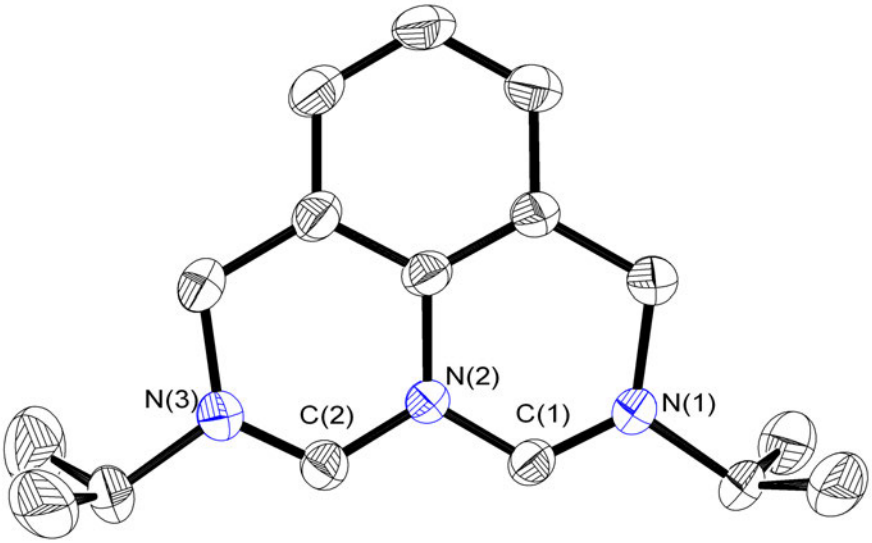

*Figure 2.3. Solid-state structure of **7a** (hydrogens and BF_4^- omitted for clarity)*

N(1)-C(1) and N(3)-C(2) bonds, shortening them. The distance between C(1) and C(2) is 2.32 Å, which is an appropriate distance to bridge two transition metal-metal multiple bonds and should not lengthen much when deprotonated to form the TADC.

Synthesis of TADC

With the diformamidinium dications, **7a-c,** in hand, we next set out to synthesize the free dicarbene. The first and majority of the attempts to synthesize a TADC used **7a** as a starting material. Because the proposed TADC would be non-aromatic, strong, non-nucleophilic bases were tried. To make isolation and detection easier, the TADC would be trapped as a dithiobiuret by reaction with sulfur after deprotonation with a base (Scheme 2.9). The first base tried was lithium diisopropylamide (LDA, made as a 0.5 M solution in hexanes, which is stable for a week at room temperature). Reaction of **7a** with two equivalents of LDA at -78 ºC in toluene, followed by reaction with excess sulfur, resulted in the formation of a non-C_2 symmetric molecule (by ^{1}H NMR spectroscopy),

which is consistent with deprotonation at a position other than the carbenic carbon (Scheme 2.9). Additionally, ESI-MS showed no nucleophilic addition products.

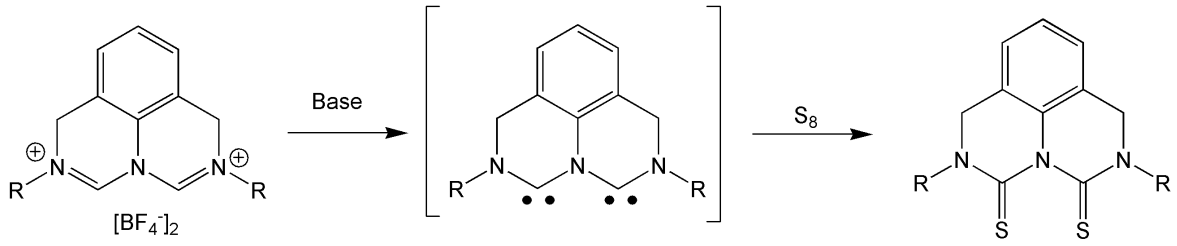

Scheme 2.9. Proposed method for detecting TADC formation

Deprotonation at undesired positions has been seen in other NHCs with acidic C-H bonds, most notably methylene-bridged bis(NHC)s.[23] In those literature cases, it was found that the weaker base potassium hexamethyldisilylazide (KHMDS) led to the desired product. When two equivalents of KHMDS were reacted with **7a** at -30 ºC in toluene, dimers and trimers of the TADC were formed as seen by ESI-MS (*vide infra*). n-Butyl lithium (two equivalents, 2.5 M in hexanes) was then used to deprotonate **7a** at -78 ºC (Table 2.1). ^{1}H NMR spectroscopy showed a non-C_2 symmetric molecule and the addition of a butyl group, which is consistent with nucleophilic addition instead of deprotonation. Similar results were seen when potassium *tert*-butoxide (KO^{t}Bu) was used. This is not surprising, given that formamidinium salts are known to react with KO^{t}Bu to form 2-tert-butoxy formaminals (Scheme 1.19).

Lithium triethylborohydride (also known as Super-Hydride®) has been used to deprotonate imidazolium salts and form air- and moisture-stable NHC-triethylborane adducts.[55] In these adducts, the triethylborane is labile, providing the free NHC when heated. However, when **7a** was reacted with two equivalents of lithium

triethylborohydride in THF, it was reduced to the corresponding 3,9-diazajulolidine derivative instead of being deprotonated at the carbenic carbons (Scheme 2.10)

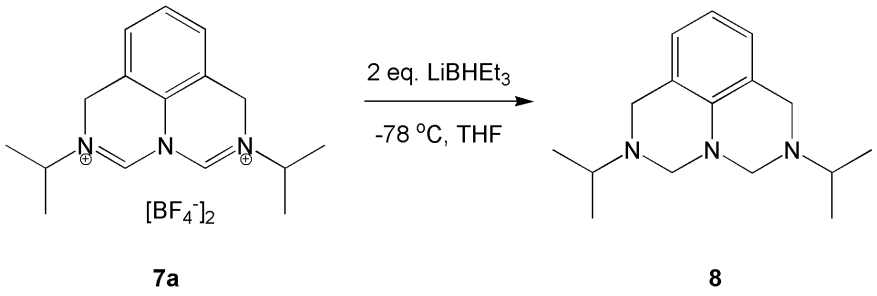

*Scheme 2.10. Reaction of **7a** with $LiBHEt_3$*

Reaction of **7a** with two equivalents of LiHMDS at low temperatures (0 ºC and -78 ºC) resulted in little to no reaction (Scheme 2.11). At room temperature, reaction with two equivalents of LiHMDS formed a TADC dimer, with trace amounts of trimer and tetramer seen by ESI-MS (*vide infra*).

Base	Solvent	Reaction time	Temperature	Trapping reagent	Results
2 eq LDA	Toluene	30 min.	-78 ºC	Sulfur	Asymmetric molecule, likely deprotonation at benzylic position
2 eq KHMDS	Toluene	30 min.	-30 ºC	Sulfur	Dimer, trimer formed
2 eq n-BuLi	Hexane	5 min.	-78 ºC	Sulfur	Nucleophilic addition
4 eq KOtBu	C_6D_6	overnight	RT	none	Nucleophilic addition
2 eq $LiBHEt_3$	THF	2 hours	-78 ºC	none	Reduction to **8**
2 eq LiHMDS	C_6D_6	5 hours	RT	none	Dimer formed
5 eq LiHMDS	C_6D_6	2 hours	RT	none	**9a** formed
4 eq LiHMDS	Toluene	4 hours	0 ºC	none	Almost no reaction/very little **9a** formed
2 eq LiHMDS	Toluene	2 hours	-78 ºC	Sulfur	No reaction

*Table 2.1. Summary of the reactions of **7a** with various bases and conditions (RT = room temperature)*

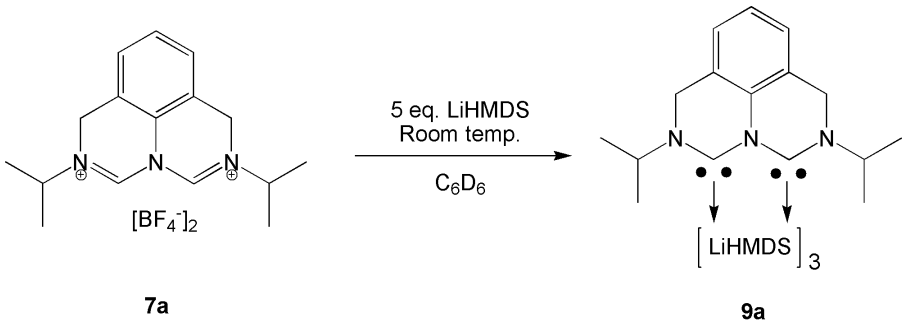

7a **9a**

*Scheme 2.11. Reaction of **7a** with LiHMDS*

However, when five equivalents of LiHMDS were used, the TADC **9a** formed. ^{1}H NMR spectra showed a C_2 symmetric molecule with three coordinated LiHMDS molecules. The coordinated LiHMDS ligands were inequivalent, resulting in two broadened signals in a 1:2 ratio. The ^{13}C NMR resonance for the carbenic carbons was δ232 in C_6D_6 (Figure 2.4). This is slightly lower that what is expected for NHCs that are in a six-membered ring (δ236-244).[56] This lower chemical shift is likely from coordination of Li^+ to the carbene, which is known to shift the ^{13}C NMR resonances of carbenes upfield. The ^{13}C NMR resonance for the carbenic carbons of **9a** is also very broad (≈ 20 Hz). A possible explanation for this is quadrapolar coupling to lithium (^{6}Li is spin 1 and ^{7}Li is spin 3/2). However, a more likely explanation is that **9a** is fluxional in solution, with the bound LiHMDS quickly exchanging. This is evidenced by the signals corresponding to the bound LiHMDS being broad as well.

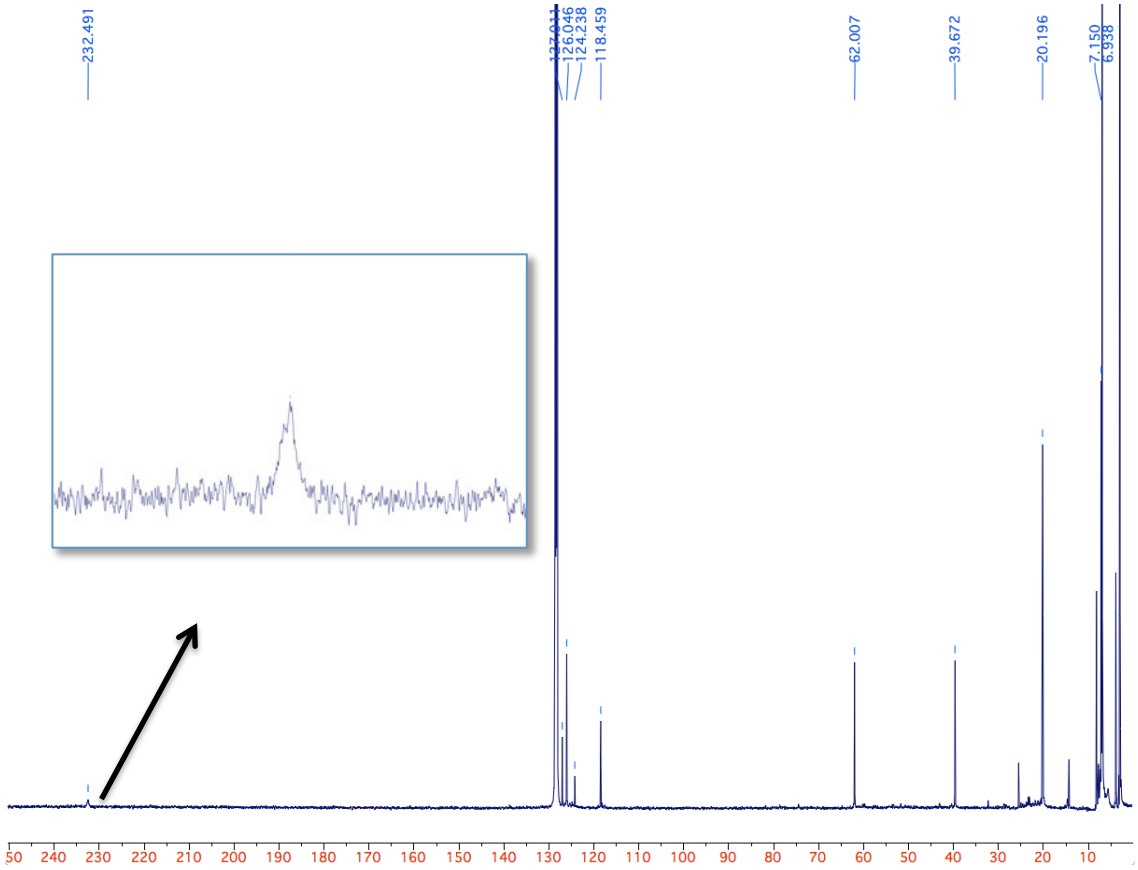

*Figure 2.4. ^{13}C NMR spectrum of **9a***

To confirm that a TADC had been formed, **9a** was reacted with excess sulfur, forming the dithiobiuret, **10a** (Scheme 2.12), as shown by ^{1}H NMR and ^{13}C NMR spectra and ESI-MS.

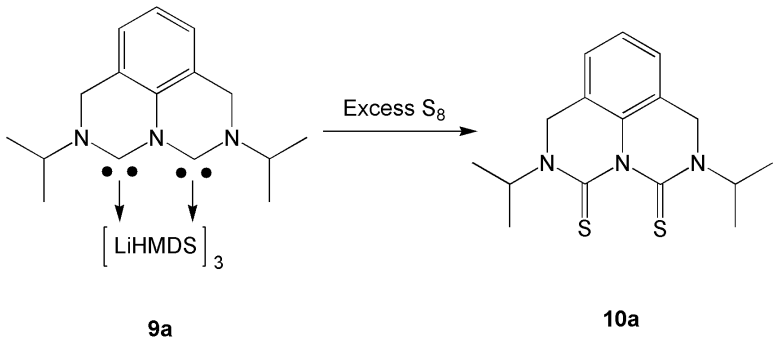

*Scheme 2.12. Reaction of **9a** with sulfur to form the dithiobiuret, **10a***

Given that LiHMDS is known to react with many metal halides, it would be advantageous to isolate the 'free' TADC in order to avoid unwanted side reactions. The crown ether 12-crown-4 is known to de-lithiate NHCs, providing 'free' NHCs.[9] When three equivalents of 12-crown-4 were added to **9a** at room temperature, a dimer was very quickly formed (< 1 minute) (Scheme 2.13). Treating **9a** with THF at room temperature produced the same result.

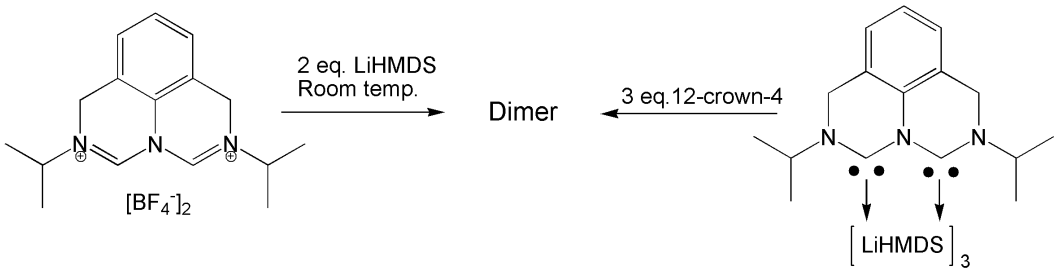

Scheme 2.13. Routes to the TADC dimer

This dimer is identical to the one formed from the reaction of **7a** and two equivalents of LiHMDS as shown by NMR spectroscopy and ESI-MS. Forming the dimer via two equivalents of LiHMDS is preferred in order to avoid the presence of 12-crown-4 signals in the NMR spectra. On the basis of ESI-MS data, this dimer also appears to be the same product that was formed from reaction of **7a** with two equivalents of KHMDS. The ^{13}C NMR spectrum of the dimer in C_6D_6 (Figure 2.8, page 43) contained at least 32 signals, which is consistent with dimerization in an asymmetric fashion, making all the carbons inequivalent. Additionally, there was a ^{13}C NMR resonance at δ 236, consistent with an NHC that is part of a hexahydropyrimidine ring. When sulfur was added to the dimer, the pseudomolecular ion shown by ESI-MS shifted from *m/z* 529 (consistent with 2 x **9a** + H_2O+H^+) to *m/z* 543 (consistent with 2 x **9a** + S

$+H^+$). Though NHCs are well known for dimerizing to form ene-tetraamines, the high degree of asymmetry and the presence of a residual carbene site in the product ruled out the possibility of **9a** dimerizing to a di-ene-hexaamine.

Analysis of TADC Dimer

In order to identify the structure of the dimer, several different NMR experiments were performed, as summarized in Table 2.1. In a ^{13}C DEPT135 NMR experiment, resonances for -CH and $–CH_3$ units appear as positive signals, while those corresponding to CH_2's show up as negative signals, and non-protonated carbons show no signal. The ^{13}C DEPT135 spectrum of the dimer (Figure 2.9, page 44) showed twenty-one positive signals and only three negative signals. By comparing these data to the ^{13}C NMR spectrum, it is possible to deduce that there must be eight non-protonated carbons. The dimerization of **9a** should produce four CH_2's and ten non-protonated carbons, given that all carbons are inequivalent, as is indicated by the ^{13}C NMR spectrum. The missing $-CH_2$ resonance indicates that one of the benzylic positions has either gained or, more likely, lost a proton. The loss of two non-protonated positions likely indicates that each of the carbenic carbons has added a proton.

Next, a set of three 2D NMR experiments were performed. These included Correlation Spectroscopy (COSY), which shows ^1H-^1H through-bond (*J*-coupling) correlations (Figure 2.10, page 45), Heteronuclear Single-Quantum Correlation (HSQC), which shows one-bond correlations between directly-bonded ^1H and ^{13}C nuclei (Figure 2.11, page 46), and Heteronuclear Multiple-Bond Correlation (HMBC), which shows long-range (two- to four-bond) correlations between ^1H and ^{13}C nuclei (Figure 2.12, page

47). Analysis of these data indicated that much of the structure of the two **9a** units remained intact, as signals were clearly present corresponding to four isopropyl units, two 1,2,3-trisubstituted benzene rings, and three benzylic -CH_2's. After assigning most of the ^{1}H NMR resonances to these moieties, it was noted that there was one more proton resonance than expected for a dimer of **9a**. These reactions were performed in C_6D_6, which precluded the possibility that an extra proton might have been abstracted from the solvent.

Another possibility is that the dimer added an equivalent of HMDS by insertion into the N-H bond by one of the carbenes. Alder, *et al.* demonstrated this reaction for a six-membered ring NHC by ^{13}C NMR spectroscopy, which showed that the six-membered ring NHC (δ 236) was in equilibrium with the HMDS adduct (δ 91.6) (Scheme 2.14).[57] In the ^{13}C NMR spectrum of the **9a** dimer, there is a CH resonance at δ 90.1 that suggests an analogous addition of HMDS. Additionally, upon closer

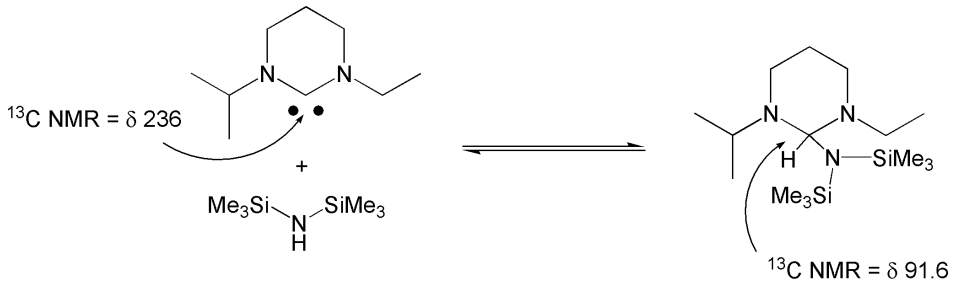

Scheme 2.14. The reversible addition of HMDS to a six-membered NHC[57]

inspection of the ESI-MS data for the dimer after reaction with sulfur, an ion of low intensity was observed at *m/z* 704, which would be consistent with 2 x **9a** + HMDS + S + H^+. Reanalyzing the sample by high-resolution ESI-MS gave an *m/z* value of 704.4351 (expected for $C_{38}H_{62}N_7Si_2S$: 704.4326), which corresponds to the expected elemental

composition for such an ion and confirms that the dimer had indeed reacted with HMDS. The *m/z* 543 ion presumably arises from a facile loss of $HMDS^-$ from this species.

With most of the structural fragments of the dimer now assigned, HMBC correlations were used to piece them together, leading to proposal of **11** as the likely structure of the dimer. A summary of the most important HMBC correlations is shown in Figure 2.6. All of the correlations shown are fully consistent with the proposed structure. A particularly useful HMBC correlation of previously unassigned signals H-20 (δ_H 7.17, s) and C-12 (δ_C 137.5, s) established the connection between the two **9a-**derived subunits via an unusual enetriamine linkage as shown. Unfortunately, there is a paucity of NMR data for enetriamines in the literature, so direct comparisons of the chemical shift values with assignments for similar compounds was not possible. Even so, the ^{13}C NMR chemical shift assigned to C-13 is δ 137.5, which is only slightly upfield from what is expected for enetetraamines (≈δ141-144). The ^{13}C NMR chemical shift assigned to C-20 is δ 111, which is considerably upfield from the expected chemical shift of an eneamine (≈δ135-142), but this difference is consistent with the C12-C20 olefin unit being in conjugation with N-11 and N-13, which donate electron density to C-20 by resonance, moving its ^{13}C NMR signal significantly upfield. The configuration about the C-20-C-12 and C-31-N-32 double bonds has not yet been determined, however this could be accomplished by NOESY (^1H-^1H through-space coupling) analysis.

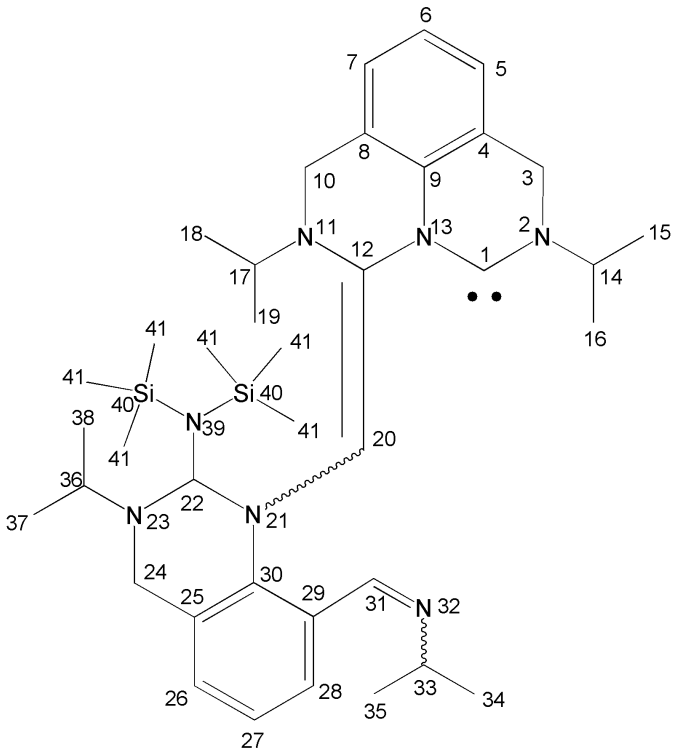

*Figure 2.5. Proposed structure of dimer **11***

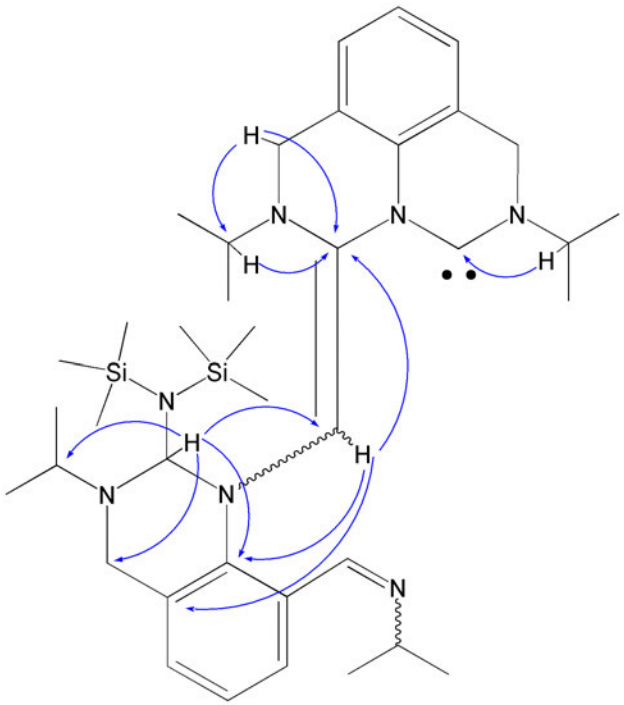

*Figure 2.6. Selected HMBC correlations in dimer **11***

Position	δ_C[a]	δ_H, mult (*J* in Hz)	COSY	HMBC
1	236.2			
2-N				
3	42.6	3.65, m	5, 7	
4	120.2			
5	124.1	6.54, d (7.5)	6	3, 7, 9
6	123.0	6.75, t (7.5)	5, 7	4, 8
7	125.1	6.61, d (7.5)	6	6, 9, 10
8	125.2			
9	130.1			
10	41.9	4.23, d (17) 3.35, d (17)	5, 7	17, 8, 9, 12
11-N				
12	137.5			
13-N				
14	59.5	3.71, m	15, 16	1
15	22.1	1.23, d (6.5)	14	
16	22.0	1.25, d (6.5)	14	
17	52.7	2.99, septet (6.5)	18, 19	12, 10
18	21.5	0.72, d (6.5)	17	
19	21.2	0.82, d (6.5)	17	
20	111.6	7.17, s	22	30, 12, 25
21-N				
22	90.1	5.02, s	20	30, 29, 20, 24, 36
23-N				
24	45.0	3.43, m	26, 28	
25	128.2			
26	126.6	6.90, dd (5.5, 1.5)	27, 28	30, 28, 24
27	118.9	6.82,t (7.5)	26, 28	28, 29
28	128.1	8.20, dd (7, 1.5)	27, 26	31, 30, 26
29	126.0			
30	144.5			
31	158.4	8.90	27, 28	30, 28, 29, 35
32-N				
33	61.5	3.60, m	34, 35	
34	25.1	1.17, d (6.5)	33	
35	24.6	0.90, d (6.5)	33	
36	46.0	3.77, m	37, 38	22, 24, 37
37	14.5	0.88, d (6.5)	36	
38	21.6	1.14, d (6.5)	36	
39-N				
40-Si				
41	3.9	0.27, s		

*Table 2.2. Summary of NMR data for dimer **11** in C_6D_6. [a] The multiplicities of the carbon resonances as determined by DEPT135 are consistent with the assignments*

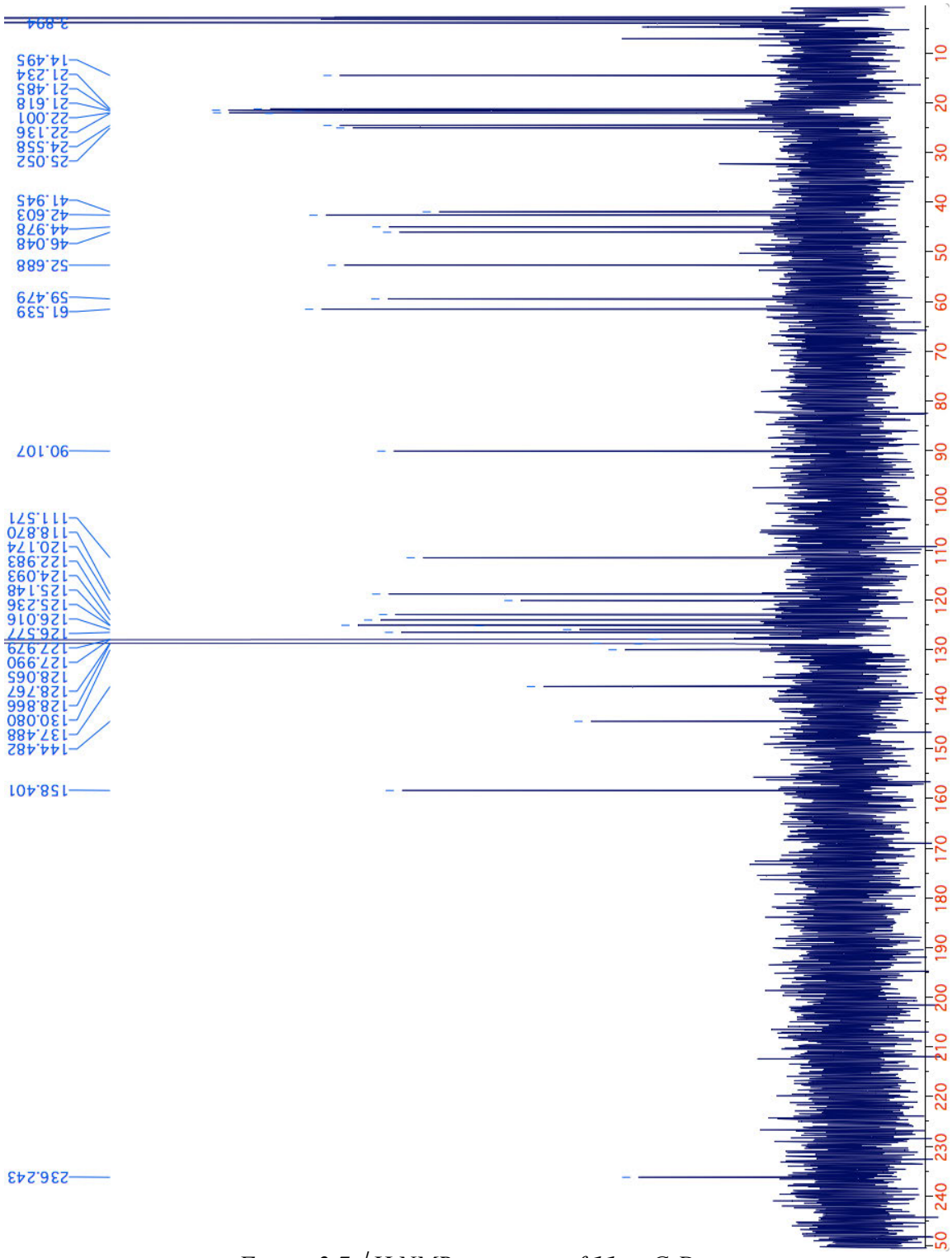

*Figure 2.7. ^{1}H NMR spectrum of **11** in C_6D_6*

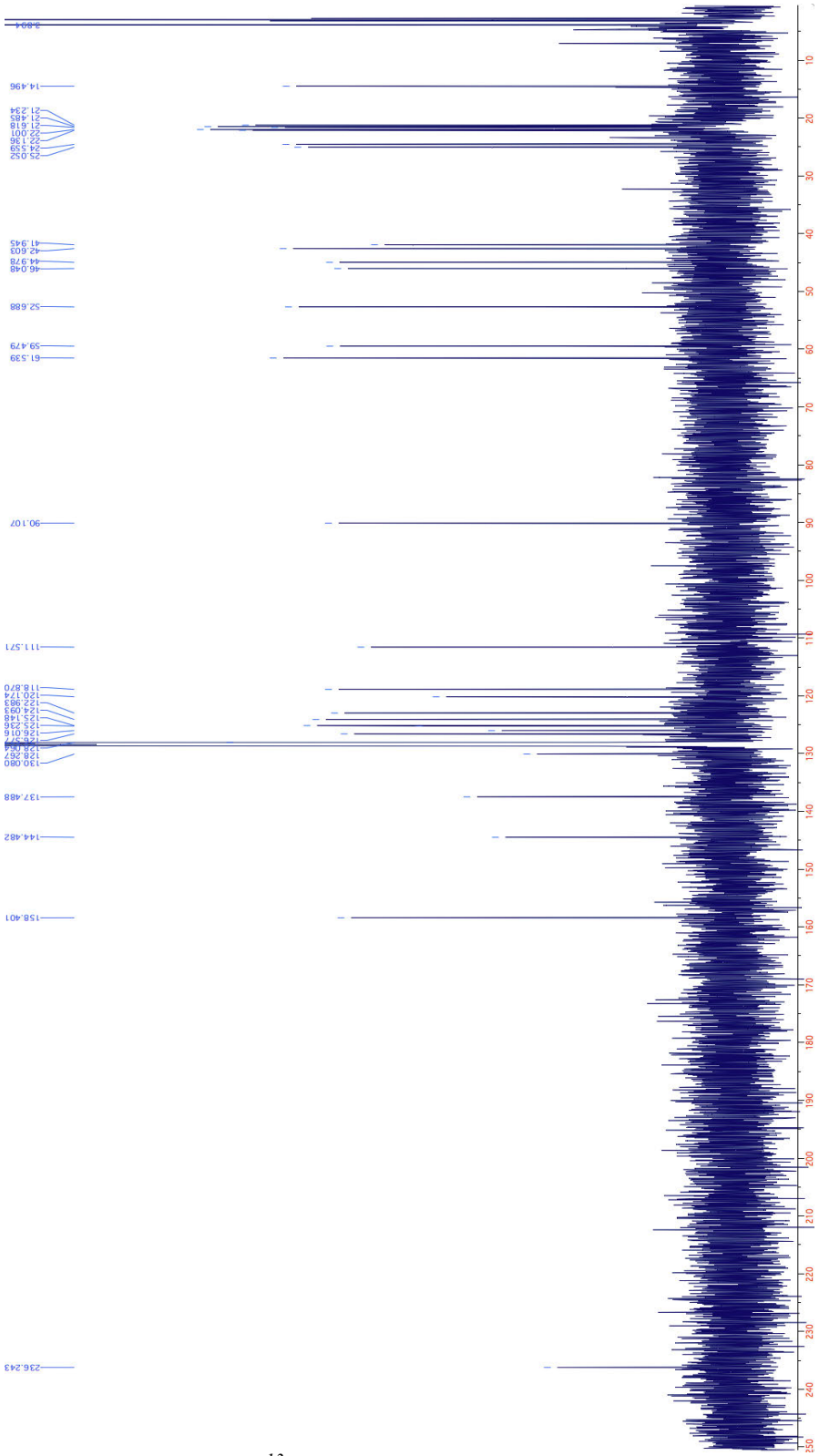

*Figure 2.8. ^{13}C NMR spectrum of **11** in C_6D_6*

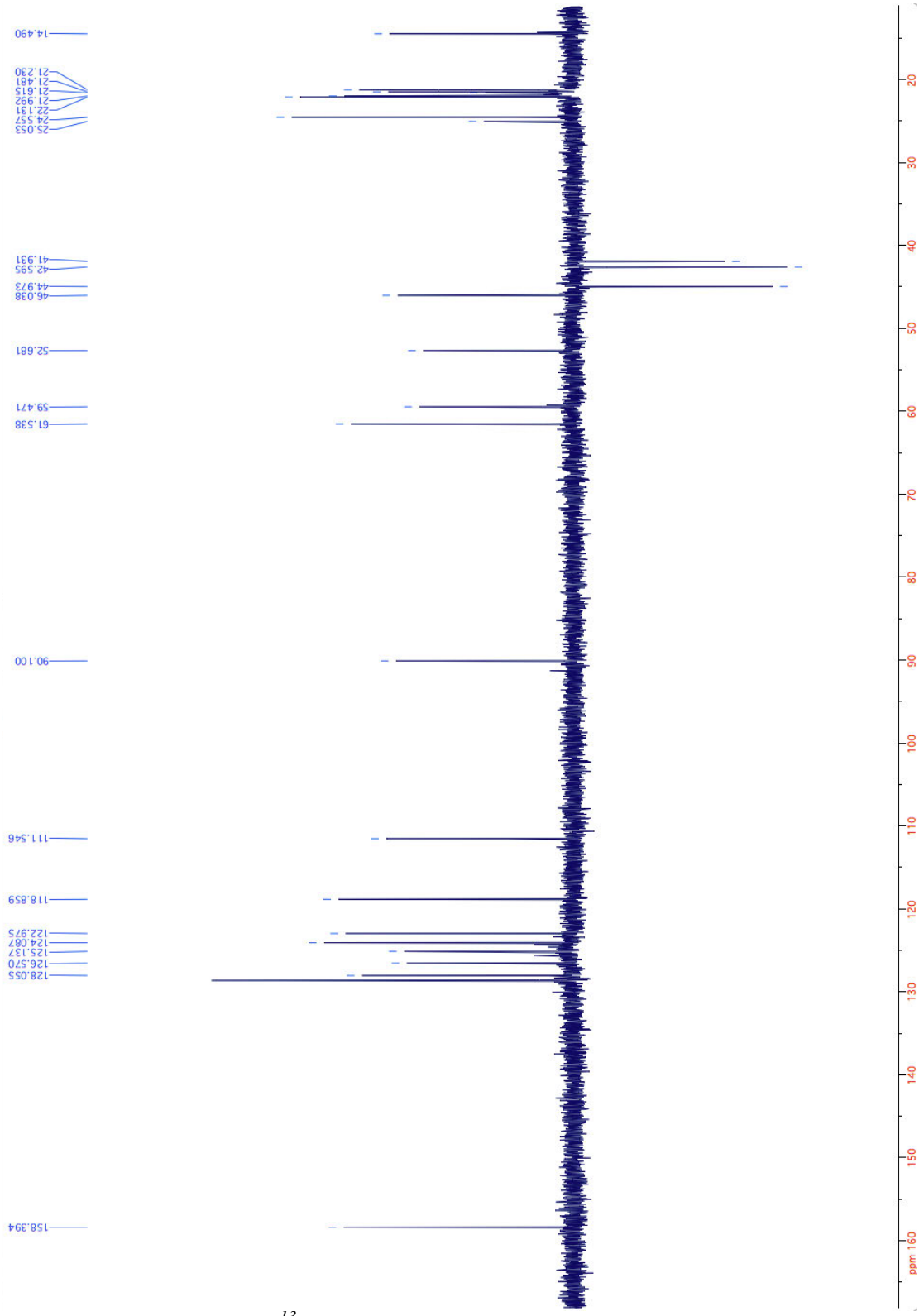

*Figure 2.9. ^{13}C DEPT135 NMR spectrum of **11** in C_6D_6*

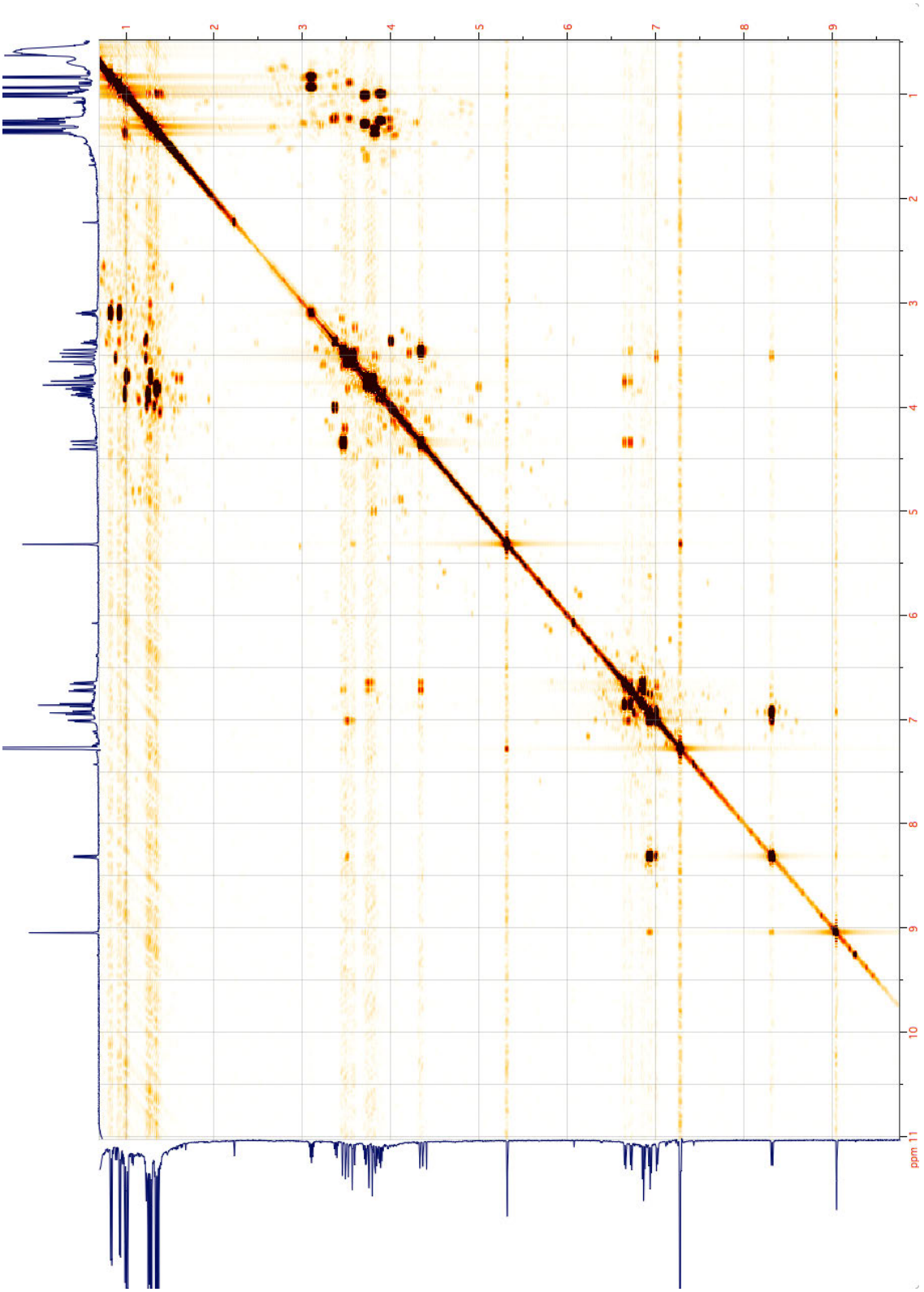

*Figure 2.10. COSY NMR spectrum of **11** in C_6D_6*

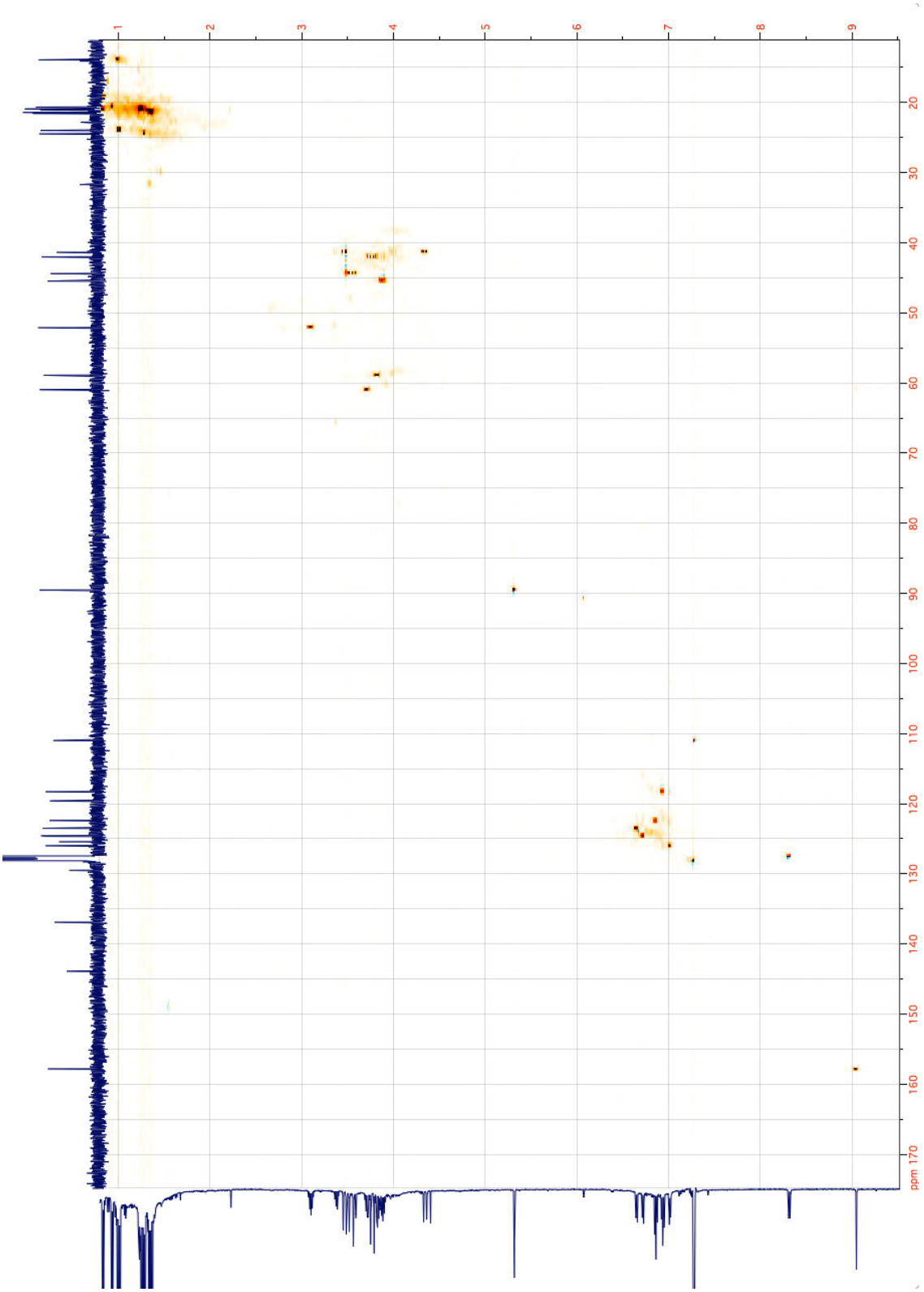

*Figure 2.11. HSQC NMR spectrum of **11** in C_6D_6*

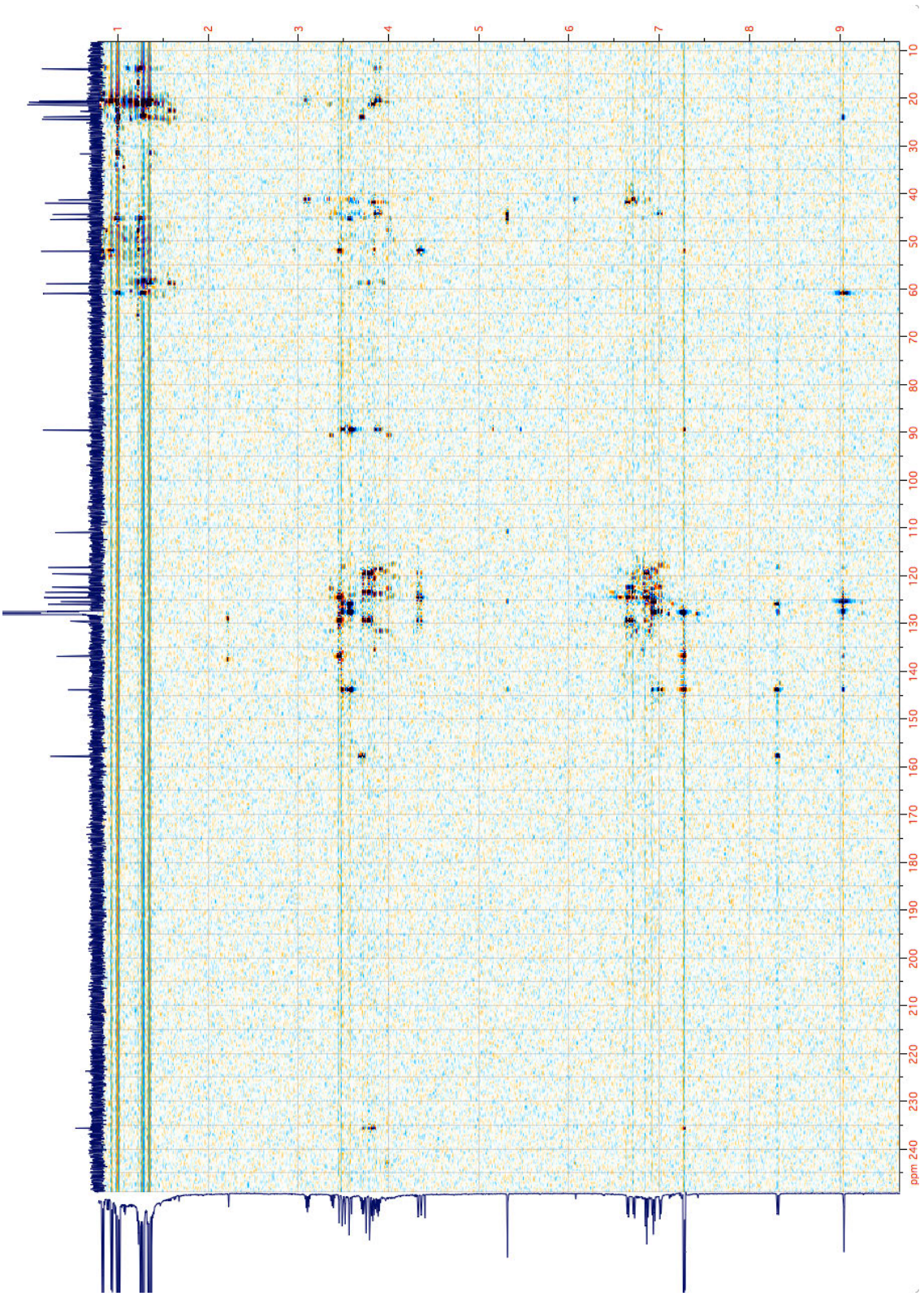

*Figure 2.12. HMBC NMR spectrum of **11** in C_6D_6*

Our proposed mechanism for the formation of **11** begins with the generation of a very sterically-congested ene-tetraamine dimer (Scheme 2.15). This intermediate could then undergo a 1,3-shift of a benzylic proton to one carbon of the ene-tetraamine unit, accompanied by cleavage of the N-C bond, producing the ene-triamine and imine moieties found in **11**. Analogous 1,3-shifts of α-protons to carbenes, coupled with loss of an R-group, have been documented in acyclic diaminocarbenes (ADACs).[58] Next, one of the remaining NHCs adds into the N-H bond of HMDS, forming **11**. If one of the remaining NHCs instead reacted with another molecule of **9a**, it would form a trimer, which has also been observed by ESI-MS.

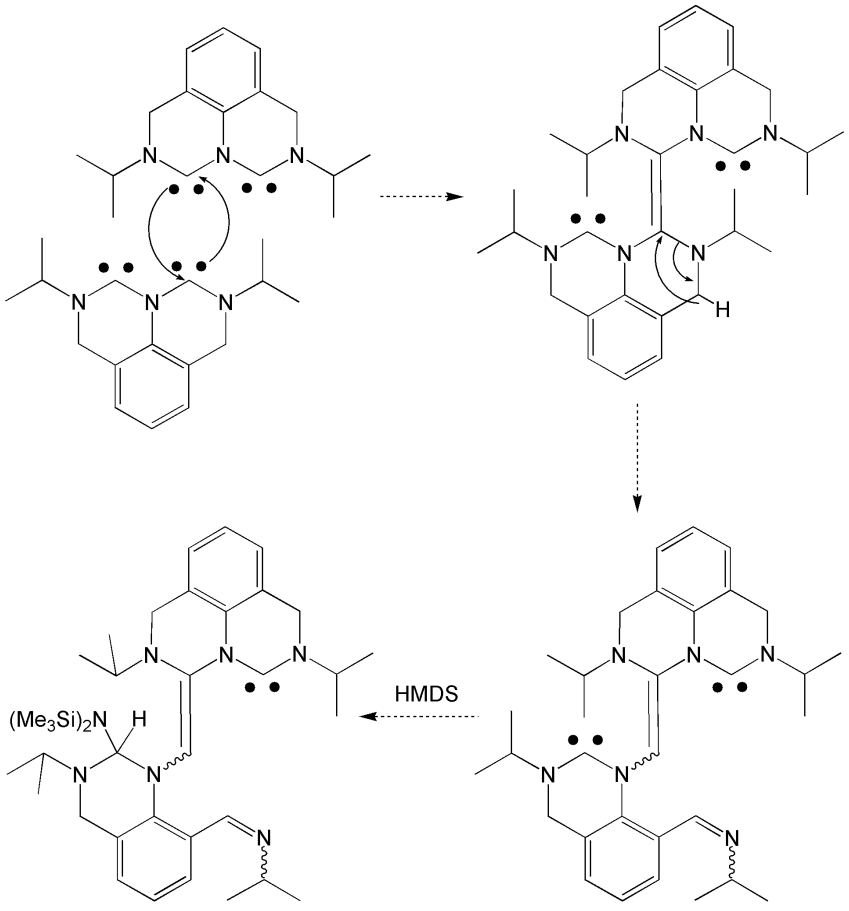

*Scheme 2.15. Proposed mechanism for the formation of **11***

Attempts to Coordinate TADC to a Metal Center

Given that we were unable to isolate a free TADC starting with **7a**, we turned our attention to **7b**, hoping that the larger N-mesityl groups would prevent dimerization. Reaction of **7b** with two equivalents of LiHMDS at room temperature in toluene resulted in a deep purple reaction mixture, which quickly turned brown after one to two seconds. ^{1}H NMR spectroscopy showed an extremely complex reaction mixture with no resonances in the δ8-9 region, indicating that there were no formamidinium cations present. Addition of five equivalents of LiHMDS gave very similar results. Performing this reaction at low temperatures led to very curious color changes. As two equivalents of LiHMDS were added dropwise to a suspension of **7b** in THF at -78 ºC, the reaction quickly turned purple, but by the time all of the LiHMDS was added to the reaction, it had returned to colorless. However, after approximately ten minutes at -78 ºC, the reaction mixture changed back to the same deep purple. After 45 minutes at -78 ºC, the dark purple reaction mixture started to turn brown, at which time excess sulfur was added to trap any carbenes. The ^{13}C and ^{1}H NMR spectra were less complicated than the previous reactions, but still quite complex. The ESI-MS revealed that a dimerization had occurred, showing that the mesityl groups are insufficiently bulky to prevent dimerization.

With the N-mesityl results in hand, it was hoped that an even bulkier R group (in this case tert-butyl) would prevent dimerization, so **7c** was synthesized using the same methodology as **7a-b**. When **7c** was treated with two or five equivalents of LiHMDS at room temperature in toluene, a deep purple solution formed. This solution appeared very

similar in color to when **7b** was treated with LiHMDS. However, unlike **7b**, this color persisted at room temperature for approximately thirty minutes, after which time the reaction mixture started to turn brown. Treating this purple/brown reaction mixture with sulfur resulted in a complex mixture that did not contain any dithiobiuret by ^{13}C NMR spectroscopy.

Reaction of **7c** with LDA at -78 ºC in toluene produced a light-yellow solution, which was then reacted with excess sulfur to trap any carbenes. NMR analysis showed a very complicated spectrum, and ESI-MS showed that no dithiobiuret or dimer had been formed.

Given that we were unable to obtain the free TADC from any of our diformamidinium dications, we next set out to trap **9a** with a metal complex (Scheme 2.16). A number of metal complexes were chosen as starting material based on their

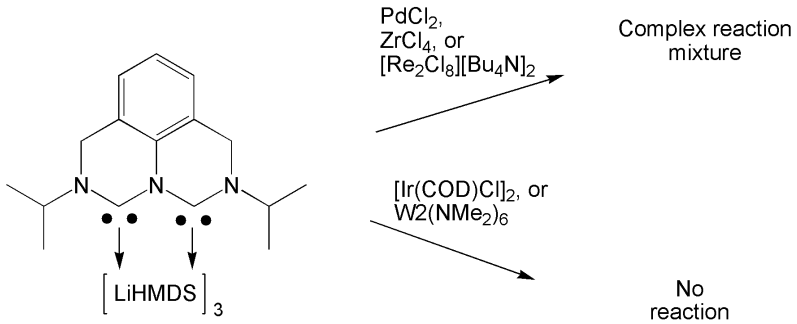

*Scheme 2.16. Attempts to ligate **9a** to a transition metal*

known propensity to form NHC complexes: $PdCl_2$, $ZrCl_4$, and $[Ir(COD)Cl]_2$. Both $PdCl_2$ and $ZrCl_4$ reacted with **9a** in C_6D_6 to form very dark reaction mixtures, which gave very complex ^1H NMR spectra. The dark mixtures appeared very similar in color to the

reaction of the starting metal complexes with LiHMDS. On the other hand, $[Ir(COD)Cl]_2$ did not react with **9a**. Ligation to dinuclear complexes with metal-metal multiple bonds was also attempted. Much like $PdCl_2$ and $ZrCl_4$, $[Bu_4N]_2[Re_2Cl_8]$ reacted with **9a** in C_6D_6 to form a dark reaction mixture, very similar in appearance to the reaction of $[Bu_4N]_2[Re_2Cl_8]$ with LiHMDS, with a very complex, uninterpretable ^1H NMR spectrum. As with $[Ir(COD)Cl]_2$, $W_2(NMe_2)_6$ did not react with **9a** in toluene.

From the results of these reactions, it was clear that it was necessary to find a transition metal starting material that was inert to LiHMDS and that also had labile ligands that could be displaced by the TADC. Tungsten hexacarbonyl ($W(CO)_6$) fits into these criteria and is well-known for making NHC complexes. Reaction of **9a** with one equivalent of $W(CO)_6$ in C_6D_6 at room temperature (Scheme 2.17) led to an orange solution (mono(NHC) tungsten carbonyl complexes are known to be yellow/orange). The ^1H NMR spectrum showed a C_2 symmetric structure with slightly broadened lines

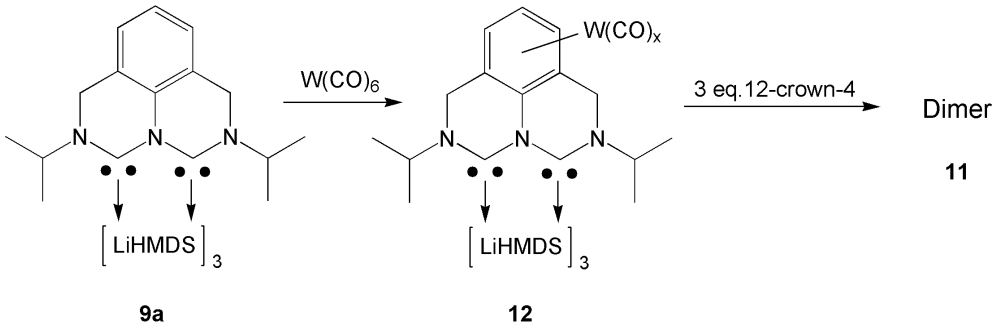

*Scheme 2.17. Reaction of **9a** with $W(CO)_6$ to form **12**, which is then decomposed to **11** with 12-crown-4*

that did not match those of **9a**. In addition, the ^{13}C NMR spectrum showed a signal at δ196 ppm with ^{183}W satellites and a very broad signal at δ232 (≈ 60 Hz). This led to the

hypothesis that the carbenic carbons were not bound to the tungsten, but instead were still bound to LiHMDS. To test this, three equivalents of 12-crown-4 were added to de-lithiate the TADC, if any was present. The ^{1}H NMR spectrum of this reaction mixture showed that the dimer, **11**, had been produced, indicating that the carbenic carbons were still bound to LiHMDS. Thus, it is likely that **12** was bound to the tungsten, not through the carbenic carbons, but through the aromatic ring as an η^6-arene complex. These types of tungsten complexes are known and are usually synthesized by heating $W(CO)_6$ with the desired aromatic. Attempts with $Cr(CO)_6$ gave very similar results.

Next, it was postulated that the TADC might be stable to dimerization if it was de-lithiated at very low temperatures, allowing for the formation of a TADC-transition metal complex. This was attempted by cooling a mixture of **9a** and $W(CO)_6$ in toluene to -78 ºC and treating it with three equivalents of 12-crown-4. After stirring for three hours at -78 ºC and then overnight at room temperature, the reaction mixture was rotovapped to a sticky solid, which was then analyzed by ^{1}H NMR spectroscopy in C_6D_6. The spectrum showed the presents of a very complicated mixture.

Photolysis of $W(CO)_6$ with UV light in THF was performed to allow for the substitution of one of the carbonyl ligands for THF, forming $W(CO)_5$(THF). Since the THF ligand is more easily displaced than the carbonyls, this substitution would hopefully aid in the coordination of the TADC. When the yellow solution of $W(CO)_5$(THF) in THF was added to a solution of **9a** in toluene, the reaction mixture instantly turned black. The ^{1}H NMR spectrum of the reaction mixture showed that dimer **11** had formed, though the spectrum also showed the presents of a number of other unknown compounds.

$W(CO)_6$ was also reacted with **9a** overnight in toluene, while being irradiated with UV light. Again, the hope was that the UV light would labilize the carbonyls, allowing for the coordination of **9a**. Unfortunately, the opposite happened, and no reaction occurred, with the ^{1}H NMR spectrum showing mostly **9a** present in the final reaction mixture.

Another methodology for forming NHC complexes uses a weak base to deprotonate the imidazolium or formamidinium salt in the presence of the transition metal starting material. Bases used for this reaction are commonly neutral, nitrogenous, and sterically-hindered bases like TEA, 1,8-diazabicycloundec-7-ene (DBU), or 1,8-bis(dimethylamino)naphthalene (also known as Proton-sponge®). In our hands, reaction of **7a** with TEA or Proton-sponge® and either $[Ir(COD)Cl]_2$ or $W(CO)_6$ resulted in no reaction, even at elevated temperatures (90 ºC). In comparison, **7a** reacted with DBU and $W(CO)_6$ at room temperature appeared to form nucleophilic addition products of DBU and **7a**, as shown by ESI-MS (Scheme 2.18).

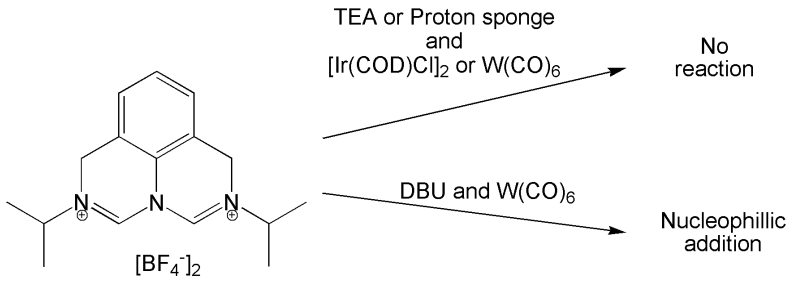

*Scheme 2.18. Attempted deprotonation and coordination of **7a** with weak bases*

Another route to NHC complexes uses a basic ligand on the transition metal to deprotonate the NHC precursor, eliminating the protonated ligand and allowing the newly

formed NHC to coordinate. Basic ligands for this reaction include hydride, alkyl, acetate, and amide ligands. It was thought that this methodology would have the advantage of the deprotonation happening very near to the metal center, allowing for quick coordination of the TADC, which would hopefully prevent any dicarbene dimerization. A good example of this methodology is the use of silver acetate to form a triazole-di-ylidene (ditz)-silver complex by Bertrand, *et al.* (Scheme 1.24).[44] Ditz is the only other known neutral dicarbene where the two carbenes are conjugated and supported by only three nitrogens, making it very electronically similar to our TADC. In our hands, however, heating **7a** in acetonitrile with two equivalents of silver acetate in a vial protected from light resulted in a very dark solution and precipitate. The ^{1}H NMR spectrum showed a very complicated mixture. It is also worth noting that Bertrand was unable to isolate free ditz.[44]

Another metal complex with basic ligands capable of deprotonating NHC precursors is $H_5Ir[P(iPr)_3]_2$. This complex has been used by Crabtree, *et al*., to make a number of NHC complexes.[59] When **7a** was heated with $H_5Ir(P(iPr)_3)_2$ in C_6D_6, no reaction occurred.

Next, it was thought that a high oxidation-state, early transition metal should have more ionic bonds with its ligands, making them more basic. There are a number of examples of zirconium[24] and tantalum[25] compounds that are able to deprotonate NHC precursors and form NHC adducts. Among these are $Zr(NMe_2)_4$ and $Zr(CH_2Ph)_4$. When either of these were heated with **7a** in C_6D_6, minimal reaction occurred. Mainly unreacted **7a** was observed by ^{1}H NMR spectroscopy, and the rest of the reaction mixture was very complex. The results were very similar when $Ta(CH_2Ph)_2Cl_3$ was used. The failure of

these reactions to form TADC complexes is likely because of the electrostatic repulsion of the dication **7a** and the very electropositive metal centers. In many of the examples where a basic ligand deprotonates the NHC precursor, the precursor has R groups which can coordinate, such as amines, phenols, and pyridines. These R groups likely help hold the NHC precursor near to the metal, aiding in the deprotonation.

Reaction of dinuclear complexes with basic ligands was also tried. One such complex is $Ta_2(PMe_3)_4Cl_6H_2$.[60] Though this compound had not been used as a base before, it was thought that the bridging hydrides could deprotonate **7a** and then allow for coordination by loss of two PMe_3 groups. However, heating **7a** with $Ta_2(PMe_3)_4Cl_6H_2$ in C_6D_6 resulted in no discernible reaction based on color change. In comparison, reaction of $W_2(NMe_2)_6$ with **7a** in refluxing C_6D_6 resulted in the production of two non-C_2 symmetric molecules. However, there were no carbene resonances observed in the ^{13}C NMR spectrum.

Attempted Stepwise Synthesis of TADC

Having had no success making either a free TADC or a TADC metal complex, we next turned our attention to synthesizing a TADC stepwise. This would involve first synthesizing a precursor with two different moieties that would allow the formation of a mono-NHC, which could then be complexed to a metal center. This metal-mono(NHC) complex would then be reacted to form the TADC-metal complex. We decided that the mono-formamidinium/mono-2-methoxyformaminal, **13**, could be first deprotonated, creating the mono-NHC, then complexed to a metal center. This complex could then be

heated, eliminating methanol and forming the TADC, which would then also complex to a metal center.

Synthesis of **13** was accomplished in a very similar fashion to **7a-c** (Scheme 2.19). However, instead of starting with the di-protonated [**6c**][HBF_4]$_2$, the mono-protonated [**6c**][HBF_4], was used. This resulted in one of the methoxy groups from the trimethylorthoformate remaining on the final product. A single crystal of this compound was grown by layering a concentrated solution of **13** in CH_2Cl_2 with hexanes.

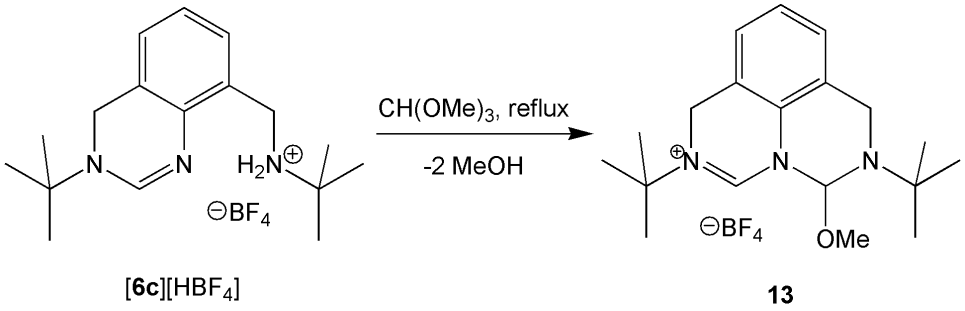

*Scheme 2.19. Synthesis of **13***

The single crystal of **13** was analyzed by X-ray diffractometry. This structure (Figure 2.13) showed that the formamidinium was sterically-hindered, with only ≈2.8 Å between C(5) and C(1). Similarly to **7a**, the C-N bond distances alternate in the formamidinium moiety, though to a much lesser extent (C(1)-N(1) = 1.309(3) Å and C(1)-N(2) = 1.325(3) Å). As expected, N(1) and N(2) are planar due to being sp^2 hybridized, while N(3) is tetrahedral because it is sp^3 hybridized.

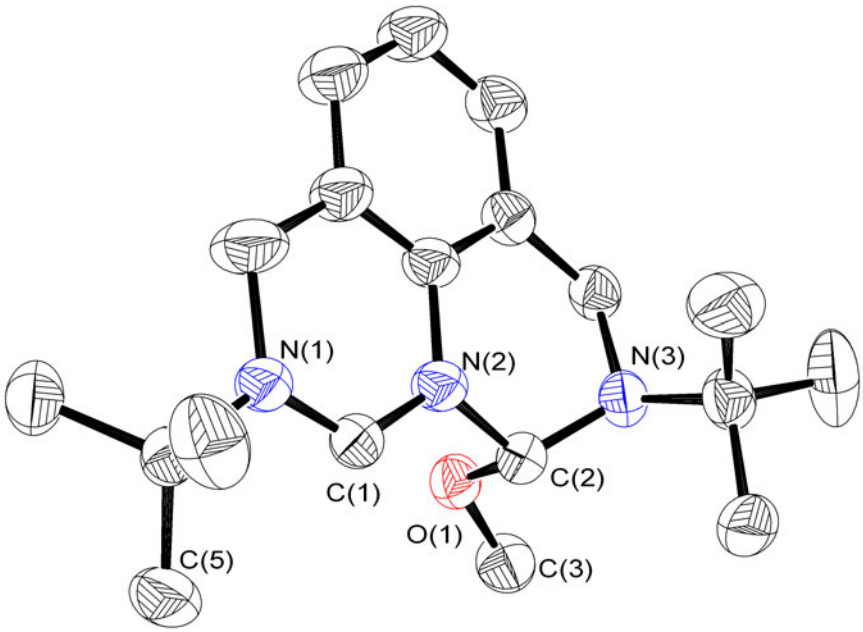

*Figure 2.13. Solid-state structure of **13** (hydrogens and BF_4^- anions omitted for clarity)*

Next, **13** was treated with one equivalent of LiHMDS in order to form the mono-NHC. However, to our surprise, by ^{1}H NMR spectroscopy, it appeared that the main product of this reaction was a C_2 symmetric molecule. The ^{13}C NMR spectrum also showed a broad resonance at δ237, which led us to conclude that a TADC, **9c$_a$**, had been formed (Scheme 2.20). This signal also exhibited splitting, which was assumed to have been caused by coupling to ^{7}Li (92% abundant), though the signal-to-noise ratio was not sufficient to be certain. The formation of the TADC was unexpected as, to the best of our knowledge, there has never been an example of 2-methoxyformaminals forming NHCs by addition of base. When excess sulfur was then added to this reaction, ESI-MS and ^{13}C and ^{1}H NMR spectroscopy confirmed the formation of the dithiobiuret, **10c**, therefore confirming the formation of a TADC.

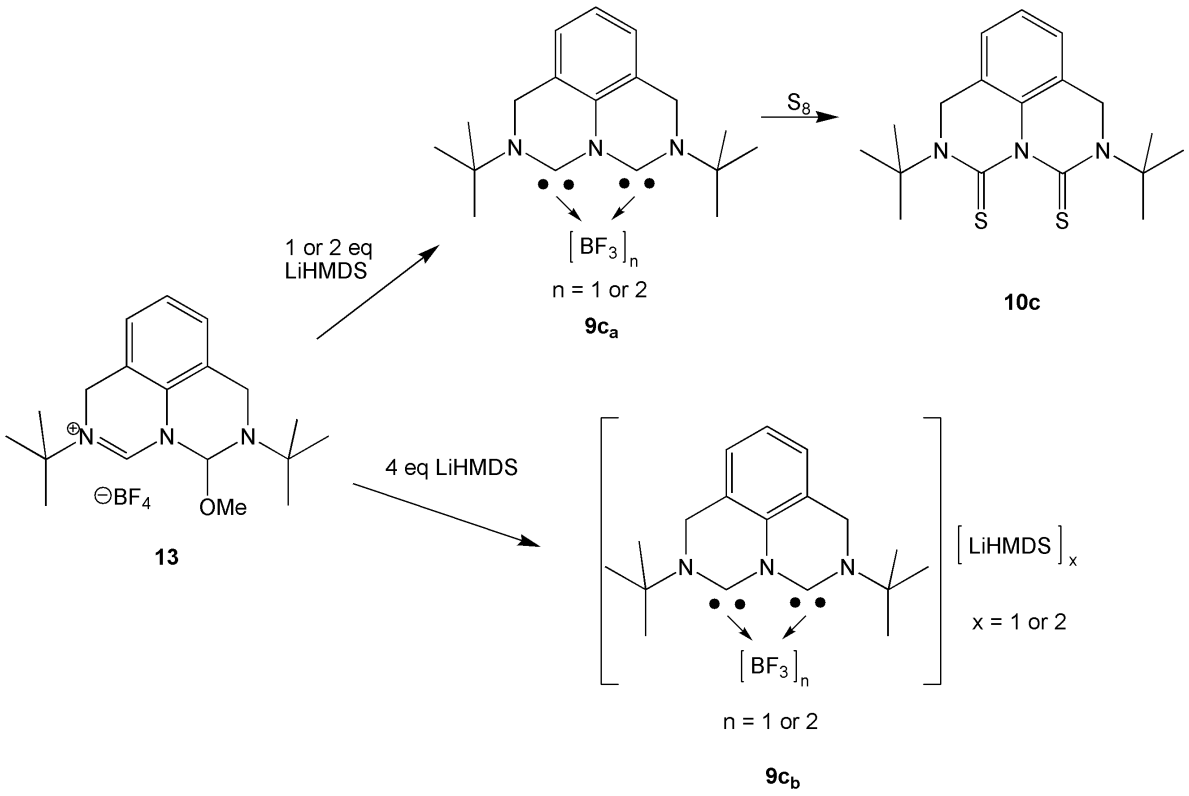

*Scheme 2.20. Reaction of **13** with LiHMDS to form TADCs **9c$_a$** and **9c$_b$** and subsequent reaction of **9c$_a$** to form dithiobiuret **10c***

Addition of two equivalents of LiHMDS to **13** also produced **9c$_a$**, but addition of three equivalents resulted in the production of a mixture of **9c$_a$** and a new TADC that had a broad ^{13}C NMR resonance at δ235, that also appeared to be coupled to a spin-active nucleus. Addition of four equivalents produced exclusively this new TADC, **9c$_b$**. These two TADCs had very similar structures by ^{1}H and ^{13}C NMR spectroscopy, with all of their resonances being only slightly shifted from one another. It remains unclear what the exact difference between these two compounds is, but our current hypothesis is that **9c$_b$** is a LiHMDS coordinated **9c$_a$**.

Because it was assumed that the TADC was also ligated to lithium, attempts were made to de-lithiate it. However, unlike **9a,** addition of 12-crown-4 or

tetramethylethylenediamine (TMEDA) to **9c$_a$** resulted in no change to ^{1}H and ^{13}C NMR spectra. A ^{13}C NMR spectrum of **9c$_b$** with higher signal-to-noise ratio was acquired (Figure 2.14). It was expected that the carbene resonance would be split into a 1:1:1:1 quadruplet due to coupling to ^{7}Li, a spin 3/2 nuclei. This spectrum showed that the carbene resonance was indeed split; however, it was split into a 1:2:2:1 quartet, indicating that the carbon was instead coupled to three spin 1/2 nuclei. This suggested that the carbene was likely bound to a BF_3. The *J*-value for the quartet was ≈20 Hz, which is consistent with a two-bond ^{19}F-^{13}C coupling. Arduengo, *et al*., have demonstrated the ligation of NHCs to BF_3, and unlike ligation to other boron compounds (i.e., BH_3, BEt_3), this coordination is irreversible.[61] Ligation of BF_3 to **9c$_a$** and **9c$_b$** also explains why addition of 12-crown-4 or TMEDA produced no reaction. The source of BF_3 would presumably be the decomposition of $LiBF_4$ to BF_3 and LiF.

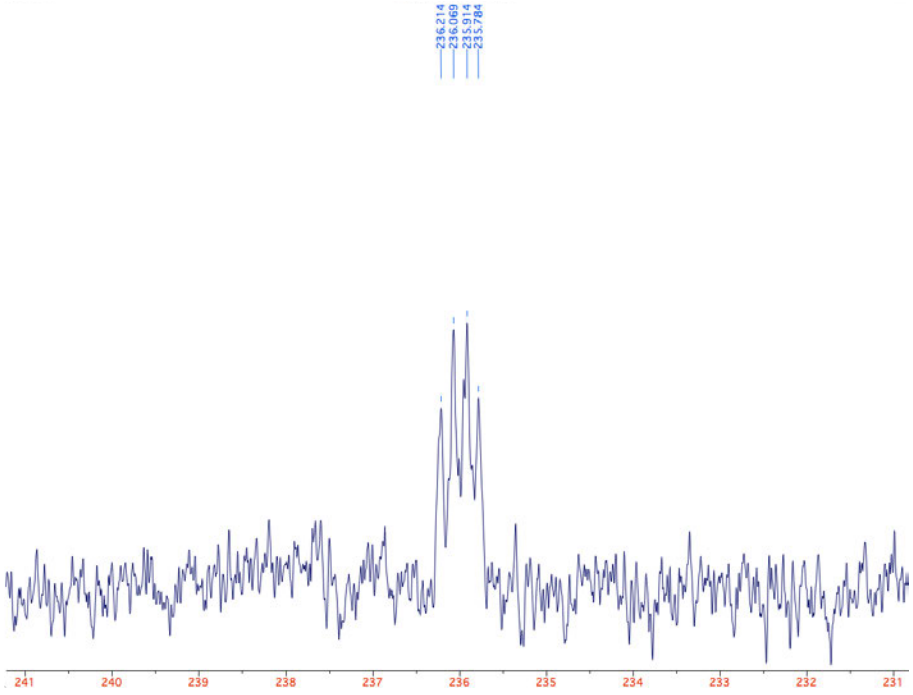

*Figure 2.14. ^{13}C NMR spectrum of the carbene resonance in **9c$_b$**, showing likely coupling to three ^{19}F nuclei*

An interesting side reaction was observed when **13** was deprotonated with two equivalents of LiHMDS in CH_2Cl_2 (Scheme 2.21). Instead of $\mathbf{9c_a}$ being produced, the di-CH_2Cl_2 adduct, **14**, was observed, as shown by ^1H and ^{13}C NMR spectroscopy and high resolution ESI-MS.

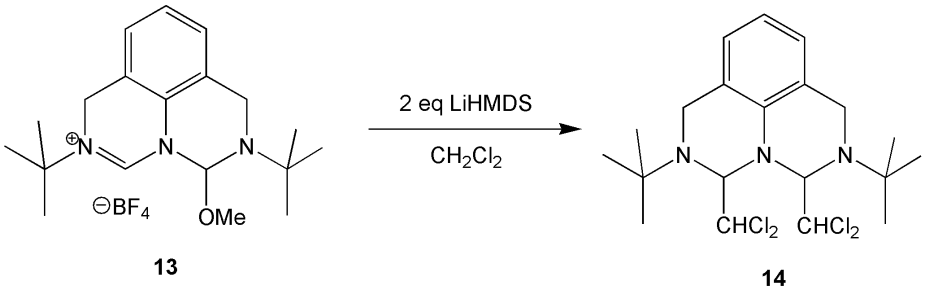

*Scheme 2.21. Formation of the di-CH_2Cl_2 adduct, **14**, via reaction of **13** with LiHMDS in CH_2Cl_2*

Before it was postulated that $\mathbf{9c_a}$ was a BF_3 adduct, attempts were made to ligate it to a metal. Inorganic reactants $PdCl_2(COD)$ (COD = 1,4-cyclooctadiene), $PdCl_2(PhCN)_2$, $[IrCl(COD)]_2$, and $Cp_2Mo_2(CO)_4$ were tried, and all resulted in no reaction, in retrospect likely because the carbene positions were blocked by BF_3. Reacting $\mathbf{9c_a}$ with $Cr(CO)_6$ appears to have produced a product much like **12**, with the ^{13}C NMR resonances being slightly shifted for the molecule, except for the carbene ^{13}C NMR resonance, which remained unchanged.

When **13** was treated with one equivalent of NaHMDS, the mono-NHC **15** (which we had originally targeted) was cleanly formed (Scheme 2.22). The ^{13}C NMR spectrum showed a non-C_2 symmetric molecule with a resonance at δ239. If two equivalents of NaHMDS were added, there was no change in the reaction products, with **15** being the

only major product. This mono-carbene was stable for a number of hours at room temperature; however, it completely decomposed to unknown compounds overnight.

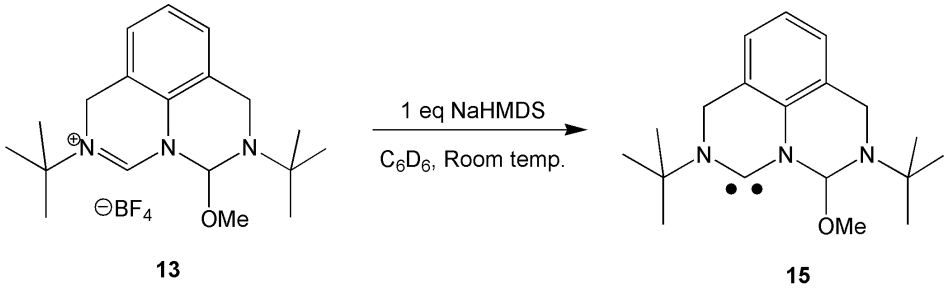

13 **15**

*Scheme 2.22. Formation of mono-NHC, **15**, via treatment of **13** with NaHMDS*

An interesting result occurred when the Li^+ of LiHMDS was chelated to 12-crown-4 prior to LiHMDS being added to **13**. In this experiment, a premixed toluene solution containing two equivalents of 12-crown-4 and two equivalents of LiHMDS was added to a suspension of **13** in toluene at room temperature, resulting in the formation of **15**. Although the reason LiHMDS leads to the TADC and NaHMDS leads to the mono-NHC is still unclear, this experiment demonstrates that lithium coordination is necessary to form either of the TADCs $\mathbf{9c_a}$ or $\mathbf{9c_b}$.

In order to see if **15** could be converted to $\mathbf{9c_a}$ or $\mathbf{9c_b}$, **13** was treated with one equivalent of NaHMDS in C_6D_6 and then filtered to remove $NaBF_4$ and any excess **13**. This light-yellow solution of **15** (confirmed by ^{1}H NMR spectroscopy) was then treated with one equivalent of LiHMDS in C_6D_6, forming a mixture of $\mathbf{9c_a}$, $\mathbf{9c_b}$ and **15** (based on ^{1}H NMR spectroscopy). The formation of the TADCs was puzzling, given that there should be very little BF_4^- in solution to act as a BF_3 source. This result also suggests that the mono-NHC **15** is likely an intermediate during the formation of $\mathbf{9c_a}$ and $\mathbf{9c_b}$.

After obtaining **15**, our next goal was to ligate it to a transition metal center. The metal complexes $PdCl_2(COD)$, $PdCl_2(PhCN)_2$, $[IrCl(COD)]_2$, $Cr(CO)_6$, and $Cp_2Mo_2(CO)_4$ were reacted with **15** at room temperature in C_6D_6. In each case there was no reaction of **15** with the transition metal starting material. This is likely a result of a combination of factors. The NHC in **15** is likely sterically-encumbered, which prevents, or at least slows down, coordination to metal centers. Because coordination is slowed, **15** decomposes before the NHC-transition metal complex is formed.

Next, it was decided that instead of deprotonating first, it might be better to thermally decompose the 2-methoxyformaminal moiety to an NHC first. It was hoped that this NHC would be less sterically-congested than **15**, hopefully allowing for quicker formation of the metal complex. A solution of one equivalent of **13** in trifluorotoluene (b.p. 103 ºC) was refluxed with one equivalent of $Cr(CO)_6$ overnight (Scheme 2.23). The

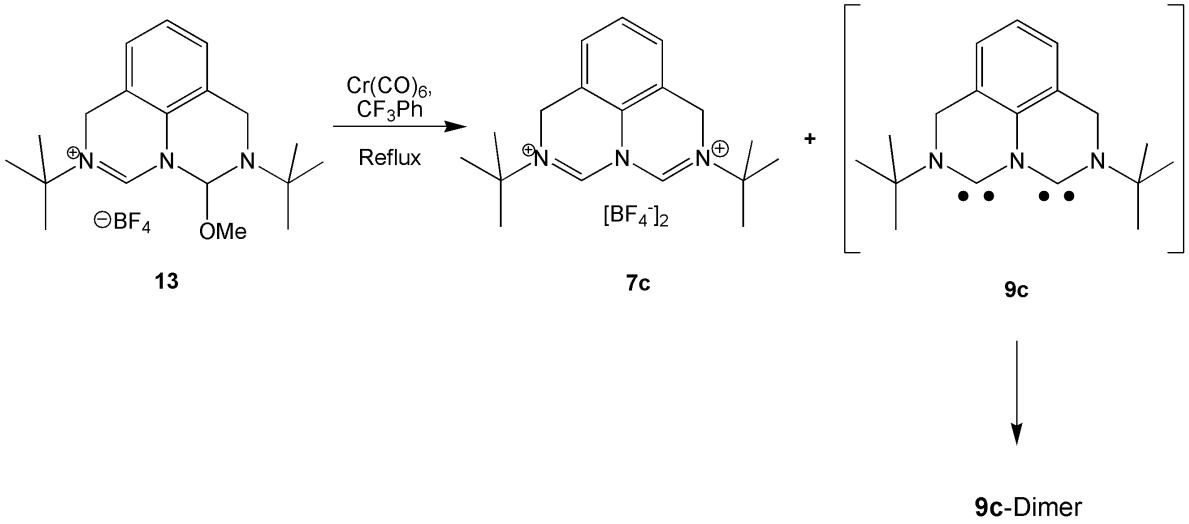

*Scheme 2.23. Heating **13** leads to the formation of **7c** and a **9c** dimer*

reaction yielded a yellow solution and a fine white precipitate. The precipitate was collected and analyzed by ^{1}H NMR spectroscopy, which showed that it was **7c**. The yellow solution was analyzed by ESI-MS, which showed an *m/z* of 584, which is consistent with $[2(\mathbf{9c})+H_2O]^+$ (the addition of water is likely an ESI-MS artifact, not occurring during the reaction itself). These data lead to the conclusion that **13** is disproportionating into the dication **7c** and the TADC **9c**, which then dimerizes.

Conclusions

Despite our best efforts, a TADC-metal complex has remained elusive. While the dications **7a-c** appeared to be promising precursors, they were very sensitive to the base that was used, with only one case resulting in the formation of an isolable TADC, **9a**. Though this was an exciting discovery, in every instance where the LiHMDS was removed from **9a**, dimerization happened quickly. Through careful study of this dimer, it was concluded that the dimer is formed via a 1,3-shift of a benzylic proton to a carbenic center. Thus, going forward, it would be beneficial to synthesize an analog to **7a-c** that has been tetra-methylated at the benzylic positions, in order to eliminate all the benzylic protons and thereby prevent dimerization. Alternatively, the stepwise approach in the synthesis of **15** might also yield results if the R groups are less bulky. This would hopefully allow for coordination of a metal complex to the mono-NHC.

Experimental

All procedures were performed under an argon atmosphere unless noted otherwise. $KMnO_4$, 2,6-dimethylnitrobenzene, isopropylamine, diisopropylamine, tert-butylamine, 2,4,6-trimethylaniline, triethylamine, thionyl chloride, 10% Pd on carbon, 65% Red Al

(Vitride) in toluene, trimethyl orthoformate (anhydrous), tetrafluoroboric acid etherate, and NaHMDS were purchased from Sigma-Aldrich and used as received. $LiAlH_4$ was purchased from TCI America and used as received. $Ta(CH_2Ph)_2Cl_2$, $PdCl_2$, $[Ir(COD)Cl]_2$, $ZrCl_4$, $W(CO)_6$, $[Bu_4N]_2[Re_2Cl_8]$, and $W_2(NMe_2)_6$ were provided by L. Messerle. All amines, 1,1,2,2-tetrachloroethane, 1,4-dioxane, CH_2Cl_2 were dried over 4Å sieves. Diglyme, diisopropylamine and DBU were dried via vacuum distillation from NaH. C_6D_6 was dried over Na. 12-Crown-4 was vacuum distilled from sodium. Triethyl orthoformate was distilled prior to use. Oxonium salts,[31] $Pd(PhCN)_2Cl_2$,[62] $Zr(NMe)_4$,[63] $Zr(CH_2Ph)_4$,[64] $IrH_5(P(iPr)_3)$[65] and $Ta_2H_2Cl_6(PMe_3)_4$[60] were synthesized following published procedures. $W(CO)_6$ was sublimed prior to use. LiHMDS was prepared via addition of 2.5 M n-BuLi in hexanes to a solution of HMDS in hexanes, which was then rotovapped to a solid. LDA was prepared as a 0.5 M solution in hexanes using diisopropylamine and 2.5 M n-BuLi in hexanes. A Thermo LCQ Deca quadrupole ion trap mass spectrometer was used to obtain nominal mass ESI-MS data. A Waters Q-TOF Premier mass spectrometer was used to obtain high-resolution ESI-MS data. NMR spectra were acquired on Bruker Fourier 300 MHz, Bruker DRX 400 MHz, Bruker AMX 360 MHz, and Bruker AVANCE 500 MHz intruments. Chemical shifts are expressed in parts per million (δ scale) downfield from tetramethylsilane and are referenced to the residual proton resonance in the deuterated NMR solvent ($CHCl_3$: δ 7.26; C_6D_5H: δ 7.15; CD_2HCN: δ 1.94; DMSO-d_5H: δ 2.50; CD_2HOD: δ 3.31) or the solvent ^{13}C resonance ($CDCl_3$: δ 77.16; C_6D_6: δ 128.36; CD_3CN: δ 118.69; DMSO-d_6: δ 39.51; CD_3OD: δ 49.15).

2-Nitroisophthalic acid (**1**). In ambient atmosphere, a three-neck, 12 L round bottom

flask was equipped with a mechanical stirrer and two reflux condensers. 2,6-Dimethylnitrobenzene (100 g, 0.662 mol) was added to a solution of $KMnO_4$ (439 g, 4.2 eq.) in 5 L of deionized (DI) water. This deep purple, biphasic mixture was then refluxed for ≈18 hours. The reaction was then cooled to room temperature and filtered through Celite. The dark brown precipitate (MnO_2) was rinsed with ≈500 mL DI water. The light yellow filtrate was then acidified to Ar < 4 with concentrated HCl, forming a white precipitate. This precipitate was then collected by filtration and rinsed with ≈250 mL water. The white solid was dried to a constant weight under vacuum with gentle heating. 2-Nitroisophthalic acid (**1**) (95.0 g, 68% yield) was obtained as a fluffy white powder. R_f = 0.30 (1:1 ethyl acetate:methanol, silica gel). ^{1}H NMR (CD_3OD, 400 MHz): δ 7.72 (t, 1H), 8.20 (d, 2H). ^{13}C NMR (CD_3OD, 100 MHz): δ 126.12, 131.65, 136.09, 151.11 (Ar), 165.73 (-O=C-OH). Negative ion ESI-MS: *m/z* 210 (M-H).

2-Nitroisophthaloyl dichloride (**2**). This is a modification of a known procedure.[52] To a suspension of 2-nitroisophthalic acid (**1**) (45.0 g, 213 mmol) in 1,1,2,2-tetrachloroethane (125 mL) in a single-neck, 500 mL round bottom flask fitted with a reflux condenser and gas inlet adapter, thionyl chloride (55 mL) was added all at once by temporarily removing the reflux condenser. This suspension was refluxed for 5 hours, after which the reaction had become a clear yellow/green solution. The solution was allowed to cool to room temperature, leading to colorless crystals. The flask was then stoppered and placed in a -40ºC freezer overnight. This cooled mixture was then quickly filtered in air and rinsed with ≈100 mL hexanes. This colorless solid was transferred to a flask and dried under vacuum. 2-Nitroisophthaloyl dichloride (**2**) (45.0 g, 85% yield) was obtained as colorless crystals. ^{1}H NMR ($CDCl_3$, 400 MHz): δ 7.91 (t, 1H), 8.41 (d, 2H).

N,N'-Diisopropyl-2-nitroisophthalamide (**3a**). Via solid addition funnel, 2-nitro-isophthaloyl dichloride (**2**) (45.0 g, 182 mmol) was slowly added over approximately 15 minutes to a solution of isopropyl amine (65 mL, 4.1 eq) in CH_2Cl_2 (450 mL) in a two neck, 1 L flask fitted with a gas inlet adapter and cooled in an ice bath. After **2** had been added, the ice bath was removed and the reaction stirred at room temperature for two hours. The precipitate was then collected by filtration. This white solid was placed in 500 mL of DI water and stirred for 30 minutes in order to remove all ammonium salts. The solid was then collected by filtration and rinsed with ≈100 mL of water and then ≈100 mL acetone. This solid was dried under vacuum to afford N,N'-diisopropyl-isophthalamide (**3a**) (50.9 g, 96%) as a white fluffy powder. ^{1}H NMR (DMSO-d_6, 400 MHz): δ 1.12 (d, 12H, -CH-(C<u>H</u>$_3$)$_2$, 3.93 (m, 2H, -C<u>H</u>-(CH$_3$)$_2$, 7.66 (m, 3H, Ar), 8.67 (d, 2H, N<u>H</u>). ^{13}C NMR (DMSO-d_6, 100 MHz): δ 22.01 (-CH-(<u>C</u>H$_3$)$_2$), 41.26 (-<u>C</u>H-(CH$_3$)$_2$), 129.75, 131.09, 131.62, 146.82 (Ar), 163.60 (-O=<u>C</u>-NH).

N,N'-Dimesityl-2-nitroisophthalamide (**3b**). Starting with 10.0 g of **2**, the same procedure as with **3a** was followed, except that 2,4,6-trimethylaniline (2 eq.) and triethylamine (2.1 eq.) were used instead of isopropyl amine. A 17.8 g, 99% yield of **3b** was obtained. ^{1}H NMR (DMSO-d_6, 400 MHz): δ 2.22 (d, 18H, Ar-C<u>H</u>$_3$), 6.92 (s, 4H, Ar), 7.89 (t, 1H, Ar), 7.98 (d, 2H, Ar), 10.20 (s, 2H, N<u>H</u>). ^{13}C NMR (DMSO-d_6, 100 MHz): δ 17.91, 20.56 (Ar-<u>C</u>H$_3$), 128.48, 130.33, 131.47, 131.56, 131.65, 135.23, 136.17, 147.09 (Ar), 163.04 (-O=<u>C</u>-NH). Positive ion ESI-MS: *m/z* 446 (M+H).

N,N'-Di-tert-butyl-2-nitroisophthalamide (**3c**). Starting with 35.0 g of **2**, the same procedure as with **3a** was followed, except that *tert*-butyl amine (4.1 eq.) was used instead of isopropyl amine and the final product was not rinsed with acetone (**3c** is

soluble in acetone). **3c** (44.1g, 97%) was obtained. ^{1}H NMR (DMSO-d_6, 300 MHz): δ 1.34 (s, 18H, -C-(C$\underline{H}_3$)$_3$), 7.59 (m, 3H, Ar), 8.39 (s, 2H, N$\underline{H}$). ^{13}C NMR (DMSO-d_6, 75 MHz): δ 28.28 (-C-(C$\underline{H}_3$)$_3$), 51.18 (-$\underline{C}$-(CH$_3$)$_3$), 129.53, 130.87, 132.61, 146.47 (Ar), 164.44 (-O=$\underline{C}$-NH).

N,N'-Diisopropyl-2-aminoisophthalamide (**4a**). In a 500 mL glass Fischer Porter reaction vessel, N,N'-diisopropyl-2-nitroisophthalamide (50.9 g, 174 mmol), 10% Pd on carbon (0.5 g), and methanol (450 mL) were combined and purged with argon. This dark grey slurry was then pressurized to 60 psi of H_2 and vigorously stirred (strong stirring was necessary, otherwise the product will form a solid layer on top of the mixture). The reaction was followed by TLC and deemed complete after 3 days (shorter reaction times were possible with higher catalyst loading). The reaction was filtered and the filtrate rotovapped to a white solid. The dark solid (a mixture of **4a** and Pd on carbon) was then placed in a Soxlet extractor and extracted with THF until no more **4a** is present in the extraction thimble as shown by TLC. The THF slurry was then rotovapped to a solid and combined with the solid obtained from the methanol solution, affording N,N'-diisopropyl-2-aminoisophthalamide (**4a**) (42.8 g, 94% yield) as a off-white, chunky powder. R_f = 0.76 (ethyl acetate, silica gel, glows vibrant blue under UV light). ^{1}H NMR (DMSO-d_6, 400 MHz): δ 1.14 (d, 12H, -CH-(C$\underline{H}_3$)$_2$), 4.06 (m, 2H, -C$\underline{H}$-(CH$_3$)$_2$, 6.54 (t, 1H, Ar), 7.56 (d, 2H, Ar), 8.10 (d, 2H, N$\underline{H}$).

N,N'-Di-mesityl-2-aminoisophthalamide (**4b**). Starting with 17.8 g of **3b**, the same procedure as with **4a** was followed, providing of **4b (**15.6 g, 94%). ^{1}H NMR (DMSO-d_6, 400 MHz): δ 2.15 (s, 12H, Ar-C$\underline{H}_3$), 2.25 (s, 6H, Ar-C$\underline{H}_3$), 6.71 (t, 1H, Ar), 6.92 (s, 4H, Ar), 7.46 (s, 2H, N$\underline{H}$), 7.90 (d, 2H, Ar), 9.59 (s, 2H, N$\underline{H}$). ^{13}C NMR (DMSO-d_6, 100

MHz): δ 18.01, 20.56 (Ar-$\underline{C}H_3$), 113.54, 117.02, 128.32, 131.79, 132.51, 135.34, 135.62, 149.89 (Ar), 167.42 (-O=$\underline{C}$-NH). Positive ion ESI-MS: *m/z* 416 (M+H).

N,N'-Di-tert-butyl-2-aminoisophthalamide (**4c**). The same procedure as **4a** was followed, except **4c** is soluble in methanol, so the Soxlet extraction step is unnecessary. **4c** (18.56 g, 90%) was obtained as an off-white chunky solid. ^{1}H NMR (DMSO-d_6, 500 MHz): δ 1.37 (s, 18H, -C-($C\underline{H}_3$)$_3$), 6.50 (t, 1H, Ar), 7.48 (d, 2H, Ar), 7.65 (s, 2H, N$\underline{H}$). ^{13}C NMR (DMSO-d_6, 125.8 MHz): δ 28.59 (-C-($\underline{C}H_3$)$_3$), 50.76 (-$\underline{C}$-(CH_3)$_3$), 113.07, 118.68, 131.22, 148.61 (Ar), 168.80 (-O=$\underline{C}$-NH).

2,6-Bis((isopropylamino)methyl)aniline (**5a**) A three-neck flask fitted with a reflux condenser, pressure equalizing addition funnel, a gas inlet adapter, and a septum and containing **4a** (20 g, 85 mmol) was flushed with argon. Dry diglyme (≈100 mL) was then transferred into the flask to create a thick slurry. The septum was then exchanged for a glass stopper. Red Al (sodium bis(2-methoxyethoxy)aluminum dihydride, also known as Vitride, 65% solution in toluene) (118 mL, 5 eq.) was added slowly over approximately 10 minutes via addition funnel, which produced a copious amount of gas evolution (presumably H_2). Addition of the Red Al also caused the solids to dissolve and turned the reaction dark yellow/orange. The reaction mixture was heated to reflux. The reaction was monitored by TLC (reaction samples for TLC were first quenched with 5 M NaOH) and deemed complete after 2.5 hours. This dark orangish-red solution was then cooled to room temperature and placed in an ice bath. To this solution, 5 M NaOH was added slowly, which caused gas evolution and formed a sticky white precipitate. 5 M NaOH (≈60 mL total) was added until a clear solution with a thick white sludge on the bottom of the flask was formed. The reaction was decanted and filtered through Celite. The filtrate

was then placed in a single-neck round bottom flask fitted with septum. A needle connected to a bubbler through the Schlenk line was first attached and then HCl gas was bubbled through the solution using a separate needle, which formed a precipitate. The HCl was bubbled through the reaction until no more precipitate was formed. This precipitate was collected and washed with ≈100 mL diethyl ether. This light yellow to off-white powder was then suspended in CH_2Cl_2 (300 mL). Under vigorous stirring, 5 M NaOH was added until all the solids dissolved and the aqueous layer remained basic. This biphasic solution was then separated and the aqueous layer extracted with CH_2Cl_2 (3 x 50 mL). The organic fractions were then combined, dried over anhydrous sodium carbonate, and rotovapped to provide **5a** (13.5 g, 75%) as a dark orange solid that melts very near to room temperature. ^{1}H NMR ($CDCl_3$, 400 MHz): δ 1.11 (d, 12H, -CH-(C<u>H</u>$_3$)$_2$, 2.84 (m, 2H, -C<u>H</u>-(CH$_3$)$_2$, 3.77 (s, 4H, Ar-C<u>H</u>$_2$), 6.58 (t, 1H, Ar), 6.96 (d, 2H, Ar). ^{13}C NMR ($CDCl_3$, 100 MHz): δ 22.34 (-CH-(<u>C</u>H$_3$)$_2$), 48.76 (Ar-<u>C</u>H$_2$), 50.69 (-<u>C</u>H-(CH$_3$)$_2$), 116.48, 124.50, 128.75, 146.98 (Ar). Positive ion ESI-MS: *m/z* 236 (M+H).

2,6-Bis((mesitylamino)methyl)aniline (**5b**) In a two-neck 100 mL round bottom flask fitted with a reflux condenser and a gas inlet adapter, **4b** (3.0 g, 7.2 mmol), 1,4-dioxane (25 mL), and $LiAlH_4$ (1.10 g, 4.0 eq.) were mixed. No visible reaction occurred. The reaction was then heated, and the reaction mixture became green and produced considerable bubbling and gas evolution. Reflux was continued for 2 days. The reaction was cooled to room temperature and quenched with 5 M NaOH. CH_2Cl_2 (20 mL) was then added and the reaction was filtered through Celite, resulting in a light yellow/orange solution, which was then rotovapped to a solid. This solid was recrystallized from 1:4 toluene:hexanes to afford a white solid, **5b** (2.32 g, 83%). ^{1}H NMR ($CDCl_3$, 300 MHz):

δ 2.26 (s, 12H, Ar-C$\underline{H}_3$), 2.35 (s, 6H, Ar-C$\underline{H}_3$), 4.03 (s, 4H, Ar-CH_2), 6.71 (t, 1H, Ar), 6.88 (s, 4H, Ar), 7.13 (d, 2H, Ar).

2,6-Bis((tert-butylamino)methyl)aniline (**5c**). Starting with 10.0 g of **4c**, the same procedure as **5a** was used, providing **5c** (8.04 g, 89%). ^{1}H NMR ($CDCl_3$, 300 MHz): δ 1.20 (s, 18H, -C-(C$\underline{H}_3$)$_3$), 3.76 (s, 2H, Ar-C$\underline{H}_2$-) 6.60 (t, 1H, Ar), 6.97 (d, 2H, Ar). ^{13}C NMR ($CDCl_3$, 75 MHz): δ 29.15 (-C-(C$\underline{H}_3$)$_3$), 46.26 (Ar-C$\underline{H}_2$-), 50.76 (-C-(CH$_3$)$_3$), 116.86, 125.21, 128.94, 147.61 (Ar).

[**6a**][HBF_4]$_2$. In an oven-dried 50 mL Schlenk flask, a slurry of **Ox$_a$** (954 mg, 1.1 eq.) in CH_2Cl_2 (20 mL) was cooled to -78 ºC in a dry ice/acetone bath. A solution of **5a** (1.00 g, 4.25 mmol) in CH_2Cl_2 (5 mL) was then quickly added and this mixture was mixed overnight, during which time it warmed to room temperature. This reaction was then taken into the glove box, where it was filtered to remove a small amount of precipitate and rotovapped to a sticky solid, which was then extracted with diethyl ether (3 x 10 mL). This solid was redissolved in CH_2Cl_2 (20 mL) and treated with tetrafluoroboric acid etherate (640 uL, 1.1 eq.), which caused a precipitate to form. This solid was collected by filtration and dried under vacuum to afford [**6a**][HBF_4]$_2$ (1.70 g, 95%) as a white powder. ^{1}H NMR (CD_3CN, 360 MHz): δ 1.38 (dd, 12H, -CH-(C$\underline{H}_3$)$_2$, 3.60 (m, 1H, -C$\underline{H}$-(CH$_3$)$_2$, 4.05 (m, 1H, -C$\underline{H}$-(CH$_3$)$_2$, 4.20 (m, 2H, Ar-C$\underline{H}_2$), 4.82 (s, 2H, Ar-C$\underline{H}_2$), 6.80 (br, 2H, N$\underline{H}$) 7.26 (d, 1H, Ar), 7.36 (t, 1H, Ar), 7.44 (d, 1H, Ar), 8.02 (d, 1H, -N-C$\underline{H}$=N-) 9.43 (br, 1H, N$\underline{H}$). ^{13}C NMR (CD_3CN, 90 MHz): δ 19.22, 19.61 (-CH-(C$\underline{H}_3$)$_2$), 44.33, 44.55 (Ar-C$\underline{H}_2$), 54.14, 59.06 (-C$\underline{H}$-(CH$_3$)$_2$), 119.31, 119.60, 128.71, 129.93, 130.09,132.69 (Ar), 150.27 (-N-C$\underline{H}$=N-). Positive ion ESI-MS: *m/z* 246 (M+H).

[**6b**][HBF_4]$_2$. Starting with 500 mg of **5b**, the same procedure as [**6a**][HBF_4]$_2$ was followed, providing [**6b**][HBF_4]$_2$ (694 mg, 94%) ^{1}H NMR (DMSO-d_6, 300 MHz): δ 1.90 (s, 6H, Ar-C$\underline{H}_3$), 2.30 (s, 12H, Ar-C$\underline{H}_3$), 3.35 (d, 4H, Ar-C$\underline{H}_2$), 3.64 (d, 1H, Ar-C$\underline{H}_2$), 4.17 (s, 2H, Ar-C$\underline{H}_2$), 6.87 (t, 1H, Ar), 6.98 (s, 2H, Ar), 7.08 (s, 2H, Ar), 7.17 (d, 2H, Ar), 8.06 (d, 1H, -N-C$\underline{H}$=N-). Positive ion ESI-MS: *m/z* 398 (M+H).

[**6c**][HBF_4]$_2$. The same procedure as [**6a**][HBF_4]$_2$ was used, providing [**6c**][HBF_4]$_2$ (823 mg, 97%). ^{1}H NMR (CD_3CN, 500 MHz): δ 1.37 (2s, 18H, -C-(C$\underline{H}_3$)$_3$), 4.24 (m, 2H, Ar-C$\underline{H}_2$-), 4.90 (m, 2H, Ar-C$\underline{H}_2$-), 7.34 (d, 1H, Ar), 7.41 (t, 1H, Ar), 7.48 (d, 1H, Ar), 8.06 (d, 1H, -N-C$\underline{H}$=N-).

7a. In an oven-dried 50 mL Schlenk flask fitted with a reflux condenser, a solution of [**6a**][HBF_4]$_2$ (1.00 g, 2.37 mmol) and trimethylorthoformate (1.2 mL, 5 eq.) in acetonitrile (20 mL) was refluxed for 4 hours, resulting in an orange solution. The reaction mixture was then brought into the glovebox and rotovapped to approximately half the volume. It was then placed in the -30 ºC freezer overnight. The resulting crystals were collected by filtration and washed with a minimal amount (> 1mL) of cold acetonitrile. Second and third crops could be obtained by reducing the volume further. The solids were combined to afford **7a** (735 mg, 72% yield) as a white powder. ^{1}H NMR (CD_3CN , 400 MHz): δ 1.54 (d, 12H, -CH-(C$\underline{H}_3$)$_2$, 4.29 (m, 2H, -C$\underline{H}$-(CH_3)$_2$, 5.04 (s, 4H, Ar-C$\underline{H}_2$), 6.80 7.32 (d, 2H, Ar), 7.57 (t, 1H, Ar), 8.77 (s, 2H, -N-C$\underline{H}$=N-). ^{13}C NMR (CD_3CN, 100 MHz): δ 19.86 (-CH-(C$\underline{H}_3$)$_2$), 47.26 (Ar-C$\underline{H}_2$), 63.34 (-C$\underline{H}$-(CH_3)$_2$), 118.06, 120.83, 127.82, 132.29, 151.51 (Ar), 151.50 (-N-C$\underline{H}$=N-).

Attempts to deprotonate 7a with strong bases. A suspension of **7a** (30 mg, 70 μmol) in toluene (5 mL) at -78 ºC was treated with LDA (0.5 M in hexanes, 250 μL, 2.1 eq) and stirred at this temperature for 30 minutes. S_8 (10 mg, 0.5 eq (4 eq S)) was then added and stirred for 1 hour at -78 ºC. The reaction was then warmed to room temperature, filtered and rotovapped to a sticky solid. The ^{1}H NMR spectrum showed a non-C_2 symmetric molecule, likely indicating that a benzylic position had been deprotonated. The same procedure was attempted except that n-Bu-Li (2.5 M in hexanes, 50 μL, 2.1 eq) was used instead of LDA. The ^{1}H NMR spectrum showed a non-C_2 symmetric molecule and what appeared to be an addition of a butyl group, indicating that the n-BuLi had nucleophilically added to **7a**. The same procedure was attempted using KO^{t}Bu (16 mg, 2.1 eq), except the reaction was performed at room temperature. The ^{1}H NMR spectrum showed a non-C_2 symmetric product that was likely the result of nucleophilic attack on the diformamidinium dication by KO^{t}Bu.

Attempts to form a TADC-transition metal complex using 7a and a weak base. Reaction of a suspension of **7a** (30 mg, 70 μmol) in toluene (5 mL) with TEA (28 mg, 4.0 eq) or Proton-sponge® (30 mg, 2.0 eq) and $[Ir(COD)Cl]_2$ (47 mg, 1.0 eq) or $W(CO)_6$ (49 mg, 2.0 eq) at room temperature or 90 ºC resulted in no reaction as shown by ^{1}H NMR spectra of the supernatants. The same reaction using DBU (21 mg, 2.0 eq) and $W(CO)_6$ (49 mg, 2.0 eq) at room temperature resulted in nucleophilic addition of DBU to **7a,** as shown by ESI-MS.

Attempts to form a TADC-transition metal complex using 7a and a transition metal complex with a basic ligand. A solution of **7a** (20 mg, 46 μmol) in acetonitrile-d_3 (1

mL) in a 5 mL vial wrapped in aluminum foil was heated to 80ºC overnight with Ag(OAc) (15 mg, 2.0 eq), resulting in a very dark solution and precipitate. The solution was analyzed by ^{1}H NMR, which showed a complex mixture. The reaction of a suspension of **7a** (30 mg, 70 μmol) and $Zr(NMe_2)_4$ (37 mg, 2 eq), $Zr(CH_2Ph)_4$ (56 mg, 2.0 eq) or $Ta(CH_2Ph)_2Cl_3$ (61 mg, 2.0 eq) in C_6D_6 (1 mL) at 80ºC for 4 hours resulted in minimal reaction products. The products that were formed were very complex by ^{1}H NMR spectroscopy. The same procedure was used to react **7a** (30 mg, 70 μmol) with $Ta_2H_2Cl_6(PMe_3)_4$ (61 mg, 1.0 eq) resulted in no reaction by ^{1}H NMR spectroscopy. This procedure was also used to react **7a** (30 mg, 70 μmol) with $W_2(NMe_2)_6$ resulting in the production of two non-C_2 symmetric molecules according to ^{1}H NMR spectroscopy. ^{13}C NMR spectroscopy was complex and showed no free or ligated carbenes.

7b. In an oven-dried 50 mL Schlenk flask fitted with a reflux condenser, a suspension of [**6b**][HBF_4]$_2$ (370 mg, 0.63 mmol) and trimethylorthoformate (100 μl, 1.5 eq.) in toluene (10 mL) were refluxed overnight. The reaction was then brought into the glovebox and the precipitate collected by filtration. This off-white powder was dried to provide **7b** (220 mg, 60% yield). ^{1}H NMR (CD_3CN, 300 MHz): δ 2.37 (s, 6H, Ar-C<u>H</u>$_3$), 2.40 (s, 12H, Ar-C<u>H</u>$_3$), 5.32 (s, 4H, Ar-CH_2), 7.19 (s, 4H, Ar), 7.42 (d, 2H, Ar), 7.70 (t, 1H, Ar), 9.00 (s, 2H, -N-C<u>H</u>=N-). ^{13}C NMR (CD_3CN, 75 MHz): δ 17.34, 21.15 (Ar-<u>C</u>H_3), 52.64 (Ar-<u>C</u>H_2), 118.09, 120.88, 128.49, 131.42, 133.04, 134.62, 135.78, 143.45 (Ar), 155.97 (-N-<u>C</u>H=N-).

Attempts to deprotonate 7b. To a suspension of **7b** (30 mg, 51 μmol) in THF (5 mL) at -78 ºC, a solution of LiHMDS (17 mg, 2.1 eq) in THF (1 mL) was added dropwise over

approximately 5 minutes, which turned the reaction purple; however, by the time all of the LiHMDS solution was added to the reaction mixture, the solution had returned to colorless. After approximately ten minutes at -78 ºC, the reaction changed back to the same deep purple. After 45 minutes at -78 ºC, the dark purple reaction started to turn brown, at which time S_8 (7 mg, 0.5 eq (4 eq S)) was added and the reaction stirred at this temperature for 2 hours. The reaction mixture was then warmed to room temperature, filtered and the filtrate rotovapped to an oily solid. The ^{13}C and ^{1}H NMR spectra were too complicated to draw any conclusions, but the ESI-MS revealed that a dimerization had occurred.

7c Starting with 200 mg, the same procedure as for **7b** was followed, except that [**6c**][HBF_4]$_2$ was refluxed in neat triethylorthoformate, providing **7c** (187 mg, 87%). ^{1}H NMR (CD_3CN, 300 MHz): δ 1.65 (d, 18H, -C-(C<u>H</u>$_3$)$_3$), 5.11 (s, 2H, Ar-C<u>H</u>$_2$-), 7.34 (d, 2H, Ar), 7.58 (t, 1H, Ar), 8.79 (s, 1H, -N-C<u>H</u>=N-). ^{13}C NMR (CD_3CN, 75 MHz): 26.69 (-C-(<u>C</u>H$_3$)$_3$), 45.46 (Ar-<u>C</u>H$_2$-), 69.30 (-<u>C</u>-(CH$_3$)$_3$), 117.61, 127.34, 131.86 (Ar) 151.28 (-N-<u>C</u>H=N-)

Attempts to deprotonate 7c. To a suspension of **7c** (30 mg, 66 μmol) in toluene (5 mL) at room temperature, LiHMDS (22 mg, 2.1 eq) was added. The reaction quickly turns purple. After 30 minutes, the reaction mixture was purple/brown and S_8 (8 mg, 0.5 eq (4 eq S)) is added and the reaction stirred for a further 2 hours at room temperature. The reaction mixture was then filtered and the filtrate rotovapped to an oily solid. The ^{1}H and ^{13}C NMR spectra were very complex, however no resonances that corresponded to a dithiobiuret were seen. The same reaction was tried with LDA (0.5 M in hexanes, 135

μL, 2.1 eq) at -78 ºC. The ^{1}H and ^{13}C NMR spectra were very complicated, and the ESI-MS showed that no dithiobiuret or dimer was formed.

3,9-Diisopropyl-3,9-diazajulolidine (**8**). In an oven-dried 50 mL Schlenk flask, a suspension of **7a** (30 mg, 70 μmol) in THF (10 mL) was cooled to -78 ºC in a dry ice/acetone bath. $LiBHEt_3$ (1.0 M in toluene, 170 μL, 2.5 eq.) was then added and the reaction mixture stirred in the bath for one hour. The reaction mixture was then removed from the bath and stirred for two hours at room temperature. The reaction was filtered through Celite and rotovapped to an oily solid, affording 3,9-diisopropyl-3,9-diazajulolidine (**8**). ^{1}H NMR (CD_3CN, 400 MHz): δ 1.10 (d, 12H, -CH-(C<u>H</u>$_3$)$_2$, 2.89 (m, 2H, -C<u>H</u>-(CH_3)$_2$, 3.88 (d, 8H, Ar-C<u>H</u>$_2$ and –N-CH_2-N-) , 6.52 (t, 1H, Ar), 6.73 (d, 2H, Ar).

9a. In a glovebox, LiHMDS (58 mg, 5.0 eq.) in C_6D_6 (0.5 mL) was added to a suspension of **7a** (30 mg, 70 μmol) in C_6D_6 (0.25 mL) in a 5 mL vial. This mixture was stirred well for 3 hours, during which time it turned yellow/orange. The reaction was then filtered through a plug of glass wool into an NMR tube to form a light yellow solution of **9a**. ^{1}H NMR (C_6D_6, 500 MHz): δ 0.34 (s, 36H, LiHMDS), 0.54 (s, 18H, LiHMDS), 1.04 (d, 12H, -CH-(C<u>H</u>$_3$)$_2$, 3.44 (s, 4H, Ar-C<u>H</u>$_2$), 4.38 (m, 2H, -C<u>H</u>-(CH_3)$_2$, 6.37 (d, 2H, Ar), 6.79 (t, 1H, Ar). ^{13}C NMR (C_6D_6, 125.8 MHz): δ 20.19 (-CH-(<u>C</u>H_3)$_2$), 39.67 (Ar-<u>C</u>H_2), 62.01 (-<u>C</u>H-(CH_3)$_2$), 118.46, 124.24, 126.04, 127.01(Ar), 232.47 (C:).

Attempted coordination of 9a to transition metal complexes. To a solution of **9a**, as prepared above, $PdCl_2$ (24 mg, 2.0 eq), $ZrCl_4$ (32 mg, 2.0 eq), or $[Bu_4N]_2[Re_2Cl_8]$ (79 mg, 1.0 eq) was added at room temperature. In each case the reaction turned very dark in

color. After stirring for two hours at room temperature, the reaction mixtures were filtered and ^{1}H NMR spectra obtained. All of the spectra were uninterpretable. The same procedure was used to react **9a** with $[Ir(COD)Cl]_2$ (47 mg, 1.0 eq) or $W_2(NMe_2)_6$ (44 mg, 1.0 eq). In these cases the ^{1}H NMR spectra showed that no reaction occurred.

9c$_a$. Starting with 30 mg of **13**, the same procedure as for **9a** was followed, except that two equivalents of LiHMDS were used. ^{1}H NMR (C_6D_6, 500 MHz): δ 1.24 (s, 18H, -C-($C\underline{H}_3$)$_3$), 3.69 (s, 4H, Ar-C$\underline{H}_2$), 6.33 (d, 2H, Ar), 6.75 (t, 1H, Ar). ^{13}C NMR (C_6D_6, 125.8 MHz): δ 29.38 (-C-($\underline{C}H_3$)$_3$), 40.60 (Ar-$\underline{C}H_2$), 62.22 (-$\underline{C}$-(CH_3)$_3$), 118.99, 122.48, 125.58, 126.58 (Ar), 237.83 ($\underline{C}$:).

Attempted coordination of 9c$_a$ to transition metal complexes. A solution of **9c$_a$** in C_6D_6 as prepared above was treated with $PdCl_2$ (26 mg, 2.0 eq), $PdCl_2(PhCN)_2$ (53 mg, 2.0 eq), $[Ir(COD)Cl]_2$ (50 mg, 1.0 eq), or $Cp_2Mo_2(CO)_4$ (31 mg, 1.0 eq). Each reaction mixture was stirred overnight. In each case, the ^{1}H NMR spectrum of the supernatant showed only starting materials.

9c$_b$. The same procedure as **9a** was followed, except that four equivalents of LiHMDS were used and **13** was used as the starting material. ^{1}H NMR (C_6D_6, 500 MHz): δ 1.19 (s, 18H, -C-($C\underline{H}_3$)$_3$), 3.89 (s, 4H, Ar-C$\underline{H}_2$), 6.50 (d, 2H, Ar), 6.89 (t, 1H, Ar). ^{13}C NMR (C_6D_6, 125.8 MHz): δ 29.20 (-C-($\underline{C}H_3$)$_3$), 40.87 (Ar-$\underline{C}H_2$), 62.02 (-$\underline{C}$-(CH_3)$_3$), 118.61, 121.94, 126.13, 127.59 (Ar), 235.95 (q, J = 20 Hz, $\underline{C}$:).

10a. A solution of **9a** in C_6D_6, as prepared above, was treated with S_8 (10 mg, 0.5 eq (4 eq S)). This was mixed for 1 hour, resulting in a yellow solution of **10a**. ^{1}H NMR (C_6D_6 , 500 MHz): δ 0.70 (d, 6H, -CH-($C\underline{H}_3$)$_2$, 0.86 (d, 6H, -CH-($C\underline{H}_3$)$_2$, 5.89 (m, 2H, -C$\underline{H}$-

$(CH_3)_2$, 6.59 (d, 2H, Ar), 6.82 (t, 1H, Ar). ^{13}C NMR ($CDCl_3$, 100 MHz): δ 18.52, 19.20 (-CH-($\underline{C}H_3)_2$), 42.69 (Ar-$\underline{C}H_2$), 52.11 (-$\underline{C}$H-$(CH_3)_2$), 121.74, 123.45, 124.73, 137.82 (Ar), 178.92 (C=S). Positive ion ESI-MS: *m/z* 326 (M+Li) and 342 (M+Na).

10c. The same procedure as **10a** was followed, except that a solution of **9c$_a$** as prepared above was used. ^{1}H NMR (C_6D_6, 500 MHz): δ 1.56 (s, 18H, -C-($C\underline{H}_3)_3$), 3.86 (d, 2H, Ar-$C\underline{H}_2$), 4.15 (d, 2H, Ar-$C\underline{H}_2$), 6.62 (d, 2H, Ar), 6.82 (t, 1H, Ar). ^{13}C NMR (C_6D_6, 125.8 MHz): δ 28.98 (-C-($\underline{C}H_3)_3$), 46.84 (Ar-$\underline{C}H_2$), 62.15 (-$\underline{C}$-$(CH_3)_3$), 122.61, 122.96, 124.44, 136.05 (Ar), 179.59 ($\underline{C}$=S). Positive ion ESI-MS: 348.2 (M+H) and 370.1 (M+Na).

Dimer (11) Method A: To a solution of **9a** in C_6D_6, as prepared above, in a NMR tube fitted with a septum, 12-crown-4 (33 μL, 3 eq.) was added via syringe and then the NMR tube was shaken by hand. There was no visible change. The reaction was then analyzed by ^{1}H and ^{13}C NMR spectroscopies, which confirmed the formation of **11**.

Method B: The same procedure as for **9a** was used, except two equivalents of LiHMDS were used. This route provided **11** more cleanly than did method A, and thus was the method of choice when preparing NMR samples. See Table 2.1 for full NMR spectroscopy details. High resolution ESI-MS: calculated for $C_{38}H_{62}N_7SSi_2$ (M+H) = 704.4326, found 704.4351.

12. In a glovebox, **7a** (30 mg, 70 μmol) was treated with a solution of LiHMDS (58 mg, 5.0 eq) in toluene (2 mL) in a 5 mL vial. This mixture was stirred for two hours and then filtered through a small plug of Celite. To this yellow/orange solution, $W(CO)_6$ (24 mg, 1.0 eq) was added and the reaction stirred overnight. This resulted in the formation of a orange solution with solids stuck to the sides of the vial. The reaction was then decanted

and rotovapped to an oil. This oil was extracted with hexanes (2 x 1 mL) and the solution dried under vacuum to provide **12**, as an orange oil. ^{1}H NMR (C_6D_6 , 500 MHz): δ 0.38 (br, LiHMDS), 1.25 (br, 12H, -CH-(C<u>H</u>$_3$)$_2$, 3.67 (s, 4H, Ar-C<u>H</u>$_2$) 3.92 (br, 2H, -C<u>H</u>-(CH$_3$)$_2$), 6.38 (d, 2H, Ar), 6.79 (t, 1H, Ar). ^{13}C NMR ($CDCl_3$, 100 MHz): δ 5.81 (LiHMDS), 20.72 (-CH-(<u>C</u>H$_3$)$_2$), 41.53 (Ar-<u>C</u>H$_2$), 60.05 (-<u>C</u>H-(CH$_3$)$_2$), 118.46, 122.71, 125.47, 126.55 (Ar), 196.86 (C=O), 232.71 (C:).

13. In an oven-dried 50 mL Schlenk flask, a slurry of **Ox$_a$** (612 mg, 1.1 eq.) in CH_2Cl_2 (20 mL) was cooled to -78 ºC in a dry ice/acetone bath. A solution of **5c** (1.00 g, 275 mmol) in CH_2Cl_2 (5 mL) was then quickly added, and this mixture was stirred overnight, during which time it warmed to room temperature. This reaction mixture was then taken into the glove box, where it was filtered to remove a small amount of precipitate. The filtrate was rotovapped to a sticky solid, which was then triterated with diethyl ether (3 x 10 mL). This was dissolved in trimethylorthoformate (10 mL) and refluxed overnight in a 50 mL Schlenk flask fitted with a reflux condenser, outside the glovebox. The reaction mixture was then rotovapped in the glovebox to a sticky solid, which was dissolved in a minimum amount of methylene chloride and layered with hexanes. This mixture was placed in a -30 ºC fridge for two days. A solid was recovered by filtration and washed with 2 mL of hexanes, providing **13** (665 mg, 60%), as large, cubic, colorless crystals. ^{1}H NMR (DMSO-d$_6$, 500 MHz): δ 1.19 (s, 9H, -C-(C<u>H</u>$_3$)$_3$), 1.50 (s, 9H, -C-(C<u>H</u>$_3$)$_3$), 3.35 (s, 3H, -O-C<u>H</u>$_3$), 4.04 (s, 2H, Ar-C<u>H</u>$_2$), 4.94 (s, 2H, Ar-C<u>H</u>$_2$), 6.15 (s, 1H, -C<u>H</u>-O-CH$_3$) 7.12 (d, 1H, Ar), 7.22 (d, 1H, Ar), 7.26 (t, 1H, Ar), 8.67 (s, 1H, -N-C<u>H</u>=N-). ^{13}C NMR (DMSO-d$_6$, 125.8 MHz): δ 26.78, 27.66 (-C-(<u>C</u>H$_3$)$_3$), 38.45, 42.86 (Ar-<u>C</u>H$_2$), 53.31,

54.06 (-C-$(CH_3)_3$), 62.15 (-O-CH_3), 94.51 (-CH-O-CH_3), 118.44, 124.30, 124.62, 124.92, 126.17, 127.09 (Ar), 147.18 (-N-CH=N-).

14. Starting with 30 mg of **13**, the same procedure as **9a** was followed, except that the reaction solvent was CH_2Cl_2. ^{1}H NMR (C_6D_6, 500 MHz): δ 1.10 (s, 18H, -C-(CH_3)$_3$), 3.80 (d, 2H, Ar-CH_2), 4.08 (d, 2H, Ar-CH_2), 5.13 (d, 2H, -CH-$CHCl_2$), 5.64 (d, 2H, -CH-$CHCl_2$), 6.70 (m, 3H, Ar). ^{13}C NMR (C_6D_6, 125.8 MHz): δ 28.67 (-C-(CH_3)$_3$), 42.08 (Ar-CH_2), 55.25 (-C-$(CH_3)_3$), 75.87 (-CH-$CHCl_2$), 78.23 (-CH-$CHCl_2$), 118.27, 121.16, 124.76, 137.29 (Ar). Positive ion ESI-MS: *m/z* 454 (M+H).

15. Starting with 30 mg of **13**, the same procedure as **9a** was followed, except that two equivalents of NaHMDS were used. ^{1}H NMR (C_6D_6, 500 MHz): δ 1.18 (s, 9H, -C-(CH_3)$_3$), 1.29 (s, 9H, -C-(CH_3)$_3$), 3.40 (s, 3H, -O-CH_3), 3.77 (dd, 2H, Ar-CH_2), 4.05 (d, 1H, Ar-CH_2), 4.43 (d, 1H, Ar-CH_2), 6.26 (s, 1H, -CH-O-CH_3) 6.60 (d, 1H, Ar), 6.84 (m, 2H, Ar) ^{13}C NMR (C_6D_6, 125.8 MHz): δ 28.56, 29.55 (-C-(CH_3)$_3$), 39.81, 41.41 (Ar-CH_2), 53.56, 53.84 (-C-$(CH_3)_3$), 59.55 (-O-CH_3), 101.46 (-CH-O-CH_3), 121.07, 122.93, 122.98, 124.13, 125.75 (Ar), 240.14 (C:).

Attempted coordination of 15 to transition metal complexes. A solution of **15** in C_6D_6 as prepared above was treated with $PdCl_2$ (26 mg, 2.0 eq), $PdCl_2(PhCN)_2$ (53 mg, 2.0 eq), $[Ir(COD)Cl]_2$ (50 mg, 1.0 eq), $Cr(CO)_6$ (33 mg, 2.0 eq) or $Cp_2Mo_2(CO)_4$ (31 mg, 1.0 eq) and stirred overnight. In each case the ^{1}H NMR spectrum of the supernatant showed that **15** had decomposed and no reaction had occurred with the starting transition metal complex.

CHAPTER III: ATTEMPTED SYNTHESIS OF TADC STARTING FROM 3,9-DIAZAJOULIDINE

Our first attempt at synthesizing a TADC started with the known compound 3,9-diazajoulolidine, **17**. Because it had a very similar structure to our desired TADC and its synthesis was already known, it was thought that that this would provide a convenient starting point.

Precursor **17** was first synthesized by Farrar in 1964 by reacting *p*-toluidine with formaldehyde.[66] However, Farrar's procedure produced complex mixtures and only provided **17** in small quantities. A more recent paper published by Johnson, *et al*., reported the production of **17** as a by-product during the synthesis of Troger's base, **16**, using hexamethylenetetramine (HMTA) and *p*-toluidine (Scheme 3.1).[67] This methodology was synthetically much simpler, though yields were poor because it was not optimized for the synthesis of **17**. Another drawback to this synthetic approach is that it only allows for aromatic R groups that are unsubstituted ortho to the amine.

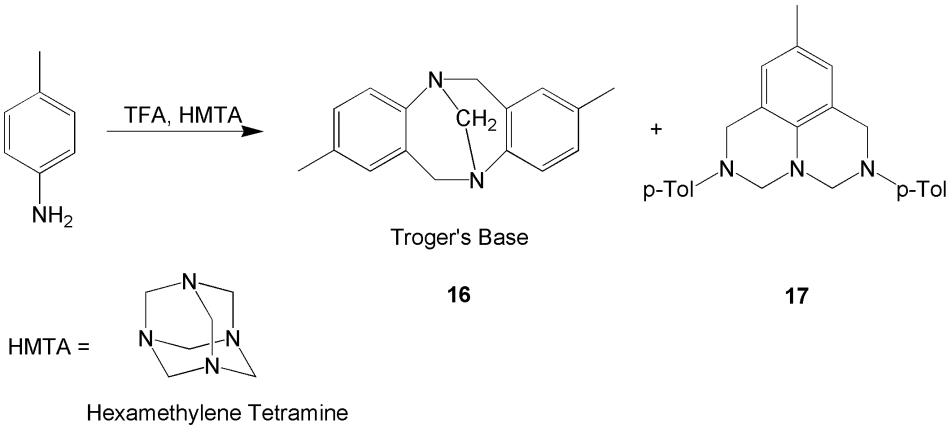

*Scheme 3.1. Synthesis of Troger's base (**16**) and 3,9-diazajoulolidine (**17**) using trifluoroacetic acid and hexamethylene tetraamine*

In order to convert **17** to a diformamidinium dication, it would be necessary to oxidize the aminal functionalities to formamidinium cations. This transformation is possible using a number of reagents, most commonly N-bromosuccinimide (NBS).[29] Addition of two equivalents of NBS to **17** should produce the diformamidinium dication **18**, a direct precursor, in theory, to the dicarbene (Scheme 3.2). Though this methodology was very limited in its possible R-groups, it seemed like a rapid path to a dicarbene.

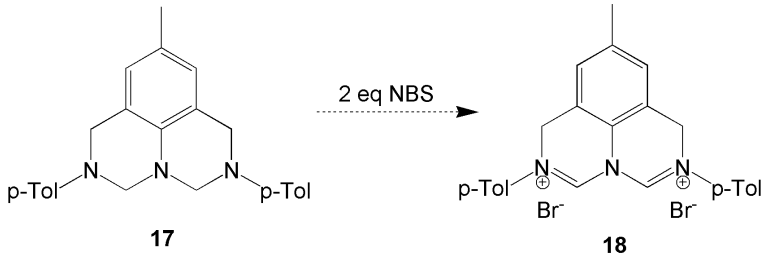

17 **18**

*Scheme 3.2. Attempted conversion of 3,9-diazajoulolidine (**17**) to the corresponding diformamidinium dication*

The first hurdle to overcome in this synthesis was optimizing the reaction of *p*-toluidine and HMTA for production of **17**. Johnson, *et al*., reported a yield of 26% by addition of trifluoroacetic acid (TFA) to a cooled, equimolar mixture of HMTA and *p*-toluidine. Isolation was accomplished via column chromatography. In our hands, it was found that the yield of **17** could be increased to 42% if the ratio of HMTA:*p*-toluidine was changed to 4:1 and the reaction was refluxed in methylene chloride. Additionally, we found that **17** could be isolated from the reaction mixture via recrystallization, greatly simplifying isolation and purification.

The next step was to oxidize the aminal to the formamidinium. When one equivalent of NBS was added to **17**, the formamidinium salt, **19a**, was obtained in good

yield (62%) (Scheme 3.3). Addition of two equivalents of NBS also resulted in the formation of **19a**, with no trace of the dication, **18**. If four equivalents of NBS were added, only brominated products were obtained, which could be expected given that NBS can brominate benzylic positions. Reactions with bromine and iodine,[68] which are also known to convert aminals to formamidiniums cations, gave similar results.

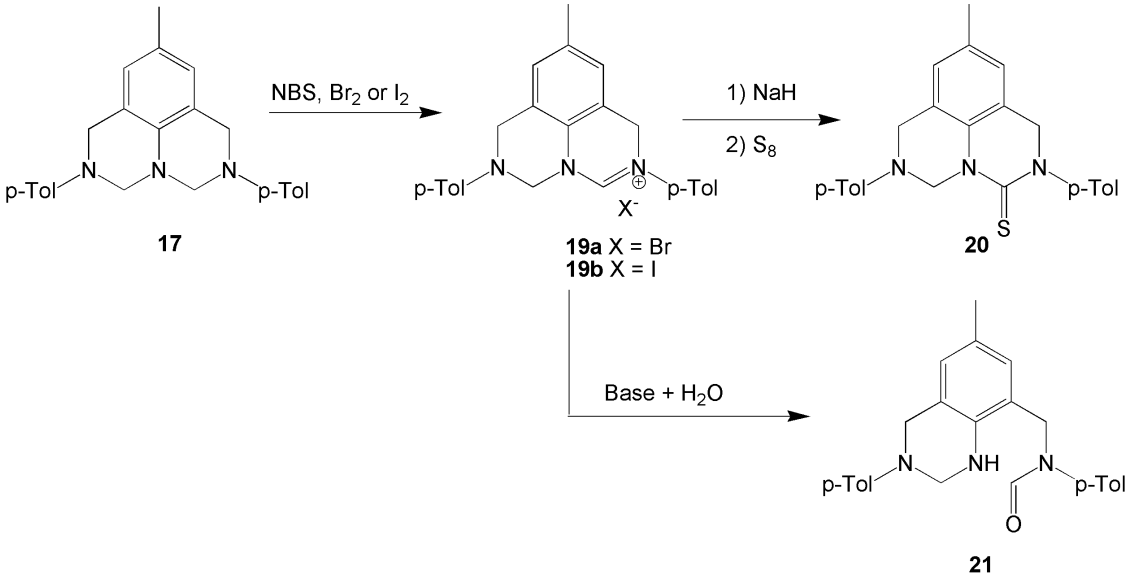

*Scheme 3.3. Synthesis of thiourea **20** from 3,9-diazajoulolidine*

An alternative way to envision this reaction is as a hydride abstraction (formally, abstraction of an H^- from an aminal creates a formamidinium cation). A reagent well-known for hydride abstraction is triphenylcarbenium tetrafluoroborate (trityl BF_4).[69] When one or two equivalents of trityl BF_4 was added to **17**, two products were formed (as shown by thin layer chromatography) (Scheme 3.4). One was colorless and the other was a very deep purple, and both had very similar structures by ^1H NMR spectroscopy. The compounds were tentatively assigned the structures **19c** and **22**. The structure of **19c** was

later confirmed by ^{1}H NMR of the anion metathesis product of **19a** with silver tetrafluoroborate.

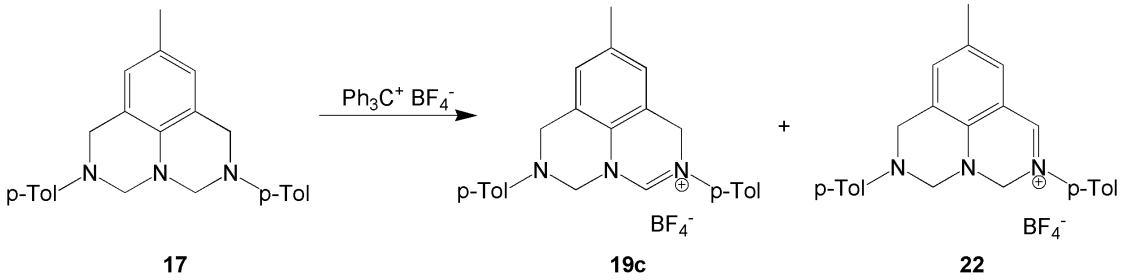

Scheme 3.4. Hydride abstraction from 3,9-diazajoulolidine using triphenylcarbenium tetrafluoroborate

Given that **17** could not be converted into the diformamidinium dication **18** under the reaction conditions that we explored, a molecule containing a formamidinium cation and a thiourea, such as **23**, was our next synthetic target. This gave the possibility of making a dicarbene stepwise via desulfurization of the thiourea, then deprotonation of the formamidinium cation, or vice versa. We started by treating **19a** with a base and then trapping the resulting NHC with S_8, affording **20** (Scheme 3.3). A number of different bases were tried, with sodium hydride with a catalytic amount of DMSO resulting in the highest yield (55%). A commonly-observed side product in this reaction was the formamide **21** (Scheme 3.3), which is produced when the NHC reacts with any water or hydroxide present in the reaction. However, when **20** was reacted with NBS, only complex mixtures were observed (Scheme 3.5). It was later discovered that NBS readily and quantitatively reacts with thioureas.[70]

Next, the possibility of directly converting **6** to the dithiobiuret was considered. Denk, *et al*., reported the conversion of cyclic formaminals to thioureas with elemental

sulfur at high temperature;[71] however, when this methodology was applied to **17,** only complex mixtures were obtained.

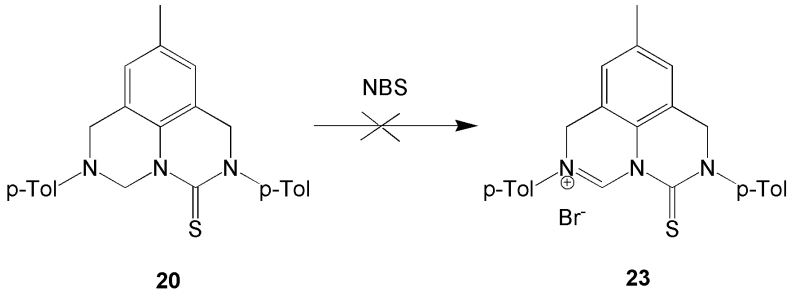

Scheme 3.5. Attempted synthesis of thiourea/formamidinium cation ***12***

Conclusions

At first, these synthetic pathways appeared to provide a simple and quick method for producing possible dicarbene precursors, however the difficulty in converting the aminal functionalities to formamidinium cations or thioureas made this methodology unusable.

Experimental

3,9-Diazajoulolidine (**17**). To a stirred suspension of p-toluidine (2.16 g, 20.0 mmol) and hexamethylene tetraamine (11.28 g, 4.0 eq) in methylene chloride (140 mL), trifluoroacetic acid (20 mL) was added. The resulting dark red solution was refluxed for 1 hour. The reaction was then cooled and treated with 10% aqueous sodium carbonate (120 mL), which turned the mixture orange. The organic phase was separated, dried over sodium carbonate, and rotovapped to dryness. This solid was then dissolved in a minimal amount of methylene chloride and washed though a short (approx. 1") silica gel column with 1:3 ethyl acetate:hexanes. This solution was rotovapped to a solid, which

was recrystallized from 1:3 ethyl acetate:hexanes. Alternatively, **17** can be isolated from the crude reaction mixture by column chromatography (1:3 ethyl acetate:hexanes, silica gel). Yield 1.02 g, 41.6%. R_f 0.36 (silica gel, 1:3 ethyl acetate:hexanes). ^{1}H NMR (DMSO-d_6, 300 MHz): δ 2.13 (s, 3H, Ar-C$\underline{H}_3$), 2.17 (s, 6H, Ar-C$\underline{H}_3$), 4.40 (s, 4H, Ar-C$\underline{H}_2$-N-), 4.54 (s, 4H, -N-C$\underline{H}_2$-N-), 6.67 (s, 2H, Ar), 7.92 (dd, 4H, Ar). ^{13}C NMR (DMSO-d_6, 75 MHz): δ 20.06, 20.31 (Ar-$\underline{C}$H$_3$), 50.11 (Ar-$\underline{C}$H$_2$-N-), 62.98 (-N-$\underline{C}$H$_2$-N-), 116.29, 119.78, 124.93, 125.72, 127.63, 129.28, 138.62, 146.69 (Ar).

Formamidinium Bromide (19a). From an aluminum foil-covered addition funnel, a solution of N-bromosuccinimide (1.43 g, 1.1 eq) in dry glyme (20 mL) was added to a solution of **6** (2.70 g, 7.31 mmol) in dry glyme (50 mL). A light blue precipitate quickly formed. This reaction mixture was stirred for 2 hours. The precipitate was then collected via filtration and dried under vacuum. Yield 2.02 g, (61.6%). ^{1}H NMR (DMSO-d_6, 300 MHz): δ 2.13 (s, 3H, Ar-C$\underline{H}_3$), 2.33 (s, 3H, Ar-C$\underline{H}_3$), 2.44 (s, 3H, Ar-C$\underline{H}_3$), 4.75 (s, 2H, Ar-C$\underline{H}_2$-N-), 5.25 (s, 2H, Ar-C$\underline{H}_2$-N-), 5.60 (s, 2H, -N-C$\underline{H}_2$-N-), 6.95 (s, 1H, Ar), 7.08 (s, 4H, Ar), 7.17 (s, 1H, Ar), 7.40 (d, 2H, Ar), 7.55 (d, 2H, Ar), 9.07 (s, 1H, -N-CH=N-).

Formamidinium Iodide (19b). Iodine (137 mg, 1.0 eq) was added to a solution of **6** (200 mg, 0.54 mmol) and triethylamine (66 mg, 1.2 eq) in dry glyme (20 mL). This very-dark mixture was stirred for 3 hours and then filtered to collect the light yellow precipitate. Yield: 176 mg, 64%. ^{1}H NMR (DMSO-d_6, 300 MHz): δ 2.19 (s, 3H, Ar-C$\underline{H}_3$), 2.29 (s, 3H, Ar-C$\underline{H}_3$), 2.38 (s, 3H, Ar-C$\underline{H}_3$), 4.78 (s, 2H, Ar-C$\underline{H}_2$-N-), 5.22 (s, 2H, Ar-C$\underline{H}_2$-N-), 5.61 (s, 2H, -N-C$\underline{H}_2$-N-), 6.95 (s, 1H, Ar), 7.08 (s, 4H, Ar), 7.17 (s, 1H, Ar), 7.40 (d, 2H, Ar), 7.55 (d, 2H, Ar), 9.03 (s, 1H, -N-CH=N-).

Formamidinium tetrafluoroborate (19c) The formamidinium bromide **8a** (2.02 g, 4.50 mmol) was suspended in dry methanol (40 mL). Dimethylformamide (DMF) was then added until all of the precipitate was dissolved (approx. 65 mL). Silver tetrafluoroborate (867 mg, 1.0 eq) was added and a precipitate quickly formed. The reaction was then rotovapped to a solid, extracted with methylene chloride, and the solution filtered through Celite. The filtrate was rotovapped to dryness. Yield 2.00g, 99%. ^{1}H NMR (DMSO-d_6, 400 MHz): δ 2.21 (s, 3H, Ar-C$\underline{H}_3$), 2.29 (s, 3H, Ar-C$\underline{H}_3$), 2.30 (s, 3H, Ar-C$\underline{H}_3$), 4.56 (s, 2H, Ar-C$\underline{H}_2$-N-), 5.02 (s, 2H, Ar-C$\underline{H}_2$-N-), 5.53 (s, 2H, -N-C$\underline{H}_2$-N-), 6.79 (s, 1H, Ar), 6.92 (d, 2H, Ar), 7.00 (s, 1H, Ar), 7.05 (d, 2H, Ar), 7.21 (d, 2H, Ar), 7.26 (s, 1H, Ar), 7.34 (d, 2H, Ar), 8.65 (s, 1H, -N-C$\underline{H}$=N-). ^{13}C NMR (DMSO-d_6, 100 MHz): 20.39, 20.91, 21.11 (Ar-$\underline{C}H_3$), 49.06, 49.47 (Ar-$\underline{C}H_2$-N-), 68.38 (-N-$\underline{C}H_2$-N-), 117.75, 117.89, 121.45, 124.44, 124.74, 125.68, 127.64, 130.18, 130.67, 131.51, 137.60, 139.05, 139.40, 143.67 (Ar), 147.47 (-N-CH=N-).

Thiourea (20). Under an atmosphere of argon, the formamidinium bromide **19a** (200 mg, 1.13 mmol) was suspended in dry THF (20 mL). Sodium hydride (60% dispersion in mineral oil, 50 mg, 1.1 eq) and dry DMSO (approx. 0.25 mL) were added and the mixture stirred for 2 hours. S_8 (40 mg, 1.1 eq (8.8 eq S)) was then added and the mixture stirred overnight. The reaction was filtered through Celite and the filtrate rotovapped to a yellow solid. The thiourea was isolated by column chromatography (1:1 ethyl acetate: hexanes, silica gel). Yield 176 mg (44%). R_f 0.72 (1:1 ethyl acetate: hexanes, silica gel). ^{1}H NMR ($CDCl_3$, 400 MHz): δ 2.26 (s, 3H, Ar-C$\underline{H}_3$), 2.28 (s, 3H, Ar-C$\underline{H}_3$), 2.39 (s, 3H, Ar-C$\underline{H}_3$), 4.54 (s, 2H, Ar-C$\underline{H}_2$-N-), 4.66 (s, 2H, Ar-C$\underline{H}_2$-N-), 5.81 (s, 2H, -N-C$\underline{H}_2$-N-),

6.69 (s, 1H, Ar), 6.90 (s, 1H, Ar), 7.08 (m, 4H, Ar), 7.05 (d, 2H, Ar), 7.25 (m, 4H, Ar). ^{13}C NMR ($CDCl_3$, 100 MHz): 20.42, 20.69, 21.18 (Ar-$\underline{C}H_3$), 50.79, 52.26 (Ar-$\underline{C}H_2$-N-), 66.71 (-N-$\underline{C}H_2$-N-), 117.54, 119.33, 121.32, 124.37, 126.57, 126.85, 129.80, 130.09, 130.33, 130.63, 133.40, 137.33, 143.78, 145.01 (Ar), 171.05 (-C=S). Positive ion ESI-MS: *m/z* 422 (M+Na).

A common byproduct of this reaction was the formamide **21**, formed when there was water or hydroxide present in the reaction. R_f 0.50 (1:1 ethyl acetate: hexanes, silica gel). ^{1}H NMR ($CDCl_3$, 400 MHz): δ 2.09 (s, 3H, Ar-C$\underline{H}_3$), 2.28 (s, 3H, Ar-C$\underline{H}_3$), 2.33 (s, 3H, Ar-C$\underline{H}_3$), 4.44 (s, 2H, Ar-C$\underline{H}_2$-N-), 4.68 (s, 2H, Ar-C$\underline{H}_2$-N-), 4.76 (s, 2H, -N-C$\underline{H}_2$-N-), 6.45 (s, 1H, Ar), 6.75 (s, 1H, Ar), 6.81 (d, 2H, Ar), 6.95 (d, 2H, Ar), 7.07 (m, 4H, Ar), 8.21 (s, 1H, -N-CO-$\underline{H}$). ^{13}C NMR ($CDCl_3$, 100 MHz): 20.33, 20.51, 20.97 (Ar-$\underline{C}H_3$), 45.96, 51.42 (Ar-$\underline{C}H_2$-N-), 62.27 (-N-$\underline{C}H_2$-N-), 117.90, 120.27, 120.87, 125.80, 126.54, 127.53, 129.66, 129.98, 130.16, 137.47, 137.49, 139.02 (Ar), 162.85 (-N-C=O).

CHAPTER IV: ORGANOMOLYBDENUM AND ORGANO-DIMOLYBENUM N-HETEROCYCLIC CARBENE COMPLEXES

As described in Chapter 1, N-heterocyclic carbenes (NHCs) are ubiquitous ligands in organometallic reagents and catalysts for organic synthesis.[2,14] NHC tunability, through changes in N-substituents and in ring size, unsaturation, and elements of the heterocycle, allows considerable control of ligand sterics and electronics. NHCs are generally described as strong σ-donors, with greater basicity than trialkylphosphines. Recent evidence has emerged that NHCs can also undergo π-backbonding from transition metals.[72] Most transition metal NHC complexes are mononuclear, with a very small number of metal-metal bonded di- and polynuclear complexes. To our knowledge there are no well-characterized metal-metal multiply-bonded complexes with NHC ligands.

One of the most studied metal-metal multiply-bonded complexes, from a small molecule reactivity perspective,[73] is the molybdenum-molybdenum triply-bonded organodimetallic $Cp_2Mo_2(CO)_4$ (Cp = cyclopentadienyl, C_5H_5) . The reactivity of other molybdenum-molybdenum triply-bonded complexes, as exemplified by $Mo_2(NEt_2)_6$[74] and $Mo_2(CH_2SiMe_3)_6$,[75] have also been studied. The Mo-Mo distance in $Cp_2Mo_2(CO)_4$, as determined by single-crystal X-ray diffractometry, is 2.448(1) Å.[76] This compound is unique in having cyclopentadienyl centroids located along the axis of the molybdenum-molybdenum bond. It also has four semi-bridging carbonyls that have led to further understanding of semi-bridging carbonyl electronics[77] and their characterization by M-CO asymmetry parameters based on structural M-C-O metrics.[78] Derivatives with pentamethylcyclopentadienyl[79] and tris(pyrazolyl)borate (Tp)[80] ligands have been

reported. A rich organometallic chemistry, for example, based on μ-phosphido derivatives of $Cp_2Mo_2(CO)_4$, has been reported recently.[81]

One specific aspect of lower-valent organodimetallic mono(cyclopentadienyl) chemistry of the Group 6 elements chromium, molybdenum, and tungsten is the generation of mononuclear organometallic radicals via scission of metal-metal bonds by thermal or photochemical methods. An initial postulate in organodimolybdenum chemistry was that compounds such as $Cp_2Mo_2(CO)_6$, with a molybdenum-molybdenum single bond, were readily cleaved to mononuclear radicals under thermal conditions; the weaker Cr-Cr bond in $Cp_2Cr_2(CO)_6$ can be cleaved photochemically.[82] This postulate is consistent with the formation of the heterodinuclear $Cp_2MoW(CO)_6$ from solution thermolysis of a mixture of $Cp_2Mo_2(CO)_6$ and $Cp_2W_2(CO)_6$.[83] However, an alternate mechanism for formation of $Cp_2Mo_2(CO)_4$ from $Cp_2Mo_2(CO)_6$, not involving M-M cleavage to radicals, has been postulated and supported experimentally.[84] While the radical $CpMo(CO)_3$ has not been isolated, isolable derivatives such as the 17-electron $TpMo(CO)_3$,[80] $TpMo(CO)_2(PEt_2Ph)$,[85] and $Tp^*Mo(CO)_3$ (Tp* = tris(3,5-dimethylpyrazolyl)borate),[86] have been reported and structurally and spectroscopically characterized.

Given the electronic similarities between carbonyl and NHC ligands, it is not surprising that NHC derivatives of mono(cyclopentadienyl) Group 6 complexes have been reported. In addition to the 18-electron $CpMo(CO)_2(IMes)H$, formed by CO substitution by an IMes (1,3-dimesitylimidazol-2-ylidene) ligand,[87] the 17-electron $CpCr(CO)_2(IMe)$ (from IMe addition to $[CpCr(CO)_3]_2$)[88] and $CpW(CO)_2(IMes)$ (of note is that $CpW(CO)_2(IMe)$ was detected in equilibrium with $[CpW(CO)_2(IMe)]_2$)[89] have

been isolated and characterized. Of relevance to this thesis, $CpMo(CO)_2(IMes)$ was characterized *in situ* by EPR spectroscopy but not isolated.[90]

Synthesis of Molybdoradicals

The reaction of $Cp_2Mo_2(CO)_4$ with two equivalents of unsaturated 1,3-dimesitylimidazol-2-ylidene (IMes) or saturated 1,3-dimesitylimidazolin-2-ylidene (SIMes) in diethyl ether at room temperature formed the yellow-orange $CpMo(CO)_2(IMes)$ (**25a)** or $CpMo(CO)_2(SIMes)$ (**25b)**, respectively, in moderate yield (44-50%) (Scheme 4.1). Both showed broad resonances in ^1H NMR spectra and two IR

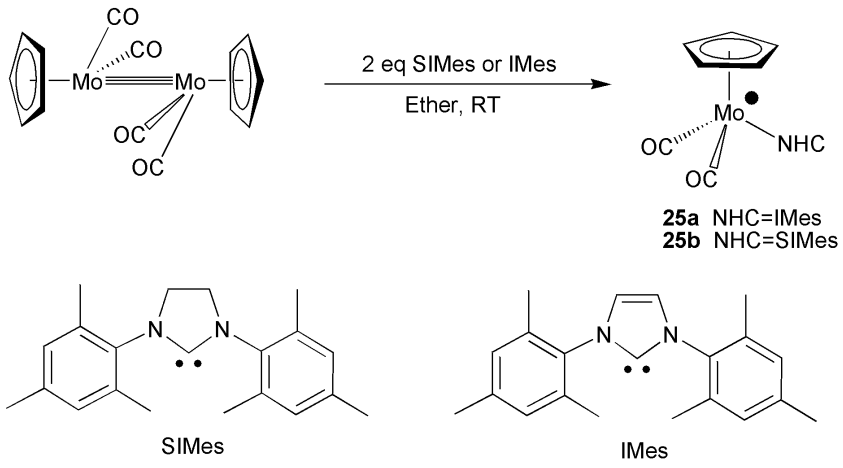

*Scheme 4.1. Synthesis of molybdoradicals **25a** and **25b***

C-O stretching frequencies consistent with C_s-symmetry. These data suggested Mo-Mo bond scission to form stable mononuclear radicals. The EPR spectra of these complexes were also recorded, confirming that these were indeed molybdenum centered radicals, with the spectrum of **25a** matching what was reported by Tumanskii, *et al*.[90] In order to ascertain the molybdoradical structural assignment, crystals of **25a** and **25b** were grown

by layering concentrated solutions in CH_2Cl_2 with hexanes at -30 ºC and studied by single-crystal X-ray diffractometry. Complex **25a** crystallized with two unique molecules in the asymmetric unit (Figure 4.1), whereas **25b** crystallized as a solvate with CH_2Cl_2 (Figure 4.2). Other than these differences and the NHC's C2-C3 bond order, the two molecules are nearly identical. The Mo-NHC bond lengths are ~2.18 Å for both, typical for low-valent Mo NHC complexes.[91]

The CO IR stretching frequencies in **25a** and **25b** provide insight into the comparative electron-donating properties of saturated vs. unsaturated five-membered ring NHCs. The IR data (Table 4.1) show a 5.3 cm^{-1} increase in the symmetric CO stretching frequencies from **25a** to **25b**, indicating the unsaturated IMes donates more electron density. This result is in agreement with other IR studies on $Ni(NHC)(CO)_3$[13] or $M(NHC)Cl(CO)_2$ (M = Rh, Ir)[92] complexes that also show IMes to be a better electron donor, though the magnitude of the difference in CO stretching frequencies is only ~ 1 cm^{-1}.

Complex	ν_{CO}, sym (cm^{-1})	ν_{CO}, asym (cm^{-1})
$CpMo(IMes)(CO)_2$ (**25a**)	1883.9 (s)	1771.5 (s)
$CpMo(SIMes)(CO)_2$ (**25b**)	1889.2 (s)	1783.4 (s)

*Table 4.1 Carbonyl IR Stretching Frequencies for **25a,b** in CH_2Cl_2*

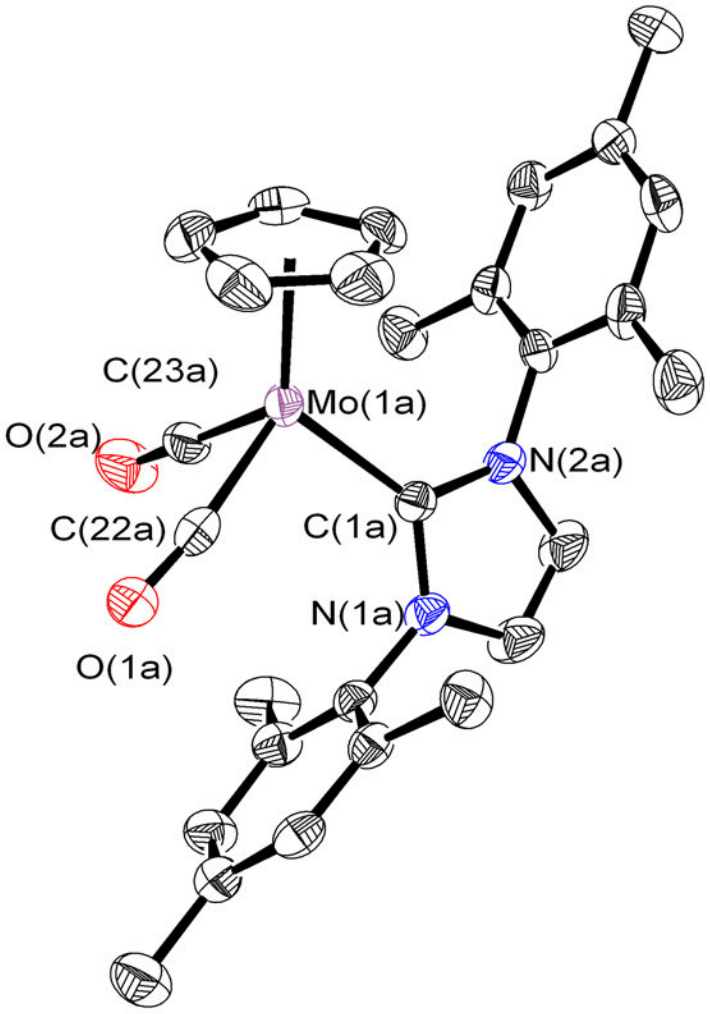

*Figure 4.1. Solid-state structure of **25a** (only one of the two unique molecules present in the asymmetric unit is pictured here, hydrogens omitted for clarity)*

	Bond Length (Å)		Angle (º)
Mo(1a)-C(1a)	2.183(4)	C(1a)-Mo(1a)-C(22a)	97.89(16)
Mo(1a)-C(22a)	1.935(5)	C(1a)-Mo(1a)-C(23a)	89.59(17)
Mo(1a)-C(23a)	1.932(4)	C(22a)-Mo(1a)-C(23a)	77.82(18)
C(22a)-O(1a)	1.178(5)	Mo(1a)-C(22a)-O(1a)	172.4(4)
C(23a)-O(2a)	1.165(5)	Mo(1a)-C(23a)-O(2a)	176.9(4)
C(1a)-N(1a)	1.374(5)	N(1a)-C(1a)-N(2a)	102.1(3)
C(1a)-N(2a)	1.378(5)		

*Table 4.2. Selected bond lengths and angles for **25a***

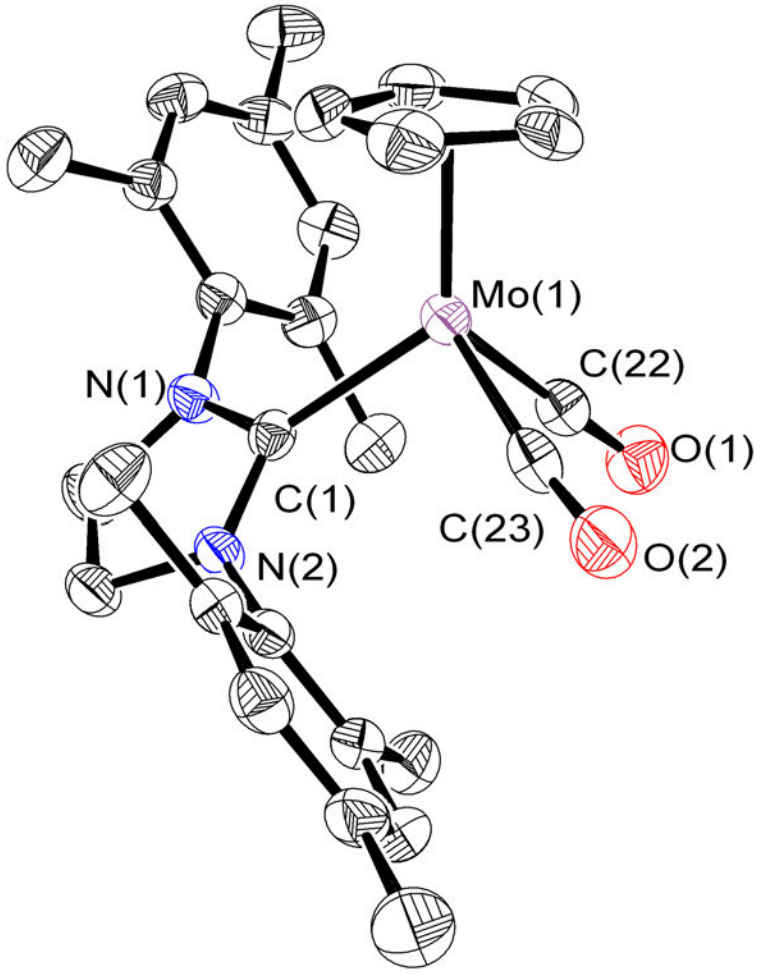

*Figure 4.2. Solid-state structure of **25b**•CH_2Cl_2 (hydrogens and lattice solvate omitted)*

	Bond Length (Å)		Angle (º)
Mo(1)-C(1)	2.177(3)	C(1)-Mo(1)-C(22)	93.20(12)
Mo(1)-C(22)	1.926(4)	C(1)-Mo(1)-C(23)	98.60(12)
Mo(1)-C(23)	1.944(4)	C(22)-Mo(1)-C(23)	77.58(14)
C(22)-O(1)	1.175(4)	Mo(1)-C(22)-O(1)	175.3(3)
C(23)-O(2)	1.167(4)	Mo(1)-C(23)-O(2)	173.2(3)
C(1)-N(1)	1.357(4)	N(1)-C(1)-N(2)	106.5(3)
C(1)-N(2)	1.350(4)		

*Table 4.3 Selected bond lengths and angles for **25b***

The superior electron-donating ability of IMes over SIMes is unexpected if only σ-donating ability is considered, given that the saturated SIMes has a higher conjugate acid pKa,[93] and is therefore a better σ -donor. However, the difference between **25a** and **25b** is likely the result of the comparative π-backbonding abilities of SIMes and IMes. The unsaturated IMes is a better net electron donor because it is also a poorer π-acceptor due to the heterocycle being aromatic. This aromaticity is disrupted if a transition metal backbonds into the π-system, so π-backbonding is therefore disfavored. Because the saturated SIMes is not aromatic, π-backbonding is not disfavored, and thus it happens more readily, leaving less electron density on the metal center. This is in agreement with studies by Nolan[72] and Bertrand[94] that have shown that π-backbonding contributes a significant portion to the NHC-metal bond for late transition metals, with π-backbonding greater for the saturated imidazolidin-2-ylidenes.

Synthesis of a Mo-Mo multiply-bonded NHC complex

It was then postulated that an NHC with less sterically-demanding N-substituents could keep the Mo-Mo bond intact. Reaction of $Cp_2Mo_2(CO)_4$ at low (-78 ºC) or room temperatures in toluene with one equivalent of unsaturated 1,3-dimethylimidazol-2-ylidene (IMe) yields a complex mixture (Scheme 4.2). The dinuclear complex

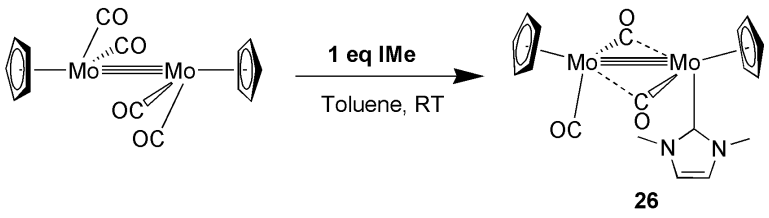

Scheme 4.2. Synthesis of **26**

$Cp_2Mo_2(CO)_3(IMe)$ (**26**) was isolated from the reaction mixture in low yield (20%). Crystals suitable for X-ray diffraction were grown from CH_2Cl_2 solution layered with toluene at -30º C. The solid-state structure (Figure 4.3) has a Mo-Mo distance of 2.5461(7) Å, ~0.1 Å longer than in $Cp_2Mo_2(CO)_4$,[76] and contains two semi-bridging and one terminal carbonyl. Similar to **25a** and **25b**, the Mo-NHC distance is 2.181(4). To the best of our knowledge, this is the first example of an NHC ligand in a metal-metal multiply-bound dinuclear compound (there is one example[95] of a dinuclear compound, heterodinuclear in this case, with a postulated metal-metal double bond observed in solution by spectroscopy).

At room temperature, the ^1H NMR spectrum of **26** in pyridine-d_5 (and in toluene-d_8) shows two broad signals for the cyclopentadienyl (Cp) groups that coalesce to a single resonance at 50 ºC (Figure 4.4). This is consistent with a fluxional process where the carbene is migrating between the two metal centers, as is common for CO ligands in dinuclear transition metal complexes, via an intermediate with a μ-IMe ligand. There is precedent for μ-NHCs in Cu and Ag complexes.[96] The CO ligands themselves are also highly fluxional, giving a single broad ^{13}C NMR resonance, even at low temperatures (-35 ºC).

During the reaction of IMe and $Cp_2Mo_2(CO)_4$, a vibrant orange precipitate was observed. The yield of this precipitate was maximized when four equivalents of IMe were used. ^1H and ^{13}C NMR spectroscopy showed a diamagnetic molecule that had a Cp:IMe ratio of 1:2. Next, it was observed that this complex was stable to, and quite soluble in, water. This allowed for a single crystal to be grown from a water/THF

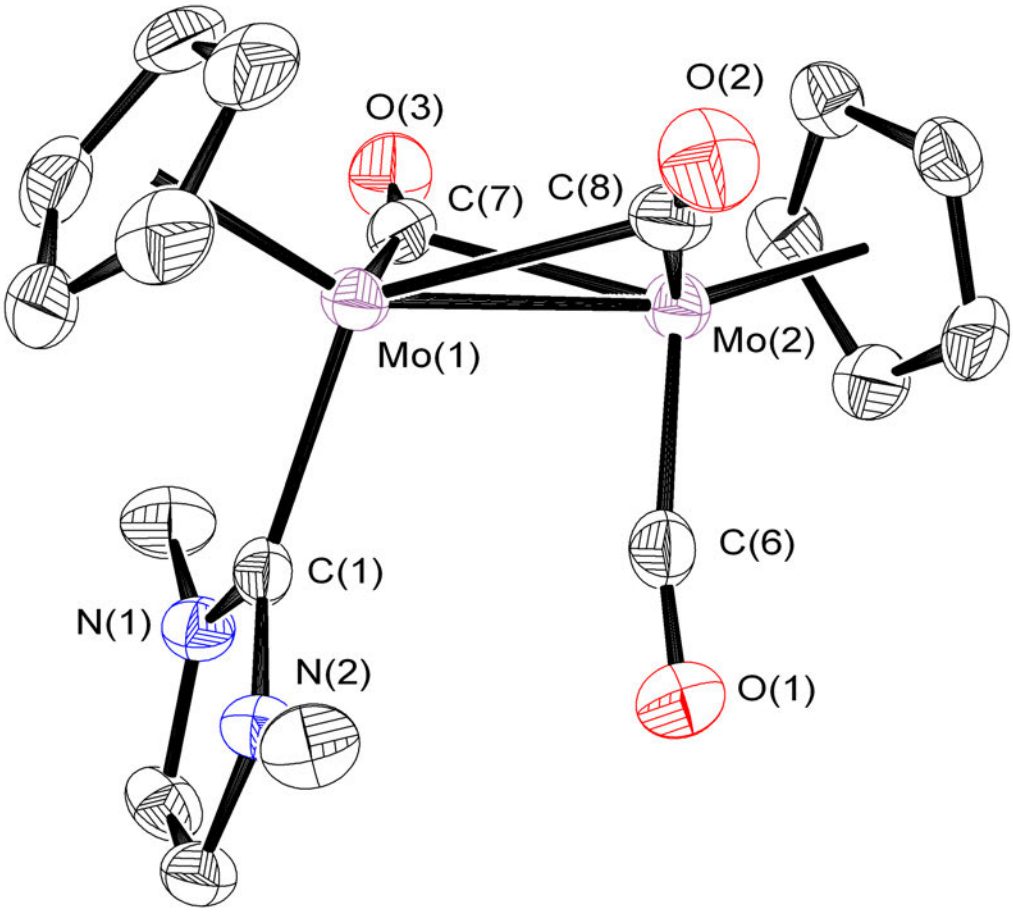

*Figure 4.3. Solid state structure of **26** (hydrogens omitted for clarity)*

	Bond Length (Å)		Angle (º)
Mo(1)-Mo(2)	2.5464(5)	Mo(2)-C(6)-O(1)	170.2(4)
Mo(1)-C(1)	2.181(4)	Mo(1)-C(7)-O(3)	163.9(4)
Mo(1)-C(7)	1.916(5)	Mo(2)-C(8)-O(2)	165.8(4)
Mo(1)-C(8)	2.510(5)	Mo(2)-Mo(1)-C(1)	102.91(10)
Mo(2)-C(6)	1.942(5)		
Mo(2)-C(8)	1.943(5)		
C(6)-O(1)	1.157(5)		
C(7)-O(3)	1.89(5)		
C(8)-O(2)	1.178(5)		

*Table 4.4. Selected bond lengths and angles for **26***

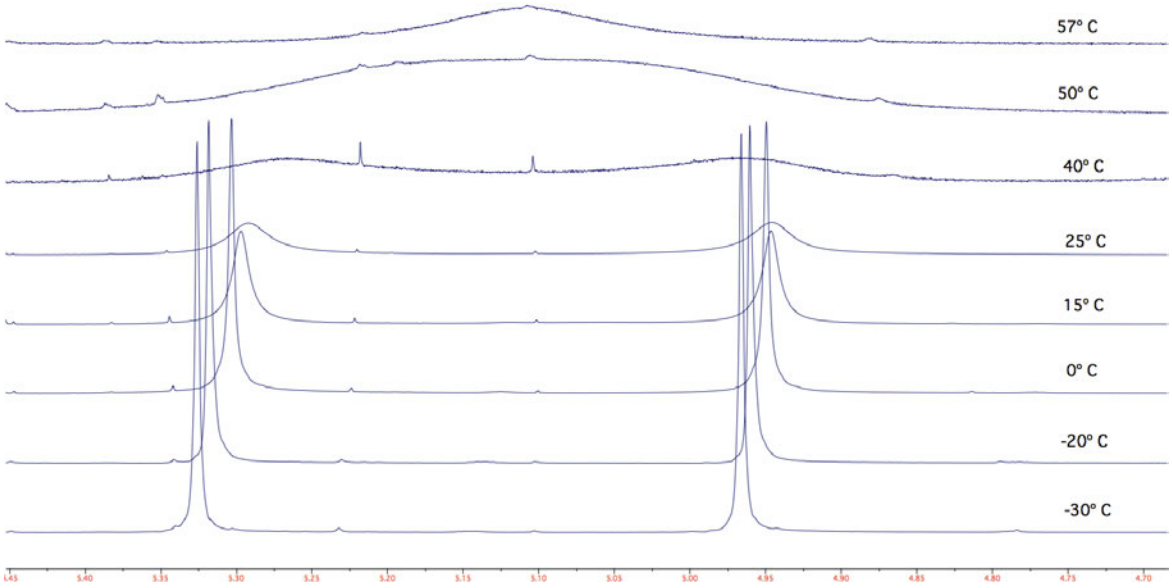

*Figure 4.4. Variable-temperature ^{1}H NMR spectra of the Cp groups on **26** in pyridine-d_5*

mixture at 0 ºC. This crystal was analyzed by single crystal X-ray diffractometry (Figure 4.5), which showed it to be the ionic, four-legged piano-stool complex *cis*-$[CpMo(CO)_2(IMe)_2]Cl$ (**27**) (Scheme 4.3). Unfortunately, the crystal was of poor quality, resulting in a high R-value, and making discussion of bond distances and angles inappropriate.

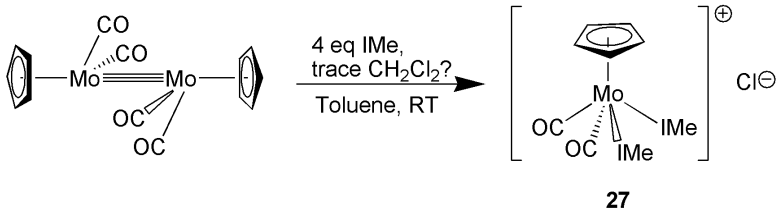

*Scheme 4.3. Synthesis of **27***

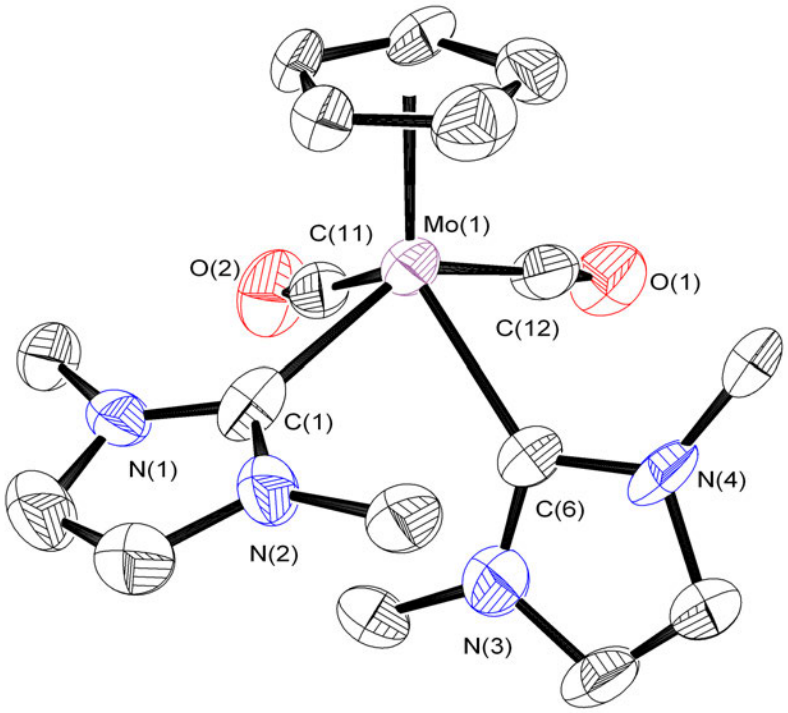

*Figure 4.5. Structure of **27** (Solvent, chloride, and hydrogen atoms omitted for clarity)*

The formation of **27** came as a bit of a surprise, given that no chlorine-containing compounds were intentionally added to the reaction. This led us to conclude that the source of the chlorine was probably adventitious CH_2Cl_2, which was a commonly-used solvent in the glove box where these syntheses were performed. The reaction likely proceeds via reaction of $Cp_2Mo_2(CO)_4$ with four equivalents of IMe to form the $CpMo(CO)_2(IMe)_2$ radical, which could abstract a chlorine atom from CH_2Cl_2, forming **27.**

Comparing **27** to $[CpMo(CO)_2(IMes)][BAr^F]$[87] shows that **27** has a lower carbonyl IR stretching frequency by 22 cm^{-1}, indicating that **27** is much more electron rich. This is to be expected as **27** has two NHC ligands, while $[CpMo(CO)_2(IMes)][BAr^F]$ only has one.

Conclusions

Reaction of $Cp_2Mo_2(CO)_4$ with the sterically-demanding NHCs IMes and SIMes yielded the molybdoradicals $CpMo(CO)_2$(IMes) (**25a)** or $CpMo(CO)_2$(SIMes) (**25b)**. By studying the carbonyl IR stretching frequencies, we were able to determine that IMes is a better electron donating ligand, most likely due to its poor π-backbonding ability. When the less sterically-demanding NHC IMe was reacted with $Cp_2Mo_2(CO)_4$, the complex $Cp_2Mo_2(CO)_3$(IMe) (**26**) could be isolated from the complex reaction mixture. This represents the first example of a metal-metal multiply bonded NHC complex that has been isolated and structurally characterized. Going forward, this reaction should be studied in greater depth, with the other product(s) being isolated and characterized. These compounds, especially the ones with Mo-Mo multiple bonds, should be tested for small molecule reactivity.

Experimental

All experiments were preformed in a dinitrogen atmosphere glovebox. Toluene and diethyl ether were purchased anhydrous from Sigma-Aldrich and used as recived. SIMes was purchased from Strem Chemicals and used as received. $Cp_2Mo_2(CO)_4$[83], IMe[97], and IMes[27] were prepared using known literature procedures. C_6D_6 was dried over sodium. A Waters Q-TOF Premier mass spectrometer was used to obtain high-resolution ESI-MS data. A Water GCT Premier mass spectrometer was used to obtain high-resolution EI-MS data. NMR spectra were recorded on a Bruker AVANCE 500 MHz instrument. Chemical shifts are expressed in parts per million (δ scale) downfield from tetramethylsilane and are referenced to the residual proton resonance in the deuterated

NMR solvent (C_6D_5H: δ 7.15; pyridine-d_4H: δ 8.74; D_2O: δ 4.80) or the solvent ^{13}C resonance (C_6D_6: δ 128.36, pyridine-d_5: δ 150.35).

$CpMo(IMes)(CO)_2$ (25a). To a stirred solution of $Cp_2Mo_2(CO)_4$ (50 mg, 0.115 mmol) in diethyl ether (10 mL), IMes (for **25a**) or SIMes (for **25b**) (70 mg, 0.230 mmol) in 1 mL diethyl ether was added dropwise over 1 minute and the dark solution stirred at room temperature for 2 hours. The volume of the solution was rotovapped to a reduced volume (~ 2 mL) and placed in the freezer overnight (-30 ºC). Yellow/orange crystals were collected by filtration to give **25a** (53 mg, 44% yield). ^1H NMR (C_6D_6, 500 MHz, integrations are approximate): δ -4.37 (br, 5H, $C_5\underline{H}_5$), 2.21 (br, 12H, Ar-$C\underline{H}_3$), 6.54 (br, Ar-$C\underline{H}_3$), 8.38 (br, 4H, Ar), 18.50 (br, 2H, -N-$C\underline{H}$=$C\underline{H}$-N-). High resolution EI-MS: $MoC_{28}O_2N_2H_{29}$, calculated 521.1288, found 521.1285 (M^+). IR (cm^{-1}, CH_2Cl_2): 1883.9, 1771.5 (ν_{CO}). EPR (toluene, 298 K): g = 2.061.

$CpMo(SIMes)(CO)_2$ (25b). The same procedure as **25a** was followed, except that SIMes was used. A 50% yield of **25b** was obtained. ^1H NMR (C_6D_6, 500 MHz, integrations are approximate): δ -3.83 (br, 5H, $C_5\underline{H}_5$), 3.33 (br, 12H, Ar-$C\underline{H}_3$), 8.14 (br, 10H, Ar-$C\underline{H}_3$ and –N-$C\underline{H}_2$-$C\underline{H}_2$-N-). High resolution EI-MS: $MoC_{28}O_2N_2H_{29}$, calculated 523.1473, found 523.1444 (M^+). IR (cm^{-1}, CH_2Cl_2): 1889.2, 1783.4(ν_{CO}). EPR (toluene, 298 K): g = 2.057.

$Cp_2Mo_2(IMe)(CO)_3$ (26). To a solution of $Cp_2Mo_2(CO)_4$ (50 mg, mmol) in 4 mL toluene, N,N'-dimethylimidazolium-2-ylidene (IMe, 11 mg, 1.0 eq) in 1 mL of toluene was added. This dark mixture was stirred for two hours and then filtered to remove any solids. The filtrate was rotovapped to a dark solid, which was extracted with 10 mL diethyl ether.

The remaining solid was collected by filtration, providing **26** (12 mg, 20%) as a dark solid. ^{1}H NMR (pyridine-d_5, 500 MHz): 3.87 (N-C<u>H</u>$_3$), 4.98 (br, 5H, C$_5$<u>H</u>$_5$), 5.33 (br, 5H, C$_5$<u>H</u>$_5$), 7.37 (s, 2H, -N-C<u>H</u>=C<u>H</u>-N-). ^{13}C NMR (pyridine-d_5, 125.8 MHz): 41.00 (N-<u>C</u>H$_3$), 91.80 (br, <u>C</u>$_5$H$_5$), 92.24 (br, <u>C</u>$_5$H$_5$), 124.82 (-N-<u>C</u>H=<u>C</u>H-N-), 188.31 (-N-<u>C</u>:-N-), 251.74 (br, Mo-<u>C</u>=O). High resolution EI-MS: $Mo_2N_2O_3C_{18}H_{18}$ calculated: 499.9436, found: 499.9463.

We observed a side product of this reaction, **[CpMo(CO)$_2$(IMe)$_2$]Cl** (**27**), as a bright orange precipitate. ^{1}H NMR (D_2O, 300 MHz): δ 3.33 (br, 12H, N-C<u>H</u>$_3$), 5.61 (s, 5H, C$_5$<u>H</u>$_5$), 7.24 (s, 4H, -N-C<u>H</u>=C<u>H</u>-N-). IR (cm^{-1}, CH_2Cl_2): 1977.6, 1856.5 (ν_{CO}). High resolution ESI-MS: $MoN_4C_{17}O_2H_{21}$ calculated: 411.0722, found: 411.0704

REFERENCES

(1) Arduengo III, A.; Harlow, R.; Kline, M. *J. Am. Chem. Soc.* **1991**, *113*, 361.

(2) (a) Nolan, S. P. *N-Heterocyclic Carbenes in Synthesis*; Wiley, 2006 (b) Díez-González, S. *N-heterocyclic Carbenes: From Laboratory Curiosities to Efficient Synthetic Tools*; RSC Pub., 2011.

(3) Iwamoto, E.; Hirai, K.; Tomioka, H. *J. Am. Chem. Soc.* **2003**, *125*, 14664.

(4) Canac, Y.; Soleilhavoup, M.; Conejero, S.; Bertrand, G. *J. Organomet. Chem.* **2004**, *689*, 3857.

(5) Lappert, M. F. *J. Organomet. Chem.* **1988**, *358*, 185.

(6) Taylor, T. E.; Hall, M. B. *J. Am. Chem. Soc.* **1984**, *106*, 1576.

(7) Alder, R.; Blake, M.; Chaker, L.; Harvey, J.; Paolini, F.; Schütz, J. *Angew. Chem. Int. Ed.* **2004**, *43*, 5896.

(8) Denk, M. K.; Hezarkhani, A.; Zheng, F.-L. *Eur. J. Inorg. Chem.* **2007**, 3527.

(9) Alder, R.; Blake, M.; Bortolotti, C.; Bufali, S.; Butts, C.; Linehan, E.; Oliva, J.; Orpen, A.; Quayle, M. *Chem. Commun.* **1999**, 1049.

(10) Magill, A.; Cavell, K.; Yates, B. *J. Am. Chem. Soc.* **2004**, *126*, 8717.

(11) Fèvre, M.; Pinaud, J.; Gnanou, Y.; Vignolle, J.; Taton, D. *Chem. Soc. Rev.* **2013**, *42*, 2142.

(12) Denk, M. K.; Rodezno, J. M.; Gupta, S.; Lough, A. J. *J. Organomet. Chem.* **2001**, *617–618*, 242.

(13) Dorta, R.; Stevens, E.; Scott, N.; Costabile, C.; Cavallo, L.; Hoff, C.; Nolan, S. *J. Am. Chem. Soc.* **2005**, *127*, 2485.

(14) de Fremont, P.; Marion, N.; Nolan, S. P. *Coord. Chem. Rev.* **2009**, *253*, 862.

(15) Glorius, F.; Peris, E. *Top. Organomet. Chem.* **2007**, *21*, 83.

(16) Hahn, F. E.; Jahnke, M. C. *Angew. Chem. Int. Ed.* **2008**, *47*, 3122.

(17) Cetinkaya, B.; Cetinkaya, E.; A. Chamizo, J.; B. Hitchcock, P.; A. Jasim, H.; Kucukbay, H.; F. Lappert, M. *Perkin Trans.* **1998**, 2047.

(18) Hahn, F.; Wittenbecher, L.; Boese, R.; Bläser, D. *Chem. Eur. J* **1999**, *5*, 1931.

(19) Poyatos, M.; Mata, J. A.; Falomir, E.; Crabtree, R. H.; Peris, E. *Organometallics* **2003**, *22*, 1110.

(20) Lee, H. M.; Chiu, P. L.; Zeng, J. Y. *Inorg. Chim. Acta* **2004**, *357*, 4313.

(21) Sémeril, D.; Bruneau, C.; Dixneuf, P. H. *Advanced Synthesis & Catalysis* **2002**, *344*, 585.

(22) Grundemann, S.; Kovacevic, A.; Albrecht, M.; Faller Robert, J. W.; Crabtree, H. *Chem. Commun.* **2001**, 2274.

(23) Weskamp, T.; Böhm, V. P. W.; Herrmann, W. A. *J. Organomet. Chem.* **2000**, *600*, 12.

(24) Romain, C.; Miqueu, K.; Sotiropoulos, J.-M.; Bellemin-Laponnaz, S.; Dagorne, S. *Angew. Chem. Int. Ed.* **2010**, *49*, 2198.

(25) Spencer, L.; Beddie, C.; Hall, M.; Fryzuk, M. *J. Am. Chem. Soc.* **2006**, *128*, 12531.

(26) Wang, H.; Lin, I. *Organometallics* **1998**, *17*, 972.

(27) Bantreil, X.; Nolan, S. P. *Nature Protocols* **2011**, *6*, 69.

(28) Herrmann, W. A. *Angew. Chem. Int. Ed.* **2002**, *41*, 1290.

(29) Mayr, M.; Wurst, K.; Ongania, K.; Buchmeiser, M. *Chem. Eur. J* **2004**, *10*, 2622.

(30) Blake, G.; Moerdyk, J.; Bielawski, C. *Organometallics* **2012**, *31*, 3373.

(31) Alder, R.; Blake, M.; Bufali, S.; Butts, C.; Orpen, A.; Schutz, J.; Williams, S. *Perkin Trans.* **2001**, 1586.

(32) Salerno, A.; Caterina, C.; Perillo, I. *Synthetic Commun.* **2000**, *30*, 3369.

(33) Davies, S.; Mortlock, A. *Tetrahedron* **1993**, *49*, 4419.

(34) Scholl, M.; Ding, S.; Lee, C.; Grubbs, R. *Org. Lett.* **1999**, *1*, 953.

(35) Vougioukalakis, G.; Grubbs, R. *Chem. Rev.* **2010**, *110*, 1746.

(36) Roy, S.; Plenio, H. *Advanced Synthesis & Catalysis* **2010**, *352*, 1014.

(37) Iwamoto, K.-i.; Hamaya, M.; Hashimoto, N.; Kimura, H.; Suzuki, Y.; Sato, M. *Tet. Lett.* **2006**, *47*, 7175.

(38) Grossmann, A.; Enders, D. *Angew. Chem. Int. Ed.* **2012**, *51*, 314.

(39) Poyatos, M.; Mata, J.; Peris, E. *Chem. Rev.* **2009**, *109*, 3677.

(40) Mata, J. A.; Poyatos, M.; Peris, E. *Coord. Chem. Rev.* **2007**, *251*, 841.

(41) Boydston, A. J.; Bielawski, C. W. *Dalton Trans.* **2006**, 4073.

(42) Tennyson, A. G.; Rosen, E. L.; Collins, M. S.; Lynch, V. M.; Bielawski, C. W. *Inorg. Chem.* **2009**, *48*, 6924.

(43) Williams, K. A.; Boydston, A. J.; Bielawski, C. W. *J. Royal Soc. Interface* **2007**, *4*, 359.

(44) Guerret, O.; Sol, S.; Gornitzka, H.; Teichert, M.; Trinquier, G.; Bertrand, G. *J. Am. Chem. Soc* **1997**, *119*, 6668.

(45) Mas-Marzá, E.; Mata, J. A.; Peris, E. *Angew. Chem. Int. Ed.* **2007**, *46*, 3729.

(46) Cotton, F. A. *Inorg. Chem.* **1998**, *37*, 5710.

(47) Cotton, F. A.; Daniels, L. M.; Murillo, C. A.; Timmons, D. J.; Wilkinson, C. C. *J. Am. Chem. Soc.* **2002**, *124*, 9249.

(48) Chisholm, M. H.; Gallucci, J.; Hadad, C. M.; Huffman, J. C.; Wilson, P. J. *J. Am. Chem. Soc.* **2003**, *125*, 16040.

(49) Cotton, F. A.; Gruhn, N. E.; Gu, J.; Huang, P.; Lichtenberger, D. L.; Murillo, C. A.; Van Dorn, L. O.; Wilkinson, C. C. *Science* **2002**, *298*, 1971.

(50) Connelly, N. G.; Geiger, W. E. *Chem. Rev.* **1996**, *96*, 877.

(51) Cotton, F. A.; Murillo, C. A.; Wang, X.; Wilkinson, C. C. *Dalton Trans.* **2006**, 4623.

(52) Pavia, M.; Moos, W.; Hershenson, F. *J. Org. Chem.* **1990**, *55*, 560.

(53) Narasimhan, S.; Balakumar, R. *Synthetic Commun.* **2000**, *30*, 4387.

(54) Andersson, P.; Munslow, I. *Modern reduction methods*, Wiley, 2008.

(55) Yamaguchi, Y.; Kashiwabara, T.; Ogata, K.; Miura, Y.; Nakamura, Y.; Kobayashi, K.; Ito, T. *Chem. Commun.* **2004**, 2160.

(56) Tapu, D.; Dixon, D.; Roe, C. *Chem. Rev.* **2009**, *109*, 3385.

(57) Lloyd-Jones, G.; Alder, R.; Owen-Smith, G. *Chem. Eur. J.* **2006**, *12*, 5361.

(58) Schulz, T.; Leibold, M.; Färber, C.; Maurer, M.; Porsch, T.; Holthausen, M.; Siemeling, U. *Chem. Commun.* **2012**, *48*, 9123.

(59) Grundemann, S.; Kovacevic, A.; Albrecht, M.; Faller, J. W.; Crabtree, R. H. *J. Am. Chem. Soc.* **2002**, *124*, 10473.

(60) Wilson, R. B.; Sattelberger, A. P.; Huffman, J. C. *J. Am. Chem. Soc.* **1982**, *104*, 858.

(61) Arduengo III, A. J.; Davidson, F.; Krafczyk, R.; Marshall, W. J.; Schmutzler, R. *Monatsh. Chem.* **2000**, *131*, 251.

(62) Anderson, G. K.; Lin, M.; Sen, A.; Gretz, E. In *Inorganic Syntheses*; John Wiley & Sons, Inc., **1990,** Vol. 28., 60.

(63) Diamond, G.; Jordan, R.; Petersen, J. *J. Am. Chem. Soc.* **1996**, *118*, 8024.

(64) Zucchini, U.; Albizzati, E.; Giannini, U. *J. Organomet. Chem.* **1971**, *26*, 357.

(65) Chatt, J.; Coffey, R. S.; Shaw, B. L. *J. Chem. Soc.* **1965**, 7391.

(66) Farrar, W. *J. Appl. Chem.* **1964**, *14*, 389.

(67) Johnson, R.; Gorman, R.; Wnuk, R.; Crittenden, N.; Aiken, J. *J. Med. Chem.* **1993**, *36*, 3202.

(68) Pytkowicz, J.; Roland, S.; Mangeney, P. *J. Organomet. Chem.* **2001**, *631*, 157.

(69) Damico, R.; Broaddus, C. *J. Org. Chem.* **1966**, *31*, 1607.

(70) Tiwari, R.; Pande, U. *Analyst* **1969**, *94*, 813.

(71) Denk, M.; Gupta, S.; Brownie, J.; Tajammul, S.; Lough, A. *Chem. Eur. J* **2001**, *7*, 4477.

(72) Fantasia, S.; Petersen, J. L.; Jacobsen, H.; Cavallo, L.; Nolan, S. P. *Organometallics* **2007**, *26*, 5880.

(73) (a) Curtis M, D.; Messerle, L.; Fotinos Nicephoros, A.; Gerlach Robert, F. In *Reactivity of Metal-Metal Bonds*; American Chemical Society, 1981; Vol. 155 (b) Curtis, M. D. *Polyhedron* **1987**, *6*, 759.

(74) Chisholm, M.; Cotton, F. A.; Frenz, B. A.; Shive, L. *J. Chem. Soc., Chem. Commun.* **1974**, *0*, 480.

(75) Huq, F.; Mowat, W.; Shortland, A.; Skapski, A. C.; Wilkinson, G. *J. Chem. Soc., Chem. Commun.* **1971**, 1079.

(76) Klingler, R.; Butler, W.; Curtis, M. *J. Am. Chem. Soc.* **1978**, *100*, 5034.

(77) Morris-Sherwood, B. J.; Powell, C. B.; Hall, M. B. *J. Am. Chem. Soc.* **1984**, *106*, 5079.

(78) Horwitz, C. P.; Shriver, D. F. In *Advances in Organometallic Chemistry*; Stone, F. G. A., Robert, W., Eds.; Academic Press, **1984**; Vol. Volume 23.

(79) Huang, J.-S.; Dahl, L. F. *J. Organomet. Chem.* **1983**, *243*, 57.

(80) Curtis, M. D.; Shiu, K. B.; Butler, W. M.; Huffman, J. C. *J. Am. Chem. Soc.* **1986**, *108*, 3335.

(81) García, M. E.; Melón, S.; Ramos, A.; Ruiz, M. A. *Dalton Trans.* **2009**, 8171.

(82) McLain, S. J. *J. Am. Chem. Soc.* **1988**, *110*, 643.

(83) Curtis, M. D.; Fotinos, N. A.; Messerle, L.; Sattelberger, A. P. *Inorg. Chem.* **1983**, *22*, 1559.

(84) Turaki, N. N.; Huggins, J. M. *Organometallics* **1985**, *4*, 1766.

(85) MacNeil, J. H.; Roszak, A. W.; Baird, M. C.; Preston, K. F.; Rheingold, A. L. *Organometallics* **1993**, *12*, 4402.

(86) Protasiewicz, J. D.; Theopold, K. H. *J. Am. Chem. Soc.* **1993**, *115*, 5559.

(87) Wu, F.; Dioumaev, V.; Szalda, D.; Hanson, J.; Bullock, R. *Organometallics* **2007**, *26*, 5079.

(88) Eide, E.; Hou, G.; Deng, S.; Wen, H.; Yang, P. **2013**.

(89) van der Eide, E.; Liu, T.; Camaioni, D.; Walter, E.; Bullock, R. *Organometallics* **2012**, *31*, 1775.

(90) Tumanskii, B.; Sheberla, D.; Molev, G.; Apeloig, Y. *Angew. Chem. Int. Ed.* **2007**, *46*, 7408.

(91) Li, S.; Kee, C. W.; Huang, K.-W.; Hor, T. S. A.; Zhao, J. *Organometallics* **2010**, *29*, 1924.

(92) Wolf, S.; Plenio, H. *J. Organomet. Chem.* **2009**, *694*, 1487.

(93) Higgins, E. M.; Sherwood, J. A.; Lindsay, A. G.; Armstrong, J.; Massey, R. S.; Alder, R. W.; O'donoghue, A. C. *Chem. Commun.* **2011**, *47*, 1559.

(94) Back, O.; Henry-Ellinger, M.; Martin, C. D.; Martin, D.; Bertrand, G. *Angew. Chem. Int. Ed.* **2013**, *52*, 2939.

(95) Wells, K.; McDonald, R.; Ferguson, M.; Cowie, M. *Organometallics* **2011**, *30*, 2654.

(96) (a) Chen, C.; Qiu, H.; Chen, W. *J. Organomet. Chem.* **2012**, *696*, 4166 (b) Catalano, V.; Munro, L.; Strasser, C.; Samin, A. *Inorg. Chem.* **2011**, *50*, 8465.

(97) Schaub, T.; Backes, M.; Radius, U. *Organometallics* **2006**, *25*, 4196.

APPENDIX A

CRYSTALLOGRAPHIC DATA FOR **7a**

Crystal data and structure refinement for mes1120 (**7a**)

Identification code	mes1120
Empirical formula	C16 H23 B2 F8 N3
Formula weight	430.99
Temperature	210(2) K
Wavelength	0.71073 Å
Crystal system	P 2_1/c
Unit cell dimensions	a = 8.2143(9) Å α= 90°
	b = 23.487(3) Å β= 93.013(5)°
	c = 10.1190(11) Å γ= 90°
Volume	1949.6(4) A^3
Z, Calculated density	4, 1.468 Mg/m^3
Absorption coefficient	0.140 mm^{-1}
F(000)	888
Crystal size	0.38 x 0.28 x 0.28 mm
Theta range for data collection	2.63 to 28.09°
Limiting indices	-10<=h<=10, -30<=k<=30, -13<=l<=13
Reflections collected / unique	15503 / 4680 [R(int) = 0.0297]
Completeness to theta = 28.09	98.6 %
Max. and min. transmission	0.9619 and 0.9487
Refinement method	Full-matrix least-squares on F^2
Data / restraints / parameters	4680 / 222 / 369
Goodness-of-fit on F F^2	1.062

Final R indices [I>2sigma(I)]	R1 = 0.0570, wR2 = 0.1556
R indices (all data)	R1 = 0.0779, wR2 = 0.1720
Largest diff. peak and hole	0.274 and -0.324 e.A^{-3}

Atomic coordinates (x 10^4) and equivalent isotropic displacement parameters ($Å^2$ x 10^3) for mes1120. U(eq) is defined as one third of the trace of the orthogonalized U^{ij} tensor.

	x	y	z	U(eq)
N(3)	-1622(2)	720(1)	8007(2)	36(1)
N(1)	1943(2)	1567(1)	5227(1)	33(1)
C(2)	-427(2)	722(1)	7250(2)	34(1)
N(2)	108(2)	1195(1)	6650(1)	32(1)
C(14)	-1957(2)	1754(1)	7641(2)	39(1)
C(1)	1394(2)	1150(1)	5878(2)	32(1)
C(15)	-689(2)	1728(1)	6808(2)	33(1)
C(10)	-139(2)	2194(1)	6135(2)	35(1)
C(11)	-888(2)	2712(1)	6330(2)	44(1)
C(16)	-2517(3)	1233(1)	8345(3)	55(1)
C(3)	3417(2)	1477(1)	4443(2)	41(1)
C(13)	-2697(3)	2274(1)	7817(2)	48(1)
C(6)	-2178(3)	168(1)	8568(3)	55(1)
C(12)	-2152(3)	2750(1)	7168(2)	51(1)
C(5)	4806(3)	1828(1)	5050(3)	58(1)
C(9)	1237(3)	2143(1)	5231(2)	47(1)
C(4)	3031(3)	1600(1)	3003(2)	62(1)
C(7)	-3736(3)	-13(1)	7827(4)	82(1)
C(8)	-2302(4)	224(2)	10044(3)	90(1)
B(15)	2977(5)	1490(2)	9000(6)	42(1)
F(6)	3514(10)	1031(2)	8273(8)	54(1)
F(10)	1571(7)	1337(4)	9619(8)	67(1)
F(11)	4182(8)	1643(4)	9950(6)	61(1)
F(12)	2644(12)	1948(2)	8159(6)	53(1)
B(15')	2992(7)	1468(3)	8976(8)	42(1)
F(6')	3128(17)	1954(3)	8206(11)	59(2)
F(12')	3108(16)	987(3)	8183(10)	48(2)
F(11')	4238(11)	1461(7)	9960(9)	66(2)
F(10')	1494(10)	1469(5)	9555(11)	59(2)
B(27)	-2193(5)	598(2)	3767(5)	59(1)

F(24)	-2646(9)	688(3)	5055(4)	62(2)
F(25)	-2370(11)	25(2)	3451(8)	65(2)
F(26)	-3181(8)	922(2)	2899(5)	52(2)
F(28)	-576(6)	758(5)	3664(8)	107(3)
B(27')	-1863(11)	650(3)	3706(8)	59(1)
F(51)	-584(15)	575(6)	2877(14)	78(4)
F(52)	-3316(14)	704(6)	2949(14)	64(4)
F(53)	-1960(20)	182(5)	4540(14)	90(4)
F(54)	-1595(18)	1139(5)	4459(13)	72(4)
B(27")	-2034(8)	607(2)	3791(6)	59(1)
F(61)	-350(7)	554(4)	3779(11)	87(2)
F(62)	-2441(10)	887(5)	4939(8)	82(3)
F(63)	-2602(16)	919(4)	2694(8)	116(3)
F(64)	-2743(9)	70(3)	3751(9)	75(2)
B(27*)	-1877(16)	531(5)	4085(12)	59(1)
F(71)	-2420(20)	296(8)	2880(16)	75(5)
F(72)	-1800(20)	1120(5)	3967(19)	64(5)
F(73)	-2950(30)	388(10)	5049(19)	90(5)
F(74)	-330(20)	321(7)	4443(19)	69(4)

Bond lengths [Å] and angles [°] for mes1120.

N(3)-C(2)	1.277(2)
N(3)-C(16)	1.461(2)
N(3)-C(6)	1.496(2)
N(1)-C(1)	1.276(2)
N(1)-C(9)	1.472(2)
N(1)-C(3)	1.496(2)
C(2)-N(2)	1.350(2)
N(2)-C(1)	1.351(2)
N(2)-C(15)	1.424(2)
C(14)-C(15)	1.375(2)
C(14)-C(13)	1.381(3)
C(14)-C(16)	1.500(3)
C(15)-C(10)	1.378(2)
C(10)-C(11)	1.383(2)
C(10)-C(9)	1.495(3)
C(11)-C(12)	1.377(3)
C(3)-C(4)	1.504(3)
C(3)-C(5)	1.512(3)

C(13)-C(12)	1.382(3)
C(6)-C(8)	1.508(4)
C(6)-C(7)	1.510(4)
B(15)-F(6)	1.3899
B(15)-F(12)	1.3900
B(15)-F(10)	1.3901
B(15)-F(11)	1.3901
B(15')-F(10')	1.3899
B(15')-F(6')	1.3900
B(15')-F(11')	1.3901
B(15')-F(12')	1.3901
B(27)-F(24)	1.3898
B(27)-F(26)	1.3900
B(27)-F(28)	1.3900
B(27)-F(25)	1.3903
B(27')-F(53)	1.3899
B(27')-F(54)	1.3900
B(27')-F(51)	1.3900
B(27')-F(52)	1.3901
B(27")-F(62)	1.3899
B(27")-F(61)	1.3900
B(27")-F(64)	1.3901
B(27")-F(63)	1.3902
B(27*)-F(72)	1.3898
B(27*)-F(74)	1.3900
B(27*)-F(73)	1.3900
B(27*)-F(71)	1.3901

C(2)-N(3)-C(16)	123.42(15)
C(2)-N(3)-C(6)	119.30(16)
C(16)-N(3)-C(6)	117.27(15)
C(1)-N(1)-C(9)	123.62(15)
C(1)-N(1)-C(3)	118.84(14)
C(9)-N(1)-C(3)	117.51(14)
N(3)-C(2)-N(2)	123.37(16)
C(2)-N(2)-C(1)	118.59(14)
C(2)-N(2)-C(15)	120.69(14)
C(1)-N(2)-C(15)	120.71(14)
C(15)-C(14)-C(13)	118.13(17)
C(15)-C(14)-C(16)	121.03(16)
C(13)-C(14)-C(16)	120.84(17)
N(1)-C(1)-N(2)	123.21(15)
C(14)-C(15)-C(10)	123.09(16)

C(14)-C(15)-N(2)	118.38(15)
C(10)-C(15)-N(2)	118.52(15)
C(15)-C(10)-C(11)	117.94(17)
C(15)-C(10)-C(9)	121.18(15)
C(11)-C(10)-C(9)	120.87(17)
C(12)-C(11)-C(10)	119.99(18)
N(3)-C(16)-C(14)	112.96(16)
N(1)-C(3)-C(4)	110.57(17)
N(1)-C(3)-C(5)	108.77(16)
C(4)-C(3)-C(5)	113.9(2)
C(14)-C(13)-C(12)	119.89(18)
N(3)-C(6)-C(8)	109.8(2)
N(3)-C(6)-C(7)	108.9(2)
C(8)-C(6)-C(7)	114.6(2)
C(11)-C(12)-C(13)	120.94(18)
N(1)-C(9)-C(10)	112.65(15)
F(6)-B(15)-F(12)	109.5
F(6)-B(15)-F(10)	109.5
F(12)-B(15)-F(10)	109.5
F(6)-B(15)-F(11)	109.5
F(12)-B(15)-F(11)	109.5
F(10)-B(15)-F(11)	109.5
F(10')-B(15')-F(6')	109.5
F(10')-B(15')-F(11')	109.5
F(6')-B(15')-F(11')	109.5
F(10')-B(15')-F(12')	109.5
F(6')-B(15')-F(12')	109.5
F(11')-B(15')-F(12')	109.5
F(24)-B(27)-F(26)	109.5
F(24)-B(27)-F(28)	109.5
F(26)-B(27)-F(28)	109.5
F(24)-B(27)-F(25)	109.5
F(26)-B(27)-F(25)	109.5
F(28)-B(27)-F(25)	109.5
F(53)-B(27')-F(54)	109.5
F(53)-B(27')-F(51)	109.5
F(54)-B(27')-F(51)	109.5
F(53)-B(27')-F(52)	109.5
F(54)-B(27')-F(52)	109.5
F(51)-B(27')-F(52)	109.5
F(62)-B(27")-F(61)	109.5
F(62)-B(27")-F(64)	109.5
F(61)-B(27")-F(64)	109.5

F(62)-B(27")-F(63)	109.5
F(61)-B(27")-F(63)	109.5
F(64)-B(27")-F(63)	109.5
F(72)-B(27*)-F(74)	109.5
F(72)-B(27*)-F(73)	109.5
F(74)-B(27*)-F(73)	109.5
F(72)-B(27*)-F(71)	109.5
F(74)-B(27*)-F(71)	109.5
F(73)-B(27*)-F(71)	109.5

Anisotropic displacement parameters ($Å^2$ x 10^3) for mes1120. The anisotropic displacement factor exponent takes the form: $-2\pi^2 [h^2 a^{*2} U^{11} + ... + 2 h k a^* b^* U^{12}]$

	U^{11}	U^{22}	U^{33}	U^{23}	U^{13}	U^{12}
N(3)	32(1)	34(1)	42(1)	1(1)	7(1)	-3(1)
N(1)	32(1)	34(1)	33(1)	0(1)	8(1)	2(1)
C(2)	31(1)	31(1)	41(1)	1(1)	4(1)	1(1)
N(2)	30(1)	28(1)	38(1)	0(1)	8(1)	1(1)
C(14)	33(1)	36(1)	49(1)	-6(1)	11(1)	-2(1)
C(1)	30(1)	32(1)	33(1)	-3(1)	5(1)	1(1)
C(15)	29(1)	29(1)	40(1)	-4(1)	5(1)	2(1)
C(10)	32(1)	33(1)	42(1)	1(1)	5(1)	2(1)
C(11)	44(1)	31(1)	58(1)	1(1)	6(1)	3(1)
C(16)	51(1)	40(1)	77(2)	-4(1)	36(1)	-2(1)
C(3)	40(1)	42(1)	42(1)	1(1)	18(1)	6(1)
C(13)	40(1)	42(1)	64(1)	-10(1)	18(1)	3(1)
C(6)	48(1)	39(1)	80(2)	14(1)	25(1)	0(1)
C(12)	47(1)	34(1)	72(1)	-9(1)	12(1)	9(1)
C(5)	37(1)	65(1)	73(2)	0(1)	14(1)	-2(1)
C(9)	50(1)	36(1)	59(1)	11(1)	21(1)	10(1)
C(4)	80(2)	68(2)	39(1)	0(1)	20(1)	14(1)
C(7)	54(2)	47(1)	146(3)	-15(2)	19(2)	-19(1)
C(8)	103(2)	92(2)	79(2)	38(2)	37(2)	11(2)
B(15)	39(1)	48(1)	40(1)	-5(1)	7(1)	2(1)
F(6)	37(2)	49(2)	76(2)	-21(1)	-1(2)	4(2)
F(10)	49(2)	83(3)	72(2)	-6(2)	22(2)	-5(2)
F(11)	61(2)	72(3)	49(2)	-4(2)	-12(2)	-10(2)
F(12)	53(3)	45(1)	61(2)	-1(1)	-7(2)	-2(2)
B(15')	39(1)	48(1)	40(1)	-5(1)	7(1)	2(1)

F(6')	44(4)	58(2)	76(3)	11(2)	6(3)	-3(2)
F(12')	34(3)	52(2)	57(2)	-12(2)	-9(2)	13(2)
F(11')	51(2)	101(5)	46(2)	-22(3)	-2(2)	10(3)
F(10')	46(3)	72(3)	60(3)	5(2)	22(2)	10(2)
B(27)	66(2)	43(1)	65(2)	-10(1)	-16(2)	3(1)
F(24)	84(3)	51(4)	49(2)	-17(2)	4(2)	-14(3)
F(25)	64(4)	30(2)	100(4)	-11(2)	4(3)	21(2)
F(26)	64(3)	23(2)	68(3)	12(2)	0(2)	1(2)
F(28)	58(3)	167(9)	96(5)	-9(5)	-3(3)	-45(4)
B(27')	66(2)	43(1)	65(2)	-10(1)	-16(2)	3(1)
F(51)	80(7)	83(7)	72(7)	-22(7)	14(6)	16(6)
F(52)	76(7)	39(7)	71(7)	13(6)	-39(6)	-10(6)
F(53)	114(9)	46(6)	112(9)	7(6)	12(8)	6(7)
F(54)	84(8)	62(7)	64(7)	-22(6)	-33(7)	4(6)
B(27")	66(2)	43(1)	65(2)	-10(1)	-16(2)	3(1)
F(61)	90(4)	63(4)	107(6)	-29(3)	-3(4)	5(3)
F(62)	88(5)	46(5)	107(5)	-36(3)	-30(4)	11(3)
F(63)	134(7)	88(5)	125(6)	28(4)	-14(5)	-4(5)
F(64)	71(4)	34(2)	119(5)	-20(3)	-15(4)	23(2)
B(27*)	66(2)	43(1)	65(2)	-10(1)	-16(2)	3(1)
F(71)	87(9)	58(8)	76(8)	-29(7)	-36(8)	2(8)
F(72)	91(9)	35(7)	62(9)	-5(7)	-36(8)	16(7)
F(73)	101(10)	80(10)	90(9)	-12(9)	-2(9)	-3(9)
F(74)	86(9)	47(8)	69(8)	-27(7)	-28(7)	29(7)

Hydrogen coordinates (x 10^4) and isotropic displacement parameters ($Å^2$ x 10^3) for mes1120.

	x	y	z	U(eq)
H(2A)	109	376	7102	41
H(1A)	1910	795	5817	38
H(10A)	-534	3039	5892	53
H(15A)	-2385	1296	9302	66
H(15B)	-3680	1174	8122	66
H(3A)	3728	1071	4525	49
H(12A)	-3569	2305	8378	58
H(5A)	-1336	-122	8408	66
H(11A)	-2652	3104	7299	61
H(5B)	4987	1728	5976	87

H(5C)	4535	2229	4977	87
H(5D)	5788	1753	4587	87
H(8A)	842	2242	4330	57
H(8B)	2090	2416	5507	57
H(4A)	2133	1360	2680	92
H(4B)	3982	1521	2504	92
H(4C)	2728	1997	2894	92
H(7A)	-3555	-39	6889	123
H(7B)	-4583	265	7967	123
H(7C)	-4071	-382	8149	123
H(7D)	-1256	341	10443	135
H(7E)	-2608	-140	10409	135
H(7F)	-3121	506	10228	135

APPENDIX B

CRYSTALLOGRAPHIC DATA FOR **13**

Crystal data and structure refinement for mes122 (**13)**.

Identification code	mes122
Empirical formula	C19.50 H31 B Cl F4 N3 O
Formula weight	445.73
Temperature	150(2) K
Wavelength	1.54160 Å
Crystal system	C 2/c
Unit cell dimensions	a = 18.7737(19) Å α= 90°
	b = 9.8686(11) Å β = 101.102(5)°
	c = 24.719(3) Å γ = 90°
Volume	4494.0(9) A^3
Z, Calculated density	8, 1.318 Mg/m^3
Absorption coefficient	1.935 mm^{-1}
F(000)	1880
Crystal size	0.32 x 0.18 x 0.14 mm
Theta range for data collection	5.08 to 61.53°
Limiting indices	-21<=h<=20, -11<=k<=11, -28<=l<=26
Reflections collected / unique	11084 / 3417 [R(int) = 0.0351]
Completeness to theta = 61.53	98.2 %
Max. and min. transmission	0.7734 and 0.5764
Refinement method	Full-matrix least-squares on F^2
Data / restraints / parameters	3417 / 21 / 328
Goodness-of-fit on F^2	1.150
Final R indices [I>2sigma(I)]	R1 = 0.0623, wR2 = 0.1714

R indices (all data)	R1 = 0.0740, wR2 = 0.1831
Extinction coefficient	0.0020(4)
Largest diff. peak and hole	0.292 and -0.258 e.A^{-3}

Atomic coordinates (x 10^4) and equivalent isotropic displacement parameters ($Å^2$ x 10^3) for mes122. U(eq) is defined as one third of the trace of the orthogonalized U^{ij} tensor.

	x	y	z	U(eq)
O(1)	5716(1)	-2770(2)	514(1)	43(1)
N(1)	4212(1)	4(2)	802(1)	41(1)
N(3)	6317(1)	-2638(2)	1434(1)	40(1)
N(2)	5286(1)	-1227(2)	1051(1)	41(1)
C(2)	5637(1)	-2583(2)	1067(1)	38(1)
C(4)	3392(1)	24(2)	670(1)	42(1)
C(1)	4571(1)	-1137(2)	889(1)	39(1)
C(8)	6323(1)	-2926(3)	2031(1)	46(1)
C(13)	5394(1)	1200(2)	1013(1)	48(1)
C(17)	6483(1)	-201(2)	1220(1)	41(1)
C(19)	6815(1)	-1589(2)	1300(1)	42(1)
C(18)	5731(1)	-53(2)	1095(1)	41(1)
C(16)	6899(1)	973(3)	1255(1)	50(1)
C(5)	3099(2)	-1303(3)	401(2)	67(1)
C(15)	6572(1)	2231(3)	1175(1)	57(1)
C(12)	4581(1)	1332(3)	887(2)	67(1)
C(3)	5907(2)	-4139(3)	408(1)	53(1)
C(14)	5822(2)	2350(3)	1056(1)	58(1)
C(7)	3145(2)	1180(3)	271(1)	60(1)
C(6)	3129(2)	259(4)	1204(1)	70(1)
C(9)	5763(3)	-4037(5)	2083(2)	52(1)
C(11)	7071(2)	-3566(9)	2267(2)	77(2)
C(10)	6189(4)	-1721(4)	2359(2)	63(2)
C(9')	6099(12)	-4240(20)	2091(8)	84(6)
C(10')	5788(10)	-1805(15)	2256(6)	61(4)
C(11')	7074(9)	-2710(20)	2369(7)	75(5)
B(9)	3915(5)	-4851(8)	1066(4)	40(1)
F(3)	3792(6)	-3990(8)	1461(4)	58(1)
F(41)	4047(3)	-4127(4)	634(2)	80(2)
F(42)	3333(4)	-5659(7)	909(4)	87(3)

F(43)	4501(5)	-5620(10)	1267(4)	117(5)
B(9')	3846(4)	-5015(7)	1155(3)	40(1)
F(3')	3885(4)	-3648(5)	1370(2)	58(1)
F(45)	3690(2)	-5884(3)	1539(1)	84(1)
F(46)	4506(3)	-5354(7)	1031(2)	77(2)
F(47)	3312(3)	-5075(6)	693(2)	89(2)
Cl(1)	5497(2)	1502(3)	2526(1)	113(1)
Cl(2)	4022(1)	2263(2)	2503(1)	97(1)
C(20)	4905(15)	2848(5)	2548(14)	63(4)

Bond lengths [Å] and angles [°] for mes122.

O(1)-C(2)	1.414(3)
O(1)-C(3)	1.435(3)
N(1)-C(1)	1.309(3)
N(1)-C(12)	1.478(3)
N(1)-C(4)	1.512(3)
N(3)-C(2)	1.418(3)
N(3)-C(19)	1.475(3)
N(3)-C(8)	1.500(3)
N(2)-C(1)	1.329(3)
N(2)-C(18)	1.420(3)
N(2)-C(2)	1.489(3)
C(2)-H(2A)	1.0000
C(4)-C(6)	1.514(4)
C(4)-C(7)	1.521(3)
C(4)-C(5)	1.523(4)
C(1)-H(1A)	0.9500
C(8)-C(10)	1.488(5)
C(8)-C(9')	1.377(19)
C(8)-C(9)	1.541(5)
C(8)-C(11')	1.510(16)
C(8)-C(11)	1.548(5)
C(8)-C(10')	1.661(14)
C(13)-C(14)	1.384(4)
C(13)-C(18)	1.385(3)
C(13)-C(12)	1.502(4)
C(17)-C(16)	1.391(3)
C(17)-C(18)	1.395(3)
C(17)-C(19)	1.502(3)

C(19)-H(19A)	0.9900
C(19)-H(19B)	0.9900
C(16)-C(15)	1.382(4)
C(16)-H(16A)	0.9500
C(5)-H(5A)	0.9800
C(5)-H(5B)	0.9800
C(5)-H(5C)	0.9800
C(15)-C(14)	1.386(4)
C(15)-H(15A)	0.9500
C(12)-H(12A)	0.9900
C(12)-H(12B)	0.9900
C(3)-H(3A)	0.9800
C(3)-H(3B)	0.9800
C(3)-H(3C)	0.9800
C(14)-H(14A)	0.9500
C(7)-H(7A)	0.9800
C(7)-H(7B)	0.9800
C(7)-H(7C)	0.9800
C(6)-H(6A)	0.9800
C(6)-H(6B)	0.9800
C(6)-H(6C)	0.9800
C(9)-H(9A)	0.9800
C(9)-H(9B)	0.9800
C(9)-H(9C)	0.9800
C(11)-H(11A)	0.9800
C(11)-H(11B)	0.9800
C(11)-H(11C)	0.9800
C(10)-H(10A)	0.9800
C(10)-H(10B)	0.9800
C(10)-H(10C)	0.9800
C(9')-H(9'A)	0.9800
C(9')-H(9'B)	0.9800
C(9')-H(9'C)	0.9800
C(10')-H(10D)	0.9800
C(10')-H(10E)	0.9800
C(10')-H(10F)	0.9800
C(11')-H(11D)	0.9800
C(11')-H(11E)	0.9800
C(11')-H(11F)	0.9800
B(9)-F(41)	1.347(8)
B(9)-F(3)	1.348(8)
B(9)-F(42)	1.348(8)
B(9)-F(43)	1.350(8)

B(9')-F(45)	1.352(7)
B(9')-F(47)	1.368(8)
B(9')-F(46)	1.375(7)
B(9')-F(3')	1.447(7)
Cl(1)-C(20)	1.740(17)
Cl(2)-C(20)	1.74(2)
C(20)-H(20A)	0.9900
C(20)-H(20B)	0.9900

C(2)-O(1)-C(3)	112.13(18)
C(1)-N(1)-C(12)	121.8(2)
C(1)-N(1)-C(4)	121.14(18)
C(12)-N(1)-C(4)	116.70(18)
C(2)-N(3)-C(19)	111.11(18)
C(2)-N(3)-C(8)	118.20(18)
C(19)-N(3)-C(8)	118.04(19)
C(1)-N(2)-C(18)	120.93(19)
C(1)-N(2)-C(2)	118.97(19)
C(18)-N(2)-C(2)	118.74(18)
O(1)-C(2)-N(3)	111.42(18)
O(1)-C(2)-N(2)	102.75(17)
N(3)-C(2)-N(2)	112.96(18)
O(1)-C(2)-H(2A)	109.8
N(3)-C(2)-H(2A)	109.8
N(2)-C(2)-H(2A)	109.8
N(1)-C(4)-C(6)	107.6(2)
N(1)-C(4)-C(7)	108.71(19)
C(6)-C(4)-C(7)	110.0(2)
N(1)-C(4)-C(5)	110.54(19)
C(6)-C(4)-C(5)	111.1(2)
C(7)-C(4)-C(5)	108.9(2)
N(1)-C(1)-N(2)	124.4(2)
N(1)-C(1)-H(1A)	117.8
N(2)-C(1)-H(1A)	117.8
C(10)-C(8)-N(3)	114.5(2)
C(10)-C(8)-C(9')	127.2(9)
N(3)-C(8)-C(9')	109.9(9)
C(10)-C(8)-C(9)	109.5(3)
N(3)-C(8)-C(9)	110.0(2)
C(9')-C(8)-C(9)	25.2(8)
C(10)-C(8)-C(11')	79.8(7)
N(3)-C(8)-C(11')	110.2(6)
C(9')-C(8)-C(11')	110.3(10)

C(9)-C(8)-C(11')	129.4(7)
C(10)-C(8)-C(11)	111.0(4)
N(3)-C(8)-C(11)	106.3(2)
C(9')-C(8)-C(11)	81.4(9)
C(9)-C(8)-C(11)	105.2(3)
C(11')-C(8)-C(11)	33.6(6)
C(10)-C(8)-C(10')	26.9(5)
N(3)-C(8)-C(10')	108.2(5)
C(9')-C(8)-C(10')	111.9(9)
C(9)-C(8)-C(10')	88.8(6)
C(11')-C(8)-C(10')	106.3(8)
C(11)-C(8)-C(10')	135.2(6)
C(14)-C(13)-C(18)	118.6(2)
C(14)-C(13)-C(12)	119.8(2)
C(18)-C(13)-C(12)	121.6(2)
C(16)-C(17)-C(18)	117.3(2)
C(16)-C(17)-C(19)	122.6(2)
C(18)-C(17)-C(19)	120.1(2)
N(3)-C(19)-C(17)	113.83(18)
N(3)-C(19)-H(19A)	108.8
C(17)-C(19)-H(19A)	108.8
N(3)-C(19)-H(19B)	108.8
C(17)-C(19)-H(19B)	108.8
H(19A)-C(19)-H(19B)	107.7
C(13)-C(18)-C(17)	122.8(2)
C(13)-C(18)-N(2)	118.1(2)
C(17)-C(18)-N(2)	119.1(2)
C(15)-C(16)-C(17)	120.8(2)
C(15)-C(16)-H(16A)	119.6
C(17)-C(16)-H(16A)	119.6
C(4)-C(5)-H(5A)	109.5
C(4)-C(5)-H(5B)	109.5
H(5A)-C(5)-H(5B)	109.5
C(4)-C(5)-H(5C)	109.5
H(5A)-C(5)-H(5C)	109.5
H(5B)-C(5)-H(5C)	109.5
C(14)-C(15)-C(16)	120.7(2)
C(14)-C(15)-H(15A)	119.6
C(16)-C(15)-H(15A)	119.6
N(1)-C(12)-C(13)	112.5(2)
N(1)-C(12)-H(12A)	109.1
C(13)-C(12)-H(12A)	109.1
N(1)-C(12)-H(12B)	109.1

C(13)-C(12)-H(12B)	109.1
H(12A)-C(12)-H(12B)	107.8
O(1)-C(3)-H(3A)	109.5
O(1)-C(3)-H(3B)	109.5
H(3A)-C(3)-H(3B)	109.5
O(1)-C(3)-H(3C)	109.5
H(3A)-C(3)-H(3C)	109.5
H(3B)-C(3)-H(3C)	109.5
C(15)-C(14)-C(13)	119.9(2)
C(15)-C(14)-H(14A)	120
C(13)-C(14)-H(14A)	120
C(4)-C(7)-H(7A)	109.5
C(4)-C(7)-H(7B)	109.5
H(7A)-C(7)-H(7B)	109.5
C(4)-C(7)-H(7C)	109.5
H(7A)-C(7)-H(7C)	109.5
H(7B)-C(7)-H(7C)	109.5
C(4)-C(6)-H(6A)	109.5
C(4)-C(6)-H(6B)	109.5
H(6A)-C(6)-H(6B)	109.5
C(4)-C(6)-H(6C)	109.5
H(6A)-C(6)-H(6C)	109.5
H(6B)-C(6)-H(6C)	109.5
C(8)-C(9)-H(9A)	109.4
C(8)-C(9)-H(9B)	109.5
H(9A)-C(9)-H(9B)	109.5
C(8)-C(9)-H(9C)	109.5
H(9A)-C(9)-H(9C)	109.5
H(9B)-C(9)-H(9C)	109.5
C(8)-C(11)-H(11A)	109.5
C(8)-C(11)-H(11B)	109.5
H(11A)-C(11)-H(11B)	109.5
C(8)-C(11)-H(11C)	109.4
H(11A)-C(11)-H(11C)	109.5
H(11B)-C(11)-H(11C)	109.5
C(8)-C(10)-H(10A)	109.6
C(8)-C(10)-H(10B)	109.4
H(10A)-C(10)-H(10B)	109.5
C(8)-C(10)-H(10C)	109.4
H(10A)-C(10)-H(10C)	109.5
H(10B)-C(10)-H(10C)	109.5
C(8)-C(9')-H(9'A)	109.2
C(8)-C(9')-H(9'B)	109.7

H(9'A)-C(9')-H(9'B)	109.5
C(8)-C(9')-H(9'C)	109.5
H(9'A)-C(9')-H(9'C)	109.5
H(9'B)-C(9')-H(9'C)	109.5
C(8)-C(10')-H(10D)	109.2
C(8)-C(10')-H(10E)	109.8
H(10D)-C(10')-H(10E)	109.5
C(8)-C(10')-H(10F)	109.4
H(10D)-C(10')-H(10F)	109.5
H(10E)-C(10')-H(10F)	109.5
C(8)-C(11')-H(11D)	109.7
C(8)-C(11')-H(11E)	109.5
H(11D)-C(11')-H(11E)	109.5
C(8)-C(11')-H(11F)	109.2
H(11D)-C(11')-H(11F)	109.5
H(11E)-C(11')-H(11F)	109.5
F(41)-B(9)-F(3)	108.9(6)
F(41)-B(9)-F(42)	110.4(6)
F(3)-B(9)-F(42)	109.8(6)
F(41)-B(9)-F(43)	109.2(6)
F(3)-B(9)-F(43)	109.3(6)
F(42)-B(9)-F(43)	109.3(6)
F(45)-B(9')-F(47)	109.6(5)
F(45)-B(9')-F(46)	109.1(5)
F(47)-B(9')-F(46)	110.5(6)
F(45)-B(9')-F(3')	109.6(5)
F(47)-B(9')-F(3')	108.9(5)
F(46)-B(9')-F(3')	109.0(5)
Cl(2)-C(20)-Cl(1)	110.6(5)
Cl(2)-C(20)-H(20A)	109.5
Cl(1)-C(20)-H(20A)	109.5
Cl(2)-C(20)-H(20B)	109.5
Cl(1)-C(20)-H(20B)	109.5
H(20A)-C(20)-H(20B)	108.1

Anisotropic displacement parameters ($Å^2$ x 10^3) for mes122. The anisotropic displacement factor exponent takes the form: $-2\pi^2 [h^2 a^{*2} U^{11} + ... + 2 h k a^* b^* U^{12}]$

	U^{11}	U^{22}	U^{33}	U^{23}	U^{13}	U^{12}
O(1)	47(1)	43(1)	37(1)	1(1)	5(1)	1(1)
N(1)	32(1)	37(1)	51(1)	2(1)	4(1)	-1(1)
N(3)	36(1)	45(1)	37(1)	5(1)	5(1)	1(1)
N(2)	33(1)	36(1)	51(1)	-1(1)	4(1)	-2(1)
C(2)	38(1)	36(1)	39(1)	2(1)	6(1)	0(1)
C(4)	33(1)	40(1)	51(2)	8(1)	4(1)	0(1)
C(1)	34(1)	39(1)	42(1)	2(1)	5(1)	-1(1)
C(8)	48(1)	53(2)	34(1)	4(1)	5(1)	-3(1)
C(13)	39(1)	38(1)	64(2)	1(1)	7(1)	-3(1)
C(17)	36(1)	46(1)	41(1)	0(1)	9(1)	-2(1)
C(19)	33(1)	48(1)	45(1)	4(1)	6(1)	-2(1)
C(18)	35(1)	39(1)	47(1)	-1(1)	7(1)	-6(1)
C(16)	35(1)	55(2)	58(2)	0(1)	9(1)	-6(1)
C(5)	40(1)	48(2)	104(3)	-5(2)	-11(2)	-4(1)
C(15)	44(2)	44(2)	83(2)	0(1)	12(1)	-10(1)
C(12)	40(2)	39(2)	117(3)	-6(2)	7(2)	-7(1)
C(3)	56(2)	50(2)	52(2)	-8(1)	9(1)	6(1)
C(14)	45(2)	41(1)	86(2)	0(1)	11(1)	-3(1)
C(7)	47(2)	60(2)	68(2)	24(1)	-2(1)	2(1)
C(6)	44(2)	105(3)	63(2)	10(2)	15(1)	-1(2)
C(9)	65(3)	54(2)	36(2)	6(2)	10(2)	-17(2)
C(11)	55(3)	118(6)	53(3)	36(3)	0(2)	15(3)
C(10)	88(4)	59(3)	42(2)	-10(2)	12(2)	-9(2)
B(9)	38(2)	39(2)	44(3)	1(2)	11(2)	0(2)
F(3)	76(2)	29(3)	67(2)	-2(2)	14(1)	-4(2)
F(41)	130(5)	50(3)	70(3)	-11(2)	46(3)	-13(3)
F(42)	44(3)	73(4)	141(9)	-30(4)	10(4)	-18(3)
F(43)	75(5)	61(4)	194(13)	-12(6)	-26(6)	33(4)
B(9')	38(2)	39(2)	44(3)	1(2)	11(2)	0(2)
F(3')	76(2)	29(3)	67(2)	-2(2)	14(1)	-4(2)
F(45)	106(3)	62(2)	89(2)	18(2)	28(2)	-16(2)
F(46)	36(2)	91(4)	106(4)	-48(3)	20(2)	-5(2)
F(47)	62(2)	124(4)	67(3)	-39(3)	-18(2)	33(3)
Cl(1)	119(2)	100(2)	112(2)	-30(1)	-2(1)	52(2)
Cl(2)	91(1)	94(1)	110(2)	-28(1)	31(1)	-35(1)
C(20)	72(14)	47(2)	70(10)	-7(5)	14(7)	2(4)

Hydrogen coordinates (x 10^4) and isotropic displacement parameters ($Å^2$ x 10^3) for mes122.

	x	y	z	U(eq)
H(2A)	5305	-3290	1169	45
H(1A)	4301	-1957	833	46
H(19A)	6980	-1857	958	51
H(19B)	7248	-1550	1600	51
H(16A)	7413	911	1335	59
H(5A)	3255	-2055	656	101
H(5B)	3286	-1440	62	101
H(5C)	2567	-1269	314	101
H(15A)	6864	3024	1202	69
H(12A)	4422	1808	1196	80
H(12B)	4436	1889	551	80
H(3A)	5956	-4224	22	79
H(3B)	5526	-4754	480	79
H(3C)	6368	-4374	649	79
H(14A)	5603	3220	1003	69
H(7A)	3331	2040	440	90
H(7B)	2613	1208	184	90
H(7C)	3332	1038	-69	90
H(6A)	3325	1118	1368	105
H(6B)	3295	-484	1461	105
H(6C)	2598	295	1130	105
H(9A)	5935	-4910	1970	78
H(9B)	5297	-3812	1846	78
H(9C)	5701	-4095	2467	78
H(11A)	7225	-4128	1983	115
H(11B)	7033	-4128	2587	115
H(11C)	7429	-2846	2379	115
H(10A)	6653	-1297	2521	95
H(10B)	5938	-2004	2654	95
H(10C)	5886	-1069	2119	95
H(9'A)	6431	-4867	1960	126
H(9'B)	5607	-4360	1875	126
H(9'C)	6098	-4415	2481	126
H(10D)	5355	-1650	1970	92
H(10E)	6050	-949	2341	92
H(10F)	5641	-2153	2589	92

H(11D)	7419	-3305	2234	113
H(11E)	7073	-2911	2756	113
H(11F)	7219	-1761	2335	113
H(20A)	5057	3354	2897	76
H(20B)	4924	3475	2238	76

Torsion angles [°] for mes122.

C(3)-O(1)-C(2)-N(3)	71.0(2)
C(3)-O(1)-C(2)-N(2)	-167.78(18)
C(19)-N(3)-C(2)-O(1)	59.0(2)
C(8)-N(3)-C(2)-O(1)	-159.83(19)
C(19)-N(3)-C(2)-N(2)	-56.0(2)
C(8)-N(3)-C(2)-N(2)	85.1(2)
C(1)-N(2)-C(2)-O(1)	83.2(2)
C(18)-N(2)-C(2)-O(1)	-83.6(2)
C(1)-N(2)-C(2)-N(3)	-156.6(2)
C(18)-N(2)-C(2)-N(3)	36.6(3)
C(1)-N(1)-C(4)-C(6)	95.3(3)
C(12)-N(1)-C(4)-C(6)	-78.3(3)
C(1)-N(1)-C(4)-C(7)	-145.6(2)
C(12)-N(1)-C(4)-C(7)	40.7(3)
C(1)-N(1)-C(4)-C(5)	-26.2(3)
C(12)-N(1)-C(4)-C(5)	160.2(3)
C(12)-N(1)-C(1)-N(2)	-1.0(4)
C(4)-N(1)-C(1)-N(2)	-174.3(2)
C(18)-N(2)-C(1)-N(1)	-5.8(4)
C(2)-N(2)-C(1)-N(1)	-172.3(2)
C(2)-N(3)-C(8)-C(10)	-82.6(4)
C(19)-N(3)-C(8)-C(10)	55.8(4)
C(2)-N(3)-C(8)-C(9')	67.9(10)
C(19)-N(3)-C(8)-C(9')	-153.6(10)
C(2)-N(3)-C(8)-C(9)	41.1(4)
C(19)-N(3)-C(8)-C(9)	179.5(3)
C(2)-N(3)-C(8)-C(11')	-170.3(9)
C(19)-N(3)-C(8)-C(11')	-31.9(9)
C(2)-N(3)-C(8)-C(11)	154.5(4)
C(19)-N(3)-C(8)-C(11)	-67.1(4)
C(2)-N(3)-C(8)-C(10')	-54.5(7)
C(19)-N(3)-C(8)-C(10')	84.0(7)
C(2)-N(3)-C(19)-C(17)	48.7(3)

C(8)-N(3)-C(19)-C(17)	-92.5(2)
C(16)-C(17)-C(19)-N(3)	160.3(2)
C(18)-C(17)-C(19)-N(3)	-21.2(3)
C(14)-C(13)-C(18)-C(17)	0.4(4)
C(12)-C(13)-C(18)-C(17)	-179.0(3)
C(14)-C(13)-C(18)-N(2)	179.9(2)
C(12)-C(13)-C(18)-N(2)	0.6(4)
C(16)-C(17)-C(18)-C(13)	-0.9(4)
C(19)-C(17)-C(18)-C(13)	-179.5(2)
C(16)-C(17)-C(18)-N(2)	179.5(2)
C(19)-C(17)-C(18)-N(2)	0.9(4)
C(1)-N(2)-C(18)-C(13)	5.8(4)
C(2)-N(2)-C(18)-C(13)	172.4(2)
C(1)-N(2)-C(18)-C(17)	-174.6(2)
C(2)-N(2)-C(18)-C(17)	-8.1(3)
C(18)-C(17)-C(16)-C(15)	0.9(4)
C(19)-C(17)-C(16)-C(15)	179.4(3)
C(17)-C(16)-C(15)-C(14)	-0.3(4)
C(1)-N(1)-C(12)-C(13)	6.7(4)
C(4)-N(1)-C(12)-C(13)	-179.7(2)
C(14)-C(13)-C(12)-N(1)	174.3(3)
C(18)-C(13)-C(12)-N(1)	-6.4(4)
C(16)-C(15)-C(14)-C(13)	-0.3(5)
C(18)-C(13)-C(14)-C(15)	0.2(4)
C(12)-C(13)-C(14)-C(15)	179.6(3)

APPENDIX C

CRYSTALLOGRAPHIC DATA FOR **25a**

Crystal data and structure refinement for mes131 (**25a**).

Identification code	mes131	
Empirical formula	C56 H58 Mo2 N4 O4	
Formula weight	1042.94	
Temperature	190(2) K	
Wavelength	0.71073 Å	
Crystal system	P -1	
Unit cell dimensions	a = 8.4556(8) Å	∂ = 78.117(5) deg.
	b = 16.4105(16) Å	ß = 81.314(5) deg.
	c = 18.7039(19) Å	γ = 86.357(5) deg.
Volume	2509.2(4) A^3	
Z, Calculated density	2, 1.380 Mg/m^3	
Absorption coefficient	0.549 mm	
F(000)	1076	
Crystal size	0.38 x 0.06 x 0.01 mm	
Theta range for data collection	2.97 to 25.00°	
Limiting indices	-10<=h<=9, -19<=k<=19, -22<=l<=22	
Reflections collected / unique	16143 / 8755 [R(int) = 0.0537]	
Completeness to theta = 25.00	99.3 %	
Max. and min. transmission	0.9945 and 0.8185	
Refinement method	Full-matrix least-squares on F^2	
Data / restraints / parameters	8755 / 0 / 606	
Goodness-of-fit on F^2	1.027	

Final R indices [I>2sigma(I)]	R1 = 0.0473, wR2 = 0.0947
R indices (all data)	R1 = 0.0912, wR2 = 0.1102
Largest diff. peak and hole	0.742 and -0.470 e.A^{-3}

Atomic coordinates (x 10^4) and equivalent isotropic displacement parameters ($Å^2$ x 10^3) for mes131. U(eq) is defined as one third of the trace of the orthogonalized U^{ij} tensor.

	x	y	z	U(eq)
Mo(1A)	3593(1)	7401(1)	2691(1)	27(1)
O(1A)	3148(4)	6952(2)	1200(2)	41(1)
C(1A)	3662(4)	8756(3)	2374(2)	25(1)
N(1A)	3450(4)	9273(2)	1716(2)	29(1)
N(2A)	3876(4)	9317(2)	2806(2)	30(1)
O(2A)	-81(4)	7485(2)	2710(2)	54(1)
C(2A)	3778(6)	10131(3)	2425(3)	42(1)
C(3A)	3517(6)	10100(3)	1742(3)	43(1)
C(4A)	3169(5)	9031(3)	1049(2)	28(1)
C(5A)	1593(5)	9068(3)	892(3)	33(1)
C(6A)	1373(5)	8860(3)	226(2)	37(1)
C(7A)	2632(5)	8627(3)	-259(2)	35(1)
C(8A)	4164(5)	8609(3)	-81(2)	33(1)
C(9A)	4468(5)	8822(3)	560(2)	29(1)
C(10A)	209(5)	9335(3)	1401(3)	48(1)
C(11A)	2348(6)	8407(3)	-973(3)	49(1)
C(12A)	6157(5)	8840(3)	726(3)	40(1)
C(13A)	4240(5)	9132(3)	3553(2)	28(1)
C(14A)	5836(5)	9164(3)	3651(3)	36(1)
C(15A)	6170(5)	9020(3)	4377(3)	40(1)
C(16A)	4984(5)	8864(3)	4981(2)	36(1)
C(17A)	3419(5)	8838(3)	4858(3)	35(1)
C(18A)	3013(5)	8973(3)	4138(2)	31(1)
C(19A)	7144(5)	9315(3)	3001(3)	49(1)
C(20A)	5389(6)	8730(3)	5756(3)	48(1)
C(21A)	1287(5)	8951(3)	4023(3)	44(1)
C(22A)	3359(5)	7175(3)	1737(3)	31(1)

C(23A)	1298(5)	7473(3)	2712(2)	33(1)
C(24A)	3775(6)	6096(3)	3479(3)	47(1)
C(25A)	3756(6)	6697(3)	3914(3)	43(1)
C(26A)	5158(6)	7141(3)	3682(3)	44(1)
C(27A)	6045(5)	6824(3)	3101(3)	47(1)
C(28A)	5186(6)	6176(3)	2969(3)	47(1)
Mo(1B)	1114(1)	2468(1)	2465(1)	27(1)
N(1B)	1835(4)	4233(2)	1373(2)	27(1)
O(1B)	1824(4)	1832(2)	995(2)	43(1)
C(1B)	1600(4)	3783(2)	2071(2)	23(1)
N(2B)	1834(4)	4350(2)	2490(2)	29(1)
O(2B)	4765(3)	2087(2)	2315(2)	46(1)
C(2B)	2213(5)	5124(3)	2050(3)	36(1)
C(3B)	2231(5)	5048(3)	1348(3)	35(1)
C(4B)	1661(5)	3932(3)	714(2)	27(1)
C(5B)	125(5)	3864(3)	554(2)	31(1)
C(6B)	-12(5)	3572(3)	-76(3)	35(1)
C(7B)	1311(5)	3374(3)	-550(3)	36(1)
C(8B)	2823(5)	3457(3)	-376(3)	36(1)
C(9B)	3021(5)	3727(3)	260(2)	30(1)
C(10B)	-1344(5)	4110(3)	1051(3)	42(1)
C(11B)	1121(6)	3090(3)	-1250(3)	53(1)
C(12B)	4679(5)	3754(3)	470(3)	40(1)
C(13B)	1631(5)	4186(2)	3281(2)	25(1)
C(14B)	2908(5)	3852(3)	3649(3)	32(1)
C(15B)	2621(5)	3670(3)	4414(3)	36(1)
C(16B)	1152(5)	3820(3)	4811(3)	39(1)
C(17B)	-69(5)	4186(3)	4417(3)	37(1)
C(18B)	150(5)	4378(3)	3654(2)	31(1)
C(19B)	4559(5)	3717(3)	3244(3)	41(1)
C(20B)	863(6)	3566(4)	5641(3)	55(2)
C(21B)	-1167(5)	4811(3)	3234(3)	44(1)
C(22B)	1538(5)	2119(3)	1527(3)	31(1)
C(23B)	3390(5)	2257(3)	2377(2)	32(1)
C(24B)	33(5)	2190(3)	3736(3)	42(1)
C(25B)	487(5)	1424(3)	3533(3)	43(1)
C(26B)	-458(5)	1303(3)	3016(3)	45(1)
C(27B)	-1510(5)	1995(3)	2895(3)	48(1)
C(28B)	-1204(5)	2555(3)	3340(3)	47(1)

Bond lengths [Å] and angles [°] for mes131.

Mo(1A)-C(23A)	1.932(4)
Mo(1A)-C(22A)	1.935(5)
Mo(1A)-C(1A)	2.183(4)
Mo(1A)-C(24A)	2.346(5)
Mo(1A)-C(28A)	2.357(5)
Mo(1A)-C(25A)	2.361(5)
Mo(1A)-C(26A)	2.390(4)
Mo(1A)-C(27A)	2.391(4)
O(1A)-C(22A)	1.178(5)
C(1A)-N(1A)	1.374(5)
C(1A)-N(2A)	1.378(5)
N(1A)-C(3A)	1.373(5)
N(1A)-C(4A)	1.441(5)
N(2A)-C(2A)	1.383(6)
N(2A)-C(13A)	1.443(5)
O(2A)-C(23A)	1.165(5)
C(2A)-C(3A)	1.340(6)
C(2A)-H(2AA)	0.9500
C(3A)-H(3AA)	0.9500
C(4A)-C(9A)	1.392(6)
C(4A)-C(5A)	1.402(5)
C(5A)-C(6A)	1.399(6)
C(5A)-C(10A)	1.496(6)
C(6A)-C(7A)	1.379(6)
C(6A)-H(6AA)	0.9500
C(7A)-C(8A)	1.383(6)
C(7A)-C(11A)	1.509(6)
C(8A)-C(9A)	1.380(6)
C(8A)-H(8AA)	0.9500
C(9A)-C(12A)	1.510(5)
C(10A)-H(10A)	0.9800
C(10A)-H(10B)	0.9800
C(10A)-H(10C)	0.9800
C(11A)-H(11A)	0.9800
C(11A)-H(11B)	0.9800
C(11A)-H(11C)	0.9800
C(12A)-H(12A)	0.9800
C(12A)-H(12B)	0.9800
C(12A)-H(12C)	0.9800
C(13A)-C(18A)	1.384(6)

C(13A)-C(14A)	1.395(5)
C(14A)-C(15A)	1.399(6)
C(14A)-C(19A)	1.506(6)
C(15A)-C(16A)	1.384(6)
C(15A)-H(15A)	0.9500
C(16A)-C(17A)	1.382(6)
C(16A)-C(20A)	1.509(6)
C(17A)-C(18A)	1.409(6)
C(17A)-H(17A)	0.9500
C(18A)-C(21A)	1.511(6)
C(19A)-H(19A)	0.9800
C(19A)-H(19B)	0.9800
C(19A)-H(19C)	0.9800
C(20A)-H(20A)	0.9800
C(20A)-H(20B)	0.9800
C(20A)-H(20C)	0.9800
C(21A)-H(21A)	0.9800
C(21A)-H(21B)	0.9800
C(21A)-H(21C)	0.9800
C(24A)-C(25A)	1.400(7)
C(24A)-C(28A)	1.405(7)
C(24A)-H(24A)	1.0000
C(25A)-C(26A)	1.396(6)
C(25A)-H(25A)	1.0000
C(26A)-C(27A)	1.397(7)
C(26A)-H(26A)	1.0000
C(27A)-C(28A)	1.406(7)
C(27A)-H(27A)	1.0000
C(28A)-H(28A)	1.0000
Mo(1B)-C(23B)	1.922(4)
Mo(1B)-C(22B)	1.932(5)
Mo(1B)-C(1B)	2.177(4)
Mo(1B)-C(26B)	2.362(4)
Mo(1B)-C(25B)	2.364(5)
Mo(1B)-C(27B)	2.365(4)
Mo(1B)-C(28B)	2.373(5)
Mo(1B)-C(24B)	2.375(5)
N(1B)-C(1B)	1.355(5)
N(1B)-C(3B)	1.389(5)
N(1B)-C(4B)	1.449(5)
O(1B)-C(22B)	1.174(5)
C(1B)-N(2B)	1.374(5)
N(2B)-C(2B)	1.391(5)

N(2B)-C(13B)	1.434(5)
O(2B)-C(23B)	1.172(5)
C(2B)-C(3B)	1.342(6)
C(2B)-H(2BA)	0.9500
C(3B)-H(3BA)	0.9500
C(4B)-C(9B)	1.390(6)
C(4B)-C(5B)	1.392(5)
C(5B)-C(6B)	1.383(6)
C(5B)-C(10B)	1.521(6)
C(6B)-C(7B)	1.383(6)
C(6B)-H(6BA)	0.9500
C(7B)-C(8B)	1.387(6)
C(7B)-C(11B)	1.512(6)
C(8B)-C(9B)	1.389(6)
C(8B)-H(8BA)	0.9500
C(9B)-C(12B)	1.518(5)
C(10B)-H(10D)	0.9800
C(10B)-H(10E)	0.9800
C(10B)-H(10F)	0.9800
C(11B)-H(11D)	0.9800
C(11B)-H(11E)	0.9800
C(11B)-H(11F)	0.9800
C(12B)-H(12D)	0.9800
C(12B)-H(12E)	0.9800
C(12B)-H(12F)	0.9800
C(13B)-C(18B)	1.389(6)
C(13B)-C(14B)	1.390(6)
C(14B)-C(15B)	1.388(6)
C(14B)-C(19B)	1.511(6)
C(15B)-C(16B)	1.383(6)
C(15B)-H(15B)	0.9500
C(16B)-C(17B)	1.392(6)
C(16B)-C(20B)	1.509(7)
C(17B)-C(18B)	1.383(6)
C(17B)-H(17B)	0.9500
C(18B)-C(21B)	1.516(6)
C(19B)-H(19D)	0.9800
C(19B)-H(19E)	0.9800
C(19B)-H(19F)	0.9800
C(19B)-H(19G)	0.9800
C(19B)-H(19H)	0.9800
C(19B)-H(19I)	0.9800
C(20B)-H(20D)	0.9800

C(20B)-H(20E)	0.9800
C(20B)-H(20F)	0.9800
C(21B)-H(21D)	0.9800
C(21B)-H(21E)	0.9800
C(21B)-H(21F)	0.9800
C(24B)-C(25B)	1.400(7)
C(24B)-C(28B)	1.405(6)
C(24B)-H(24B)	1.0000
C(25B)-C(26B)	1.395(6)
C(25B)-H(25B)	1.0000
C(26B)-C(27B)	1.399(7)
C(26B)-H(26B)	1.0000
C(27B)-C(28B)	1.420(7)
C(27B)-H(27B)	1.0000
C(28B)-H(28B)	1.0000

C(23A)-Mo(1A)-C(22A)	77.82(18)
C(23A)-Mo(1A)-C(1A)	89.59(17)
C(22A)-Mo(1A)-C(1A)	97.89(16)
C(23A)-Mo(1A)-C(24A)	98.13(18)
C(22A)-Mo(1A)-C(24A)	106.06(18)
C(1A)-Mo(1A)-C(24A)	155.88(17)
C(23A)-Mo(1A)-C(28A)	126.70(19)
C(22A)-Mo(1A)-C(28A)	91.74(18)
C(1A)-Mo(1A)-C(28A)	143.70(16)
C(24A)-Mo(1A)-C(28A)	34.76(18)
C(23A)-Mo(1A)-C(25A)	100.01(18)
C(22A)-Mo(1A)-C(25A)	140.50(18)
C(1A)-Mo(1A)-C(25A)	121.60(17)
C(24A)-Mo(1A)-C(25A)	34.60(17)
C(28A)-Mo(1A)-C(25A)	57.56(18)
C(23A)-Mo(1A)-C(26A)	130.13(19)
C(22A)-Mo(1A)-C(26A)	145.96(18)
C(1A)-Mo(1A)-C(26A)	100.84(15)
C(24A)-Mo(1A)-C(26A)	56.99(16)
C(28A)-Mo(1A)-C(26A)	57.03(17)
C(25A)-Mo(1A)-C(26A)	34.17(16)
C(23A)-Mo(1A)-C(27A)	154.69(18)
C(22A)-Mo(1A)-C(27A)	112.32(19)
C(1A)-Mo(1A)-C(27A)	110.88(16)
C(24A)-Mo(1A)-C(27A)	57.20(17)

C(28A)-Mo(1A)-C(27A)	34.44(17)
C(25A)-Mo(1A)-C(27A)	56.97(17)
C(26A)-Mo(1A)-C(27A)	33.99(17)
N(1A)-C(1A)-N(2A)	102.1(3)
N(1A)-C(1A)-Mo(1A)	129.8(3)
N(2A)-C(1A)-Mo(1A)	128.1(3)
C(3A)-N(1A)-C(1A)	112.4(4)
C(3A)-N(1A)-C(4A)	120.4(4)
C(1A)-N(1A)-C(4A)	127.2(3)
C(1A)-N(2A)-C(2A)	111.8(4)
C(1A)-N(2A)-C(13A)	127.4(3)
C(2A)-N(2A)-C(13A)	120.7(4)
C(3A)-C(2A)-N(2A)	106.8(4)
C(3A)-C(2A)-H(2AA)	126.6
N(2A)-C(2A)-H(2AA)	126.6
C(2A)-C(3A)-N(1A)	106.9(4)
C(2A)-C(3A)-H(3AA)	126.5
N(1A)-C(3A)-H(3AA)	126.5
C(9A)-C(4A)-C(5A)	122.2(4)
C(9A)-C(4A)-N(1A)	119.3(4)
C(5A)-C(4A)-N(1A)	118.4(4)
C(6A)-C(5A)-C(4A)	116.8(4)
C(6A)-C(5A)-C(10A)	121.2(4)
C(4A)-C(5A)-C(10A)	122.0(4)
C(7A)-C(6A)-C(5A)	122.3(4)
C(7A)-C(6A)-H(6AA)	118.8
C(5A)-C(6A)-H(6AA)	118.8
C(6A)-C(7A)-C(8A)	118.5(4)
C(6A)-C(7A)-C(11A)	120.8(4)
C(8A)-C(7A)-C(11A)	120.7(4)
C(9A)-C(8A)-C(7A)	122.1(4)
C(9A)-C(8A)-H(8AA)	118.9
C(7A)-C(8A)-H(8AA)	118.9
C(8A)-C(9A)-C(4A)	118.0(4)
C(8A)-C(9A)-C(12A)	121.3(4)
C(4A)-C(9A)-C(12A)	120.7(4)
C(5A)-C(10A)-H(10A)	109.5
C(5A)-C(10A)-H(10B)	109.5
H(10A)-C(10A)-H(10B)	109.5
C(5A)-C(10A)-H(10C)	109.5
H(10A)-C(10A)-H(10C)	109.5
H(10B)-C(10A)-H(10C)	109.5
C(7A)-C(11A)-H(11A)	109.5

C(7A)-C(11A)-H(11B)	109.5
H(11A)-C(11A)-H(11B)	109.5
C(7A)-C(11A)-H(11C)	109.5
H(11A)-C(11A)-H(11C)	109.5
H(11B)-C(11A)-H(11C)	109.5
C(9A)-C(12A)-H(12A)	109.5
C(9A)-C(12A)-H(12B)	109.5
H(12A)-C(12A)-H(12B)	109.5
C(9A)-C(12A)-H(12C)	109.5
H(12A)-C(12A)-H(12C)	109.5
H(12B)-C(12A)-H(12C)	109.5
C(18A)-C(13A)-C(14A)	122.7(4)
C(18A)-C(13A)-N(2A)	119.8(4)
C(14A)-C(13A)-N(2A)	117.5(4)
C(13A)-C(14A)-C(15A)	117.1(4)
C(13A)-C(14A)-C(19A)	121.1(4)
C(15A)-C(14A)-C(19A)	121.7(4)
C(16A)-C(15A)-C(14A)	122.4(4)
C(16A)-C(15A)-H(15A)	118.8
C(14A)-C(15A)-H(15A)	118.8
C(17A)-C(16A)-C(15A)	118.5(4)
C(17A)-C(16A)-C(20A)	120.7(4)
C(15A)-C(16A)-C(20A)	120.8(4)
C(16A)-C(17A)-C(18A)	121.6(4)
C(16A)-C(17A)-H(17A)	119.2
C(18A)-C(17A)-H(17A)	119.2
C(13A)-C(18A)-C(17A)	117.8(4)
C(13A)-C(18A)-C(21A)	122.1(4)
C(17A)-C(18A)-C(21A)	120.1(4)
C(14A)-C(19A)-H(19A)	109.5
C(14A)-C(19A)-H(19B)	109.5
H(19A)-C(19A)-H(19B)	109.5
C(14A)-C(19A)-H(19C)	109.5
H(19A)-C(19A)-H(19C)	109.5
H(19B)-C(19A)-H(19C)	109.5
C(16A)-C(20A)-H(20A)	109.5
C(16A)-C(20A)-H(20B)	109.5
H(20A)-C(20A)-H(20B)	109.5
C(16A)-C(20A)-H(20C)	109.5
H(20A)-C(20A)-H(20C)	109.5
H(20B)-C(20A)-H(20C)	109.5
C(18A)-C(21A)-H(21A)	109.5
C(18A)-C(21A)-H(21B)	109.5

H(21A)-C(21A)-H(21B)	109.5
C(18A)-C(21A)-H(21C)	109.5
H(21A)-C(21A)-H(21C)	109.5
H(21B)-C(21A)-H(21C)	109.5
O(1A)-C(22A)-Mo(1A)	172.4(4)
O(2A)-C(23A)-Mo(1A)	176.9(4)
C(25A)-C(24A)-C(28A)	108.2(4)
C(25A)-C(24A)-Mo(1A)	73.3(3)
C(28A)-C(24A)-Mo(1A)	73.1(3)
C(25A)-C(24A)-H(24A)	125.7
C(28A)-C(24A)-H(24A)	125.7
Mo(1A)-C(24A)-H(24A)	125.7
C(26A)-C(25A)-C(24A)	107.8(5)
C(26A)-C(25A)-Mo(1A)	74.0(3)
C(24A)-C(25A)-Mo(1A)	72.1(3)
C(26A)-C(25A)-H(25A)	125.8
C(24A)-C(25A)-H(25A)	125.8
Mo(1A)-C(25A)-H(25A)	125.8
C(25A)-C(26A)-C(27A)	108.5(4)
C(25A)-C(26A)-Mo(1A)	71.8(2)
C(27A)-C(26A)-Mo(1A)	73.0(3)
C(25A)-C(26A)-H(26A)	125.6
C(27A)-C(26A)-H(26A)	125.6
Mo(1A)-C(26A)-H(26A)	125.6
C(26A)-C(27A)-C(28A)	107.9(4)
C(26A)-C(27A)-Mo(1A)	73.0(3)
C(28A)-C(27A)-Mo(1A)	71.5(2)
C(26A)-C(27A)-H(27A)	125.9
C(28A)-C(27A)-H(27A)	125.9
Mo(1A)-C(27A)-H(27A)	125.9
C(24A)-C(28A)-C(27A)	107.6(5)
C(24A)-C(28A)-Mo(1A)	72.2(3)
C(27A)-C(28A)-Mo(1A)	74.1(3)
C(24A)-C(28A)-H(28A)	125.9
C(27A)-C(28A)-H(28A)	125.9
Mo(1A)-C(28A)-H(28A)	125.9
C(23B)-Mo(1B)-C(22B)	78.71(17)
C(23B)-Mo(1B)-C(1B)	87.58(16)
C(22B)-Mo(1B)-C(1B)	98.24(16)
C(23B)-Mo(1B)-C(26B)	115.42(18)
C(22B)-Mo(1B)-C(26B)	92.61(18)
C(1B)-Mo(1B)-C(26B)	156.18(16)
C(23B)-Mo(1B)-C(25B)	95.64(17)

C(22B)-Mo(1B)-C(25B)	117.39(18)
C(1B)-Mo(1B)-C(25B)	144.20(17)
C(26B)-Mo(1B)-C(25B)	34.34(16)
C(23B)-Mo(1B)-C(27B)	149.67(19)
C(22B)-Mo(1B)-C(27B)	101.11(18)
C(1B)-Mo(1B)-C(27B)	122.04(17)
C(26B)-Mo(1B)-C(27B)	34.44(16)
C(25B)-Mo(1B)-C(27B)	57.07(16)
C(23B)-Mo(1B)-C(28B)	142.73(19)
C(22B)-Mo(1B)-C(28B)	134.57(17)
C(1B)-Mo(1B)-C(28B)	100.51(16)
C(26B)-Mo(1B)-C(28B)	57.70(18)
C(25B)-Mo(1B)-C(28B)	57.34(17)
C(27B)-Mo(1B)-C(28B)	34.88(17)
C(23B)-Mo(1B)-C(24B)	108.80(17)
C(22B)-Mo(1B)-C(24B)	149.60(18)
C(1B)-Mo(1B)-C(24B)	111.26(17)
C(26B)-Mo(1B)-C(24B)	57.28(18)
C(25B)-Mo(1B)-C(24B)	34.38(16)
C(27B)-Mo(1B)-C(24B)	57.27(17)
C(28B)-Mo(1B)-C(24B)	34.42(16)
C(1B)-N(1B)-C(3B)	112.3(4)
C(1B)-N(1B)-C(4B)	125.5(3)
C(3B)-N(1B)-C(4B)	122.2(4)
N(1B)-C(1B)-N(2B)	103.1(3)
N(1B)-C(1B)-Mo(1B)	129.9(3)
N(2B)-C(1B)-Mo(1B)	126.9(3)
C(1B)-N(2B)-C(2B)	111.4(4)
C(1B)-N(2B)-C(13B)	124.8(3)
C(2B)-N(2B)-C(13B)	123.7(4)
C(3B)-C(2B)-N(2B)	106.8(4)
C(3B)-C(2B)-H(2BA)	126.6
N(2B)-C(2B)-H(2BA)	126.6
C(2B)-C(3B)-N(1B)	106.5(4)
C(2B)-C(3B)-H(3BA)	126.8
N(1B)-C(3B)-H(3BA)	126.8
C(9B)-C(4B)-C(5B)	122.1(4)
C(9B)-C(4B)-N(1B)	119.3(4)
C(5B)-C(4B)-N(1B)	118.6(4)
C(6B)-C(5B)-C(4B)	117.6(4)
C(6B)-C(5B)-C(10B)	121.4(4)
C(4B)-C(5B)-C(10B)	121.0(4)
C(5B)-C(6B)-C(7B)	122.2(4)

C(5B)-C(6B)-H(6BA)	118.9
C(7B)-C(6B)-H(6BA)	118.9
C(6B)-C(7B)-C(8B)	118.7(4)
C(6B)-C(7B)-C(11B)	120.9(4)
C(8B)-C(7B)-C(11B)	120.4(4)
C(7B)-C(8B)-C(9B)	121.2(4)
C(7B)-C(8B)-H(8BA)	119.4
C(9B)-C(8B)-H(8BA)	119.4
C(8B)-C(9B)-C(4B)	118.2(4)
C(8B)-C(9B)-C(12B)	120.5(4)
C(4B)-C(9B)-C(12B)	121.2(4)
C(5B)-C(10B)-H(10D)	109.5
C(5B)-C(10B)-H(10E)	109.5
H(10D)-C(10B)-H(10E)	109.5
C(5B)-C(10B)-H(10F)	109.5
H(10D)-C(10B)-H(10F)	109.5
H(10E)-C(10B)-H(10F)	109.5
C(7B)-C(11B)-H(11D)	109.5
C(7B)-C(11B)-H(11E)	109.5
H(11D)-C(11B)-H(11E)	109.5
C(7B)-C(11B)-H(11F)	109.5
H(11D)-C(11B)-H(11F)	109.5
H(11E)-C(11B)-H(11F)	109.5
C(9B)-C(12B)-H(12D)	109.5
C(9B)-C(12B)-H(12E)	109.5
H(12D)-C(12B)-H(12E)	109.5
C(9B)-C(12B)-H(12F)	109.5
H(12D)-C(12B)-H(12F)	109.5
H(12E)-C(12B)-H(12F)	109.5
C(18B)-C(13B)-C(14B)	122.2(4)
C(18B)-C(13B)-N(2B)	118.2(3)
C(14B)-C(13B)-N(2B)	119.6(4)
C(15B)-C(14B)-C(13B)	117.1(4)
C(15B)-C(14B)-C(19B)	120.7(4)
C(13B)-C(14B)-C(19B)	122.2(4)
C(16B)-C(15B)-C(14B)	122.8(4)
C(16B)-C(15B)-H(15B)	118.6
C(14B)-C(15B)-H(15B)	118.6
C(15B)-C(16B)-C(17B)	117.7(4)
C(15B)-C(16B)-C(20B)	121.1(4)
C(17B)-C(16B)-C(20B)	121.1(4)
C(18B)-C(17B)-C(16B)	121.8(4)
C(18B)-C(17B)-H(17B)	119.1

C(16B)-C(17B)-H(17B)	119.1
C(17B)-C(18B)-C(13B)	118.2(4)
C(17B)-C(18B)-C(21B)	121.1(4)
C(13B)-C(18B)-C(21B)	120.6(4)
C(14B)-C(19B)-H(19D)	109.5
C(14B)-C(19B)-H(19E)	109.5
H(19D)-C(19B)-H(19E)	109.5
C(14B)-C(19B)-H(19F)	109.5
H(19D)-C(19B)-H(19F)	109.5
H(19E)-C(19B)-H(19F)	109.5
C(14B)-C(19B)-H(19G)	109.5
H(19D)-C(19B)-H(19G)	141.1
H(19E)-C(19B)-H(19G)	56.3
H(19F)-C(19B)-H(19G)	56.3
C(14B)-C(19B)-H(19H)	109.5
H(19D)-C(19B)-H(19H)	56.3
H(19E)-C(19B)-H(19H)	141.1
H(19F)-C(19B)-H(19H)	56.3
H(19G)-C(19B)-H(19H)	109.5
C(14B)-C(19B)-H(19I)	109.5
H(19D)-C(19B)-H(19I)	56.3
H(19E)-C(19B)-H(19I)	56.3
H(19F)-C(19B)-H(19I)	141.1
H(19G)-C(19B)-H(19I)	109.5
H(19H)-C(19B)-H(19I)	109.5
C(16B)-C(20B)-H(20D)	109.5
C(16B)-C(20B)-H(20E)	109.5
H(20D)-C(20B)-H(20E)	109.5
C(16B)-C(20B)-H(20F)	109.5
H(20D)-C(20B)-H(20F)	109.5
H(20E)-C(20B)-H(20F)	109.5
C(18B)-C(21B)-H(21D)	109.5
C(18B)-C(21B)-H(21E)	109.5
H(21D)-C(21B)-H(21E)	109.5
C(18B)-C(21B)-H(21F)	109.5
H(21D)-C(21B)-H(21F)	109.5
H(21E)-C(21B)-H(21F)	109.5
O(1B)-C(22B)-Mo(1B)	173.6(4)
O(2B)-C(23B)-Mo(1B)	176.4(4)
C(25B)-C(24B)-C(28B)	108.2(4)
C(25B)-C(24B)-Mo(1B)	72.4(3)
C(28B)-C(24B)-Mo(1B)	72.7(3)
C(25B)-C(24B)-H(24B)	125.7

C(28B)-C(24B)-H(24B)	125.7
Mo(1B)-C(24B)-H(24B)	125.7
C(26B)-C(25B)-C(24B)	108.6(4)
C(26B)-C(25B)-Mo(1B)	72.7(3)
C(24B)-C(25B)-Mo(1B)	73.2(3)
C(26B)-C(25B)-H(25B)	125.5
C(24B)-C(25B)-H(25B)	125.5
Mo(1B)-C(25B)-H(25B)	125.5
C(25B)-C(26B)-C(27B)	107.9(5)
C(25B)-C(26B)-Mo(1B)	72.9(2)
C(27B)-C(26B)-Mo(1B)	72.9(3)
C(25B)-C(26B)-H(26B)	125.8
C(27B)-C(26B)-H(26B)	125.8
Mo(1B)-C(26B)-H(26B)	125.8
C(26B)-C(27B)-C(28B)	108.2(4)
C(26B)-C(27B)-Mo(1B)	72.6(2)
C(28B)-C(27B)-Mo(1B)	72.9(2)
C(26B)-C(27B)-H(27B)	125.7
C(28B)-C(27B)-H(27B)	125.7
Mo(1B)-C(27B)-H(27B)	125.7
C(24B)-C(28B)-C(27B)	107.1(5)
C(24B)-C(28B)-Mo(1B)	72.9(3)
C(27B)-C(28B)-Mo(1B)	72.3(3)
C(24B)-C(28B)-H(28B)	126.2
C(27B)-C(28B)-H(28B)	126.2
Mo(1B)-C(28B)-H(28B)	126.2

Anisotropic displacement parameters (A^2 x 10^3) for mes131. The anisotropic displacement factor exponent takes the form: $-2\pi^2 [h^2 a^{*2} U^{11} + ... + 2 h k a^* b^* U^{12}]$

	U^{11}	U^{22}	U^{33}	U^{23}	U^{13}	U^{12}
Mo(1A)	26(1)	24(1)	32(1)	-3(1)	-9(1)	-3(1)
O(1A)	54(2)	39(2)	32(2)	-7(2)	-7(2)	-9(2)
C(1A)	20(2)	31(3)	24(3)	-3(2)	1(2)	-3(2)
N(1A)	34(2)	24(2)	28(2)	-3(2)	-3(2)	0(2)
N(2A)	36(2)	21(2)	30(2)	-3(2)	-6(2)	-2(2)
O(2A)	26(2)	91(3)	44(2)	-5(2)	-7(2)	-9(2)
C(2A)	64(3)	20(3)	43(3)	-7(2)	-4(3)	-4(2)
C(3A)	63(3)	24(3)	38(3)	-2(2)	-4(2)	3(2)
C(4A)	32(2)	24(2)	26(3)	-3(2)	-4(2)	-1(2)
C(5A)	29(2)	35(3)	33(3)	-3(2)	-4(2)	3(2)
C(6A)	28(2)	49(3)	33(3)	-3(2)	-6(2)	-1(2)
C(7A)	35(3)	36(3)	32(3)	-2(2)	-5(2)	-7(2)
C(8A)	30(2)	35(3)	28(3)	-1(2)	8(2)	-4(2)
C(9A)	28(2)	23(2)	32(3)	-2(2)	-3(2)	0(2)
C(10A)	36(3)	62(4)	42(3)	-8(3)	-2(2)	14(2)
C(11A)	49(3)	63(4)	36(3)	-15(3)	-8(2)	-3(3)
C(12A)	26(2)	46(3)	47(3)	-9(3)	-5(2)	-1(2)
C(13A)	33(2)	25(3)	28(3)	-10(2)	-7(2)	-4(2)
C(14A)	29(2)	40(3)	41(3)	-14(2)	2(2)	-11(2)
C(15A)	27(2)	50(3)	47(3)	-17(3)	-8(2)	-8(2)
C(16A)	44(3)	36(3)	31(3)	-7(2)	-8(2)	-8(2)
C(17A)	34(3)	39(3)	32(3)	-10(2)	4(2)	-7(2)
C(18A)	31(2)	28(3)	35(3)	-9(2)	1(2)	-5(2)
C(19A)	37(3)	65(4)	48(3)	-18(3)	4(2)	-16(3)
C(20A)	59(3)	55(4)	33(3)	-9(3)	-15(2)	-7(3)
C(21A)	28(2)	56(3)	48(3)	-12(3)	-6(2)	-3(2)
C(22A)	30(2)	25(3)	36(3)	-1(2)	0(2)	-4(2)
C(23A)	32(3)	42(3)	25(3)	-4(2)	-5(2)	-5(2)
C(24A)	59(3)	24(3)	58(4)	5(3)	-26(3)	-2(2)
C(25A)	53(3)	40(3)	31(3)	7(2)	-13(2)	3(2)
C(26A)	54(3)	32(3)	50(3)	-2(3)	-35(3)	-2(2)
C(27A)	31(3)	52(4)	54(4)	3(3)	-14(2)	7(2)
C(28A)	55(3)	39(3)	54(4)	-17(3)	-28(3)	24(3)
Mo(1B)	23(1)	24(1)	33(1)	-3(1)	-5(1)	-3(1)
N(1B)	28(2)	25(2)	29(2)	-2(2)	-8(2)	-2(2)
O(1B)	50(2)	42(2)	38(2)	-10(2)	-8(2)	4(2)
C(1B)	18(2)	25(2)	26(3)	-5(2)	-7(2)	2(2)

N(2B)	34(2)	26(2)	28(2)	0(2)	-10(2)	-6(2)
O(2B)	27(2)	48(2)	63(2)	-14(2)	-7(2)	3(2)
C(2B)	49(3)	21(3)	39(3)	-2(2)	-11(2)	-10(2)
C(3B)	46(3)	25(3)	32(3)	2(2)	-8(2)	-7(2)
C(4B)	32(2)	25(3)	25(3)	-3(2)	-8(2)	-3(2)
C(5B)	27(2)	31(3)	32(3)	-3(2)	-5(2)	2(2)
C(6B)	32(2)	38(3)	35(3)	-1(2)	-16(2)	2(2)
C(7B)	44(3)	31(3)	31(3)	0(2)	-11(2)	5(2)
C(8B)	36(3)	38(3)	30(3)	-4(2)	-1(2)	6(2)
C(9B)	26(2)	29(3)	31(3)	-1(2)	-2(2)	-1(2)
C(10B)	28(2)	55(3)	46(3)	-15(3)	-9(2)	1(2)
C(11B)	63(3)	67(4)	37(3)	-22(3)	-17(3)	4(3)
C(12B)	32(2)	48(3)	39(3)	-8(3)	-6(2)	-3(2)
C(13B)	32(2)	18(2)	26(3)	-1(2)	-7(2)	-3(2)
C(14B)	36(2)	24(3)	35(3)	-3(2)	-6(2)	-8(2)
C(15B)	34(3)	36(3)	37(3)	0(2)	-15(2)	-2(2)
C(16B)	40(3)	40(3)	38(3)	-8(2)	-7(2)	-3(2)
C(17B)	33(3)	42(3)	33(3)	-8(2)	-2(2)	4(2)
C(18B)	30(2)	30(3)	34(3)	-9(2)	-6(2)	0(2)
C(19B)	28(2)	48(3)	48(3)	-9(3)	-7(2)	-3(2)
C(20B)	58(3)	70(4)	34(3)	-5(3)	-7(3)	3(3)
C(21B)	38(3)	53(3)	45(3)	-17(3)	-14(2)	11(2)
C(22B)	24(2)	29(3)	38(3)	3(2)	-10(2)	-2(2)
C(23B)	36(3)	26(3)	33(3)	-3(2)	-3(2)	-6(2)
C(24B)	37(3)	50(3)	37(3)	-3(3)	2(2)	-12(2)
C(25B)	38(3)	38(3)	48(3)	7(3)	-4(2)	-13(2)
C(26B)	42(3)	34(3)	57(4)	-4(3)	1(3)	-20(2)
C(27B)	25(2)	62(4)	54(4)	2(3)	-5(2)	-21(3)
C(28B)	34(3)	38(3)	57(4)	1(3)	17(2)	-1(2)

Hydrogen coordinates (x 10^4) and isotropic displacement parameters (A^2 x 10^3) for mes131.

	x	y	z	U(eq)
H(2AA)	3877	10619	2611	51
H(3AA)	3400	10561	1351	51
H(6AA)	319	8880	103	45
H(8AA)	5036	8445	-411	40

H(10A)	287	9043	1908	72
H(10B)	-794	9198	1258	72
H(10C)	228	9937	1372	72
H(11A)	1316	8140	-900	73
H(11B)	3206	8024	-1128	73
H(11C)	2338	8915	-1355	73
H(12A)	6896	8587	371	60
H(12B)	6230	8527	1227	60
H(12C)	6442	9419	687	60
H(15A)	7249	9029	4460	47
H(17A)	2596	8726	5268	42
H(19A)	7033	9886	2724	74
H(19B)	7062	8922	2679	74
H(19C)	8188	9234	3176	74
H(20A)	4435	8555	6110	72
H(20B)	5756	9251	5843	72
H(20C)	6238	8297	5820	72
H(21A)	1004	9460	3684	65
H(21B)	594	8913	4498	65
H(21C)	1143	8465	3814	65
H(24A)	2996	5641	3561	56
H(25A)	2957	6747	4357	52
H(26A)	5517	7574	3923	52
H(27A)	7146	6988	2857	57
H(28A)	5580	5790	2626	57
H(2BA)	2419	5612	2215	43
H(3BA)	2468	5469	919	42
H(6BA)	-1050	3505	-188	42
H(8BA)	3740	3326	-699	43
H(10D)	-2291	4131	803	63
H(10E)	-1200	4658	1157	63
H(10F)	-1488	3697	1514	63
H(11D)	376	2632	-1134	80
H(11E)	2164	2898	-1475	80
H(11F)	699	3555	-1596	80
H(12D)	4876	4322	516	59
H(12E)	5483	3585	88	59
H(12F)	4750	3372	943	59
H(15B)	3471	3432	4677	43
H(17B)	-1080	4307	4679	44
H(19D)	5071	4254	3063	62
H(19E)	4471	3457	2825	62
H(19F)	5205	3352	3580	62

H(19G)	4761	3121	3249	62
H(19H)	5360	3919	3487	62
H(19I)	4626	4023	2732	62
H(20D)	1758	3736	5848	83
H(20E)	774	2960	5782	83
H(20F)	-133	3836	5833	83
H(21D)	-2169	4814	3574	66
H(21E)	-1308	4513	2845	66
H(21F)	-876	5385	3010	66
H(24B)	436	2409	4133	51
H(25B)	1266	1005	3764	52
H(26B)	-478	783	2818	54
H(27B)	-2406	2053	2593	58
H(28B)	-1845	3074	3409	56

Torsion angles [°] for mes131.

C(23A)-Mo(1A)-C(1A)-N(1A)	-72.3(4)
C(22A)-Mo(1A)-C(1A)-N(1A)	5.3(4)
C(24A)-Mo(1A)-C(1A)-N(1A)	178.4(4)
C(28A)-Mo(1A)-C(1A)-N(1A)	109.2(4)
C(25A)-Mo(1A)-C(1A)-N(1A)	-173.8(3)
C(26A)-Mo(1A)-C(1A)-N(1A)	156.8(3)
C(27A)-Mo(1A)-C(1A)-N(1A)	122.9(3)
C(23A)-Mo(1A)-C(1A)-N(2A)	104.9(4)
C(22A)-Mo(1A)-C(1A)-N(2A)	-177.4(3)
C(24A)-Mo(1A)-C(1A)-N(2A)	-4.3(6)
C(28A)-Mo(1A)-C(1A)-N(2A)	-73.5(4)
C(25A)-Mo(1A)-C(1A)-N(2A)	3.4(4)
C(26A)-Mo(1A)-C(1A)-N(2A)	-26.0(4)
C(27A)-Mo(1A)-C(1A)-N(2A)	-59.8(4)
N(2A)-C(1A)-N(1A)-C(3A)	-0.4(4)
Mo(1A)-C(1A)-N(1A)-C(3A)	177.4(3)
N(2A)-C(1A)-N(1A)-C(4A)	-179.9(4)
Mo(1A)-C(1A)-N(1A)-C(4A)	-2.1(6)
N(1A)-C(1A)-N(2A)-C(2A)	0.6(4)
Mo(1A)-C(1A)-N(2A)-C(2A)	-177.2(3)
N(1A)-C(1A)-N(2A)-C(13A)	-176.4(4)

Mo(1A)-C(1A)-N(2A)-C(13A)	5.8(6)
C(1A)-N(2A)-C(2A)-C(3A)	-0.6(5)
C(13A)-N(2A)-C(2A)-C(3A)	176.6(4)
N(2A)-C(2A)-C(3A)-N(1A)	0.3(5)
C(1A)-N(1A)-C(3A)-C(2A)	0.1(5)
C(4A)-N(1A)-C(3A)-C(2A)	179.6(4)
C(3A)-N(1A)-C(4A)-C(9A)	95.7(5)
C(1A)-N(1A)-C(4A)-C(9A)	-84.9(5)
C(3A)-N(1A)-C(4A)-C(5A)	-80.2(5)
C(1A)-N(1A)-C(4A)-C(5A)	99.2(5)
C(9A)-C(4A)-C(5A)-C(6A)	1.9(6)
N(1A)-C(4A)-C(5A)-C(6A)	177.6(4)
C(9A)-C(4A)-C(5A)-C(10A)	-176.9(4)
N(1A)-C(4A)-C(5A)-C(10A)	-1.2(6)
C(4A)-C(5A)-C(6A)-C(7A)	0.1(7)
C(10A)-C(5A)-C(6A)-C(7A)	178.9(4)
C(5A)-C(6A)-C(7A)-C(8A)	-0.8(7)
C(5A)-C(6A)-C(7A)-C(11A)	-179.9(4)
C(6A)-C(7A)-C(8A)-C(9A)	-0.4(7)
C(11A)-C(7A)-C(8A)-C(9A)	178.7(4)
C(7A)-C(8A)-C(9A)-C(4A)	2.2(7)
C(7A)-C(8A)-C(9A)-C(12A)	-176.9(4)
C(5A)-C(4A)-C(9A)-C(8A)	-3.0(6)
N(1A)-C(4A)-C(9A)-C(8A)	-178.7(4)
C(5A)-C(4A)-C(9A)-C(12A)	176.1(4)
N(1A)-C(4A)-C(9A)-C(12A)	0.4(6)
C(1A)-N(2A)-C(13A)-C(18A)	-84.9(5)
C(2A)-N(2A)-C(13A)-C(18A)	98.3(5)
C(1A)-N(2A)-C(13A)-C(14A)	98.2(5)
C(2A)-N(2A)-C(13A)-C(14A)	-78.6(5)
C(18A)-C(13A)-C(14A)-C(15A)	0.5(7)
N(2A)-C(13A)-C(14A)-C(15A)	177.4(4)
C(18A)-C(13A)-C(14A)-C(19A)	178.2(4)
N(2A)-C(13A)-C(14A)-C(19A)	-5.0(6)
C(13A)-C(14A)-C(15A)-C(16A)	-1.0(7)
C(19A)-C(14A)-C(15A)-C(16A)	-178.7(5)
C(14A)-C(15A)-C(16A)-C(17A)	1.1(7)
C(14A)-C(15A)-C(16A)-C(20A)	-178.6(4)
C(15A)-C(16A)-C(17A)-C(18A)	-0.6(7)
C(20A)-C(16A)-C(17A)-C(18A)	179.1(4)
C(14A)-C(13A)-C(18A)-C(17A)	-0.1(7)
N(2A)-C(13A)-C(18A)-C(17A)	-176.8(4)
C(14A)-C(13A)-C(18A)-C(21A)	179.2(4)

N(2A)-C(13A)-C(18A)-C(21A)	2.5(6)
C(16A)-C(17A)-C(18A)-C(13A)	0.1(7)
C(16A)-C(17A)-C(18A)-C(21A)	-179.2(4)
C(23A)-Mo(1A)-C(22A)-O(1A)	-71(3)
C(1A)-Mo(1A)-C(22A)-O(1A)	-159(3)
C(24A)-Mo(1A)-C(22A)-O(1A)	24(3)
C(28A)-Mo(1A)-C(22A)-O(1A)	56(3)
C(25A)-Mo(1A)-C(22A)-O(1A)	20(3)
C(26A)-Mo(1A)-C(22A)-O(1A)	78(3)
C(27A)-Mo(1A)-C(22A)-O(1A)	85(3)
C(22A)-Mo(1A)-C(23A)-O(2A)	41(7)
C(1A)-Mo(1A)-C(23A)-O(2A)	139(8)
C(24A)-Mo(1A)-C(23A)-O(2A)	-64(8)
C(28A)-Mo(1A)-C(23A)-O(2A)	-42(8)
C(25A)-Mo(1A)-C(23A)-O(2A)	-99(8)
C(26A)-Mo(1A)-C(23A)-O(2A)	-117(7)
C(27A)-Mo(1A)-C(23A)-O(2A)	-76(8)
C(23A)-Mo(1A)-C(24A)-C(25A)	-95.9(3)
C(22A)-Mo(1A)-C(24A)-C(25A)	-175.5(3)
C(1A)-Mo(1A)-C(24A)-C(25A)	11.7(6)
C(28A)-Mo(1A)-C(24A)-C(25A)	115.6(4)
C(26A)-Mo(1A)-C(24A)-C(25A)	37.3(3)
C(27A)-Mo(1A)-C(24A)-C(25A)	78.0(3)
C(23A)-Mo(1A)-C(24A)-C(28A)	148.5(3)
C(22A)-Mo(1A)-C(24A)-C(28A)	68.9(3)
C(1A)-Mo(1A)-C(24A)-C(28A)	-103.9(5)
C(25A)-Mo(1A)-C(24A)-C(28A)	-115.6(4)
C(26A)-Mo(1A)-C(24A)-C(28A)	-78.3(3)
C(27A)-Mo(1A)-C(24A)-C(28A)	-37.6(3)
C(28A)-C(24A)-C(25A)-C(26A)	-0.7(5)
Mo(1A)-C(24A)-C(25A)-C(26A)	-65.9(3)
C(28A)-C(24A)-C(25A)-Mo(1A)	65.2(3)
C(23A)-Mo(1A)-C(25A)-C(26A)	-154.9(3)
C(22A)-Mo(1A)-C(25A)-C(26A)	122.2(3)
C(1A)-Mo(1A)-C(25A)-C(26A)	-59.1(3)
C(24A)-Mo(1A)-C(25A)-C(26A)	115.3(4)
C(28A)-Mo(1A)-C(25A)-C(26A)	77.8(3)
C(27A)-Mo(1A)-C(25A)-C(26A)	36.6(3)
C(23A)-Mo(1A)-C(25A)-C(24A)	89.8(3)
C(22A)-Mo(1A)-C(25A)-C(24A)	6.9(4)
C(1A)-Mo(1A)-C(25A)-C(24A)	-174.4(3)
C(28A)-Mo(1A)-C(25A)-C(24A)	-37.5(3)
C(26A)-Mo(1A)-C(25A)-C(24A)	-115.3(4)

C(27A)-Mo(1A)-C(25A)-C(24A)	-78.7(3)
C(24A)-C(25A)-C(26A)-C(27A)	0.4(5)
Mo(1A)-C(25A)-C(26A)-C(27A)	-64.3(3)
C(24A)-C(25A)-C(26A)-Mo(1A)	64.7(3)
C(23A)-Mo(1A)-C(26A)-C(25A)	33.2(4)
C(22A)-Mo(1A)-C(26A)-C(25A)	-105.9(4)
C(1A)-Mo(1A)-C(26A)-C(25A)	131.9(3)
C(24A)-Mo(1A)-C(26A)-C(25A)	-37.7(3)
C(28A)-Mo(1A)-C(26A)-C(25A)	-79.5(3)
C(27A)-Mo(1A)-C(26A)-C(25A)	-116.7(4)
C(23A)-Mo(1A)-C(26A)-C(27A)	149.8(3)
C(22A)-Mo(1A)-C(26A)-C(27A)	10.8(5)
C(1A)-Mo(1A)-C(26A)-C(27A)	-111.4(3)
C(24A)-Mo(1A)-C(26A)-C(27A)	78.9(3)
C(28A)-Mo(1A)-C(26A)-C(27A)	37.2(3)
C(25A)-Mo(1A)-C(26A)-C(27A)	116.7(4)
C(25A)-C(26A)-C(27A)-C(28A)	0.1(5)
Mo(1A)-C(26A)-C(27A)-C(28A)	-63.4(3)
C(25A)-C(26A)-C(27A)-Mo(1A)	63.5(3)
C(23A)-Mo(1A)-C(27A)-C(26A)	-63.9(6)
C(22A)-Mo(1A)-C(27A)-C(26A)	-173.5(3)
C(1A)-Mo(1A)-C(27A)-C(26A)	78.1(3)
C(24A)-Mo(1A)-C(27A)-C(26A)	-78.3(3)
C(28A)-Mo(1A)-C(27A)-C(26A)	-116.2(5)
C(25A)-Mo(1A)-C(27A)-C(26A)	-36.8(3)
C(23A)-Mo(1A)-C(27A)-C(28A)	52.3(6)
C(22A)-Mo(1A)-C(27A)-C(28A)	-57.3(4)
C(1A)-Mo(1A)-C(27A)-C(28A)	-165.7(3)
C(24A)-Mo(1A)-C(27A)-C(28A)	38.0(3)
C(25A)-Mo(1A)-C(27A)-C(28A)	79.4(3)
C(26A)-Mo(1A)-C(27A)-C(28A)	116.2(5)
C(25A)-C(24A)-C(28A)-C(27A)	0.8(5)
Mo(1A)-C(24A)-C(28A)-C(27A)	66.2(3)
C(25A)-C(24A)-C(28A)-Mo(1A)	-65.4(3)
C(26A)-C(27A)-C(28A)-C(24A)	-0.5(5)
Mo(1A)-C(27A)-C(28A)-C(24A)	-64.9(3)
C(26A)-C(27A)-C(28A)-Mo(1A)	64.4(3)
C(23A)-Mo(1A)-C(28A)-C(24A)	-40.1(4)
C(22A)-Mo(1A)-C(28A)-C(24A)	-116.2(3)
C(1A)-Mo(1A)-C(28A)-C(24A)	137.9(3)
C(25A)-Mo(1A)-C(28A)-C(24A)	37.4(3)
C(26A)-Mo(1A)-C(28A)-C(24A)	78.2(3)
C(27A)-Mo(1A)-C(28A)-C(24A)	114.9(5)

C(23A)-Mo(1A)-C(28A)-C(27A)	-155.1(3)
C(22A)-Mo(1A)-C(28A)-C(27A)	128.9(3)
C(1A)-Mo(1A)-C(28A)-C(27A)	23.0(5)
C(24A)-Mo(1A)-C(28A)-C(27A)	-114.9(5)
C(25A)-Mo(1A)-C(28A)-C(27A)	-77.6(3)
C(26A)-Mo(1A)-C(28A)-C(27A)	-36.7(3)
C(3B)-N(1B)-C(1B)-N(2B)	1.0(4)
C(4B)-N(1B)-C(1B)-N(2B)	-177.2(3)
C(3B)-N(1B)-C(1B)-Mo(1B)	-175.5(3)
C(4B)-N(1B)-C(1B)-Mo(1B)	6.2(5)
C(23B)-Mo(1B)-C(1B)-N(1B)	88.8(3)
C(22B)-Mo(1B)-C(1B)-N(1B)	10.5(4)
C(26B)-Mo(1B)-C(1B)-N(1B)	-105.7(5)
C(25B)-Mo(1B)-C(1B)-N(1B)	-175.0(3)
C(27B)-Mo(1B)-C(1B)-N(1B)	-98.2(4)
C(28B)-Mo(1B)-C(1B)-N(1B)	-127.9(3)
C(24B)-Mo(1B)-C(1B)-N(1B)	-162.0(3)
C(23B)-Mo(1B)-C(1B)-N(2B)	-87.1(3)
C(22B)-Mo(1B)-C(1B)-N(2B)	-165.3(3)
C(26B)-Mo(1B)-C(1B)-N(2B)	78.5(5)
C(25B)-Mo(1B)-C(1B)-N(2B)	9.2(5)
C(27B)-Mo(1B)-C(1B)-N(2B)	86.0(4)
C(28B)-Mo(1B)-C(1B)-N(2B)	56.3(3)
C(24B)-Mo(1B)-C(1B)-N(2B)	22.2(4)
N(1B)-C(1B)-N(2B)-C(2B)	-0.4(4)
Mo(1B)-C(1B)-N(2B)-C(2B)	176.3(3)
N(1B)-C(1B)-N(2B)-C(13B)	176.4(3)
Mo(1B)-C(1B)-N(2B)-C(13B)	-6.9(5)
C(1B)-N(2B)-C(2B)-C(3B)	-0.4(5)
C(13B)-N(2B)-C(2B)-C(3B)	-177.2(4)
N(2B)-C(2B)-C(3B)-N(1B)	1.0(5)
C(1B)-N(1B)-C(3B)-C(2B)	-1.3(5)
C(4B)-N(1B)-C(3B)-C(2B)	177.0(4)
C(1B)-N(1B)-C(4B)-C(9B)	-103.6(5)
C(3B)-N(1B)-C(4B)-C(9B)	78.3(5)
C(1B)-N(1B)-C(4B)-C(5B)	77.0(5)
C(3B)-N(1B)-C(4B)-C(5B)	-101.1(5)
C(9B)-C(4B)-C(5B)-C(6B)	0.8(6)
N(1B)-C(4B)-C(5B)-C(6B)	-179.8(4)
C(9B)-C(4B)-C(5B)-C(10B)	-178.7(4)
N(1B)-C(4B)-C(5B)-C(10B)	0.7(6)
C(4B)-C(5B)-C(6B)-C(7B)	-1.9(7)
C(10B)-C(5B)-C(6B)-C(7B)	177.6(4)

C(5B)-C(6B)-C(7B)-C(8B)	1.3(7)
C(5B)-C(6B)-C(7B)-C(11B)	-177.5(4)
C(6B)-C(7B)-C(8B)-C(9B)	0.4(7)
C(11B)-C(7B)-C(8B)-C(9B)	179.2(4)
C(7B)-C(8B)-C(9B)-C(4B)	-1.4(7)
C(7B)-C(8B)-C(9B)-C(12B)	175.5(4)
C(5B)-C(4B)-C(9B)-C(8B)	0.8(6)
N(1B)-C(4B)-C(9B)-C(8B)	-178.6(4)
C(5B)-C(4B)-C(9B)-C(12B)	-176.1(4)
N(1B)-C(4B)-C(9B)-C(12B)	4.5(6)
C(1B)-N(2B)-C(13B)-C(18B)	-92.6(5)
C(2B)-N(2B)-C(13B)-C(18B)	83.7(5)
C(1B)-N(2B)-C(13B)-C(14B)	88.0(5)
C(2B)-N(2B)-C(13B)-C(14B)	-95.6(5)
C(18B)-C(13B)-C(14B)-C(15B)	3.6(6)
N(2B)-C(13B)-C(14B)-C(15B)	-177.1(4)
C(18B)-C(13B)-C(14B)-C(19B)	-174.3(4)
N(2B)-C(13B)-C(14B)-C(19B)	5.0(6)
C(13B)-C(14B)-C(15B)-C(16B)	-1.1(7)
C(19B)-C(14B)-C(15B)-C(16B)	176.8(4)
C(14B)-C(15B)-C(16B)-C(17B)	-1.4(7)
C(14B)-C(15B)-C(16B)-C(20B)	176.3(4)
C(15B)-C(16B)-C(17B)-C(18B)	1.5(7)
C(20B)-C(16B)-C(17B)-C(18B)	-176.1(4)
C(16B)-C(17B)-C(18B)-C(13B)	0.9(7)
C(16B)-C(17B)-C(18B)-C(21B)	-177.3(4)
C(14B)-C(13B)-C(18B)-C(17B)	-3.5(6)
N(2B)-C(13B)-C(18B)-C(17B)	177.2(4)
C(14B)-C(13B)-C(18B)-C(21B)	174.6(4)
N(2B)-C(13B)-C(18B)-C(21B)	-4.7(6)
C(23B)-Mo(1B)-C(22B)-O(1B)	70(3)
C(1B)-Mo(1B)-C(22B)-O(1B)	156(3)
C(26B)-Mo(1B)-C(22B)-O(1B)	-45(3)
C(25B)-Mo(1B)-C(22B)-O(1B)	-20(3)
C(27B)-Mo(1B)-C(22B)-O(1B)	-79(3)
C(28B)-Mo(1B)-C(22B)-O(1B)	-90(3)
C(24B)-Mo(1B)-C(22B)-O(1B)	-38(3)
C(22B)-Mo(1B)-C(23B)-O(2B)	-52(6)
C(1B)-Mo(1B)-C(23B)-O(2B)	-150(6)
C(26B)-Mo(1B)-C(23B)-O(2B)	36(6)
C(25B)-Mo(1B)-C(23B)-O(2B)	65(6)
C(27B)-Mo(1B)-C(23B)-O(2B)	41(7)
C(28B)-Mo(1B)-C(23B)-O(2B)	105(6)

C(24B)-Mo(1B)-C(23B)-O(2B)	98(6)
C(23B)-Mo(1B)-C(24B)-C(25B)	-71.7(3)
C(22B)-Mo(1B)-C(24B)-C(25B)	28.2(5)
C(1B)-Mo(1B)-C(24B)-C(25B)	-166.6(2)
C(26B)-Mo(1B)-C(24B)-C(25B)	37.0(3)
C(27B)-Mo(1B)-C(24B)-C(25B)	78.2(3)
C(28B)-Mo(1B)-C(24B)-C(25B)	116.2(4)
C(23B)-Mo(1B)-C(24B)-C(28B)	172.0(3)
C(22B)-Mo(1B)-C(24B)-C(28B)	-88.1(4)
C(1B)-Mo(1B)-C(24B)-C(28B)	77.2(3)
C(26B)-Mo(1B)-C(24B)-C(28B)	-79.3(3)
C(25B)-Mo(1B)-C(24B)-C(28B)	-116.2(4)
C(27B)-Mo(1B)-C(24B)-C(28B)	-38.1(3)
C(28B)-C(24B)-C(25B)-C(26B)	-0.2(5)
Mo(1B)-C(24B)-C(25B)-C(26B)	-64.6(3)
C(28B)-C(24B)-C(25B)-Mo(1B)	64.4(3)
C(23B)-Mo(1B)-C(25B)-C(26B)	-128.3(3)
C(22B)-Mo(1B)-C(25B)-C(26B)	-48.1(4)
C(1B)-Mo(1B)-C(25B)-C(26B)	138.0(3)
C(27B)-Mo(1B)-C(25B)-C(26B)	37.5(3)
C(28B)-Mo(1B)-C(25B)-C(26B)	79.2(3)
C(24B)-Mo(1B)-C(25B)-C(26B)	116.3(4)
C(23B)-Mo(1B)-C(25B)-C(24B)	115.4(3)
C(22B)-Mo(1B)-C(25B)-C(24B)	-164.4(3)
C(1B)-Mo(1B)-C(25B)-C(24B)	21.7(4)
C(26B)-Mo(1B)-C(25B)-C(24B)	-116.3(4)
C(27B)-Mo(1B)-C(25B)-C(24B)	-78.8(3)
C(28B)-Mo(1B)-C(25B)-C(24B)	-37.0(3)
C(24B)-C(25B)-C(26B)-C(27B)	-0.1(5)
Mo(1B)-C(25B)-C(26B)-C(27B)	-65.0(3)
C(24B)-C(25B)-C(26B)-Mo(1B)	64.9(3)
C(23B)-Mo(1B)-C(26B)-C(25B)	59.8(4)
C(22B)-Mo(1B)-C(26B)-C(25B)	138.6(3)
C(1B)-Mo(1B)-C(26B)-C(25B)	-104.2(5)
C(27B)-Mo(1B)-C(26B)-C(25B)	-115.5(5)
C(28B)-Mo(1B)-C(26B)-C(25B)	-78.1(3)
C(24B)-Mo(1B)-C(26B)-C(25B)	-37.0(3)
C(23B)-Mo(1B)-C(26B)-C(27B)	175.3(3)
C(22B)-Mo(1B)-C(26B)-C(27B)	-105.9(3)
C(1B)-Mo(1B)-C(26B)-C(27B)	11.3(6)
C(25B)-Mo(1B)-C(26B)-C(27B)	115.5(5)
C(28B)-Mo(1B)-C(26B)-C(27B)	37.4(3)
C(24B)-Mo(1B)-C(26B)-C(27B)	78.5(3)

C(25B)-C(26B)-C(27B)-C(28B)	0.4(5)
Mo(1B)-C(26B)-C(27B)-C(28B)	-64.6(3)
C(25B)-C(26B)-C(27B)-Mo(1B)	65.0(3)
C(23B)-Mo(1B)-C(27B)-C(26B)	-8.4(6)
C(22B)-Mo(1B)-C(27B)-C(26B)	78.2(3)
C(1B)-Mo(1B)-C(27B)-C(26B)	-174.6(3)
C(25B)-Mo(1B)-C(27B)-C(26B)	-37.3(3)
C(28B)-Mo(1B)-C(27B)-C(26B)	-116.1(4)
C(24B)-Mo(1B)-C(27B)-C(26B)	-78.5(3)
C(23B)-Mo(1B)-C(27B)-C(28B)	107.7(4)
C(22B)-Mo(1B)-C(27B)-C(28B)	-165.7(3)
C(1B)-Mo(1B)-C(27B)-C(28B)	-58.6(3)
C(26B)-Mo(1B)-C(27B)-C(28B)	116.1(4)
C(25B)-Mo(1B)-C(27B)-C(28B)	78.7(3)
C(24B)-Mo(1B)-C(27B)-C(28B)	37.6(3)
C(25B)-C(24B)-C(28B)-C(27B)	0.5(5)
Mo(1B)-C(24B)-C(28B)-C(27B)	64.7(3)
C(25B)-C(24B)-C(28B)-Mo(1B)	-64.2(3)
C(26B)-C(27B)-C(28B)-C(24B)	-0.5(5)
Mo(1B)-C(27B)-C(28B)-C(24B)	-65.1(3)
C(26B)-C(27B)-C(28B)-Mo(1B)	64.5(3)
C(23B)-Mo(1B)-C(28B)-C(24B)	-12.5(5)
C(22B)-Mo(1B)-C(28B)-C(24B)	134.8(3)
C(1B)-Mo(1B)-C(28B)-C(24B)	-112.4(3)
C(26B)-Mo(1B)-C(28B)-C(24B)	78.0(3)
C(25B)-Mo(1B)-C(28B)-C(24B)	37.0(3)
C(27B)-Mo(1B)-C(28B)-C(24B)	114.9(4)
C(23B)-Mo(1B)-C(28B)-C(27B)	-127.4(4)
C(22B)-Mo(1B)-C(28B)-C(27B)	19.9(4)
C(1B)-Mo(1B)-C(28B)-C(27B)	132.7(3)
C(26B)-Mo(1B)-C(28B)-C(27B)	-36.9(3)
C(25B)-Mo(1B)-C(28B)-C(27B)	-77.9(3)
C(24B)-Mo(1B)-C(28B)-C(27B)	-114.9(4)

APPENDIX D

CRYSTALLOGRAPHIC DATA FOR **25b**

Crystal data and structure refinement for mes 124 (**25b**).

Identification code	mes124
Empirical formula	C29 H33 Cl2 Mo N2 O2
Formula weight	608.41
Temperature	190(2) K
Wavelength	0.71073 Å
Crystal system, space group	P 2_1/n
Unit cell dimensions	a = 8.3612(9) Å ∂ = 90°
	b= 16.2241(17) Å ß = 90.431(5)°
	c = 20.663(3) Å γ = 90 °
Volume	2802.9(6) A^3
Z, Calculated density	4, 1.442 Mg/m^3
Absorption coefficient	0.687 mm^{-1}
F(000)	1252
Crystal size	0.19 x 0.06 x 0.04 mm
Theta range for data collection	2.91 to 27.90°
Limiting indices	-10<=h<=10, -21<=k<=21, -27<=l<=26
Reflections collected / unique	24133 / 6667 [R(int) = 0.0831]
Completeness to theta = 27.90	99.8 %
Max. and min. transmission	0.9730 and 0.8805
Refinement method	Full-matrix least-squares on F^2
Data / restraints / parameters	6667 / 0 / 320
Goodness-of-fit on F^2	1.020

Final R indices [I>2sigma(I)]	R1 = 0.0460, wR2 = 0.0992
R indices (all data)	R1 = 0.0885, wR2 = 0.1148
Largest diff. peak and hole	0.785 and -0.586 e.A^{-3}

Atomic coordinates (x 10^4) and equivalent isotropic displacement parameters ($Å^2$ x 10^3) for mes124. U(eq) is defined as one third of the trace of the orthogonalized U^{ij} tensor.

	x	y	z	U(eq)
Mo(1)	1327(1)	5232(1)	2972(1)	27(1)
N(2)	1286(3)	7066(2)	2418(1)	27(1)
N(1)	2001(3)	7061(2)	3430(1)	28(1)
C(1)	1590(3)	6566(2)	2926(1)	25(1)
C(13)	760(4)	6825(2)	1786(1)	26(1)
C(4)	2625(4)	6786(2)	4040(1)	28(1)
C(7)	3870(4)	6315(2)	5240(2)	36(1)
C(9)	4227(4)	6541(2)	4087(2)	32(1)
C(14)	1869(4)	6713(2)	1300(2)	30(1)
C(5)	1655(4)	6832(2)	4593(2)	31(1)
C(18)	-881(4)	6761(2)	1664(2)	29(1)
C(24)	1028(4)	4122(2)	3699(2)	35(1)
C(2)	1376(4)	7950(2)	2582(2)	34(1)
C(26)	-648(4)	5218(2)	3789(2)	44(1)
C(25)	722(4)	4838(2)	4057(2)	39(1)
C(8)	4810(4)	6298(2)	4687(2)	39(1)
C(6)	2310(4)	6583(2)	5180(2)	36(1)
C(15)	1321(4)	6531(2)	680(2)	39(1)
C(28)	-156(4)	4044(2)	3218(2)	36(1)
C(10)	-26(4)	7167(3)	4563(2)	46(1)
C(16)	-294(4)	6457(2)	539(2)	38(1)
C(21)	-2108(4)	6876(3)	2188(2)	45(1)
C(19)	3642(4)	6745(2)	1440(2)	42(1)
C(12)	5347(4)	6568(2)	3519(2)	42(1)
C(27)	-1204(4)	4724(2)	3269(2)	46(1)
C(20)	-859(5)	6244(3)	-140(2)	56(1)
C(17)	-1369(4)	6579(2)	1033(2)	35(1)
C(3)	2123(4)	7938(2)	3252(2)	39(1)
O(2)	1213(3)	4788(2)	1510(1)	50(1)
O(1)	4850(3)	4878(2)	2608(1)	46(1)

C(22)	3538(4)	5038(2)	2766(2)	33(1)
C(11)	4582(4)	6082(3)	5888(2)	52(1)
C(23)	1229(4)	5005(2)	2049(2)	35(1)
Cl(2)	2588(1)	1402(1)	6577(1)	66(1)
Cl(1)	777(2)	316(1)	5735(1)	86(1)
C(29)	2220(5)	380(2)	6347(2)	54(1)

Bond lengths [Å] and angles [°] for mes124.

Mo(1)-C(22)	1.926(4)
Mo(1)-C(23)	1.944(4)
Mo(1)-C(1)	2.177(3)
Mo(1)-C(28)	2.350(3)
Mo(1)-C(27)	2.357(4)
Mo(1)-C(24)	2.360(3)
Mo(1)-C(26)	2.370(3)
Mo(1)-C(25)	2.390(3)
N(2)-C(1)	1.350(4)
N(2)-C(13)	1.431(4)
N(2)-C(2)	1.475(4)
N(1)-C(1)	1.357(4)
N(1)-C(4)	1.432(4)
N(1)-C(3)	1.472(4)
C(13)-C(14)	1.384(4)
C(13)-C(18)	1.397(4)
C(4)-C(9)	1.400(4)
C(4)-C(5)	1.409(4)
C(7)-C(6)	1.379(5)
C(7)-C(8)	1.392(5)
C(7)-C(11)	1.508(4)
C(9)-C(8)	1.387(4)
C(9)-C(12)	1.507(5)
C(14)-C(15)	1.387(4)
C(14)-C(19)	1.510(4)
C(5)-C(6)	1.387(4)
C(5)-C(10)	1.508(5)
C(18)-C(17)	1.395(4)
C(18)-C(21)	1.509(5)

C(24)-C(25)	1.401(5)
C(24)-C(28)	1.403(5)
C(24)-H(24A)	1.0000
C(2)-C(3)	1.515(4)
C(2)-H(2A)	0.9900
C(2)-H(2B)	0.9900
C(26)-C(25)	1.411(5)
C(26)-C(27)	1.416(5)
C(26)-H(26A)	1.0000
C(25)-H(25A)	1.0000
C(8)-H(8A)	0.9500
C(6)-H(6A)	0.9500
C(15)-C(16)	1.385(5)
C(15)-H(15A)	0.9500
C(28)-C(27)	1.414(5)
C(28)-H(28A)	1.0000
C(10)-H(10A)	0.9800
C(10)-H(10B)	0.9800
C(10)-H(10C)	0.9800
C(16)-C(17)	1.380(5)
C(16)-C(20)	1.516(4)
C(21)-H(21A)	0.9800
C(21)-H(21B)	0.9800
C(21)-H(21C)	0.9800
C(19)-H(19A)	0.9800
C(19)-H(19B)	0.9800
C(19)-H(19C)	0.9800
C(19)-H(19D)	0.9800
C(19)-H(19E)	0.9800
C(19)-H(19F)	0.9800
C(12)-H(12A)	0.9800
C(12)-H(12B)	0.9800
C(12)-H(12C)	0.9800
C(12)-H(12D)	0.9800
C(12)-H(12E)	0.9800
C(12)-H(12F)	0.9800
C(27)-H(27A)	1.0000
C(20)-H(20A)	0.9800
C(20)-H(20B)	0.9800
C(20)-H(20C)	0.9800
C(17)-H(17A)	0.9500
C(3)-H(3A)	0.9900
C(3)-H(3B)	0.9900

O(2)-C(23)	1.167(4)
O(1)-C(22)	1.175(4)
C(11)-H(11A)	0.9800
C(11)-H(11B)	0.9800
C(11)-H(11C)	0.9800
Cl(2)-C(29)	1.753(4)
Cl(1)-C(29)	1.744(4)
C(29)-H(29A)	0.9900
C(29)-H(29B)	0.9900

C(22)-Mo(1)-C(23)	77.58(14)
C(22)-Mo(1)-C(1)	93.20(12)
C(23)-Mo(1)-C(1)	98.60(12)
C(22)-Mo(1)-C(28)	114.99(13)
C(23)-Mo(1)-C(28)	92.21(13)
C(1)-Mo(1)-C(28)	151.44(12)
C(22)-Mo(1)-C(27)	149.94(14)
C(23)-Mo(1)-C(27)	99.07(14)
C(1)-Mo(1)-C(27)	116.75(12)
C(28)-Mo(1)-C(27)	34.95(12)
C(22)-Mo(1)-C(24)	97.05(13)
C(23)-Mo(1)-C(24)	118.43(13)
C(1)-Mo(1)-C(24)	142.88(12)
C(28)-Mo(1)-C(24)	34.66(11)
C(27)-Mo(1)-C(24)	57.83(12)
C(22)-Mo(1)-C(26)	146.22(13)
C(23)-Mo(1)-C(26)	132.23(14)
C(1)-Mo(1)-C(26)	96.42(12)
C(28)-Mo(1)-C(26)	57.73(13)
C(27)-Mo(1)-C(26)	34.85(13)
C(24)-Mo(1)-C(26)	57.41(12)
C(22)-Mo(1)-C(25)	112.00(13)
C(23)-Mo(1)-C(25)	149.57(13)
C(1)-Mo(1)-C(25)	109.20(12)
C(28)-Mo(1)-C(25)	57.41(12)
C(27)-Mo(1)-C(25)	57.67(13)
C(24)-Mo(1)-C(25)	34.32(12)
C(26)-Mo(1)-C(25)	34.48(12)
C(1)-N(2)-C(13)	126.9(3)
C(1)-N(2)-C(2)	113.5(2)
C(13)-N(2)-C(2)	119.3(2)
C(1)-N(1)-C(4)	125.3(3)
C(1)-N(1)-C(3)	113.5(2)

C(4)-N(1)-C(3)	119.7(2)
N(2)-C(1)-N(1)	106.5(3)
N(2)-C(1)-Mo(1)	127.8(2)
N(1)-C(1)-Mo(1)	125.5(2)
C(14)-C(13)-C(18)	121.5(3)
C(14)-C(13)-N(2)	119.8(3)
C(18)-C(13)-N(2)	118.6(3)
C(9)-C(4)-C(5)	121.0(3)
C(9)-C(4)-N(1)	119.5(3)
C(5)-C(4)-N(1)	119.3(3)
C(6)-C(7)-C(8)	118.1(3)
C(6)-C(7)-C(11)	121.8(3)
C(8)-C(7)-C(11)	120.1(3)
C(8)-C(9)-C(4)	118.2(3)
C(8)-C(9)-C(12)	119.2(3)
C(4)-C(9)-C(12)	122.5(3)
C(13)-C(14)-C(15)	118.6(3)
C(13)-C(14)-C(19)	121.2(3)
C(15)-C(14)-C(19)	120.1(3)
C(6)-C(5)-C(4)	117.9(3)
C(6)-C(5)-C(10)	120.2(3)
C(4)-C(5)-C(10)	121.9(3)
C(17)-C(18)-C(13)	117.6(3)
C(17)-C(18)-C(21)	120.1(3)
C(13)-C(18)-C(21)	122.3(3)
C(25)-C(24)-C(28)	108.6(3)
C(25)-C(24)-Mo(1)	74.01(19)
C(28)-C(24)-Mo(1)	72.29(18)
C(25)-C(24)-H(24A)	125.5
C(28)-C(24)-H(24A)	125.5
Mo(1)-C(24)-H(24A)	125.5
N(2)-C(2)-C(3)	102.4(2)
N(2)-C(2)-H(2A)	111.3
C(3)-C(2)-H(2A)	111.3
N(2)-C(2)-H(2B)	111.3
C(3)-C(2)-H(2B)	111.3
H(2A)-C(2)-H(2B)	109.2
C(25)-C(26)-C(27)	108.2(3)
C(25)-C(26)-Mo(1)	73.5(2)
C(27)-C(26)-Mo(1)	72.1(2)
C(25)-C(26)-H(26A)	125.7
C(27)-C(26)-H(26A)	125.7
Mo(1)-C(26)-H(26A)	125.7

C(24)-C(25)-C(26)	107.8(3)
C(24)-C(25)-Mo(1)	71.67(19)
C(26)-C(25)-Mo(1)	72.00(19)
C(24)-C(25)-H(25A)	126.0
C(26)-C(25)-H(25A)	126.0
Mo(1)-C(25)-H(25A)	126.0
C(9)-C(8)-C(7)	122.1(3)
C(9)-C(8)-H(8A)	118.9
C(7)-C(8)-H(8A)	118.9
C(7)-C(6)-C(5)	122.6(3)
C(7)-C(6)-H(6A)	118.7
C(5)-C(6)-H(6A)	118.7
C(16)-C(15)-C(14)	121.9(3)
C(16)-C(15)-H(15A)	119.1
C(14)-C(15)-H(15A)	119.1
C(24)-C(28)-C(27)	108.2(3)
C(24)-C(28)-Mo(1)	73.05(18)
C(27)-C(28)-Mo(1)	72.8(2)
C(24)-C(28)-H(28A)	125.7
C(27)-C(28)-H(28A)	125.7
Mo(1)-C(28)-H(28A)	125.7
C(5)-C(10)-H(10A)	109.5
C(5)-C(10)-H(10B)	109.5
H(10A)-C(10)-H(10B)	109.5
C(5)-C(10)-H(10C)	109.5
H(10A)-C(10)-H(10C)	109.5
H(10B)-C(10)-H(10C)	109.5
C(17)-C(16)-C(15)	118.0(3)
C(17)-C(16)-C(20)	121.1(3)
C(15)-C(16)-C(20)	120.8(3)
C(18)-C(21)-H(21A)	109.5
C(18)-C(21)-H(21B)	109.5
H(21A)-C(21)-H(21B)	109.5
C(18)-C(21)-H(21C)	109.5
H(21A)-C(21)-H(21C)	109.5
H(21B)-C(21)-H(21C)	109.5
C(14)-C(19)-H(19A)	109.5
C(14)-C(19)-H(19B)	109.5
H(19A)-C(19)-H(19B)	109.5
C(14)-C(19)-H(19C)	109.5
H(19A)-C(19)-H(19C)	109.5
H(19B)-C(19)-H(19C)	109.5
C(14)-C(19)-H(19D)	109.5

H(19A)-C(19)-H(19D)	141.1
H(19B)-C(19)-H(19D)	56.3
H(19C)-C(19)-H(19D)	56.3
C(14)-C(19)-H(19E)	109.5
H(19A)-C(19)-H(19E)	56.3
H(19B)-C(19)-H(19E)	141.1
H(19C)-C(19)-H(19E)	56.3
H(19D)-C(19)-H(19E)	109.5
C(14)-C(19)-H(19F)	109.5
H(19A)-C(19)-H(19F)	56.3
H(19B)-C(19)-H(19F)	56.3
H(19C)-C(19)-H(19F)	141.1
H(19D)-C(19)-H(19F)	109.5
H(19E)-C(19)-H(19F)	109.5
C(9)-C(12)-H(12A)	109.5
C(9)-C(12)-H(12B)	109.5
H(12A)-C(12)-H(12B)	109.5
C(9)-C(12)-H(12C)	109.5
H(12A)-C(12)-H(12C)	109.5
H(12B)-C(12)-H(12C)	109.5
C(9)-C(12)-H(12D)	109.5
H(12A)-C(12)-H(12D)	141.1
H(12B)-C(12)-H(12D)	56.3
H(12C)-C(12)-H(12D)	56.3
C(9)-C(12)-H(12E)	109.5
H(12A)-C(12)-H(12E)	56.3
H(12B)-C(12)-H(12E)	141.1
H(12C)-C(12)-H(12E)	56.3
H(12D)-C(12)-H(12E)	109.5
C(9)-C(12)-H(12F)	109.5
H(12A)-C(12)-H(12F)	56.3
H(12B)-C(12)-H(12F)	56.3
H(12C)-C(12)-H(12F)	141.1
H(12D)-C(12)-H(12F)	109.5
H(12E)-C(12)-H(12F)	109.5
C(28)-C(27)-C(26)	107.3(3)
C(28)-C(27)-Mo(1)	72.25(19)
C(26)-C(27)-Mo(1)	73.1(2)
C(28)-C(27)-H(27A)	126.1
C(26)-C(27)-H(27A)	126.1
Mo(1)-C(27)-H(27A)	126.1
C(16)-C(20)-H(20A)	109.5
C(16)-C(20)-H(20B)	109.5

H(20A)-C(20)-H(20B)	109.5
C(16)-C(20)-H(20C)	109.5
H(20A)-C(20)-H(20C)	109.5
H(20B)-C(20)-H(20C)	109.5
C(16)-C(17)-C(18)	122.3(3)
C(16)-C(17)-H(17A)	118.8
C(18)-C(17)-H(17A)	118.8
N(1)-C(3)-C(2)	102.3(2)
N(1)-C(3)-H(3A)	111.3
C(2)-C(3)-H(3A)	111.3
N(1)-C(3)-H(3B)	111.3
C(2)-C(3)-H(3B)	111.3
H(3A)-C(3)-H(3B)	109.2
O(1)-C(22)-Mo(1)	175.3(3)
C(7)-C(11)-H(11A)	109.5
C(7)-C(11)-H(11B)	109.5
H(11A)-C(11)-H(11B)	109.5
C(7)-C(11)-H(11C)	109.5
H(11A)-C(11)-H(11C)	109.5
H(11B)-C(11)-H(11C)	109.5
O(2)-C(23)-Mo(1)	173.2(3)
Cl(1)-C(29)-Cl(2)	111.8(2)
Cl(1)-C(29)-H(29A)	109.3
Cl(2)-C(29)-H(29A)	109.3
Cl(1)-C(29)-H(29B)	109.3
Cl(2)-C(29)-H(29B)	109.3
H(29A)-C(29)-H(29B)	107.9

Anisotropic displacement parameters ($Å^2$ x 10^3) for mes124. The anisotropic displacement factor exponent takes the form: $-2\pi^2 [h^2 a^{*2} U^{11} + ... + 2 h k a^* b^* U^{12}]$

	U^{11}	U^{22}	U^{33}	U^{23}	U^{13}	U^{12}
Mo(1)	28(1)	23(1)	29(1)	2(1)	0(1)	0(1)
N(2)	38(2)	20(1)	24(1)	1(1)	-2(1)	1(1)
N(1)	38(2)	23(1)	24(1)	0(1)	-2(1)	-2(1)
C(1)	21(2)	26(2)	27(2)	-2(1)	2(1)	0(1)
C(13)	35(2)	22(2)	23(2)	2(1)	-2(1)	1(1)
C(4)	34(2)	24(2)	26(2)	-4(1)	-4(1)	-4(1)
C(7)	38(2)	43(2)	27(2)	5(2)	-7(2)	-8(2)

C(9)	33(2)	33(2)	31(2)	-5(2)	0(1)	-7(2)
C(14)	32(2)	28(2)	29(2)	3(1)	4(1)	1(1)
C(5)	33(2)	32(2)	28(2)	0(1)	-1(1)	-2(1)
C(18)	32(2)	25(2)	30(2)	3(1)	1(1)	4(1)
C(24)	35(2)	30(2)	40(2)	12(2)	2(2)	-2(2)
C(2)	46(2)	25(2)	31(2)	3(1)	-2(2)	0(2)
C(26)	45(2)	36(2)	52(2)	3(2)	24(2)	2(2)
C(25)	51(2)	38(2)	29(2)	5(2)	6(2)	-9(2)
C(8)	30(2)	45(2)	41(2)	3(2)	-9(2)	-3(2)
C(6)	38(2)	42(2)	28(2)	-2(2)	2(2)	-8(2)
C(15)	54(2)	37(2)	26(2)	-1(2)	10(2)	7(2)
C(28)	39(2)	30(2)	40(2)	6(2)	1(2)	-12(2)
C(10)	37(2)	60(3)	40(2)	-3(2)	3(2)	7(2)
C(16)	55(2)	33(2)	25(2)	3(2)	-4(2)	4(2)
C(21)	34(2)	58(3)	42(2)	-6(2)	5(2)	2(2)
C(19)	37(2)	42(2)	46(2)	0(2)	9(2)	5(2)
C(12)	37(2)	49(2)	39(2)	-7(2)	4(2)	-5(2)
C(27)	25(2)	56(3)	58(2)	15(2)	4(2)	-2(2)
C(20)	81(3)	57(3)	30(2)	-5(2)	-16(2)	8(2)
C(17)	37(2)	33(2)	36(2)	4(2)	-8(2)	4(2)
C(3)	53(2)	27(2)	38(2)	-2(2)	-7(2)	-6(2)
O(2)	80(2)	36(2)	33(1)	-6(1)	-7(1)	2(1)
O(1)	32(1)	47(2)	59(2)	-1(1)	5(1)	3(1)
C(22)	34(2)	29(2)	35(2)	1(1)	-3(2)	-1(1)
C(11)	47(2)	73(3)	37(2)	14(2)	-11(2)	-5(2)
C(23)	38(2)	23(2)	43(2)	1(2)	-5(2)	0(1)
Cl(2)	68(1)	49(1)	82(1)	-16(1)	-6(1)	7(1)
Cl(1)	97(1)	71(1)	90(1)	-9(1)	-37(1)	-1(1)

Hydrogen coordinates (x 10^4) and isotropic displacement parameters (Å^2 x 10^3) for mes124.

	x	y	z	U(eq)
H(24A)	1866	3702	3804	42
H(2A)	300	8204	2587	41
H(2B)	2057	8253	2272	41
H(26A)	-1204	5712	3967	53
H(25A)	1309	5019	4456	47
H(8A)	5886	6114	4722	46
H(6A)	1660	6597	5554	43

H(15A)	2076	6455	344	47
H(28A)	-310	3557	2928	43
H(10A)	-500	7146	4995	68
H(10B)	-669	6833	4263	68
H(10C)	-2	7739	4412	68
H(21A)	-3183	6807	2004	67
H(21B)	-2005	7430	2373	67
H(21C)	-1933	6464	2529	67
H(19A)	4234	6653	1039	63
H(19B)	3923	6317	1756	63
H(19C)	3920	7288	1618	63
H(19D)	3817	6852	1902	63
H(19E)	4129	7188	1186	63
H(19F)	4131	6217	1324	63
H(12A)	4760	6748	3132	62
H(12B)	5792	6017	3445	62
H(12C)	6218	6956	3610	62
H(12D)	6420	6399	3660	62
H(12E)	5388	7130	3346	62
H(12F)	4961	6191	3181	62
H(27A)	-2227	4801	3022	55
H(20A)	-2030	6217	-149	84
H(20B)	-417	5709	-266	84
H(20C)	-495	6668	-442	84
H(17A)	-2480	6536	941	42
H(3A)	3251	8121	3242	47
H(3B)	1520	8290	3555	47
H(11A)	3762	6128	6222	79
H(11B)	5472	6454	5991	79
H(11C)	4974	5514	5870	79
H(29A)	3227	127	6194	65
H(29B)	1854	63	6728	65

APPENDIX E

CRYSTALLOGRAPHIC DATA FOR **26**

Crystal data and structure refinement for mes129a (**26**).

Identification code	mes129a
Empirical formula	C18 H18 Mo2 N2 O3
Formula weight	502.22
Temperature	190(2) K
Wavelength	0.71073 Å
Crystal system	P 2_1/c
Unit cell dimensions	a = 9.1792(9) Å α = 90°
	b = 25.031(3) Å β = 108.572(5)°
	c = 8.0903(8) Å γ = 90°
Volume 1	762.1(3) A^3
Z, Calculated density	4, 1.893 Mg/m^3
Absorption coefficient	1.443 mm^{-1}
F(000)	992
Crystal size	0.20 x 0.15 x 0.08 mm
Theta range for data collection	2.78 to 25.34°
Limiting indices	-11<=h<=10, -30<=k<=28, -9<=l<=9
Reflections collected / unique	11066 / 3210 [R(int) = 0.0429]
Completeness to theta = 25.34°	99.8 %
Max. and min. transmission	0.8933 and 0.7613
Refinement method	Full-matrix least-squares on F^2
Data / restraints / parameters	3210 / 190 / 256
Goodness-of-fit on F^2	0.926
Final R indices [I>2sigma(I)]	R1 = 0.0334, wR2 = 0.0944

R indices (all data)	R1 = 0.0503, wR2 = 0.1072
Largest diff. peak and hole	0.703 and -0.663 e.A^{-3}

Atomic coordinates (x 10^4) and equivalent isotropic displacement parameters ($Å^2$ x 10^3) for mes122. U(eq) is defined as one third of the trace of the orthogonalized U^{ij} tensor.

	x	y	z	U(eq)
Mo(1)	2622(1)	4096(1)	899(1)	25(1)
C(1)	4418(5)	3490(2)	1683(5)	26(1)
N(1)	4455(4)	3017(1)	2544(5)	30(1)
O(1)	4051(4)	3450(1)	-2468(4)	44(1)
Mo(2)	927(1)	3761(1)	-2061(1)	27(1)
O(2)	1876(4)	4927(1)	-2492(4)	45(1)
N(2)	5802(4)	3500(1)	1416(5)	28(1)
C(2)	6650(5)	3045(2)	2028(5)	31(1)
O(3)	-74(4)	3418(1)	1209(4)	45(1)
C(3)	5797(5)	2746(2)	2727(6)	34(1)
C(4)	3263(6)	2824(2)	3242(7)	44(1)
C(5)	6404(5)	3943(2)	646(6)	36(1)
C(6)	2949(5)	3569(2)	-2156(6)	32(1)
C(7)	921(5)	3645(2)	846(6)	32(1)
C(8)	1605(5)	4495(2)	-2096(6)	34(1)
C(9)	3007(6)	4350(2)	3802(6)	42(1)
C(10)	1853(6)	4661(2)	2658(6)	40(1)
C(11)	2534(6)	4971(2)	1669(6)	43(1)
C(12)	4107(6)	4857(2)	2199(6)	42(1)
C(13)	4421(6)	4478(2)	3512(6)	42(1)
C(14A)	-262(8)	3527(5)	-4996(9)	43(3)
C(15A)	-363(9)	3072(3)	-3988(13)	41(3)
C(16A)	-1307(10)	3207(3)	-2960(9)	37(2)
C(17A)	-1790(7)	3746(3)	-3333(10)	34(2)
C(18A)	-1143(10)	3943(2)	-4590(10)	35(2)
C(14B)	-38(10)	3249(5)	-4640(15)	30(3)
C(15B)	-680(16)	3047(3)	-3383(15)	28(3)
C(16B)	-1600(14)	3455(7)	-3005(15)	39(3)
C(17B)	-1528(15)	3909(4)	-4030(20)	39(4)
C(18B)	-563(16)	3782(5)	-5038(13)	34(3)

Bond lengths [Å] and angles [°] for mes129a.

Mo(1)-C(7)	1.916(5)
Mo(1)-C(1)	2.181(4)
Mo(1)-C(10)	2.272(4)
Mo(1)-C(11)	2.287(4)
Mo(1)-C(9)	2.349(5)
Mo(1)-C(12)	2.383(4)
Mo(1)-C(13)	2.426(4)
Mo(1)-C(8)	2.510(5)
Mo(1)-Mo(2)	2.5464(5)
C(1)-N(2)	1.355(5)
C(1)-N(1)	1.367(5)
N(1)-C(3)	1.373(5)
N(1)-C(4)	1.464(5)
O(1)-C(6)	1.157(5)
Mo(2)-C(6)	1.942(5)
Mo(2)-C(8)	1.943(5)
Mo(2)-C(18B)	2.361(10)
Mo(2)-C(17B)	2.337(11)
Mo(2)-C(14A)	2.350(7)
Mo(2)-C(14B)	2.367(9)
Mo(2)-C(18A)	2.352(7)
Mo(2)-C(15A)	2.372(7)
Mo(2)-C(16B)	2.329(12)
Mo(2)-C(15B)	2.347(10)
Mo(2)-C(17A)	2.376(6)
Mo(2)-C(16A)	2.388(6)
O(2)-C(8)	1.178(5)
N(2)-C(2)	1.379(5)
N(2)-C(5)	1.463(5)
C(2)-C(3)	1.333(6)
C(2)-H(2A)	0.9500
O(3)-C(7)	1.189(5)
C(3)-H(3A)	0.9500
C(4)-H(4A)	0.9800
C(4)-H(4B)	0.9800
C(4)-H(4C)	0.9800
C(5)-H(5A)	0.9800
C(5)-H(5B)	0.9800
C(5)-H(5C)	0.9800
C(9)-C(10)	1.400(7)

C(9)-C(13)	1.427(7)
C(9)-H(9A)	1.0000
C(10)-C(11)	1.397(6)
C(10)-H(10A)	1.0000
C(11)-C(12)	1.399(7)
C(11)-H(11A)	1.0000
C(12)-C(13)	1.385(7)
C(12)-H(12A)	1.0000
C(13)-H(13A)	1.0000
C(14A)-C(15A)	1.4200
C(14A)-C(18A)	1.4200
C(14A)-H(14A)	0.9500
C(15A)-C(16A)	1.4200
C(15A)-H(15A)	0.9500
C(16A)-C(17A)	1.4200
C(16A)-H(16A)	0.9500
C(17A)-C(18A)	1.4200
C(17A)-H(17A)	0.9500
C(18A)-H(18A)	0.9500
C(14B)-C(15B)	1.4200
C(14B)-C(18B)	1.4200
C(14B)-H(14B)	0.9500
C(15B)-C(16B)	1.4200
C(15B)-H(15B)	0.9500
C(16B)-C(17B)	1.4200
C(16B)-H(16B)	0.9500
C(17B)-C(18B)	1.4200
C(17B)-H(17B)	0.9500
C(18B)-H(18B)	0.9500

C(7)-Mo(1)-C(1)	97.59(17)
C(7)-Mo(1)-C(10)	88.08(18)
C(1)-Mo(1)-C(10)	127.41(16)
C(7)-Mo(1)-C(11)	118.06(18)
C(1)-Mo(1)-C(11)	132.59(17)
C(10)-Mo(1)-C(11)	35.68(16)
C(7)-Mo(1)-C(9)	92.46(18)
C(1)-Mo(1)-C(9)	92.19(16)
C(10)-Mo(1)-C(9)	35.23(17)
C(11)-Mo(1)-C(9)	58.35(17)
C(7)-Mo(1)-C(12)	145.86(17)
C(1)-Mo(1)-C(12)	98.90(16)
C(10)-Mo(1)-C(12)	58.27(17)

C(11)-Mo(1)-C(12)	34.79(16)
C(9)-Mo(1)-C(12)	57.30(17)
C(7)-Mo(1)-C(13)	125.08(18)
C(1)-Mo(1)-C(13)	77.23(16)
C(10)-Mo(1)-C(13)	57.99(18)
C(11)-Mo(1)-C(13)	57.21(17)
C(9)-Mo(1)-C(13)	34.73(17)
C(12)-Mo(1)-C(13)	33.45(17)
C(7)-Mo(1)-C(8)	99.37(17)
C(1)-Mo(1)-C(8)	124.92(14)
C(10)-Mo(1)-C(8)	105.22(16)
C(11)-Mo(1)-C(8)	81.21(17)
C(9)-Mo(1)-C(8)	138.49(16)
C(12)-Mo(1)-C(8)	95.32(17)
C(13)-Mo(1)-C(8)	128.70(16)
C(7)-Mo(1)-Mo(2)	62.34(13)
C(1)-Mo(1)-Mo(2)	102.91(10)
C(10)-Mo(1)-Mo(2)	125.12(13)
C(11)-Mo(1)-Mo(2)	120.51(13)
C(9)-Mo(1)-Mo(2)	151.83(13)
C(12)-Mo(1)-Mo(2)	140.41(13)
C(13)-Mo(1)-Mo(2)	172.57(13)
C(8)-Mo(1)-Mo(2)	45.19(11)
N(2)-C(1)-N(1)	103.0(3)
N(2)-C(1)-Mo(1)	126.9(3)
N(1)-C(1)-Mo(1)	130.1(3)
C(1)-N(1)-C(3)	111.1(3)
C(1)-N(1)-C(4)	125.5(4)
C(3)-N(1)-C(4)	123.4(4)
C(6)-Mo(2)-C(8)	85.37(18)
C(6)-Mo(2)-C(18B)	102.4(4)
C(8)-Mo(2)-C(18B)	92.8(3)
C(6)-Mo(2)-C(17B)	137.6(4)
C(8)-Mo(2)-C(17B)	94.8(4)
C(18B)-Mo(2)-C(17B)	35.18(14)
C(6)-Mo(2)-C(14A)	92.3(2)
C(8)-Mo(2)-C(14A)	105.6(3)
C(18B)-Mo(2)-C(14A)	16.9(2)
C(17B)-Mo(2)-C(14A)	46.8(2)
C(6)-Mo(2)-C(14B)	85.7(2)
C(8)-Mo(2)-C(14B)	122.1(4)
C(18B)-Mo(2)-C(14B)	34.95(12)
C(17B)-Mo(2)-C(14B)	58.46(16)

C(14A)-Mo(2)-C(14B)	18.5(2)
C(6)-Mo(2)-C(18A)	122.1(3)
C(8)-Mo(2)-C(18A)	88.71(18)
C(18B)-Mo(2)-C(18A)	20.5(3)
C(17B)-Mo(2)-C(18A)	16.3(3)
C(14A)-Mo(2)-C(18A)	35.16(9)
C(14B)-Mo(2)-C(18A)	50.7(2)
C(6)-Mo(2)-C(15A)	94.4(2)
C(8)-Mo(2)-C(15A)	140.6(3)
C(18B)-Mo(2)-C(15A)	48.7(2)
C(17B)-Mo(2)-C(15A)	59.8(2)
C(14A)-Mo(2)-C(15A)	35.00(9)
C(14B)-Mo(2)-C(15A)	19.8(2)
C(18A)-Mo(2)-C(15A)	58.20(11)
C(6)-Mo(2)-C(16B)	140.4(4)
C(8)-Mo(2)-C(16B)	126.6(5)
C(18B)-Mo(2)-C(16B)	58.66(17)
C(17B)-Mo(2)-C(16B)	35.43(16)
C(14A)-Mo(2)-C(16B)	59.5(2)
C(14B)-Mo(2)-C(16B)	58.58(16)
C(18A)-Mo(2)-C(16B)	48.2(3)
C(15A)-Mo(2)-C(16B)	46.3(2)
C(6)-Mo(2)-C(15B)	105.2(4)
C(8)-Mo(2)-C(15B)	150.6(2)
C(18B)-Mo(2)-C(15B)	58.41(15)
C(17B)-Mo(2)-C(15B)	58.74(18)
C(14A)-Mo(2)-C(15B)	47.7(2)
C(14B)-Mo(2)-C(15B)	35.05(12)
C(18A)-Mo(2)-C(15B)	62.3(2)
C(15A)-Mo(2)-C(15B)	15.8(2)
C(16B)-Mo(2)-C(15B)	35.35(15)
C(6)-Mo(2)-C(17A)	149.69(17)
C(8)-Mo(2)-C(17A)	107.8(3)
C(18B)-Mo(2)-C(17A)	51.1(3)
C(17B)-Mo(2)-C(17A)	19.3(3)
C(14A)-Mo(2)-C(17A)	58.18(10)
C(14B)-Mo(2)-C(17A)	64.1(2)
C(18A)-Mo(2)-C(17A)	34.95(8)
C(15A)-Mo(2)-C(17A)	57.88(10)
C(16B)-Mo(2)-C(17A)	18.9(3)
C(15B)-Mo(2)-C(17A)	51.0(3)
C(6)-Mo(2)-C(16A)	125.7(3)
C(8)-Mo(2)-C(16A)	142.4(3)

C(18B)-Mo(2)-C(16A)	62.6(2)
C(17B)-Mo(2)-C(16A)	48.4(3)
C(14A)-Mo(2)-C(16A)	58.01(11)
C(14B)-Mo(2)-C(16A)	51.2(2)
C(18A)-Mo(2)-C(16A)	57.98(10)
C(15A)-Mo(2)-C(16A)	34.71(9)
C(16B)-Mo(2)-C(16A)	16.3(3)
C(15B)-Mo(2)-C(16A)	20.9(2)
C(17A)-Mo(2)-C(16A)	34.68(8)
C(1)-N(2)-C(2)	112.2(3)
C(1)-N(2)-C(5)	125.7(4)
C(2)-N(2)-C(5)	122.1(3)
C(3)-C(2)-N(2)	106.0(4)
C(3)-C(2)-H(2A)	127.0
N(2)-C(2)-H(2A)	127.0
C(2)-C(3)-N(1)	107.7(4)
C(2)-C(3)-H(3A)	126.1
N(1)-C(3)-H(3A)	126.1
N(1)-C(4)-H(4A)	109.5
N(1)-C(4)-H(4B)	109.5
H(4A)-C(4)-H(4B)	109.5
N(1)-C(4)-H(4C)	109.5
H(4A)-C(4)-H(4C)	109.5
H(4B)-C(4)-H(4C)	109.5
N(2)-C(5)-H(5A)	109.5
N(2)-C(5)-H(5B)	109.5
H(5A)-C(5)-H(5B)	109.5
N(2)-C(5)-H(5C)	109.5
H(5A)-C(5)-H(5C)	109.5
H(5B)-C(5)-H(5C)	109.5
O(1)-C(6)-Mo(2)	170.2(4)
O(3)-C(7)-Mo(1)	163.9(4)
O(3)-C(7)-Mo(2)	123.2(3)
Mo(1)-C(7)-Mo(2)	71.98(14)
O(2)-C(8)-Mo(2)	165.8(4)
O(2)-C(8)-Mo(1)	125.6(3)
Mo(2)-C(8)-Mo(1)	68.40(14)
C(10)-C(9)-C(13)	107.6(4)
C(10)-C(9)-Mo(1)	69.4(3)
C(13)-C(9)-Mo(1)	75.6(3)
C(10)-C(9)-H(9A)	126.0
C(13)-C(9)-H(9A)	126.0
Mo(1)-C(9)-H(9A)	126.0

C(11)-C(10)-C(9)	107.9(4)
C(11)-C(10)-Mo(1)	72.7(2)
C(9)-C(10)-Mo(1)	75.4(3)
C(11)-C(10)-H(10A)	125.7
C(9)-C(10)-H(10A)	125.7
Mo(1)-C(10)-H(10A)	125.7
C(10)-C(11)-C(12)	108.4(5)
C(10)-C(11)-Mo(1)	71.6(2)
C(12)-C(11)-Mo(1)	76.3(3)
C(10)-C(11)-H(11A)	125.4
C(12)-C(11)-H(11A)	125.4
Mo(1)-C(11)-H(11A)	125.4
C(13)-C(12)-C(11)	108.5(5)
C(13)-C(12)-Mo(1)	75.0(3)
C(11)-C(12)-Mo(1)	68.9(3)
C(13)-C(12)-H(12A)	125.7
C(11)-C(12)-H(12A)	125.7
Mo(1)-C(12)-H(12A)	125.7
C(12)-C(13)-C(9)	107.6(4)
C(12)-C(13)-Mo(1)	71.6(3)
C(9)-C(13)-Mo(1)	69.7(3)
C(12)-C(13)-H(13A)	126.2
C(9)-C(13)-H(13A)	126.2
Mo(1)-C(13)-H(13A)	126.2
C(15A)-C(14A)-C(18A)	108
C(15A)-C(14A)-Mo(2)	73.4(3)
C(18A)-C(14A)-Mo(2)	72.5(2)
C(15A)-C(14A)-H(14A)	126.2
C(18A)-C(14A)-H(14A)	125.8
Mo(2)-C(14A)-H(14A)	119.9
C(16A)-C(15A)-C(14A)	108
C(16A)-C(15A)-Mo(2)	73.3(2)
C(14A)-C(15A)-Mo(2)	71.6(3)
C(16A)-C(15A)-H(15A)	126
C(14A)-C(15A)-H(15A)	126
Mo(2)-C(15A)-H(15A)	120.9
C(17A)-C(16A)-C(15A)	108
C(17A)-C(16A)-Mo(2)	72.2(2)
C(15A)-C(16A)-Mo(2)	72.0(2)
C(17A)-C(16A)-H(16A)	126
C(15A)-C(16A)-H(16A)	126
Mo(2)-C(16A)-H(16A)	121.5
C(16A)-C(17A)-C(18A)	108.0

C(16A)-C(17A)-Mo(2)	73.1(3)
C(18A)-C(17A)-Mo(2)	71.6(2)
C(16A)-C(17A)-H(17A)	126.0
C(18A)-C(17A)-H(17A)	126.0
Mo(2)-C(17A)-H(17A)	121.0
C(17A)-C(18A)-C(14A)	108.0
C(17A)-C(18A)-Mo(2)	73.5(2)
C(14A)-C(18A)-Mo(2)	72.3(3)
C(17A)-C(18A)-H(18A)	126.0
C(14A)-C(18A)-H(18A)	126.0
Mo(2)-C(18A)-H(18A)	120.0
C(15B)-C(14B)-C(18B)	108.0
C(15B)-C(14B)-Mo(2)	71.7(4)
C(18B)-C(14B)-Mo(2)	72.3(4)
C(15B)-C(14B)-H(14B)	126.4
C(18B)-C(14B)-H(14B)	125.6
Mo(2)-C(14B)-H(14B)	121.7
C(16B)-C(15B)-C(14B)	108.0
C(16B)-C(15B)-Mo(2)	71.6(4)
C(14B)-C(15B)-Mo(2)	73.2(4)
C(16B)-C(15B)-H(15B)	126.0
C(14B)-C(15B)-H(15B)	126.0
Mo(2)-C(15B)-H(15B)	120.9
C(17B)-C(16B)-C(15B)	108.0
C(17B)-C(16B)-Mo(2)	72.6(4)
C(15B)-C(16B)-Mo(2)	73.0(4)
C(17B)-C(16B)-H(16B)	126.0
C(15B)-C(16B)-H(16B)	126.0
Mo(2)-C(16B)-H(16B)	120.2
C(16B)-C(17B)-C(18B)	108.0
C(16B)-C(17B)-Mo(2)	72.0(4)
C(18B)-C(17B)-Mo(2)	73.3(4)
C(16B)-C(17B)-H(17B)	126.0
C(18B)-C(17B)-H(17B)	126.0
Mo(2)-C(17B)-H(17B)	120.5
C(17B)-C(18B)-C(14B)	108.0
C(17B)-C(18B)-Mo(2)	71.5(4)
C(14B)-C(18B)-Mo(2)	72.8(4)
C(17B)-C(18B)-H(18B)	126.0
C(14B)-C(18B)-H(18B)	126.0
Mo(2)-C(18B)-H(18B)	121.5

Anisotropic displacement parameters ($Å^2$ x 10^3) for mes129a. The anisotropic displacement factor exponent takes the form: $-2\pi^2 [h^2 a^{*2} U^{11} + ... + 2 h k a^* b^* U^{12}]$

	U^{11}	U^{22}	U^{33}	U^{23}	U^{13}	U^{12}
Mo(1)	23(1)	23(1)	27(1)	-1(1)	7(1)	1(1)
C(1)	26(2)	29(2)	21(2)	-2(2)	5(2)	-1(2)
N(1)	29(2)	26(2)	34(2)	0(2)	10(2)	1(2)
O(1)	39(2)	55(2)	42(2)	-3(2)	19(2)	7(2)
Mo(2)	25(1)	27(1)	28(1)	-2(1)	6(1)	-1(1)
O(2)	54(2)	30(2)	48(2)	4(2)	13(2)	-3(2)
N(2)	24(2)	26(2)	34(2)	0(2)	10(2)	0(1)
C(2)	27(2)	30(2)	35(2)	-2(2)	7(2)	6(2)
O(3)	35(2)	58(2)	46(2)	0(2)	20(2)	-10(2)
C(3)	33(3)	23(2)	40(3)	5(2)	2(2)	6(2)
C(4)	44(3)	34(3)	60(3)	5(2)	25(3)	3(2)
C(5)	34(3)	32(2)	46(3)	1(2)	21(2)	-6(2)
C(6)	34(3)	33(2)	25(2)	-2(2)	5(2)	0(2)
C(7)	29(2)	36(2)	31(2)	-6(2)	10(2)	2(2)
C(8)	30(2)	32(3)	37(3)	-5(2)	6(2)	8(2)
C(9)	56(3)	37(3)	31(3)	-12(2)	11(2)	-3(2)
C(10)	45(3)	36(3)	45(3)	-11(2)	21(2)	8(2)
C(11)	59(3)	22(2)	46(3)	-9(2)	16(3)	2(2)
C(12)	42(3)	29(3)	53(3)	-17(2)	13(3)	-12(2)
C(13)	38(3)	37(3)	39(3)	-20(2)	-4(2)	1(2)
C(14A)	42(5)	55(7)	27(4)	-13(5)	6(4)	1(5)
C(15A)	37(5)	39(4)	39(7)	-18(3)	2(4)	-2(4)
C(16A)	29(5)	34(5)	41(4)	-4(4)	2(3)	-12(4)
C(17A)	28(3)	38(5)	35(5)	3(4)	9(3)	-3(4)
C(18A)	29(5)	43(4)	29(5)	3(3)	3(3)	1(3)
C(14B)	31(6)	28(7)	32(6)	-6(5)	10(5)	-5(5)
C(15B)	26(7)	35(5)	22(7)	-5(4)	6(5)	-9(4)
C(16B)	29(5)	49(9)	42(6)	-13(6)	15(5)	-6(6)
C(17B)	31(6)	46(6)	29(8)	-11(5)	-4(5)	6(5)
C(18B)	32(7)	37(7)	26(5)	3(6)	-2(4)	-4(6)

Hydrogen coordinates (x 10^4) and isotropic displacement parameters ($Å^2$ x 10^3) for mes129a.

	x	y	z	U(eq)
H(2A)	7641	2962	1965	38
H(3A)	6069	2405	3256	41
H(4A)	2943	3115	3859	66
H(4B)	3671	2528	4051	66
H(4C)	2377	2699	2281	66
H(5A)	5549	4133	-187	53
H(5B)	7094	3803	41	53
H(5C)	6972	4189	1569	53
H(9A)	2884	4114	4748	50
H(10A)	778	4701	2688	49
H(11A)	2017	5266	861	51
H(12A)	4886	5039	1768	50
H(13A)	5457	4332	4174	50
H(14A)	298	3549	-5800	51
H(15A)	117	2737	-4000	49
H(16A)	-1570	2978	-2164	44
H(17A)	-2432	3939	-2829	41
H(18A)	-1277	4292	-5076	42
H(14B)	625	3060	-5128	36
H(15B)	-520	2699	-2884	34
H(16B)	-2165	3428	-2207	47
H(17B)	-2036	4240	-4034	46
H(18B)	-312	4012	-5839	41

Torsion angles [°] for mes129a.

C(7)-Mo(1)-C(1)-N(2)	156.6(4)
C(10)-Mo(1)-C(1)-N(2)	-110.0(4)
C(11)-Mo(1)-C(1)-N(2)	-63.3(4)
C(9)-Mo(1)-C(1)-N(2)	-110.6(4)
C(12)-Mo(1)-C(1)-N(2)	-53.4(4)
C(13)-Mo(1)-C(1)-N(2)	-79.0(4)
C(8)-Mo(1)-C(1)-N(2)	49.6(4)
Mo(2)-Mo(1)-C(1)-N(2)	93.3(3)

C(7)-Mo(1)-C(1)-N(1)	-23.6(4)
C(10)-Mo(1)-C(1)-N(1)	69.8(4)
C(11)-Mo(1)-C(1)-N(1)	116.5(4)
C(9)-Mo(1)-C(1)-N(1)	69.2(4)
C(12)-Mo(1)-C(1)-N(1)	126.4(4)
C(13)-Mo(1)-C(1)-N(1)	100.8(4)
C(8)-Mo(1)-C(1)-N(1)	-130.6(3)
Mo(2)-Mo(1)-C(1)-N(1)	-86.8(4)
N(2)-C(1)-N(1)-C(3)	-2.2(4)
Mo(1)-C(1)-N(1)-C(3)	178.0(3)
N(2)-C(1)-N(1)-C(4)	176.0(4)
Mo(1)-C(1)-N(1)-C(4)	-3.8(6)
N(1)-C(1)-N(2)-C(2)	2.0(4)
Mo(1)-C(1)-N(2)-C(2)	-178.1(3)
N(1)-C(1)-N(2)-C(5)	-175.4(4)
Mo(1)-C(1)-N(2)-C(5)	4.5(6)
C(1)-N(2)-C(2)-C(3)	-1.2(5)
C(5)-N(2)-C(2)-C(3)	176.3(4)
N(2)-C(2)-C(3)-N(1)	-0.2(5)
C(1)-N(1)-C(3)-C(2)	1.5(5)
C(4)-N(1)-C(3)-C(2)	-176.7(4)
C(8)-Mo(2)-C(6)-O(1)	-95(2)
C(18B)-Mo(2)-C(6)-O(1)	-3(2)
C(17B)-Mo(2)-C(6)-O(1)	-3(2)
C(14A)-Mo(2)-C(6)-O(1)	11(2)
C(14B)-Mo(2)-C(6)-O(1)	28(2)
C(18A)-Mo(2)-C(6)-O(1)	-9(2)
C(15A)-Mo(2)-C(6)-O(1)	46(2)
C(16B)-Mo(2)-C(6)-O(1)	53(2)
C(15B)-Mo(2)-C(6)-O(1)	57(2)
C(17A)-Mo(2)-C(6)-O(1)	23(3)
C(16A)-Mo(2)-C(6)-O(1)	62(2)
C(1)-Mo(1)-C(7)-O(3)	97.7(14)
C(10)-Mo(1)-C(7)-O(3)	-29.8(14)
C(11)-Mo(1)-C(7)-O(3)	-49.9(14)
C(9)-Mo(1)-C(7)-O(3)	5.2(14)
C(12)-Mo(1)-C(7)-O(3)	-20.6(16)
C(13)-Mo(1)-C(7)-O(3)	18.0(15)
C(8)-Mo(1)-C(7)-O(3)	-134.9(14)
Mo(2)-Mo(1)-C(7)-O(3)	-161.6(15)
C(1)-Mo(1)-C(7)-Mo(2)	-100.64(12)
C(10)-Mo(1)-C(7)-Mo(2)	131.87(15)
C(11)-Mo(1)-C(7)-Mo(2)	111.73(17)

C(9)-Mo(1)-C(7)-Mo(2)	166.83(14)
C(12)-Mo(1)-C(7)-Mo(2)	141.0(3)
C(13)-Mo(1)-C(7)-Mo(2)	179.67(14)
C(8)-Mo(1)-C(7)-Mo(2)	26.76(13)
C(6)-Mo(2)-C(7)-O(3)	-132.7(4)
C(8)-Mo(2)-C(7)-O(3)	137.8(4)
C(18B)-Mo(2)-C(7)-O(3)	21.5(8)
C(17B)-Mo(2)-C(7)-O(3)	36.7(5)
C(14A)-Mo(2)-C(7)-O(3)	-8.8(7)
C(14B)-Mo(2)-C(7)-O(3)	-30.8(6)
C(18A)-Mo(2)-C(7)-O(3)	38.4(5)
C(15A)-Mo(2)-C(7)-O(3)	-29.1(4)
C(16B)-Mo(2)-C(7)-O(3)	10.6(6)
C(15B)-Mo(2)-C(7)-O(3)	-23.2(5)
C(17A)-Mo(2)-C(7)-O(3)	28.1(4)
C(16A)-Mo(2)-C(7)-O(3)	-5.7(5)
C(6)-Mo(2)-C(7)-Mo(1)	53.35(19)
C(8)-Mo(2)-C(7)-Mo(1)	-36.15(18)
C(18B)-Mo(2)-C(7)-Mo(1)	-152.5(6)
C(17B)-Mo(2)-C(7)-Mo(1)	-137.3(3)
C(14A)-Mo(2)-C(7)-Mo(1)	177.2(5)
C(14B)-Mo(2)-C(7)-Mo(1)	155.2(3)
C(18A)-Mo(2)-C(7)-Mo(1)	-135.5(2)
C(15A)-Mo(2)-C(7)-Mo(1)	156.96(16)
C(16B)-Mo(2)-C(7)-Mo(1)	-163.4(5)
C(15B)-Mo(2)-C(7)-Mo(1)	162.8(3)
C(17A)-Mo(2)-C(7)-Mo(1)	-145.9(2)
C(16A)-Mo(2)-C(7)-Mo(1)	-179.7(3)
C(6)-Mo(2)-C(8)-O(2)	91.7(15)
C(18B)-Mo(2)-C(8)-O(2)	-10.6(16)
C(17B)-Mo(2)-C(8)-O(2)	-45.8(16)
C(14A)-Mo(2)-C(8)-O(2)	0.6(16)
C(14B)-Mo(2)-C(8)-O(2)	9.7(16)
C(18A)-Mo(2)-C(8)-O(2)	-30.6(15)
C(15A)-Mo(2)-C(8)-O(2)	0.3(17)
C(16B)-Mo(2)-C(8)-O(2)	-62.8(16)
C(15B)-Mo(2)-C(8)-O(2)	-21.5(19)
C(17A)-Mo(2)-C(8)-O(2)	-60.4(15)
C(16A)-Mo(2)-C(8)-O(2)	-56.8(16)
C(6)-Mo(2)-C(8)-Mo(1)	-80.28(14)
C(18B)-Mo(2)-C(8)-Mo(1)	177.5(4)
C(17B)-Mo(2)-C(8)-Mo(1)	142.3(4)
C(14A)-Mo(2)-C(8)-Mo(1)	-171.40(18)

C(14B)-Mo(2)-C(8)-Mo(1)	-162.3(2)
C(18A)-Mo(2)-C(8)-Mo(1)	157.4(3)
C(15A)-Mo(2)-C(8)-Mo(1)	-171.6(3)
C(16B)-Mo(2)-C(8)-Mo(1)	125.2(3)
C(15B)-Mo(2)-C(8)-Mo(1)	166.5(8)
C(17A)-Mo(2)-C(8)-Mo(1)	127.64(17)
C(16A)-Mo(2)-C(8)-Mo(1)	131.2(4)
C(7)-Mo(1)-C(8)-O(2)	148.2(4)
C(1)-Mo(1)-C(8)-O(2)	-105.6(4)
C(10)-Mo(1)-C(8)-O(2)	57.7(4)
C(11)-Mo(1)-C(8)-O(2)	31.0(4)
C(9)-Mo(1)-C(8)-O(2)	43.6(5)
C(12)-Mo(1)-C(8)-O(2)	-0.9(4)
C(13)-Mo(1)-C(8)-O(2)	-3.3(5)
Mo(2)-Mo(1)-C(8)-O(2)	-177.6(5)
C(7)-Mo(1)-C(8)-Mo(2)	-34.20(17)
C(1)-Mo(1)-C(8)-Mo(2)	71.97(19)
C(10)-Mo(1)-C(8)-Mo(2)	-124.75(16)
C(11)-Mo(1)-C(8)-Mo(2)	-151.39(17)
C(9)-Mo(1)-C(8)-Mo(2)	-138.8(2)
C(12)-Mo(1)-C(8)-Mo(2)	176.72(15)
C(13)-Mo(1)-C(8)-Mo(2)	174.33(15)
C(7)-Mo(1)-C(9)-C(10)	-83.2(3)
C(1)-Mo(1)-C(9)-C(10)	179.1(3)
C(11)-Mo(1)-C(9)-C(10)	38.6(3)
C(12)-Mo(1)-C(9)-C(10)	80.0(3)
C(13)-Mo(1)-C(9)-C(10)	115.5(4)
C(8)-Mo(1)-C(9)-C(10)	24.0(4)
Mo(2)-Mo(1)-C(9)-C(10)	-57.8(4)
C(7)-Mo(1)-C(9)-C(13)	161.4(3)
C(1)-Mo(1)-C(9)-C(13)	63.7(3)
C(10)-Mo(1)-C(9)-C(13)	-115.5(4)
C(11)-Mo(1)-C(9)-C(13)	-76.8(3)
C(12)-Mo(1)-C(9)-C(13)	-35.5(3)
C(8)-Mo(1)-C(9)-C(13)	-91.5(4)
Mo(2)-Mo(1)-C(9)-C(13)	-173.3(2)
C(13)-C(9)-C(10)-C(11)	0.5(5)
Mo(1)-C(9)-C(10)-C(11)	-66.0(3)
C(13)-C(9)-C(10)-Mo(1)	66.5(3)
C(7)-Mo(1)-C(10)-C(11)	-148.6(3)
C(1)-Mo(1)-C(10)-C(11)	113.3(3)
C(9)-Mo(1)-C(10)-C(11)	114.4(4)
C(12)-Mo(1)-C(10)-C(11)	37.4(3)

C(13)-Mo(1)-C(10)-C(11)	77.0(3)
C(8)-Mo(1)-C(10)-C(11)	-49.4(3)
Mo(2)-Mo(1)-C(10)-C(11)	-94.9(3)
C(7)-Mo(1)-C(10)-C(9)	97.0(3)
C(1)-Mo(1)-C(10)-C(9)	-1.1(4)
C(11)-Mo(1)-C(10)-C(9)	-114.4(4)
C(12)-Mo(1)-C(10)-C(9)	-77.0(3)
C(13)-Mo(1)-C(10)-C(9)	-37.3(3)
C(8)-Mo(1)-C(10)-C(9)	-163.8(3)
Mo(2)-Mo(1)-C(10)-C(9)	150.8(2)
C(9)-C(10)-C(11)-C(12)	-0.3(5)
Mo(1)-C(10)-C(11)-C(12)	-68.1(3)
C(9)-C(10)-C(11)-Mo(1)	67.8(3)
C(7)-Mo(1)-C(11)-C(10)	36.1(4)
C(1)-Mo(1)-C(11)-C(10)	-97.7(3)
C(9)-Mo(1)-C(11)-C(10)	-38.1(3)
C(12)-Mo(1)-C(11)-C(10)	-115.1(5)
C(13)-Mo(1)-C(11)-C(10)	-79.4(3)
C(8)-Mo(1)-C(11)-C(10)	132.1(3)
Mo(2)-Mo(1)-C(11)-C(10)	108.9(3)
C(7)-Mo(1)-C(11)-C(12)	151.2(3)
C(1)-Mo(1)-C(11)-C(12)	17.4(4)
C(10)-Mo(1)-C(11)-C(12)	115.1(5)
C(9)-Mo(1)-C(11)-C(12)	77.0(3)
C(13)-Mo(1)-C(11)-C(12)	35.7(3)
C(8)-Mo(1)-C(11)-C(12)	-112.8(3)
Mo(2)-Mo(1)-C(11)-C(12)	-136.0(3)
C(10)-C(11)-C(12)-C(13)	-0.1(5)
Mo(1)-C(11)-C(12)-C(13)	-65.0(3)
C(10)-C(11)-C(12)-Mo(1)	64.9(3)
C(7)-Mo(1)-C(12)-C(13)	68.0(4)
C(1)-Mo(1)-C(12)-C(13)	-50.0(3)
C(10)-Mo(1)-C(12)-C(13)	78.8(3)
C(11)-Mo(1)-C(12)-C(13)	117.2(4)
C(9)-Mo(1)-C(12)-C(13)	36.9(3)
C(8)-Mo(1)-C(12)-C(13)	-176.6(3)
Mo(2)-Mo(1)-C(12)-C(13)	-173.0(2)
C(7)-Mo(1)-C(12)-C(11)	-49.2(5)
C(1)-Mo(1)-C(12)-C(11)	-167.2(3)
C(10)-Mo(1)-C(12)-C(11)	-38.4(3)
C(9)-Mo(1)-C(12)-C(11)	-80.3(3)
C(13)-Mo(1)-C(12)-C(11)	-117.2(4)
C(8)-Mo(1)-C(12)-C(11)	66.2(3)

Mo(2)-Mo(1)-C(12)-C(11)	69.9(3)
C(11)-C(12)-C(13)-C(9)	0.4(5)
Mo(1)-C(12)-C(13)-C(9)	-60.7(3)
C(11)-C(12)-C(13)-Mo(1)	61.1(3)
C(10)-C(9)-C(13)-C(12)	-0.6(5)
Mo(1)-C(9)-C(13)-C(12)	61.9(3)
C(10)-C(9)-C(13)-Mo(1)	-62.4(3)
C(7)-Mo(1)-C(13)-C(12)	-140.5(3)
C(1)-Mo(1)-C(13)-C(12)	129.1(3)
C(10)-Mo(1)-C(13)-C(12)	-79.7(3)
C(11)-Mo(1)-C(13)-C(12)	-37.2(3)
C(9)-Mo(1)-C(13)-C(12)	-117.6(4)
C(8)-Mo(1)-C(13)-C(12)	4.3(4)
Mo(2)-Mo(1)-C(13)-C(12)	37.2(11)
C(7)-Mo(1)-C(13)-C(9)	-22.9(4)
C(1)-Mo(1)-C(13)-C(9)	-113.3(3)
C(10)-Mo(1)-C(13)-C(9)	37.9(3)
C(11)-Mo(1)-C(13)-C(9)	80.4(3)
C(12)-Mo(1)-C(13)-C(9)	117.6(4)
C(8)-Mo(1)-C(13)-C(9)	121.9(3)
Mo(2)-Mo(1)-C(13)-C(9)	154.8(8)
C(6)-Mo(2)-C(14A)-C(15A)	94.4(5)
C(8)-Mo(2)-C(14A)-C(15A)	-179.7(4)
C(18B)-Mo(2)-C(14A)-C(15A)	-138.0(10)
C(17B)-Mo(2)-C(14A)-C(15A)	-97.9(4)
C(14B)-Mo(2)-C(14A)-C(15A)	25.4(7)
C(18A)-Mo(2)-C(14A)-C(15A)	-115.61(11)
C(16B)-Mo(2)-C(14A)-C(15A)	-56.1(4)
C(15B)-Mo(2)-C(14A)-C(15A)	-14.2(4)
C(17A)-Mo(2)-C(14A)-C(15A)	-78.18(14)
C(16A)-Mo(2)-C(14A)-C(15A)	-37.08(9)
C(6)-Mo(2)-C(14A)-C(18A)	-150.0(4)
C(8)-Mo(2)-C(14A)-C(18A)	-64.1(4)
C(18B)-Mo(2)-C(14A)-C(18A)	-22.4(9)
C(17B)-Mo(2)-C(14A)-C(18A)	17.7(4)
C(14B)-Mo(2)-C(14A)-C(18A)	141.0(8)
C(15A)-Mo(2)-C(14A)-C(18A)	115.61(11)
C(16B)-Mo(2)-C(14A)-C(18A)	59.5(4)
C(15B)-Mo(2)-C(14A)-C(18A)	101.5(4)
C(17A)-Mo(2)-C(14A)-C(18A)	37.43(9)
C(16A)-Mo(2)-C(14A)-C(18A)	78.53(13)
C(18A)-C(14A)-C(15A)-C(16A)	0
Mo(2)-C(14A)-C(15A)-C(16A)	64.7(2)

C(18A)-C(14A)-C(15A)-Mo(2)	-64.7(2)
C(6)-Mo(2)-C(15A)-C(16A)	156.2(4)
C(8)-Mo(2)-C(15A)-C(16A)	-115.7(7)
C(18B)-Mo(2)-C(15A)-C(16A)	-101.1(4)
C(17B)-Mo(2)-C(15A)-C(16A)	-59.5(4)
C(14A)-Mo(2)-C(15A)-C(16A)	-116.09(12)
C(14B)-Mo(2)-C(15A)-C(16A)	-139.8(7)
C(18A)-Mo(2)-C(15A)-C(16A)	-78.43(13)
C(16B)-Mo(2)-C(15A)-C(16A)	-17.9(4)
C(15B)-Mo(2)-C(15A)-C(16A)	22.1(10)
C(17A)-Mo(2)-C(15A)-C(16A)	-36.97(9)
C(6)-Mo(2)-C(15A)-C(14A)	-87.7(4)
C(8)-Mo(2)-C(15A)-C(14A)	0.4(7)
C(18B)-Mo(2)-C(15A)-C(14A)	15.0(4)
C(17B)-Mo(2)-C(15A)-C(14A)	56.6(4)
C(14B)-Mo(2)-C(15A)-C(14A)	-23.7(7)
C(18A)-Mo(2)-C(15A)-C(14A)	37.66(9)
C(16B)-Mo(2)-C(15A)-C(14A)	98.2(4)
C(15B)-Mo(2)-C(15A)-C(14A)	138.2(10)
C(17A)-Mo(2)-C(15A)-C(14A)	79.12(14)
C(16A)-Mo(2)-C(15A)-C(14A)	116.09(12)
C(14A)-C(15A)-C(16A)-C(17A)	0
Mo(2)-C(15A)-C(16A)-C(17A)	63.7(2)
C(14A)-C(15A)-C(16A)-Mo(2)	-63.7(2)
C(6)-Mo(2)-C(16A)-C(17A)	-146.1(5)
C(8)-Mo(2)-C(16A)-C(17A)	-6.0(7)
C(18B)-Mo(2)-C(16A)-C(17A)	-60.3(3)
C(17B)-Mo(2)-C(16A)-C(17A)	-20.8(4)
C(14A)-Mo(2)-C(16A)-C(17A)	-79.06(14)
C(14B)-Mo(2)-C(16A)-C(17A)	-100.2(3)
C(18A)-Mo(2)-C(16A)-C(17A)	-37.33(9)
C(15A)-Mo(2)-C(16A)-C(17A)	-116.46(12)
C(16B)-Mo(2)-C(16A)-C(17A)	11.3(9)
C(15B)-Mo(2)-C(16A)-C(17A)	-133.1(7)
C(6)-Mo(2)-C(16A)-C(15A)	-29.7(5)
C(8)-Mo(2)-C(16A)-C(15A)	110.5(7)
C(18B)-Mo(2)-C(16A)-C(15A)	56.1(3)
C(17B)-Mo(2)-C(16A)-C(15A)	95.7(4)
C(14A)-Mo(2)-C(16A)-C(15A)	37.40(9)
C(14B)-Mo(2)-C(16A)-C(15A)	16.3(3)
C(18A)-Mo(2)-C(16A)-C(15A)	79.13(14)
C(16B)-Mo(2)-C(16A)-C(15A)	127.8(9)
C(15B)-Mo(2)-C(16A)-C(15A)	-16.6(7)

C(17A)-Mo(2)-C(16A)-C(15A)	116.46(12)
C(15A)-C(16A)-C(17A)-C(18A)	0
Mo(2)-C(16A)-C(17A)-C(18A)	63.6(2)
C(15A)-C(16A)-C(17A)-Mo(2)	-63.6(2)
C(6)-Mo(2)-C(17A)-C(16A)	63.8(9)
C(8)-Mo(2)-C(17A)-C(16A)	176.2(4)
C(18B)-Mo(2)-C(17A)-C(16A)	97.3(3)
C(17B)-Mo(2)-C(17A)-C(16A)	126.7(7)
C(14A)-Mo(2)-C(17A)-C(16A)	78.52(14)
C(14B)-Mo(2)-C(17A)-C(16A)	58.5(2)
C(18A)-Mo(2)-C(17A)-C(16A)	116.18(12)
C(15A)-Mo(2)-C(17A)-C(16A)	37.00(9)
C(16B)-Mo(2)-C(17A)-C(16A)	-9.8(7)
C(15B)-Mo(2)-C(17A)-C(16A)	19.6(3)
C(6)-Mo(2)-C(17A)-C(18A)	-52.4(9)
C(8)-Mo(2)-C(17A)-C(18A)	60.0(4)
C(18B)-Mo(2)-C(17A)-C(18A)	-18.8(3)
C(17B)-Mo(2)-C(17A)-C(18A)	10.5(7)
C(14A)-Mo(2)-C(17A)-C(18A)	-37.65(9)
C(14B)-Mo(2)-C(17A)-C(18A)	-57.7(2)
C(15A)-Mo(2)-C(17A)-C(18A)	-79.17(14)
C(16B)-Mo(2)-C(17A)-C(18A)	-126.0(7)
C(15B)-Mo(2)-C(17A)-C(18A)	-96.6(3)
C(16A)-Mo(2)-C(17A)-C(18A)	-116.18(12)
C(16A)-C(17A)-C(18A)-C(14A)	0
Mo(2)-C(17A)-C(18A)-C(14A)	64.6(3)
C(16A)-C(17A)-C(18A)-Mo(2)	-64.6(3)
C(15A)-C(14A)-C(18A)-C(17A)	0
Mo(2)-C(14A)-C(18A)-C(17A)	-65.3(2)
C(15A)-C(14A)-C(18A)-Mo(2)	65.3(2)
C(6)-Mo(2)-C(18A)-C(17A)	151.8(4)
C(8)-Mo(2)-C(18A)-C(17A)	-124.4(5)
C(18B)-Mo(2)-C(18A)-C(17A)	134.1(7)
C(17B)-Mo(2)-C(18A)-C(17A)	-12.4(9)
C(14A)-Mo(2)-C(18A)-C(17A)	115.66(12)
C(14B)-Mo(2)-C(18A)-C(17A)	100.7(3)
C(15A)-Mo(2)-C(18A)-C(17A)	78.17(13)
C(16B)-Mo(2)-C(18A)-C(17A)	20.6(3)
C(15B)-Mo(2)-C(18A)-C(17A)	60.6(3)
C(16A)-Mo(2)-C(18A)-C(17A)	37.03(9)
C(6)-Mo(2)-C(18A)-C(14A)	36.2(5)
C(8)-Mo(2)-C(18A)-C(14A)	119.9(5)
C(18B)-Mo(2)-C(18A)-C(14A)	18.4(7)

C(17B)-Mo(2)-C(18A)-C(14A)	-128.1(9)
C(14B)-Mo(2)-C(18A)-C(14A)	-14.9(3)
C(15A)-Mo(2)-C(18A)-C(14A)	-37.49(9)
C(16B)-Mo(2)-C(18A)-C(14A)	-95.0(3)
C(15B)-Mo(2)-C(18A)-C(14A)	-55.0(3)
C(17A)-Mo(2)-C(18A)-C(14A)	-115.66(12)
C(16A)-Mo(2)-C(18A)-C(14A)	-78.62(14)
C(6)-Mo(2)-C(14B)-C(15B)	124.5(7)
C(8)-Mo(2)-C(14B)-C(15B)	-153.7(7)
C(18B)-Mo(2)-C(14B)-C(15B)	-116.6(2)
C(17B)-Mo(2)-C(14B)-C(15B)	-79.3(3)
C(14A)-Mo(2)-C(14B)-C(15B)	-124.9(8)
C(18A)-Mo(2)-C(14B)-C(15B)	-96.9(4)
C(15A)-Mo(2)-C(14B)-C(15B)	8.5(7)
C(16B)-Mo(2)-C(14B)-C(15B)	-37.50(16)
C(17A)-Mo(2)-C(14B)-C(15B)	-58.2(4)
C(16A)-Mo(2)-C(14B)-C(15B)	-19.7(4)
C(6)-Mo(2)-C(14B)-C(18B)	-119.0(8)
C(8)-Mo(2)-C(14B)-C(18B)	-37.2(7)
C(17B)-Mo(2)-C(14B)-C(18B)	37.25(16)
C(14A)-Mo(2)-C(14B)-C(18B)	-8.3(8)
C(18A)-Mo(2)-C(14B)-C(18B)	19.6(4)
C(15A)-Mo(2)-C(14B)-C(18B)	125.0(7)
C(16B)-Mo(2)-C(14B)-C(18B)	79.1(2)
C(15B)-Mo(2)-C(14B)-C(18B)	116.6(2)
C(17A)-Mo(2)-C(14B)-C(18B)	58.4(4)
C(16A)-Mo(2)-C(14B)-C(18B)	96.9(4)
C(18B)-C(14B)-C(15B)-C(16B)	0
Mo(2)-C(14B)-C(15B)-C(16B)	63.6(4)
C(18B)-C(14B)-C(15B)-Mo(2)	-63.6(4)
C(6)-Mo(2)-C(15B)-C(16B)	-174.6(7)
C(8)-Mo(2)-C(15B)-C(16B)	-66.3(14)
C(18B)-Mo(2)-C(15B)-C(16B)	-79.1(2)
C(17B)-Mo(2)-C(15B)-C(16B)	-37.66(15)
C(14A)-Mo(2)-C(15B)-C(16B)	-95.6(4)
C(14B)-Mo(2)-C(15B)-C(16B)	-116.1(2)
C(18A)-Mo(2)-C(15B)-C(16B)	-56.0(4)
C(15A)-Mo(2)-C(15B)-C(16B)	-126.7(9)
C(17A)-Mo(2)-C(15B)-C(16B)	-16.0(4)
C(16A)-Mo(2)-C(15B)-C(16B)	16.4(8)
C(6)-Mo(2)-C(15B)-C(14B)	-58.4(7)
C(8)-Mo(2)-C(15B)-C(14B)	49.8(14)
C(18B)-Mo(2)-C(15B)-C(14B)	36.98(15)

C(17B)-Mo(2)-C(15B)-C(14B)	78.5(2)
C(14A)-Mo(2)-C(15B)-C(14B)	20.5(3)
C(18A)-Mo(2)-C(15B)-C(14B)	60.2(3)
C(15A)-Mo(2)-C(15B)-C(14B)	-10.6(9)
C(16B)-Mo(2)-C(15B)-C(14B)	116.1(2)
C(17A)-Mo(2)-C(15B)-C(14B)	100.2(4)
C(16A)-Mo(2)-C(15B)-C(14B)	132.5(8)
C(14B)-C(15B)-C(16B)-C(17B)	0
Mo(2)-C(15B)-C(16B)-C(17B)	64.7(4)
C(14B)-C(15B)-C(16B)-Mo(2)	-64.7(4)
C(6)-Mo(2)-C(16B)-C(17B)	-107.5(11)
C(8)-Mo(2)-C(16B)-C(17B)	30.2(7)
C(18B)-Mo(2)-C(16B)-C(17B)	-37.35(15)
C(14A)-Mo(2)-C(16B)-C(17B)	-57.0(3)
C(14B)-Mo(2)-C(16B)-C(17B)	-78.5(2)
C(18A)-Mo(2)-C(16B)-C(17B)	-15.3(3)
C(15A)-Mo(2)-C(16B)-C(17B)	-98.2(3)
C(15B)-Mo(2)-C(16B)-C(17B)	-115.73(19)
C(17A)-Mo(2)-C(16B)-C(17B)	23.1(8)
C(16A)-Mo(2)-C(16B)-C(17B)	-136.7(9)
C(6)-Mo(2)-C(16B)-C(15B)	8.2(11)
C(8)-Mo(2)-C(16B)-C(15B)	145.9(7)
C(18B)-Mo(2)-C(16B)-C(15B)	78.4(2)
C(17B)-Mo(2)-C(16B)-C(15B)	115.73(19)
C(14A)-Mo(2)-C(16B)-C(15B)	58.7(3)
C(14B)-Mo(2)-C(16B)-C(15B)	37.18(14)
C(18A)-Mo(2)-C(16B)-C(15B)	100.4(3)
C(15A)-Mo(2)-C(16B)-C(15B)	17.5(3)
C(17A)-Mo(2)-C(16B)-C(15B)	138.9(8)
C(16A)-Mo(2)-C(16B)-C(15B)	-21.0(8)
C(15B)-C(16B)-C(17B)-C(18B)	0
Mo(2)-C(16B)-C(17B)-C(18B)	65.0(4)
C(15B)-C(16B)-C(17B)-Mo(2)	-65.0(4)
C(6)-Mo(2)-C(17B)-C(16B)	115.5(10)
C(8)-Mo(2)-C(17B)-C(16B)	-156.1(7)
C(18B)-Mo(2)-C(17B)-C(16B)	115.90(19)
C(14A)-Mo(2)-C(17B)-C(16B)	97.0(3)
C(14B)-Mo(2)-C(17B)-C(16B)	78.9(2)
C(18A)-Mo(2)-C(17B)-C(16B)	135.5(9)
C(15A)-Mo(2)-C(17B)-C(16B)	55.9(3)
C(15B)-Mo(2)-C(17B)-C(16B)	37.57(16)
C(17A)-Mo(2)-C(17B)-C(16B)	-22.7(7)
C(16A)-Mo(2)-C(17B)-C(16B)	14.9(3)

C(6)-Mo(2)-C(17B)-C(18B)	-0.4(10)
C(8)-Mo(2)-C(17B)-C(18B)	88.0(7)
C(14A)-Mo(2)-C(17B)-C(18B)	-18.9(3)
C(14B)-Mo(2)-C(17B)-C(18B)	-37.01(15)
C(18A)-Mo(2)-C(17B)-C(18B)	19.6(8)
C(15A)-Mo(2)-C(17B)-C(18B)	-60.0(3)
C(16B)-Mo(2)-C(17B)-C(18B)	-115.90(19)
C(15B)-Mo(2)-C(17B)-C(18B)	-78.3(2)
C(17A)-Mo(2)-C(17B)-C(18B)	-138.6(8)
C(16A)-Mo(2)-C(17B)-C(18B)	-101.0(3)
C(16B)-C(17B)-C(18B)-C(14B)	0
Mo(2)-C(17B)-C(18B)-C(14B)	64.1(4)
C(16B)-C(17B)-C(18B)-Mo(2)	-64.1(4)
C(15B)-C(14B)-C(18B)-C(17B)	0
Mo(2)-C(14B)-C(18B)-C(17B)	-63.2(4)
C(15B)-C(14B)-C(18B)-Mo(2)	63.2(4)
C(6)-Mo(2)-C(18B)-C(17B)	179.7(7)
C(8)-Mo(2)-C(18B)-C(17B)	-94.4(7)
C(14A)-Mo(2)-C(18B)-C(17B)	125.5(8)
C(14B)-Mo(2)-C(18B)-C(17B)	116.4(2)
C(18A)-Mo(2)-C(18B)-C(17B)	-15.6(8)
C(15A)-Mo(2)-C(18B)-C(17B)	94.8(3)
C(16B)-Mo(2)-C(18B)-C(17B)	37.63(15)
C(15B)-Mo(2)-C(18B)-C(17B)	79.3(2)
C(17A)-Mo(2)-C(18B)-C(17B)	16.3(4)
C(16A)-Mo(2)-C(18B)-C(17B)	55.8(3)
C(6)-Mo(2)-C(18B)-C(14B)	63.3(7)
C(8)-Mo(2)-C(18B)-C(14B)	149.2(7)
C(17B)-Mo(2)-C(18B)-C(14B)	-116.4(2)
C(14A)-Mo(2)-C(18B)-C(14B)	9.1(8)
C(18A)-Mo(2)-C(18B)-C(14B)	-132.0(8)
C(15A)-Mo(2)-C(18B)-C(14B)	-21.6(3)
C(16B)-Mo(2)-C(18B)-C(14B)	-78.8(2)
C(15B)-Mo(2)-C(18B)-C(14B)	-37.09(15)
C(17A)-Mo(2)-C(18B)-C(14B)	-100.1(4)
C(16A)-Mo(2)-C(18B)-C(14B)	-60.6(3)

APPENDIX F

CRYSTALLOGRAPHIC DATA FOR **27**

Crystal data and structure refinement for mes133 (**27**).

Formula weight	444.73
Temperature	190(2) K
Wavelength	0.71073 Å
Crystal system	C 2/m
Unit cell dimensions	a = 14.525(2) Å α = 90 deg. b = 21.089(4) Å β = 105.486(9) deg. c = 16.992(2) Å γ = 90 deg
Volume	5016.0(13) $Å^3$
Z, Calculated density	10, 1.472 Mg/m^3
Absorption coefficient	0.777 mm^{-1}
F(000)	2296
Crystal size	0.38 x 0.04 x 0.03 mm
Theta range for data collection	1.91 to 25.29°
Limiting indices	-17<=h<=17, -25<=k<=25, -20<=l<=20
Reflections collected / unique	11924 / 4344 [R(int) = 0.1350]
Completeness to theta = 25.29	92.1 %
Max. and min. transmission	0.9808 and 0.7566
Refinement method	Full-matrix least-squares on F^2
Data / restraints / parameters	4344 / 0 / 271
Goodness-of-fit on F^2	1.042
Final R indices [I>2sigma(I)]	R1 = 0.1064, wR2 = 0.2625
R indices (all data)	R1 = 0.2063, wR2 = 0.3249
Largest diff. peak and hole	1.409 and -1.737 $e.Å^{-3}$

APPENDIX G

SELECTED NMR SPECTRA

^{1}H NMR spectra of **7a**

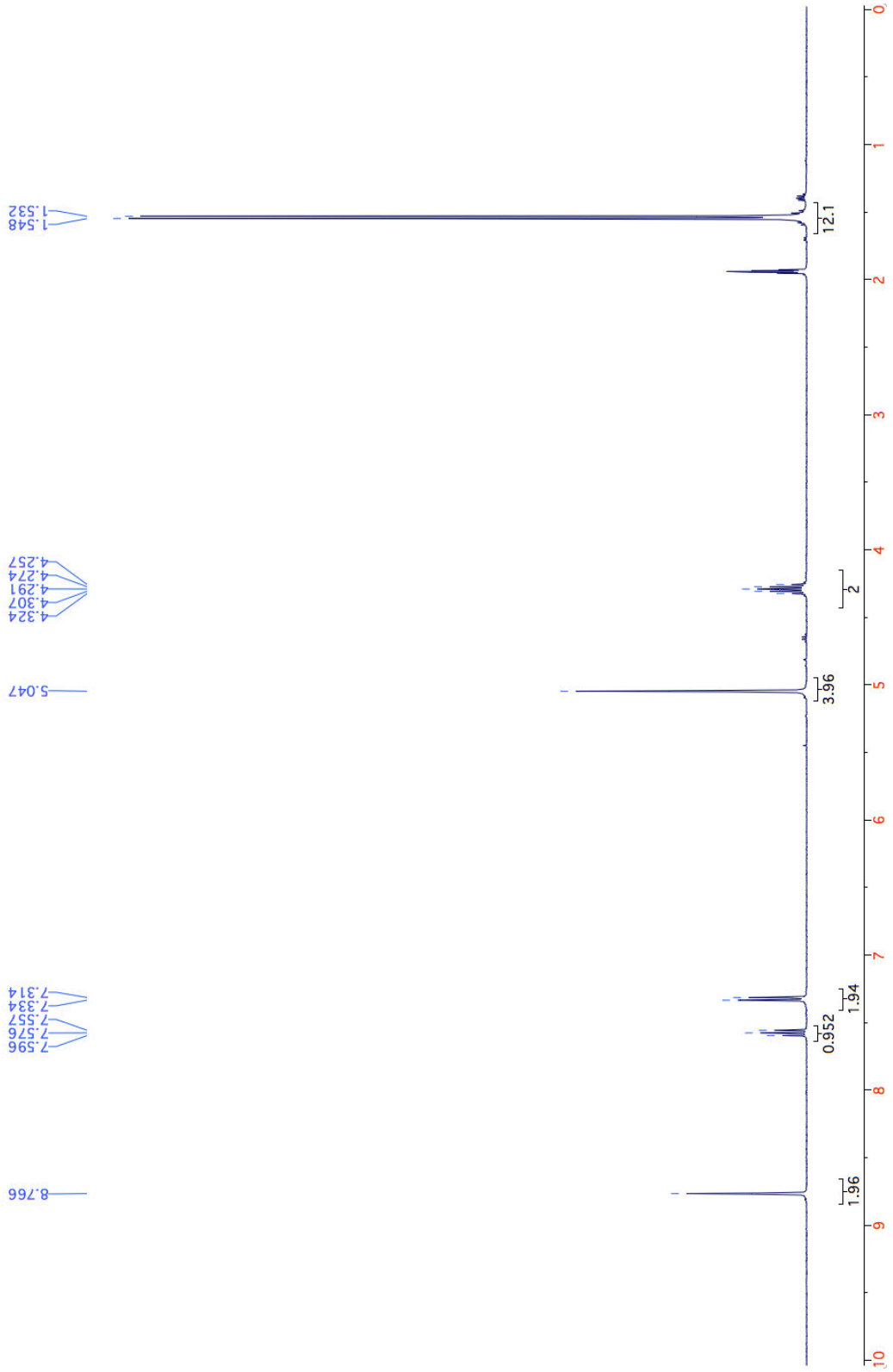

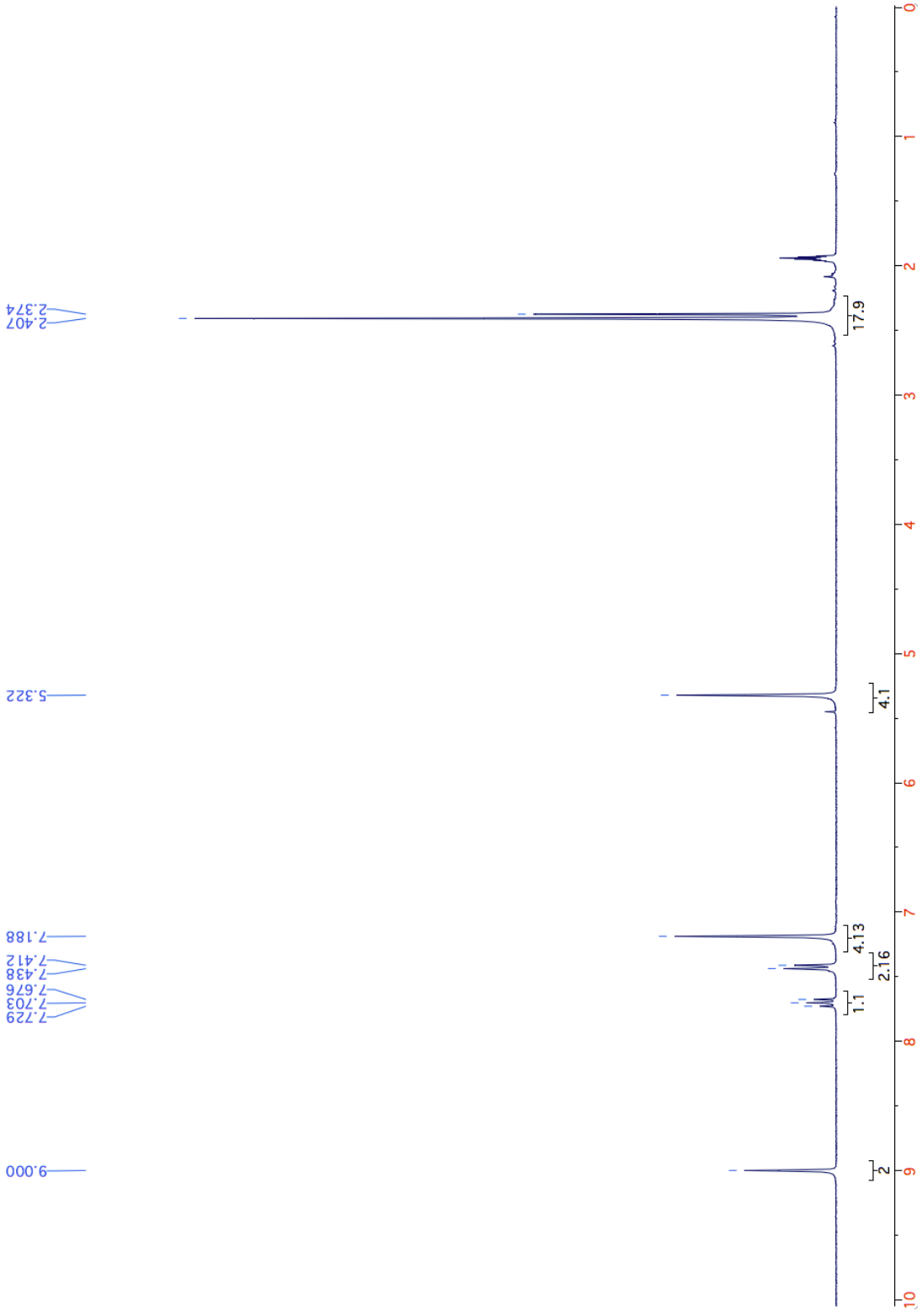

^{1}H NMR spectra of **7b**

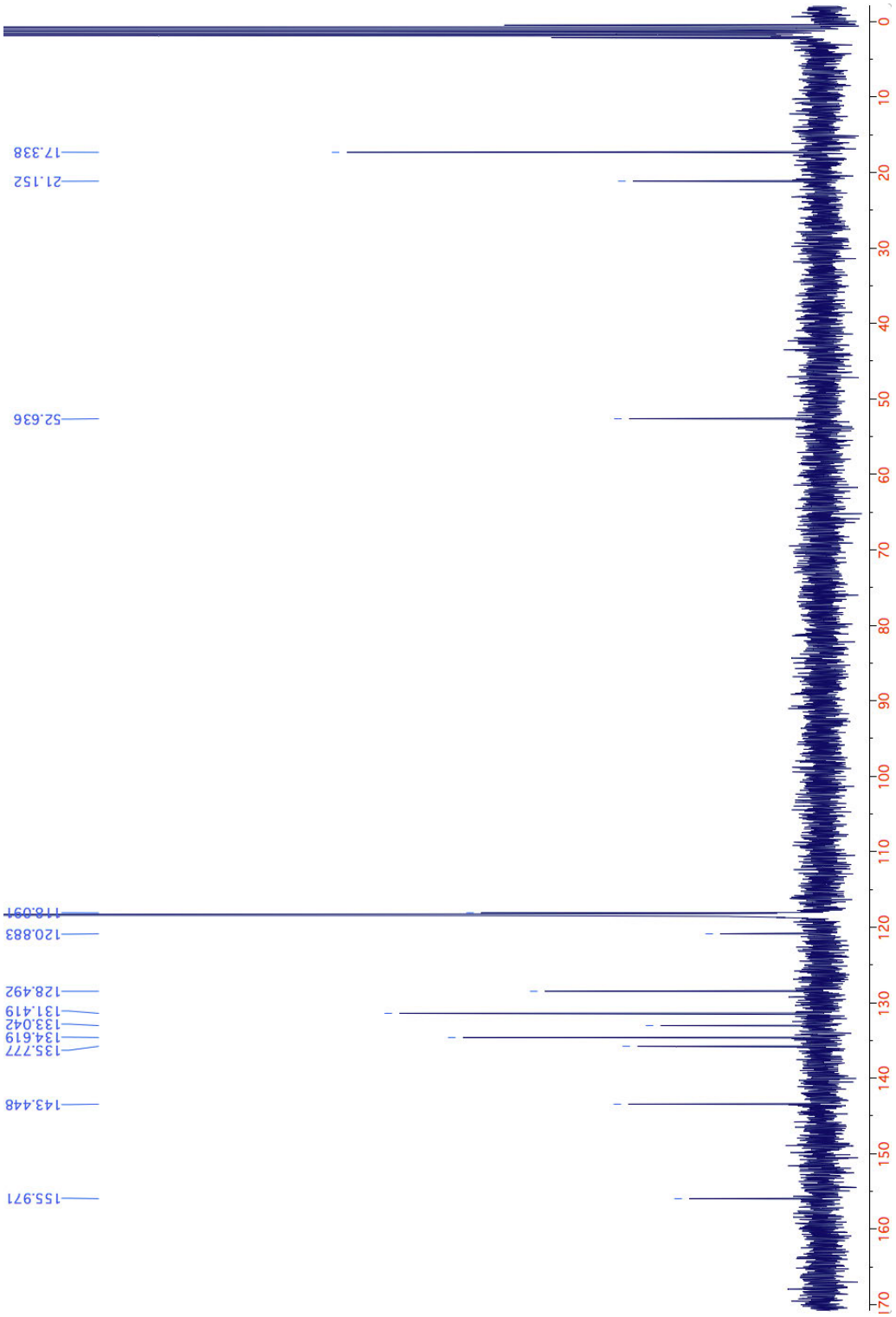

^{13}C NMR spectra of **7b**

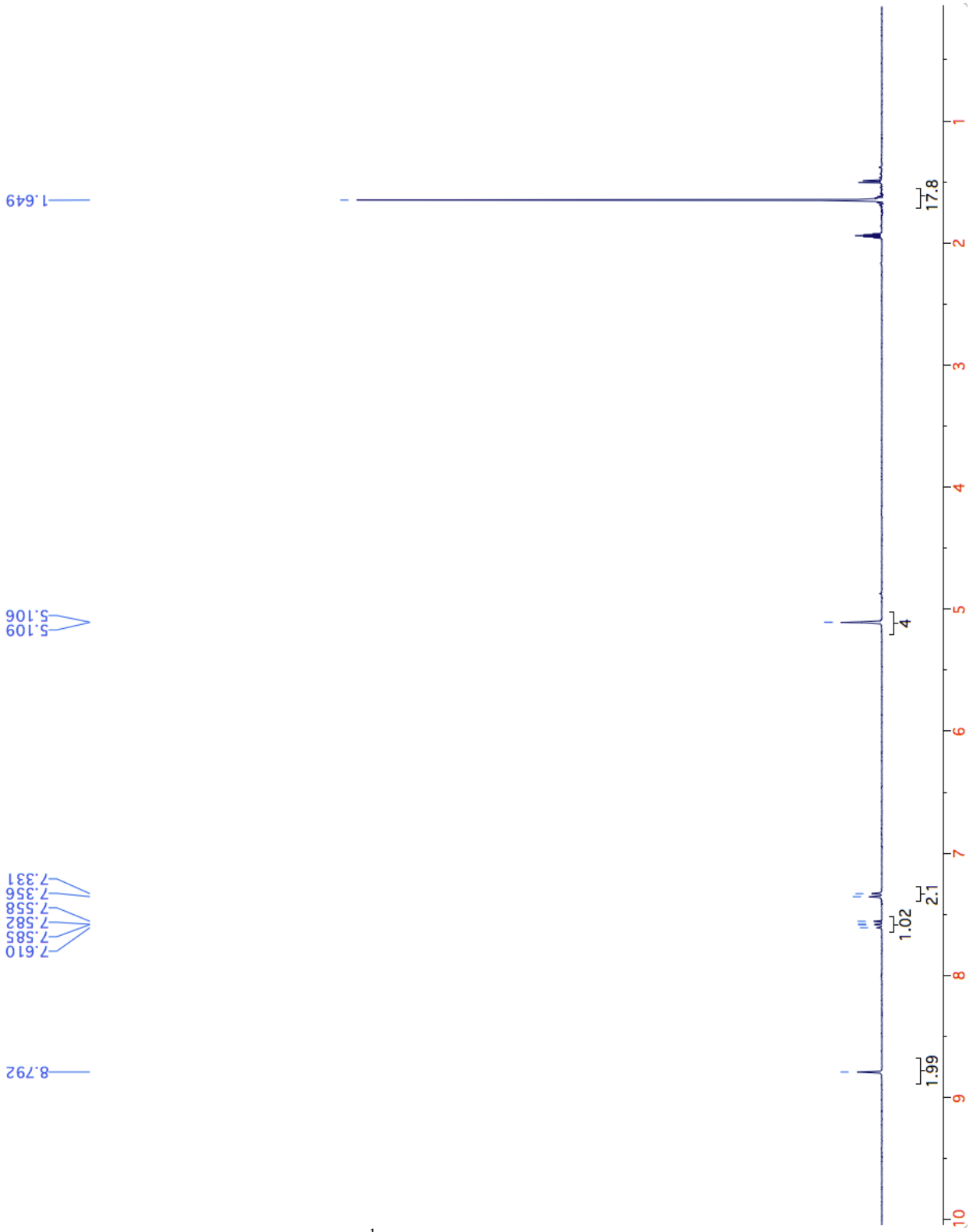

^{1}H NMR spectra of **7c**

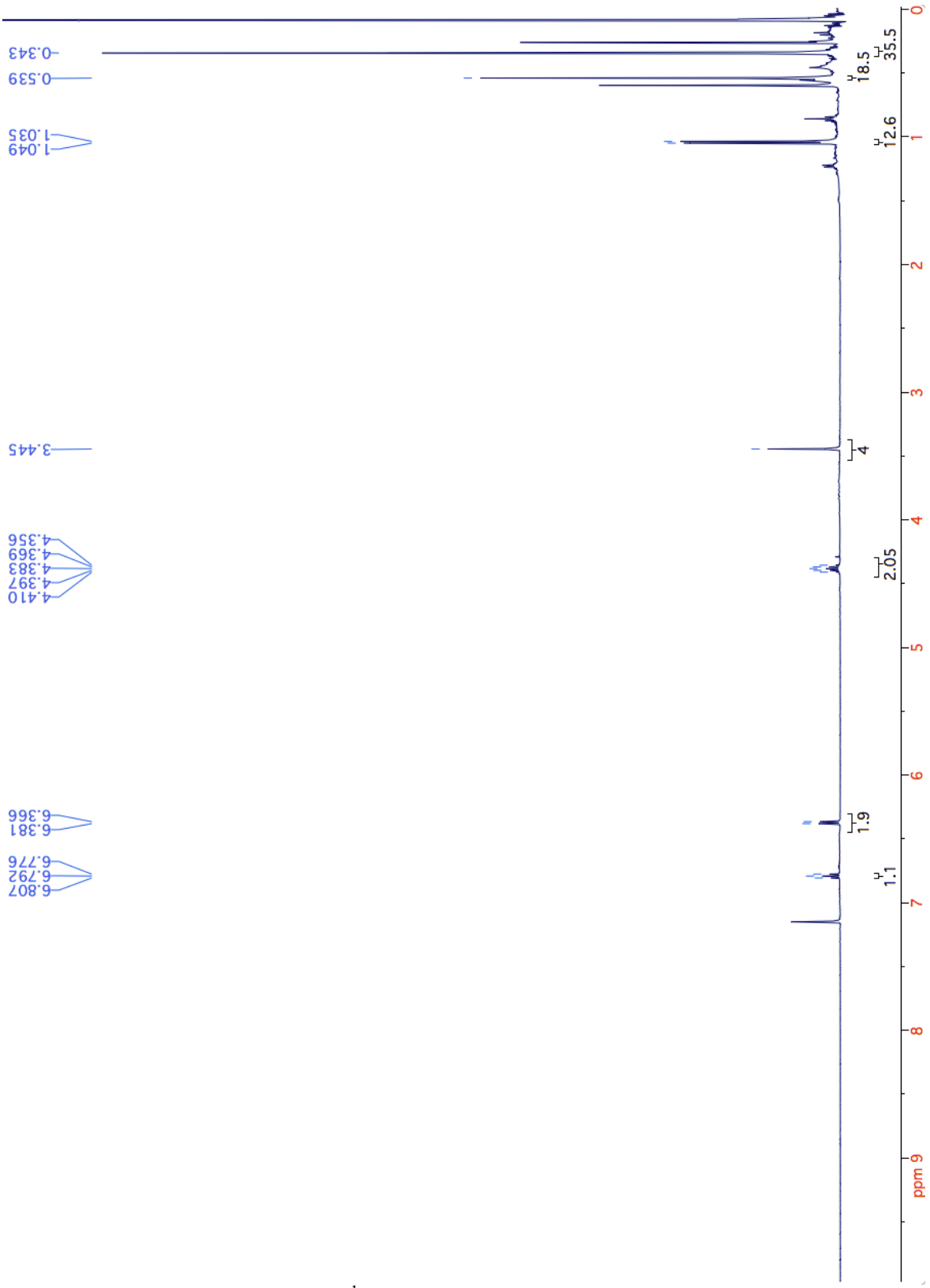

^{1}H NMR spectra of **9a**

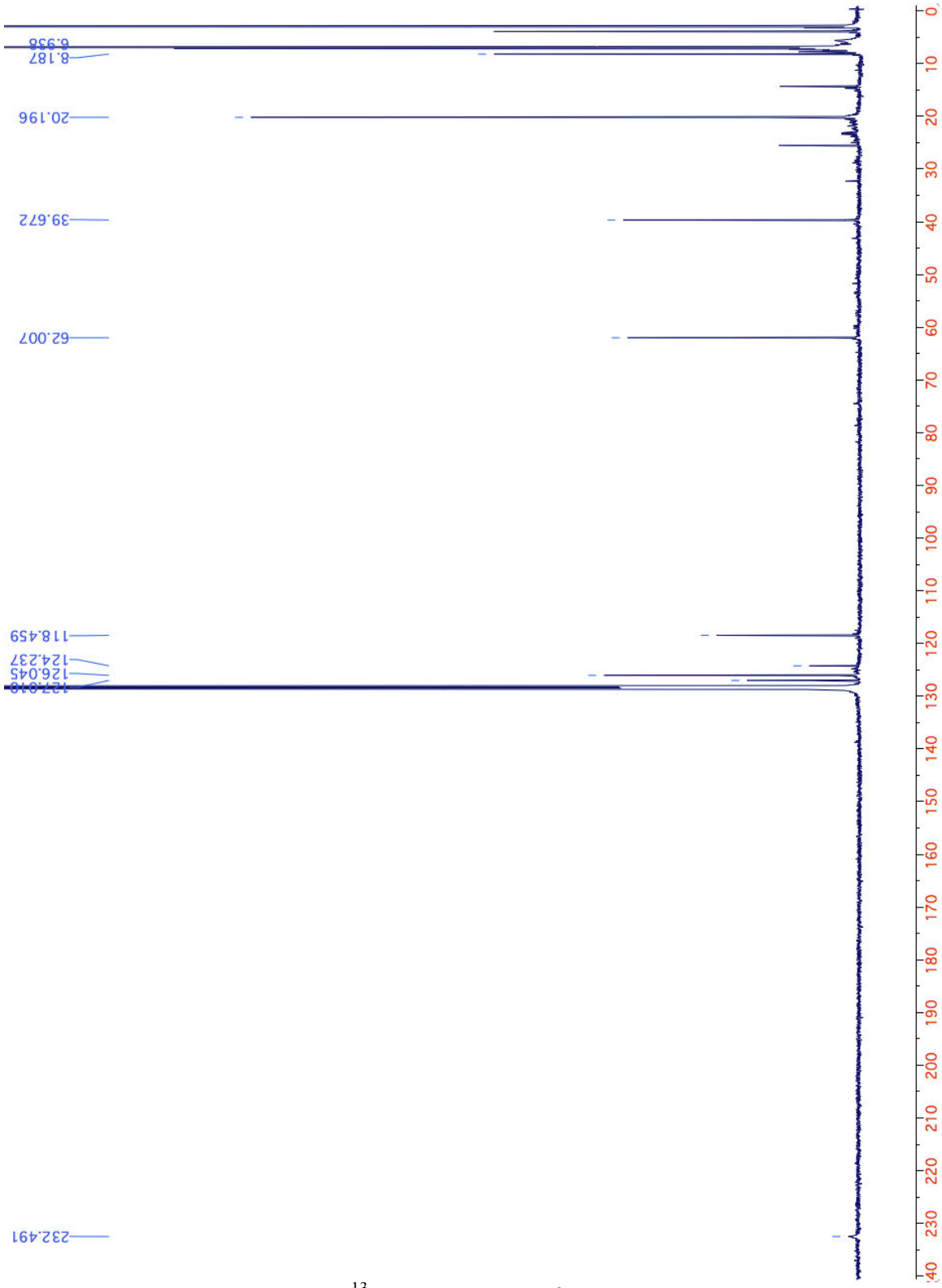

^{13}C NMR spectra of **9a**

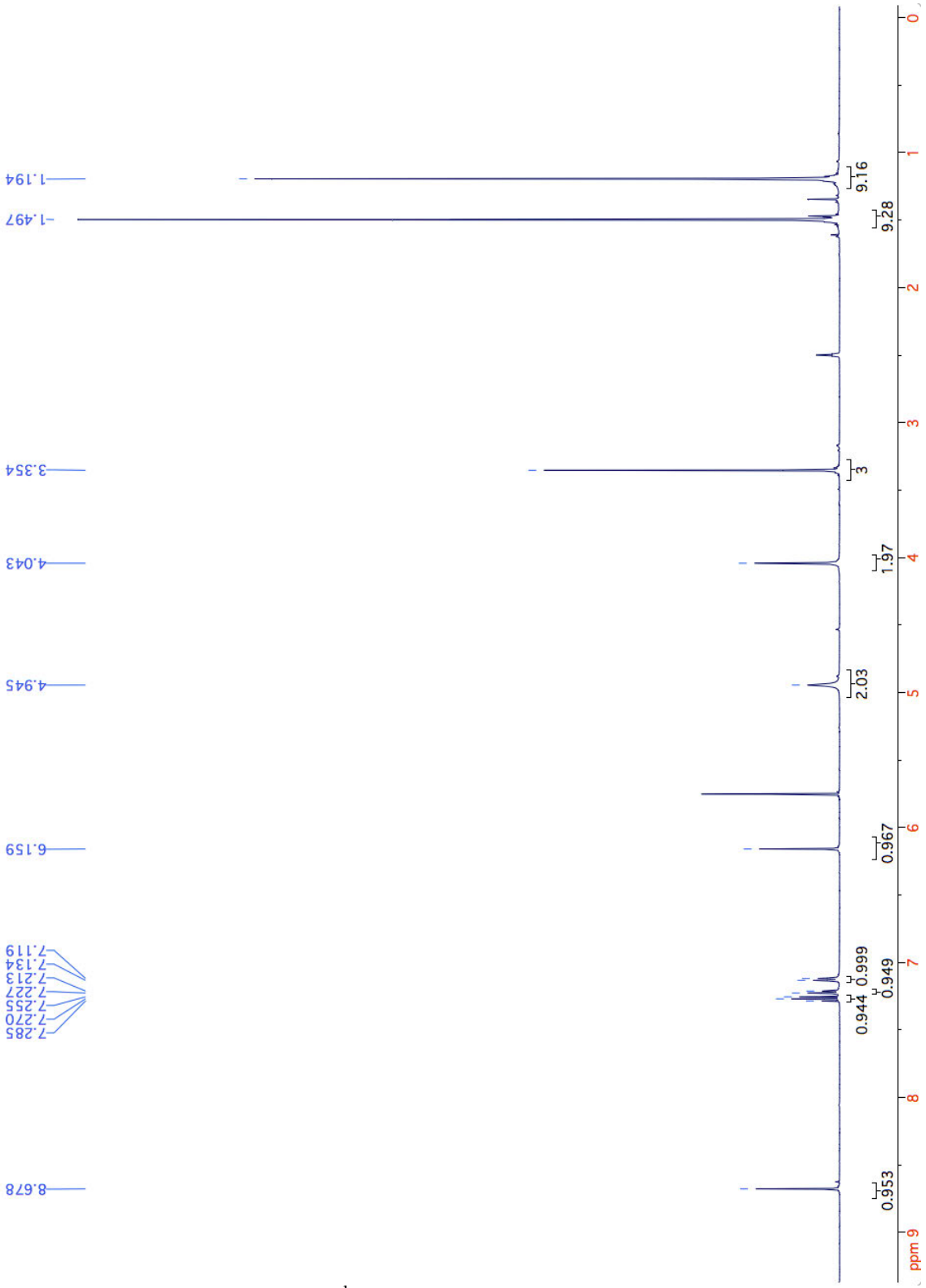

^{1}H NMR spectra of **13**

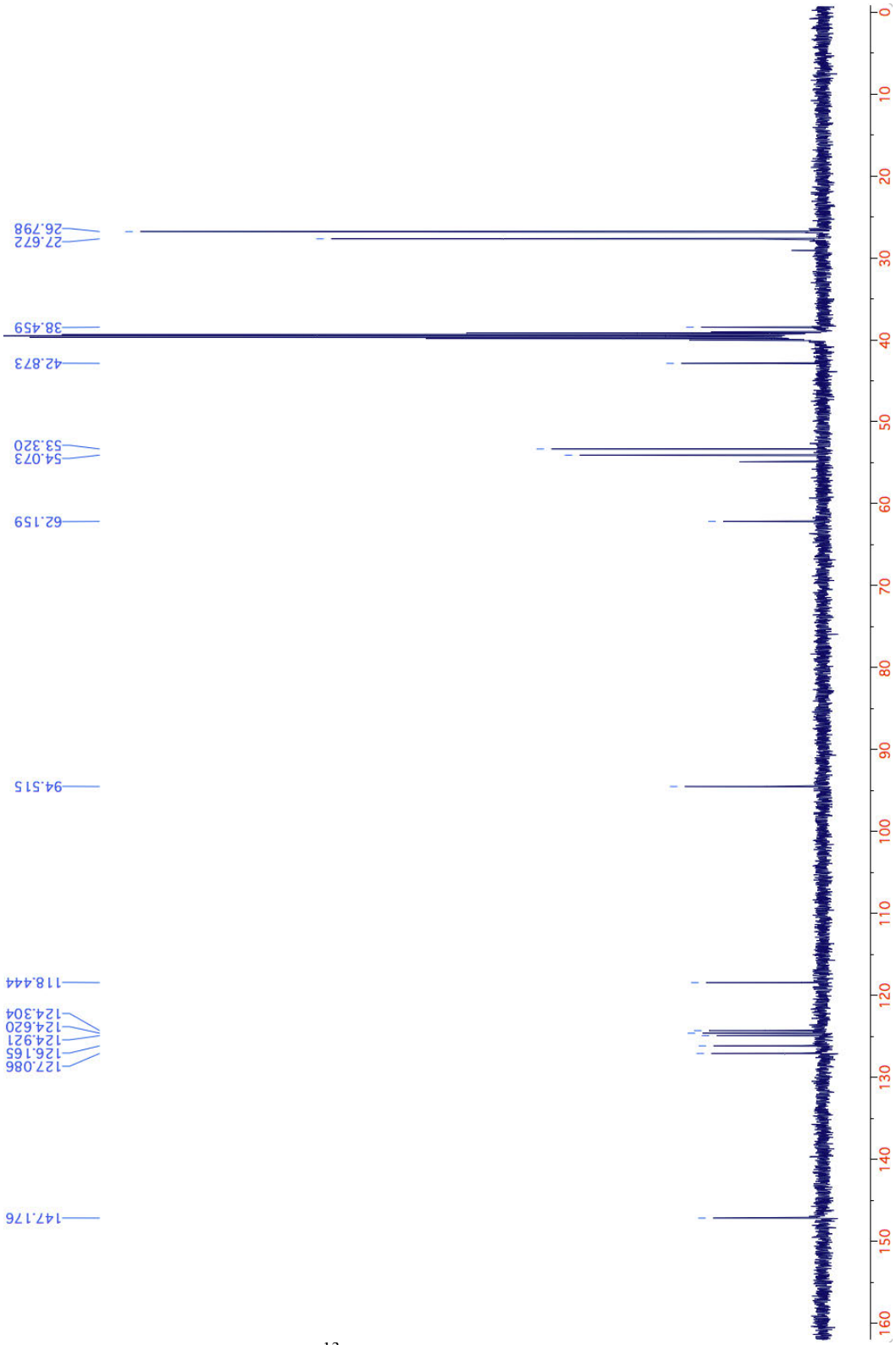

^{13}C NMR spectra of **13**

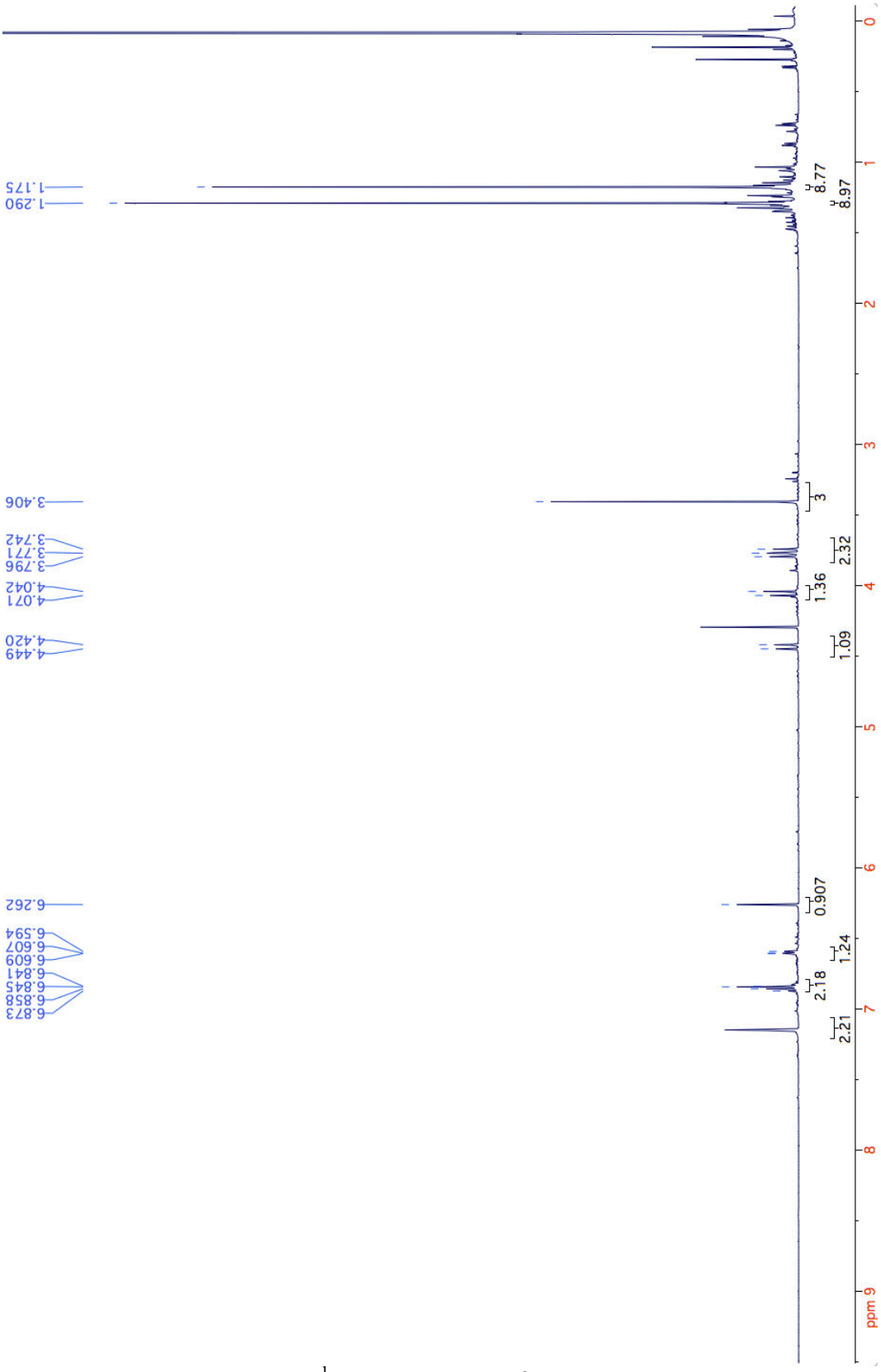

^{1}H NMR spectra of **15**

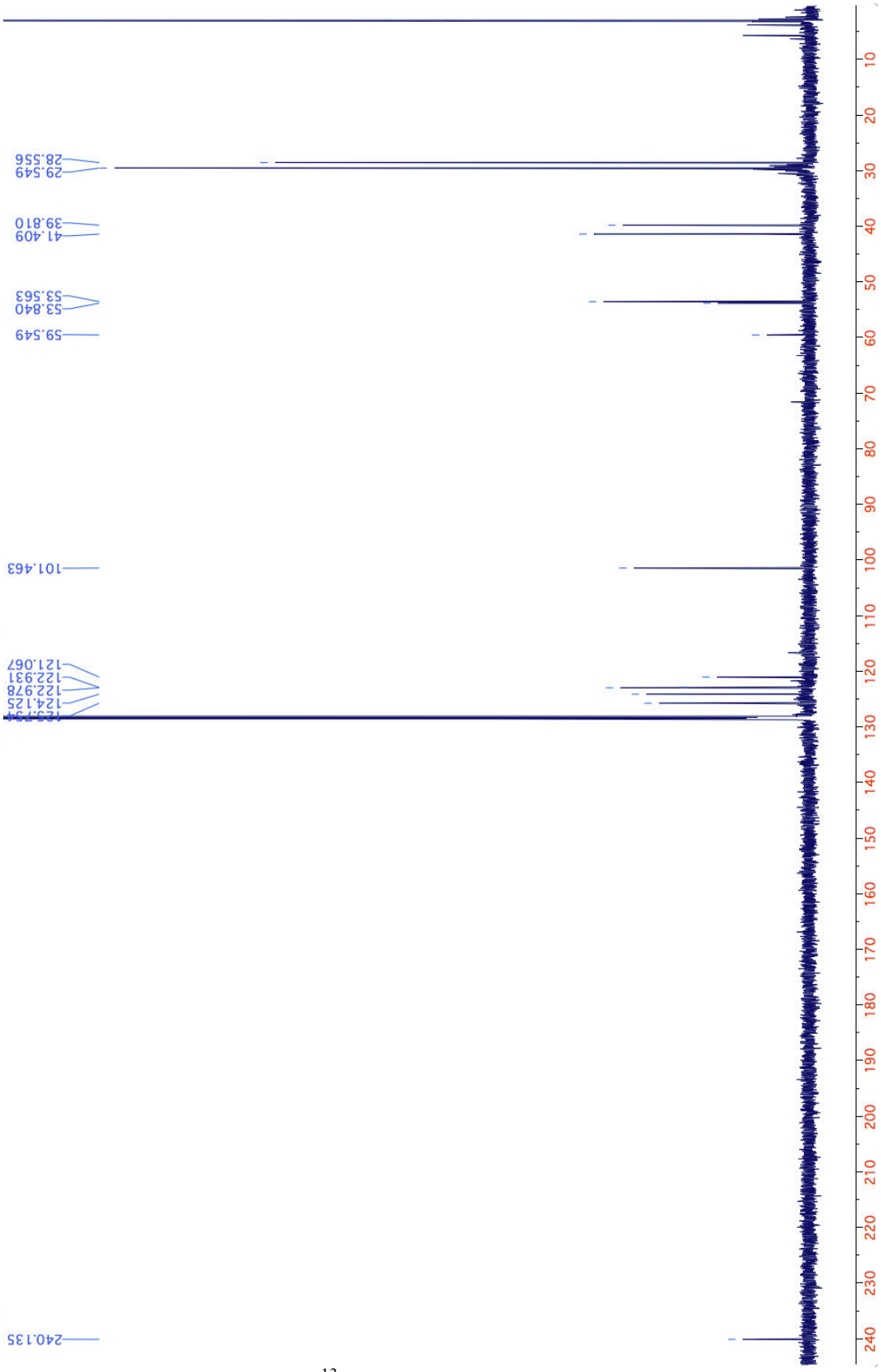

^{13}C NMR spectra of **15**